

# PINNED CONNECTIONS

I. Harms

Master of Science thesis





---

# PINNED CONNECTIONS

---

MASTER THESIS

submitted in partial fulfilment of the  
requirements for the degree of

MASTER OF SCIENCE

in

STRUCTURAL ENGINEERING

by

Ivo Harms

## **Thesis committee**

- Prof.ir. F.S.K. Bijlaard, University of Delft, Steel and Timber Constructions (Chairman)
- Ir. R. Abspoel, University of Delft, Steel and Timber Constructions
- Dr. Ir. P.C.J Hoogenboom, University of Delft, Structural Mechanics
- P.S. van der Mel, Msc., Mammoet Solutions
- Ir. L.J.M. Houben, Road and Railway Engineering



Department of Steel and Timber constructions  
Faculty CEG, Delft University of Technology  
Delft, the Netherlands



Mammoet Europe B.V.  
Karel Doormanweg 47  
Schiedam, the Netherlands



# Preface

This master thesis is written to finalize the master study Structural Engineering at the University of Technology at Delft. The work is done from September 2014 until May 2015, at the office of Mammoet Solutions in Schiedam. The report presents research about the calculation methods of pinned connections. The conclusions of this report can be used to improve the calculation methods at the Mammoet Solutions department.

Without the help of others I would not have reached the same results presented in this report. I would like to thank Mammoet Solutions for offering the opportunity to graduate within a company like Mammoet. I want to thank all the employees of Mammoet Solutions who contributed in any way, for their interest and helpful advices. In particular I would like to thank Stephan van der Mel for his guidance in the use of the program Ansys. Secondly I would like to thank my other committee members for their enthusiasm on the subject and their input and questions during this master thesis.

Ivo Harms

Schiedam, May 2015



---

# Summary

Mammoet is a worldwide operating lifting and transportation company. To remain the market leader, Mammoet improves their operating methods and develops new equipment. Within this equipment, pinned connections are very common for example in cranes.

The capacity of a pinned connection is general determined according to certain standards. Disadvantages of standards are the limitation of their scope, the limited extent of the output and most important, the differences between the various standards. A comparative study on analytical methods and standards for the calculation of pinned connections points out the differences between the standards.

Another way to determine the capacity of pinned connections is using Finite Element Method (FEM) programs. FEM programs have no limits in their scope to analyze pinned connections. Disadvantages of FEM programs are that results and output have to be assessed and interpreted by a competent person on validity. A FEM analysis for a wide range of geometries should provide more information in addition to the standards. By comparing the standards with the FEM results, a clear method is developed which clearly interprets the FEM results. This method determines capacities for geometries which are not covered by a standard or for specific checks.

In a literature study all analytical and empirical backgrounds are studied, which often form the basis of the standards. All these methods and standards include different calculation rules, restrictions and have different design factors. A comparative study points out that most standards provide simple unity checks to determine the capacity, but due their simplicity they are not always accurate. The EN13001-3-1 standard and the ASME BTH-1 standard include unity checks which are dependent on most geometry parameters and seem to be most accurate compared to the FEM results.

Pinned connections can be modelled in different ways in a FEM program. With smart assumptions and choices the computation time of a FEM analysis can significantly be reduced. To save computation time a 2D FEM model is used to determine the internal stresses/strains for connections without cheek plates. If cheek plates are applied, a 3D FEM model is preferred. Elastic analysis shows that the peak stress in the model is sensitive for different element types and mesh sizes. Plastic analysis provides more uniform results for different element types and mesh sizes and is therefore preferred.

With a FEM analysis the stress/strain distributions are calculated and plotted for the capacities according to the standards. This results in different magnitudes of stresses and strains due to the simplified unity check formulas, which don't include all geometric effects. It can be concluded that the FEM results do not automatically agree with the capacities according to the standards.

The influence of the load and geometry on the magnitude of plastic strains is studied with a FEM program. It is concluded that the magnitude and location of plastic strains is dependent on many geometric parameters. A method is developed to manually provide additional capacities based on these FEM results.

In this method the FEM results are predicted with a formula with an accuracy of  $\pm 10\%$ , without doing a time consuming FEM analysis. An advantage of these formulas and method is their wide range of applicability.

To improve this report some additional work is recommended. Some simplifications and unaddressed issues deserve more detailed investigation.

- Validate the results for other steel grades than S690, to prove the expansion of the FEM results of steel grade S690
- Study the effect of tapered eyes
- Study the effect of oblique and perpendicular loads
- Study the effect of various clearances for the load distribution between the cheek plates and the mid plate

# Table of Contents

<b>Preface</b> .....	<b>iii</b>
<b>Summary</b> .....	<b>v</b>
<b>1 Introduction</b> .....	<b>1</b>
1.1 Motivation .....	1
1.2 Purpose .....	2
1.3 Structure.....	4
1.4 Terms symbols and definitions .....	5
<b>2 Applications and backgrounds</b> .....	<b>7</b>
2.1 General .....	7
2.2 Mammoet .....	7
2.3 History .....	8
2.4 Theoretical background .....	9
2.4.1 Analytical background.....	10
2.4.2 Empirical background .....	12
2.4.3 Standards.....	14
2.5 Conclusion .....	16
<b>3 Comparative study</b> .....	<b>19</b>
3.1 Reference eyes .....	19
3.2 Parameter influences .....	24
3.2.1 Influence of the eye radius.....	24
3.2.2 Influence of the eccentricity .....	25
3.2.3 Influence of the clearance.....	26
3.2.4 Influence of the steel grade .....	27
3.2.5 Influence of load angle and tapered eyes.....	29

3.3	Design factor influences.....	31
3.4	Conclusion/ Recommendation .....	33
3.4.1	Remarkable results.....	33
3.4.2	Lack of information and recommendation .....	33
<b>4</b>	<b>FEM modeling.....</b>	<b>35</b>
4.1	Introduction .....	35
4.2	Geometry .....	36
4.3	Mesh .....	37
4.3.1	Element type.....	37
4.3.2	Numerical integration.....	38
4.3.3	Pin-hole contact .....	39
4.3.4	Element size .....	40
4.3.5	Conclusion .....	40
4.4	Analysis types .....	41
4.4.1	Elastic analysis .....	42
4.4.2	Plastic analysis .....	43
4.4.3	Possible analysis methods .....	44
4.5	Conclusion .....	46
<b>5</b>	<b>FEM analysis.....</b>	<b>49</b>
5.1	Analysis of the results based on the capacities of the standards .....	50
5.1.1	Influence of $R_{eye}$ .....	50
5.1.2	Influence of the eccentricity .....	50
5.1.3	Influence of the clearance.....	51
5.1.4	Conclusion .....	53
5.2	Analysis of the loads based on plastic strains .....	55
5.2.1	Influence of $R_{eye}$ .....	55
5.2.2	Influence of the eccentricity .....	58
5.2.3	Influence of the clearance.....	58
5.2.4	Conclusion .....	60
5.3	Cheek plates .....	61
5.3.1	Load distribution between the cheek plates and the mid plate.....	61
5.3.2	Other effects .....	63
<b>6</b>	<b>Comparison FEM versus theory .....</b>	<b>67</b>
<b>7</b>	<b>Post processing FEM results.....</b>	<b>69</b>

---

---

7.1	Assumptions.....	69
7.2	Formulas .....	69
7.2.1	Tension in the net section.....	69
7.2.2	Fracture beyond the hole.....	72
7.2.3	Bearing.....	73
7.2.4	Yielding .....	75
7.2.5	Dishing.....	77
7.2.6	Load distribution for applying cheek plates .....	77
7.3	Use of formulas.....	78
7.3.1	Method to determine additional capacities .....	78
<b>8</b>	<b>Conclusion and recommendation .....</b>	<b>81</b>
8.1	Conclusion .....	81
8.2	Recommendation.....	82
	<b>Bibliography.....</b>	<b>83</b>
	<b>Appendices .....</b>	<b>85</b>
<b>A</b>	<b>Literature study .....</b>	<b>86</b>
A.1	Introduction .....	86
A.2	Pinned connections.....	86
A.2.1	General .....	86
A.2.2	Mammoet.....	88
A.2.3	History.....	90
A.3	Analytical background.....	93
A.4	Empirical background.....	98
A.5	Standards.....	100
A.6	Comparison / summary.....	105
<b>B</b>	<b>Capacity calculations.....</b>	<b>107</b>
B.1	Analytical background.....	107
B.2	Empirical background.....	110
B.3	Standards.....	120
<b>C</b>	<b>Comparative study.....</b>	<b>133</b>
C.1	Reference eyes .....	133
C.2	Parameter influences .....	152
C.3	Design factor influences.....	166
C.3.1	Variance influences with NEN6786 .....	179

---

C.3.2	Variance influences without NEN6786 .....	181
<b>D</b>	<b>FEM Modeling</b> .....	<b>184</b>
<b>E</b>	<b>FEM Analysis</b> .....	<b>191</b>
E.1	Analysis of the results based on the capacities of the standards .....	191
E.2	Analysis of the loads based on results.....	199
E.3	Analysis of cheek plates .....	208
<b>F</b>	<b>FEM and Formula results</b> .....	<b>213</b>
F.1	Results .....	213
F.2	Formulas .....	234
<b>G</b>	<b>Spreadsheet</b> .....	<b>238</b>

---

# 1 Introduction

## 1.1 Motivation

Mammoet is a worldwide operating lifting and transportation company with a long history. One of their famous operations is the salvage of the Russian nuclear submarine Kursk in the Barents Sea. Mammoet has wide range of projects in which they have been involved. To remain the market leader Mammoet improves their operating methods and develops new equipment. Much equipment is used temporary. For transport limitations it must be easy to assemble and disassemble the equipment. Within the equipment of Mammoet, pinned connections are very common, as they offer many advantages over e.g. welding, clamping or bolting. Pinned connections are simple and robust; they contain a small number of parts and can often be assembled without specialist tools.

For the calculation of pinned connections generally two methods are available:

1. Analytical methods, either described in codes and standards, or published in scientific literature.
2. Numerical methods with finite element software.

At Mammoet both calculation methods are used frequently by engineers, where the analytical methods prevail. In the following both methods will be shortly discussed, and advantages and disadvantages will be pointed out.

### Analytical methods

Analytical methods for the calculation of pinned connections already exist since the beginning of the 20<sup>th</sup> century. Many of these methods are named after the researcher who has proposed and published them. Examples of well-known analytical methods are the theories of Bleich [1], and Poócza [2]. These and other theories are often quite complex and therefore in more recent years analytical methods have evolved in simplified calculation rules incorporated in codes and standards. These codes and standards are an easy tool to design pinned connections. Some examples of standards which include calculation rules for pinned connections are Eurocode-1993-1-8 [3], EN13001-1-3 [4], ASME BTH-1-2011 [5] and NEN 6786 [6].

Analytical methods have two major advantages over numerical methods, being:

1. Simple to work with, once they are incorporated in calculation software like Excel or Mathcad
2. Well defined checks are included

Disadvantages of analytical methods are the limitation of their scope (not all kind of loads or geometry might be possible or covered by the method), the limited extent of the output (generally an analytical

method does not give details on stresses and deformations), and most important, the differences between the various methods. Mammoet is working worldwide and often has to comply with local regulations, referring to local codes and standards. From the experience with working according to various codes and standards, it has become clear that there are significant differences between the standards. A comparative study on analytical methods and standards for the calculation of pinned connections will be a first step to improve the performance of Mammoet engineering.

### **Numerical methods**

Commercial finite element software is available since the 1980's, and has ever since made an enormous progress. Finite element software ranges from simple linear-elastic shell models to very sophisticated elasto-plastic, non-linear solid models containing specific features as contact elements, initial deformations and gaps. Finite element calculations can cope with all possible geometries, boundary conditions and load conditions. FEM programs have no limits in their scope to analyze pinned connections. Disadvantages of FEM programs are that results and output have to be assessed and interpreted by a competent person on validity. This person also has to decide the relevant checks to be made. This requires engineering judgment and is less straight forward than analytical methods in which the rules for checking are included. Another disadvantage is that general a FEM analysis takes a lot more time than simple analytical methods.

## **1.2 Purpose**

In recent years great progress has been made in the field of modeling pinned connections in advanced FEM software at the Mammoet Solutions Department. Detailed calculations of many pinned connections justify deviating from standards for specific checks. The purpose of this thesis is to develop a specific Mammoet standard for the design of pinned connections like Figure 1-1 including the use of cheek plates (Figure 1-2 and Figure 1-3). Geometries like Figure 1-1 are covered by most methods and standards. This report should provide the main differences between the used methods and standards. A method which provides clarity about FEM results should be provided for geometries which are not covered by a standard, or for specific checks.

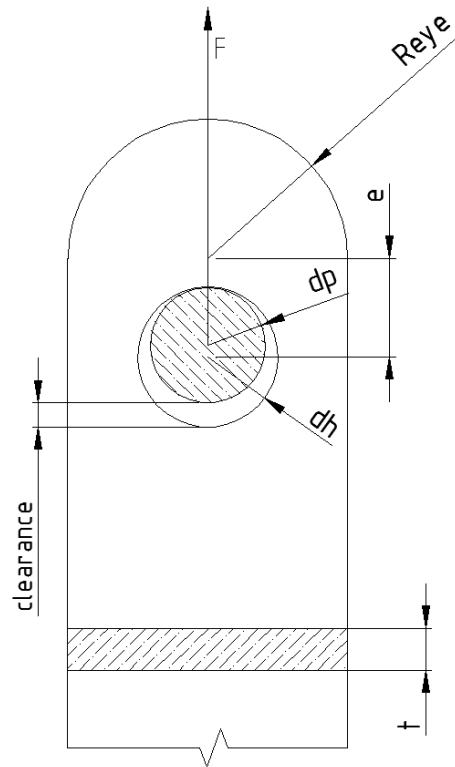


Figure 1-1: Standard geometry pinned connection<sup>1</sup>

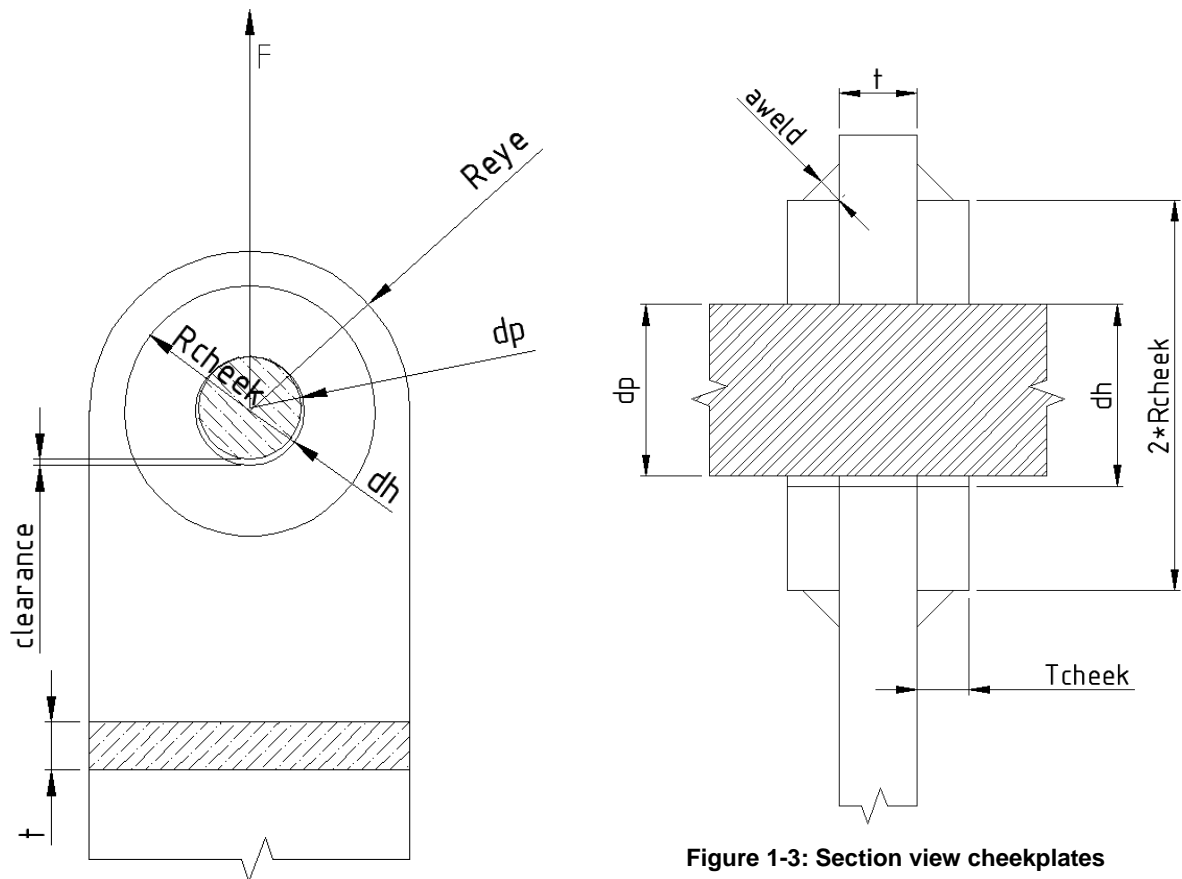


Figure 1-2: Front view of cheekplates

Figure 1-3: Section view cheekplates

<sup>1</sup> Explanation of symbols follows in paragraph 1.4

### 1.3 Structure

Analytical theories and standards are compared with FEM analysis to improve the designs and validate a deviation of the currently used standards at Mammoet. A literature study in appendix A is the basis for comparing different theories and applications of pinned connections. Chapter 2 is a brief description of the findings in the literature study and provides some knowledge about the application, the history and theoretical background about pinned connections. In chapter 3 a comparative study between different analytical and empirical theories and standards is done to point out the differences between the standards. In chapter 4 the finite element model is determined, which is used in chapter 5 to analyze all kind of geometries. Chapter 6 summarizes the results of chapter 5 and provides a comparison of the FEM analysis results with the analytical theories and standards. The results are used in chapter 7 to develop and formulate formulas to predict FEM results. These formulas can validate geometries which do not fulfill the geometry requirements according to the standards.

## 1.4 Terms symbols and definitions

$a_{\text{weld}}$	-	Weld throat
clearance	-	Clearance parameter between pin and hole
$d_h$	-	hole diameter
DOF	-	Degree Of Freedom
$d_p$	-	pin diameter
$e$	-	eccentricity
$E$	-	Shape parameter
$F$	-	Applied load
FEM	-	Finite Element Method
$f_u$	-	ultimate tensile stress
$f_y$	-	yield stress
$f_{yp}$	-	yield stress pin
$G$	-	Shape parameter
$R_{\text{eye}}$	-	eye radius
$R_{\text{cheek}}$	-	Radius cheek plate
$s$	-	clearance between eyes
SLS	-	Serviceability Limit State
$t$	-	thickness main plate
$T_{\text{cheek}}$	-	thickness cheek plate
$t_2$	-	thickness side eyes
ULS	-	Ultimate Limit State



## 2 Applications and backgrounds

### 2.1 General

Pinned connections are one of the simplest steel to steel connections. They are easy to fabricate, and easy to assemble or disassemble. A pinned connection has only one pin (or bolt, axle) going through a lapped type connection, like pad eyes or eye bars. A pinned connection allows rotation and only transfers shear forces through the pin. Pinned connections cannot resist bending moments. Structural parts which are connected with pinned connections are therefore often statically determined.

Pinned connections can be used as column base like in Figure 2-1 or in a bracing system like Figure 2-2.



Figure 2-1: Typical 2-1 connection (one part at the foundation, two parts at the column) ([7])



Figure 2-2: Bracing system ([7])

### 2.2 Mammoet

Pinned connections are commonly used at Mammoet for all different type of equipment. Assembly and disassembly of components is a frequently occurring operation at Mammoet and is easy with pinned connections. In Figure 2-3 some disassembled components are shown which can be transported on containers (Figure 2-4).

After transport the disassembled components can be connected (Figure 2-5) on site. Depending on the size and application of the connection this can be done by hand or with hydraulic tools. With clearances in connections assembling and disassembling is easier. But the allowable clearance is also dependent on the application of the connection. Some connections are not only designed to connect components, but are the center of rotation (pivot) of the equipment and are loaded under different

---

angles. In that case clearances are not allowed. In the equipment of Mammoet a lot pinned connections are notable. In Figure 2-6 the pivots are easily notable. In a detailed look one might see the connections of the braced parts too (white painted in booms of the crane).



**Figure 2-3: Disassembled parts which can be transported on containers**



**Figure 2-4: Disassembled part on container**

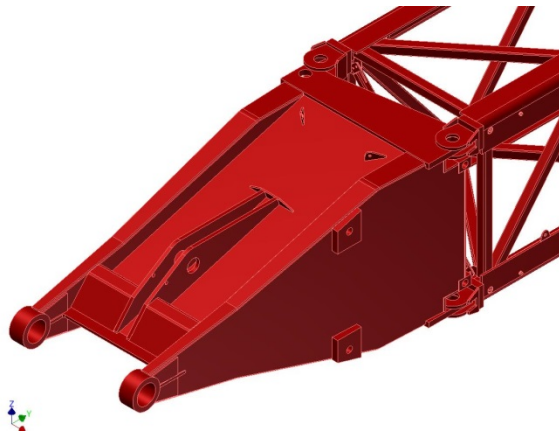


**Figure 2-5: Model of two assembled parts**



**Figure 2-6: Application of equipment**

## 2.3 History

In the end of the 19<sup>th</sup> century and the beginning of the 20<sup>th</sup> century some bridge designers started to make standards for pinned connections. The first bridge type that was developed with pinned connections was the suspension bridge like Figure 2-8, where the suspension “cable” was composed of “eye bars” (Figure 2-7) [8].

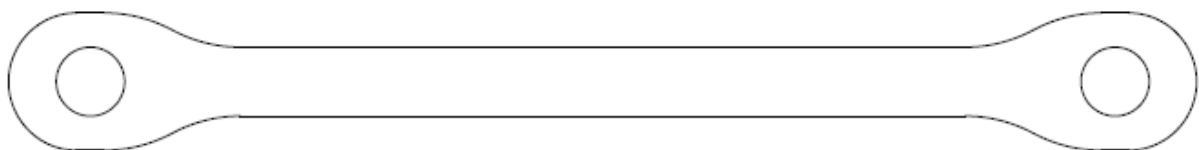


**Figure 2-7: Typical eye bar**

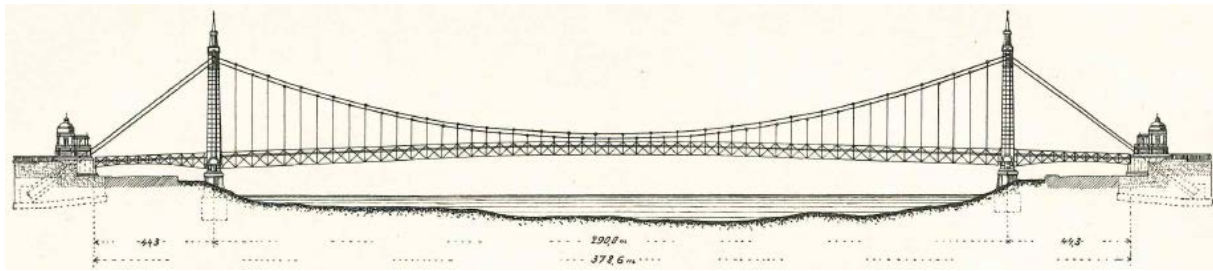


Figure 2-8: Elisabeth Bridge in Budapest ( [8], Fig. 41.)

There was hardly any information about stress distributions in the eye at that time. With rough approximations, experimental results and experience the first connections were designed depending on the width of the bar and/or the diameter of the hole, see Figure 2-9.

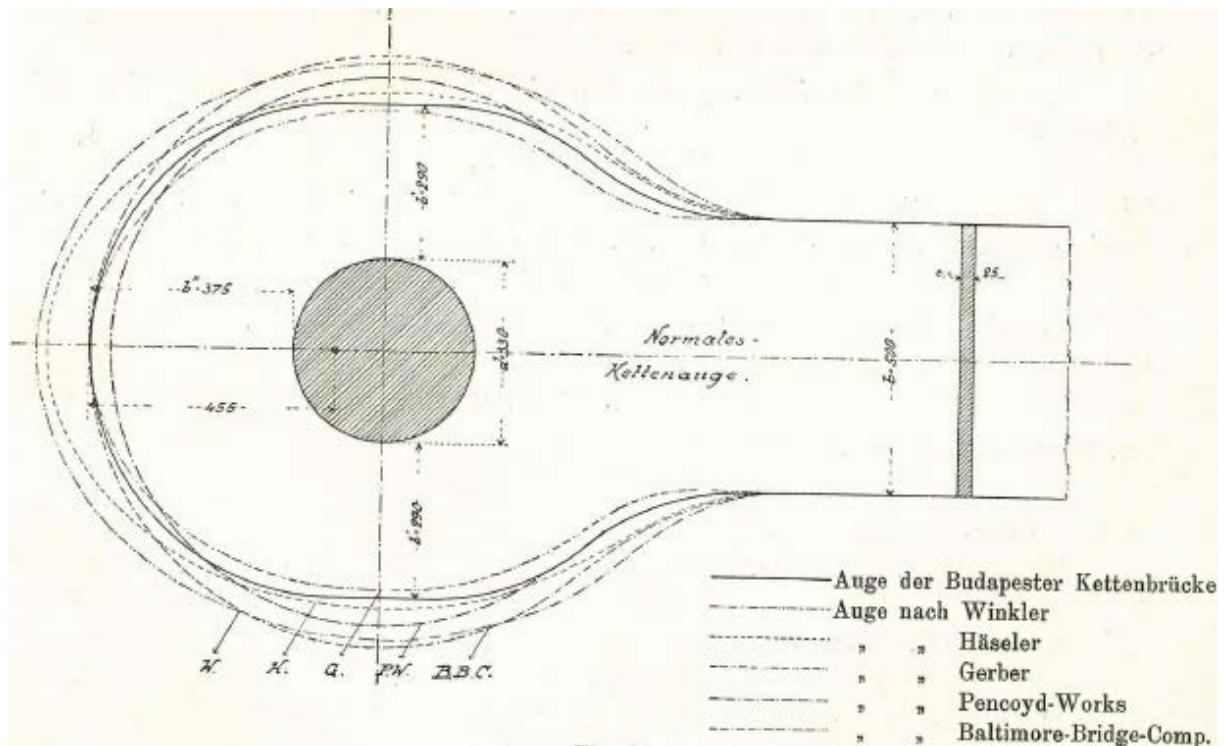


Figure 2-9: Standard geometries in the late 19th century/ early 20th century ( [8], Fig. 69.)

It is interesting that the recommendation of Winkler is the basis of the currently used standard EN-1993-1-8 [3]. In the beginning of the 20<sup>th</sup> century the stress distribution in the eyes were not so clear. With experimental results of a reference eye the first stress concentration factors were derived for the design of pinned connections. To improve the design of pinned connection researchers did a lot of research and experiments for more detailed calculations of pinned connections.

In the beginning of the 20<sup>th</sup> century the first theories were derived with mathematics. In the end of the 20<sup>th</sup> century and the beginning of the 21<sup>st</sup> century more research is done with finite element (FEM) programs. In paragraph 2.4 these findings and backgrounds are summarized.

## 2.4 Theoretical background

Although pinned connections were already used since the 19<sup>th</sup> century, the first theories were derived in the beginning of the 20<sup>th</sup> century.

### 2.4.1 Analytical background

**G. Schaper** [9] assumed that for small clearances the bearing load on the eye is just radial orientated. The resultants of these radial stresses are equal to  $H$  and  $P/2$  (Figure 2-10), which can be used to derive the stresses in the eye.

**Dr. Ing. F. Bleich** [1] assumed a radial orientated bearing load too and with this distributed load, he derived a set of equations from which the stress concentration factors at A in Figure 2-11 can be calculated.

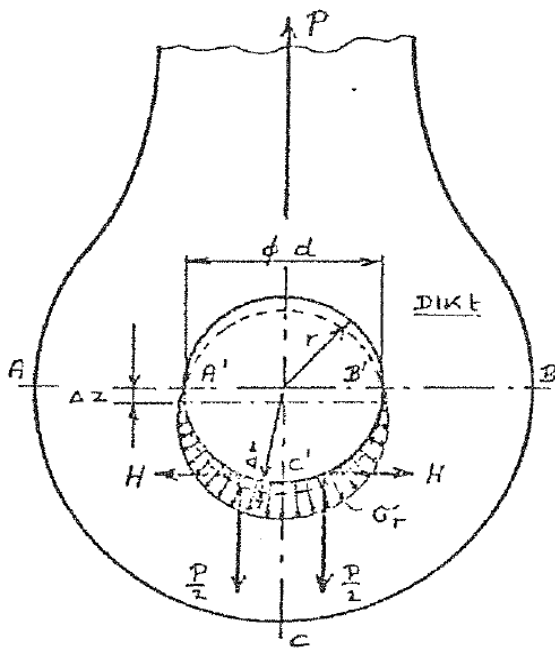


Figure 2-10: Theory of Schaper ([9], fig.4)

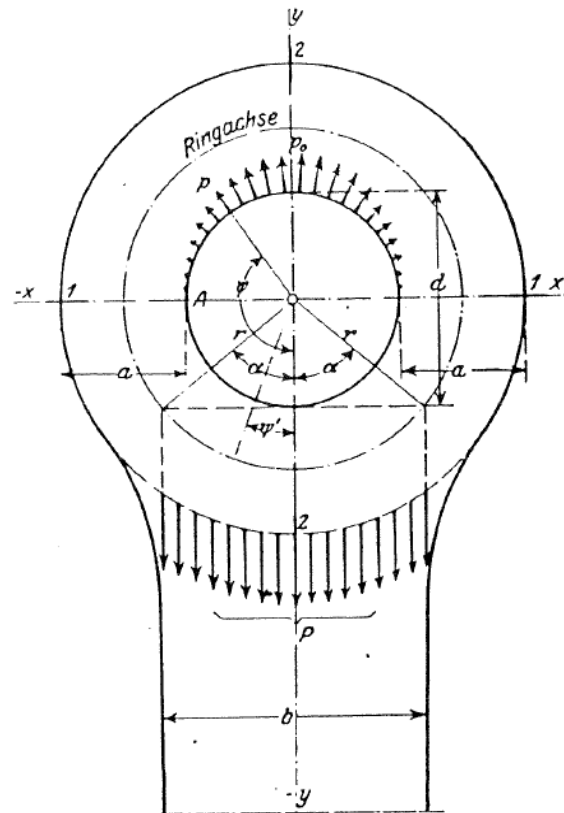


Figure 2-11: Theory of Bleich ([1], Abb. 201)

**H. Reissner and F. Strauch** [10] assumed a sinusoidal distributed and radial orientated bearing load, and also derived a formula to calculate the stresses at point A in Figure 2-11.

**W. Reidelbach** [11] made the assumption that there is not only a radial orientated bearing load but also a shear stress is transferred via the contact (Figure 2-12). With these assumptions he derived stress concentration factors not only at point A in Figure 2-11. He derived formulas to calculate the stress concentration factors through a whole section next to the eye and on top of the eye, see Figure 2-13.

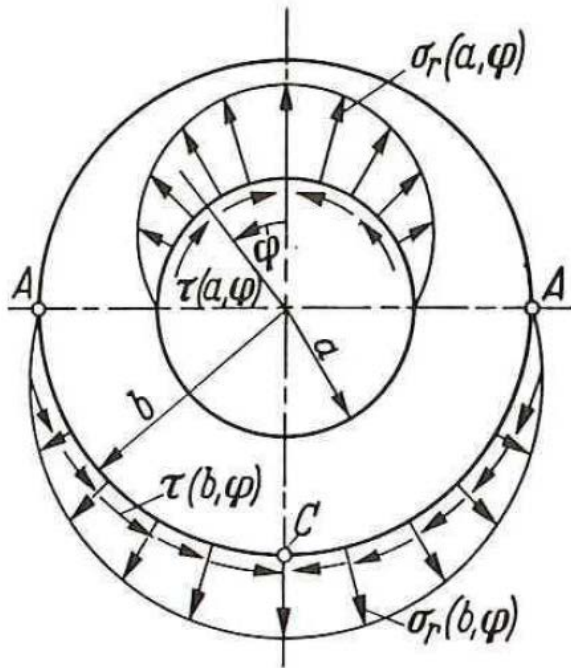


Figure 2-12: Load introduction according to Reidelbach ([11], Bild 3)

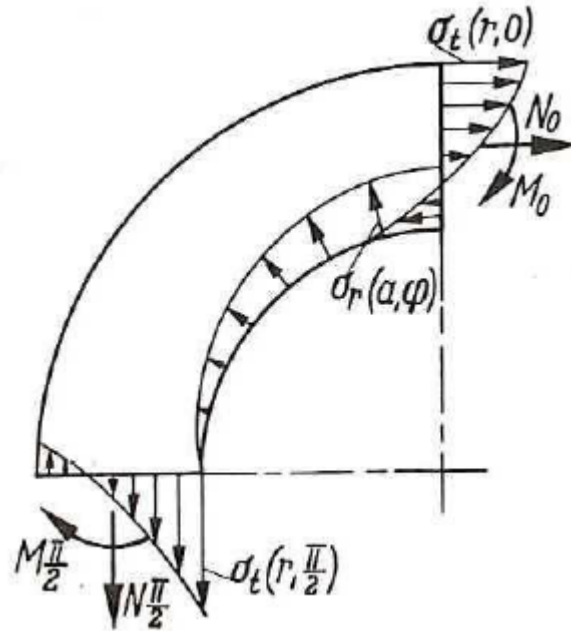


Figure 2-13: Stress distributions through whole sections according to Reidelbach ([11], Bild 10)

Dipl. -Ing. A. Poócza [2] was the first one which assumed a varying section height (e.g. the section on top of the eye is larger than the section next to the hole, so include the effect of eccentricities) of the eye. He assumed a resultant bearing load according to Figure 2-14, and derived equations to calculate the stress concentration factor at A in Figure 2-11, and at the top of the eye.

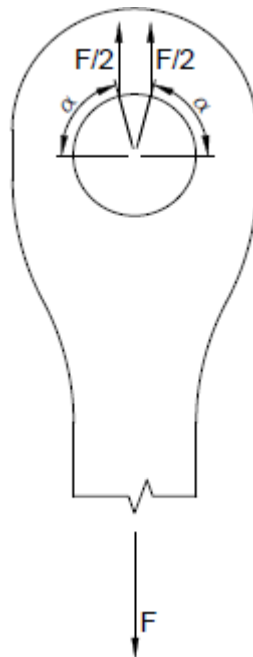


Figure 2-14: Load according to Poócza

H. Hertz did research [12] to contact stress when two surfaces are in contact. Nowadays his theory is still useful to calculate surface stresses between two elastic bodies. For pinned connections this can be useful to calculate the bearing stress. However this theory is only valid for elastic strains/stresses, and if the capacity is limited to those stresses it provides conservative results.

All analytical backgrounds are based on a certain load introduction on the eye. With these loads and certain theories the stress distributions or stress concentrations are calculated. All theories are based on elastic material behavior. Differences in outcome of these theories are because of different assumptions, simplifications and calculation methods.

## 2.4.2 Empirical background

To give more value and clarity about the analytical theories many engineers did research and experiments about pinned connections. Much of data is gained from experiments and later on most data is gained from FEM analysis.

**Peterson** [13] and **J.C. Ekvall** [14] studied various experiments to derive the stress concentration factors for different type of pinned connections under different load orientations. Peterson only derived the stress concentration factor, while Ekvall used the stress concentration factor to determine the capacity of pinned connections.

**C. Petersen** [15] summarized and analyzed a lot of literature and experiments about pinned connections. He derived a formula to calculate stress concentration factors. Petersen also derived the unity checks for failure, which are the basis of the EN-1993-1-8 [3] and are frequently used at Mammoet.

**P. Dietz** [16] and **Dip. Ing. Z. Guo-Geruschkat** [17] did research with FEM programs to check the effect of certain input parameters on the load introduction and the stress distribution of the eye. They did a detailed research not only on the magnitude of the highest stress (or at the stress concentrations), but on the stress distribution through whole sections.

**D. Duerr** [18] compared and summarized different theoretical and experimental studies about pinned connections. He derived formulas to calculate the capacity for different failure criteria (see Figure 2-15 to Figure 2-19). All these capacities for different failure criteria are verified with experimental data. These formulas to calculate the capacities are used in the ASME BTH-1 standard [5].

In contrast to the analytical theories, empirical researches are not only based on elastic behavior of the connection. Duerr and Ekvall did research to failure loads, so in that case plasticity is included. Peterson, Dietz, and Guo-Geruschkat studied the elastic behavior of pinned connections.

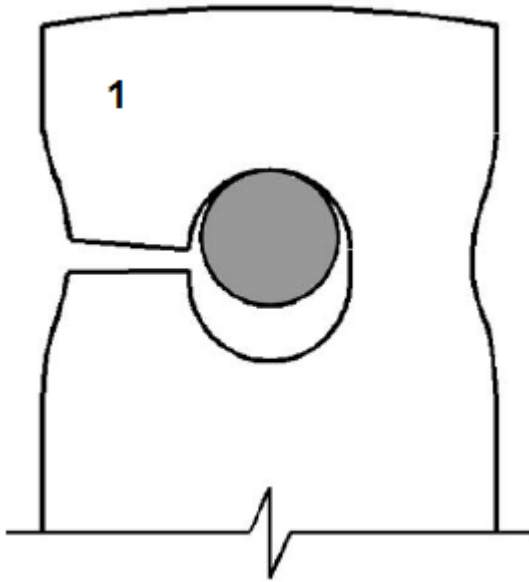


Figure 2-15: Tension in the net section ( [18], Fig. 9.a)

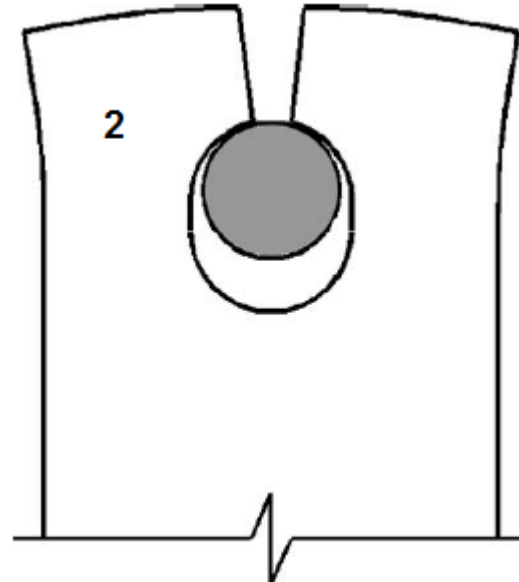


Figure 2-16: Fracture beyond the hole ( [18], Fig. 9.b)

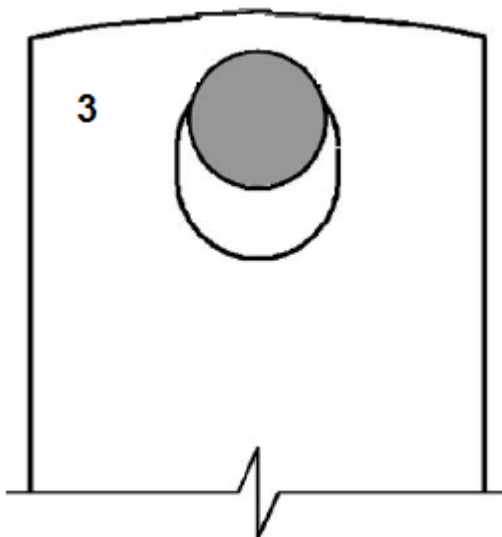


Figure 2-17: Bearing failure

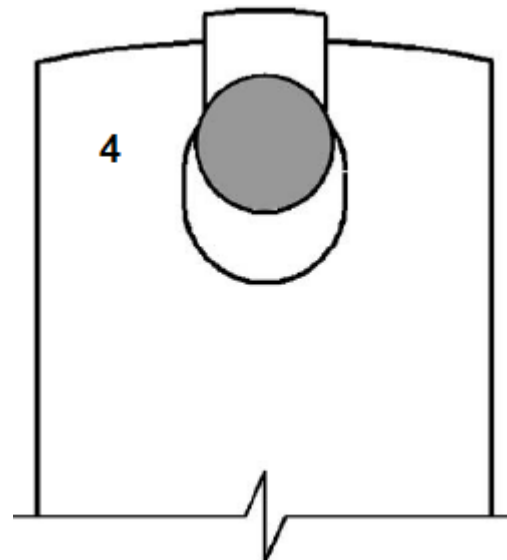


Figure 2-18: Shear failure ( [18], Fig. 9.c)

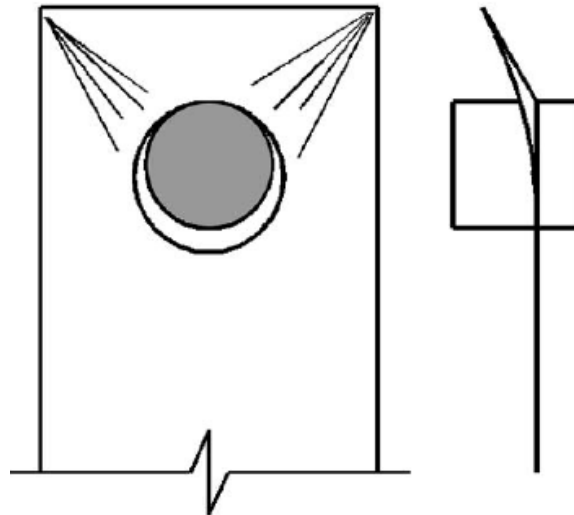


Figure 2-19: Out of plane instability, (Dishing) ( [18], Fig. 9.d)

### 2.4.3 Standards

As already mentioned Mammoet is a worldwide operating company which has to deal with different regulations and legislations. Therefore different standards are currently used at Mammoet. These standards have different ways to check the capacity, and also have different design restrictions. Because none of these standards cover all design criteria which are applied at Mammoet, it is currently not very clear which standard one should use. The following standards are currently used at Mammoet:

- DIN18800 Part 1
- NEN6772
- EN1993-1-8
- EN13001-3-1
- ASME BTH-1
- AISC

Because Eurocode (EN) standards overrule national standards like NEN (in the Netherlands) and DIN (in Germany) standards, DIN 18800 Part 1 and NEN6772 are not explained in detail.

In the literature study in appendix A also two other standards (NEN6786 and the Stress Analysis Manual) are included which are not used at Mammoet. These standards might be valuable because they have other design and geometry restrictions (including tapered eyes and perpendicular/ oblique loads).

The following standards are shortly explained:

- EN1993-1-8 [3]
- EN13001-3-1 [4]
- ASME BTH-1 [5]
- AISC 360-10 [19]
- NEN6786 [6]
- Stress Analysis Manual [20]

More detailed explanations including calculations are in Appendix B.

The **EN1993-1-8** is a European standard which describes the calculation rules for all type of connections, including pinned connections for steel structures. The standard covers steel grades S235 up to S700 and restricts the geometry of the pinned connection. From these geometry restrictions

capacity checks can be derived which are explained in Appendix B. It provides the following capacity calculations:

- Eye tension in the net section ( Figure 2-15)
- Eye fracture beyond the hole/ shear ( Figure 2-16 and Figure 2-18)
- Eye bearing ( Figure 2-17)
- Pin bearing
- Pin bending
- Pin shear
- Pin combined bending + shear

The **EN13001-3-1** is a European standard which specify design methods for cranes. This standard covers a wider set of geometries in comparison to the EN1993-1-8. This standard covers steel grades which are in accordance to equation ( 2-1 ). The clearance between the hole and the pin are assumed to be conform EN ISO 286-2:2010, tolerances H11/h11 or closer. In case of a larger clearance, higher values of  $k$  (stress concentration factor) shall be used.

$$f_u / f_y \geq 1.05 \quad (2-1)$$

The capacities are derived using design charts and calculation formulas which are explained in Appendix B. It provides the following capacity calculations:

- Eye tension in the net section ( Figure 2-15)
- Eye bearing ( Figure 2-17)
- Eye shear ( Figure 2-18)
- Pin bearing
- Pin bending

The **ASME BTH-1** is an American standard which provides minimum structural and mechanical design and electrical component selection criteria for ASME B30.20, Below-the-Hook Lifting Devices. A design factor  $N_D$  of 2 or 3 should be applied to lower the capacity with a factor  $N_D$ . These design factors are based on the variance and reliability of the load and capacity. The following capacity calculations are in accordance to the theories of Duerr.

- Eye tension in the net section ( Figure 2-15)
- Eye fracture beyond the hole ( Figure 2-16)
- Eye bearing ( Figure 2-17)
- Eye shear (Figure 2-18)
- Pin bearing
- Pin bending
- Pin shear

The **AISC 360-10** is an American standard for structural steel buildings. Part of this standard is about the design of pinned connections. It recommends that the clearance should not be larger than 1mm. This standard allows two methods to determine the capacity:

- The Allowable Strength Design (ASD) method which lowers the capacity with a factor of 2
- The Load and Resistance Factor Design (LRFD) method which lowers the capacity with a factor 1/0.75 and multiplies the load with a load factor.

A load factor of 1.5 is commonly applied. In that case both methods provide similar capacities so only the LRFD method is used to calculate the following capacities:

- Eye tension in the net section ( Figure 2-15)
- Eye bearing ( Figure 2-17)
- Eye shear (Figure 2-18)
- Eye gross section of the eye bar

The **NEN 6786** is a Dutch standard which describes technical provisions about the design of mechanical equipment and electrical installations of all types of moveable bridges for road and rail transport. This standard is normally not used at Mammoet. Because the load direction perpendicular to the eye geometry is included in this standard, it might be valuable for comparison with FEM results. This standard provides the following capacity calculations for small and large clearances in case of parallel and perpendicular loads:

- Eye tension in the net section ( Figure 2-15)
- Eye fracture beyond the hole ( Figure 2-16)
- Eye shear (Figure 2-18)

In 1969 the American Airforce developed the **Stress Analysis Manual**. This manual is developed by the American Airforce, and is therefore a manual for aerospace engineers. Part of this manual is about pinned connections. Chapter 9 of this manual presents methods of analyzing eyes (lugs) and their pins and bushings under various loading angles. This standard is not used at Mammoet. Because this standard includes oblique and perpendicular loads, it might be valuable for comparison with FEM results. This standard provides the following capacity calculations:

- Eye tension in the net section ( Figure 2-15)
- Eye fracture beyond the hole ( Figure 2-16)
- Eye bearing ( Figure 2-17)
- Pin bending
- Pin shear
- Pin combined bending + shear

Standards provide obviously ways to calculate the capacity of pinned connections. The calculations are relatively simple since all analytical theories and/or empirical backgrounds are simplified to small formulas or charts. Unfortunately all standards provide different capacity calculations and therefore the outcome of the standards is different. Some are based on elastic behavior while others are based on the real failure load. Also different standards include different safety levels. To compare the standards with each other the ULS loads are used.

## 2.5 Conclusion

It is clear that already a lot of research is done about pinned connections. Unfortunately all this research did not provide a clear standard for all type of pinned connections which are used at Mammoet. Cheek plates and oblique loads are not mentioned in most references. Nowadays some different standards are used at Mammoet with different design restrictions. To develop a clear calculation method for Mammoet, all references are compared by a numerical analysis. A FEM analysis with the program ANSYS [21] should provide more clarity about the compared references.

In Table 2-1 all backgrounds<sup>2</sup> and standards are summarized in a table with possible capacity criteria. It is clear that most literature is about tensile in the net section of the eye (Figure 2-15). This failure mechanism provides most uncertainties and questions. The stress distributions in the pin are less mentioned in the literature because it's clearer how these stresses are distributed. A comparative study in chapter 3 will indicate the differences of the theoretical backgrounds.

---

<sup>2</sup> A = Analytical background, E = Empirical background, N = Numerical background, S = Standard

	Possible failure criteria							
	Background	Tensile in net section	Fracture beyond hole	Bearing	Shear	Bending pin	Shear pin	Extra info, influence parameters
Hertz	A			x				Clearance
Schaper	A			x				
Bleich	A	x	x	x				
Reissner	A	x						
Reidelbach	A	x						
Poócza	A	x	x					
Peterson	E	x						Clearance
Ekvall	E	x						Tapered eyes and oblique loads
Petersen	E	x	x			x	x	
Dietz	N	x		x				Clearance
Guo-Geruschkat	N	x						Clearance, tapered eyes and oblique loads
Duerr	E	x	x		x			Clearance and tapered eyes
EN1993-1-8	S	x	x	x		x	x	Clearance, geometry restrictions
EN13001-3-1	S	x		x	x	x	x	
ASME BTH-1	S	x	x	x	x	x	x	Clearance
AISC 360-10	S	x		x	x			Geometry restrictions
NEN6786	S	x	x					Clearance, and oblique loads
Stress Analysis Manual	S	x	x	x		x	x	Tapered eyes and oblique loads

Table 2-1: Possible failure criteria



## 3 Comparative study

In paragraph 2.4 all different theories are studied and explained. Table 2-1 provides all failure criteria and influence parameters. There are a lot of differences in the scope and outcome of these methods. To provide more clarity a numerical comparison is done. In paragraph 3.1 some reference eyes with their outcomes are studied. Paragraph 3.2 describes the influence of different parameters for some standards. The influence of the design factors is described in Paragraph 3.3. A recommendation is stated in paragraph 3.4.

### 3.1 Reference eyes

As starting point three different eye geometries are compared by all methods. One which is critical for tension in the net section according to the EN1993-1-8, one which is critical for fracture beyond the hole according to the EN1993-1-8 and one which is critical for bearing according to the EN1993-1-8. Based on these three reference eyes the capacities for all methods are plotted in Chart 3-1 to Chart 3-3. This paragraph describes these capacities and explains their differences. In these charts capacities for the following three failure criteria are shown.

- Tension in the net section (see Figure 2-15)
- Fracture beyond the hole (see Figure 2-16)
- Bearing (see Figure 2-17)

Other failure criteria are not compared in this chart cause only very few theories include them. The numerical capacities of the reference eyes are shown in Table C-1. Note that all capacities are the ULS capacities.

All input parameters for reference eye 1 are listed in Table C-1, and the geometry is shown in Figure 3-1. Reference eye 2 has no eccentricity (0mm instead of 50mm) in comparison with reference eye 1 (Figure 3-2), so shear and fracture beyond the hole become more critical. Reference eye 3 has a larger eye radius (150mm instead of 100mm) in comparison with reference eye 1 (Figure 3-3), and therefore bearing becomes more critical.

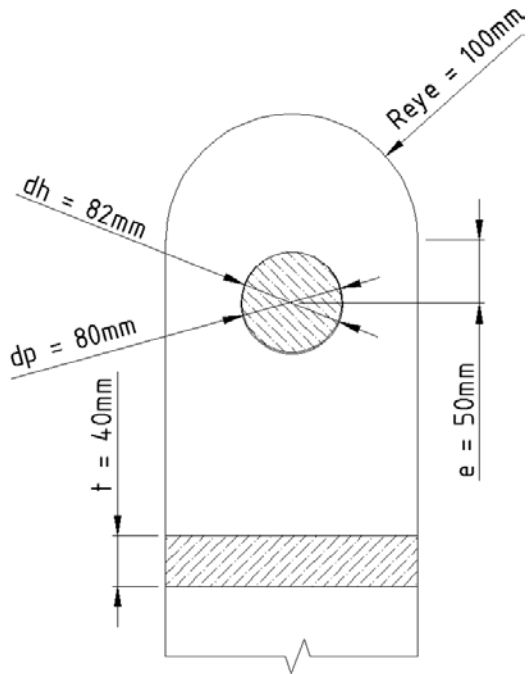


Figure 3-1: Geometry of reference eye 1

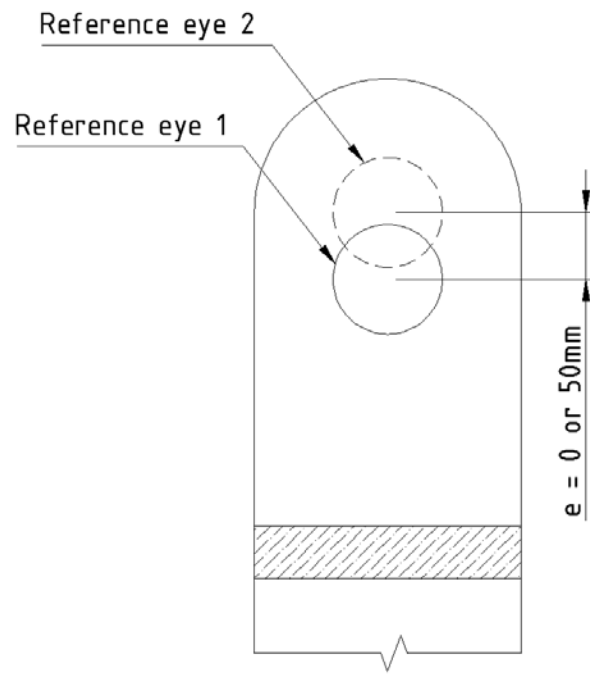


Figure 3-2: Geometries of reference eye 1 and 2

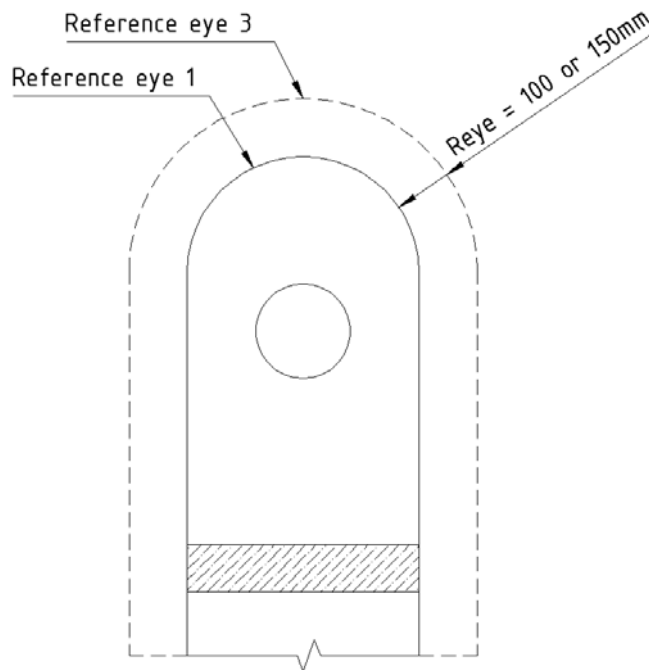


Figure 3-3: Geometries of reference eye 1 and 3

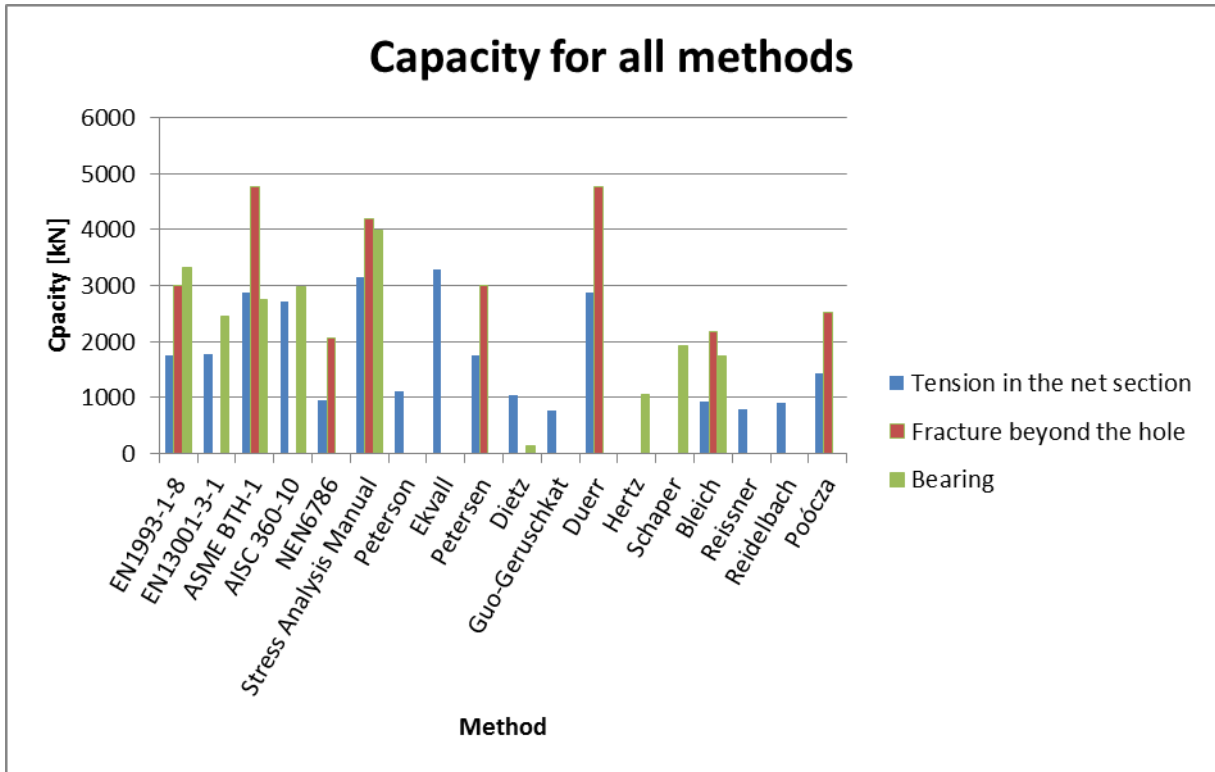


Chart 3-1: Capacities reference eye 1

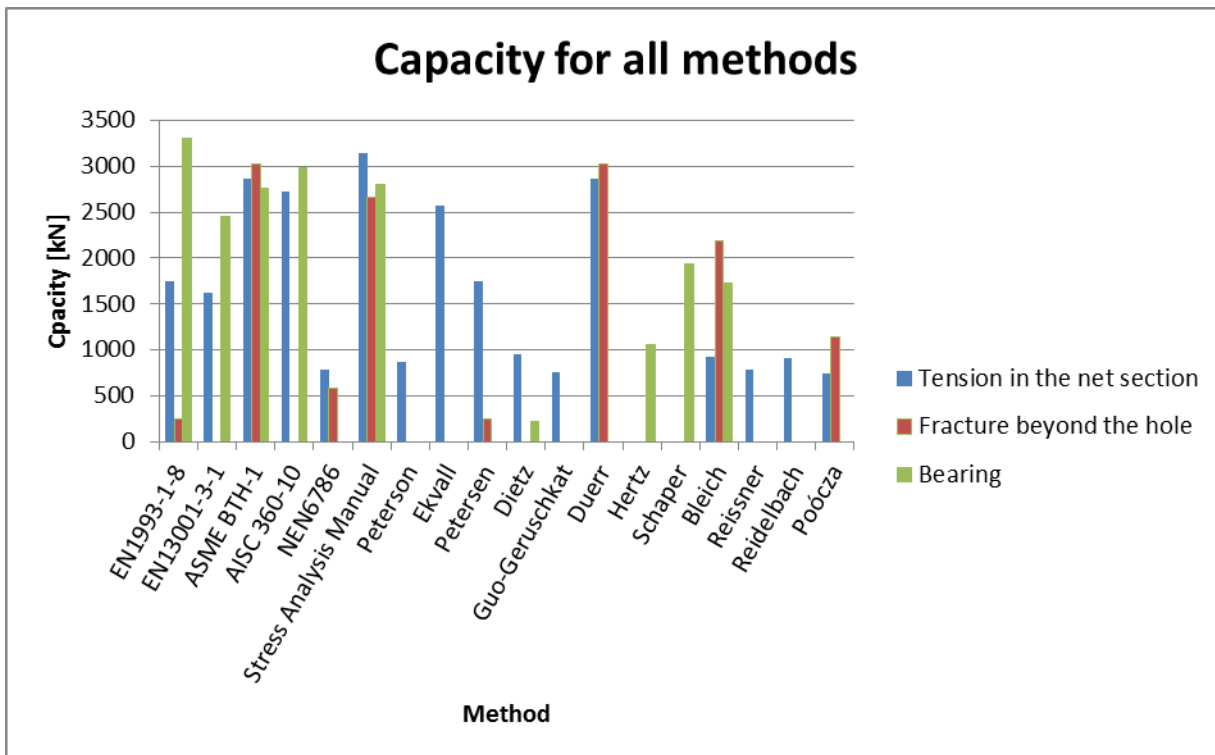
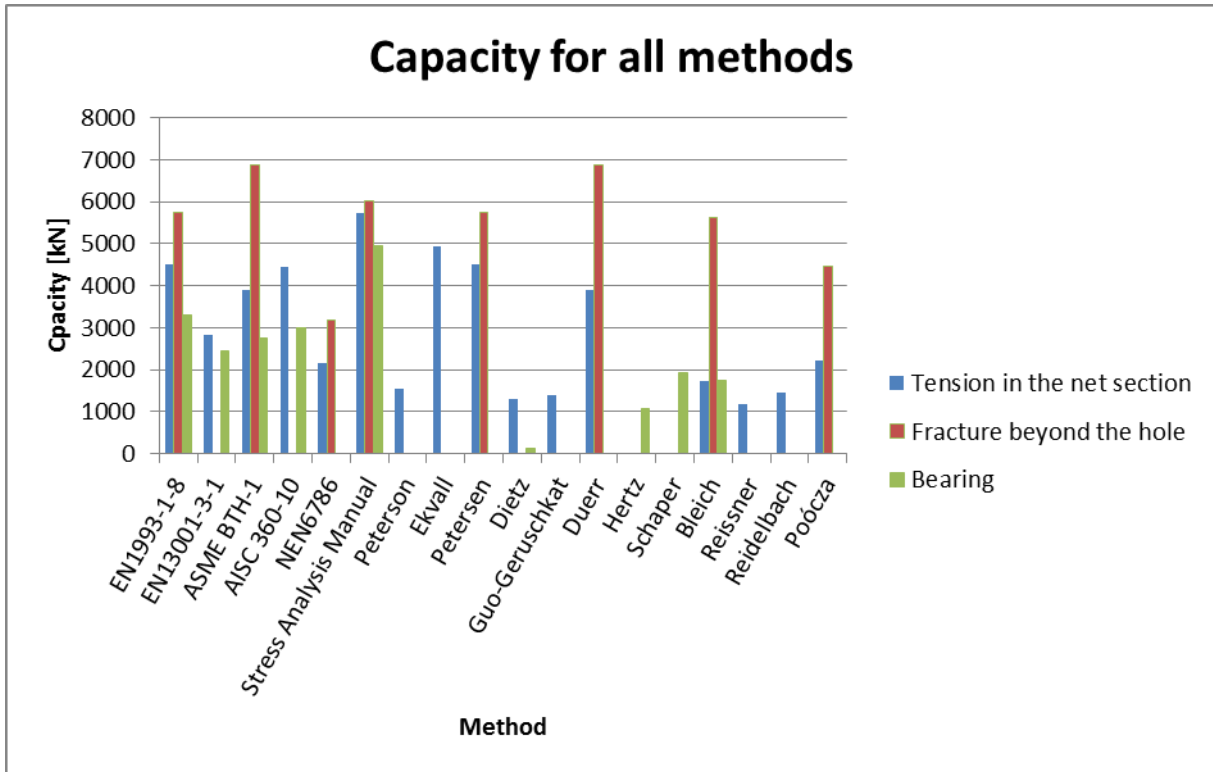
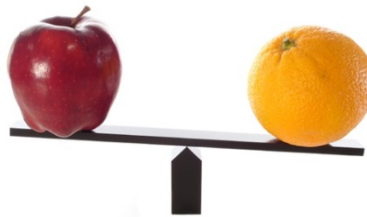


Chart 3-2: Capacities reference eye 2



**Chart 3-3: Capacities reference eye 3**

It is hard to provide any conclusions from Chart 3-1 to Chart 3-3. All methods are compared, but the outcome of the methods, the capacities are different. Even the critical failure mechanisms differ from each other. One reason is “comparing apples to oranges”.



**Figure 3-4: Comparing apples to oranges<sup>3</sup>**

As already mentioned in chapter 2, some theories are based on elastic material behavior, while others are based on the ultimate capacity of pinned connections. Some standards provide checks just between them (partial plastic behavior). It is straightforward that there are a lot of differences between the elastic capacity (when yielding starts to occur) and the ultimate capacity of pinned connections. This is due to plasticity and stress redistributions. Subdividing all methods in different categories provides more similar outcomes. The methods are categorized into the following three categories:

- Elastic methods, which provide “Elastic capacity”
  - Peterson
  - Dietz
  - Guo-Geruschkat
  - Hertz

<sup>3</sup> <https://bluedragonfly10.files.wordpress.com/2011/06/applesoranges2.jpg>

- Schaper
- Bleich
- Reissner
- Reidelbach
- Poócza
- NEN6786
- Fully plastic methods, which provide “Ultimate capacity”
  - ASME BTH-1
  - AISC 360-10
  - Ekvall
  - Duerr
  - Stress Analysis Manual
- Partial plastic methods, which provide “Reduced ultimate capacity”
  - EN1993-1-8
  - EN13001-3-1
  - Petersen

The variances of the methods are plotted in Chart 3-4 to Chart 3-6 for different categories and for different failure mechanisms. The variance determined as follows:

$$\mu = \text{average outcomes} \tag{3-1}$$

$$\sigma = \text{standard deviation outcomes} \tag{3-2}$$

$$V = \sigma / \mu = \text{variance outcomes} \tag{3-3}$$

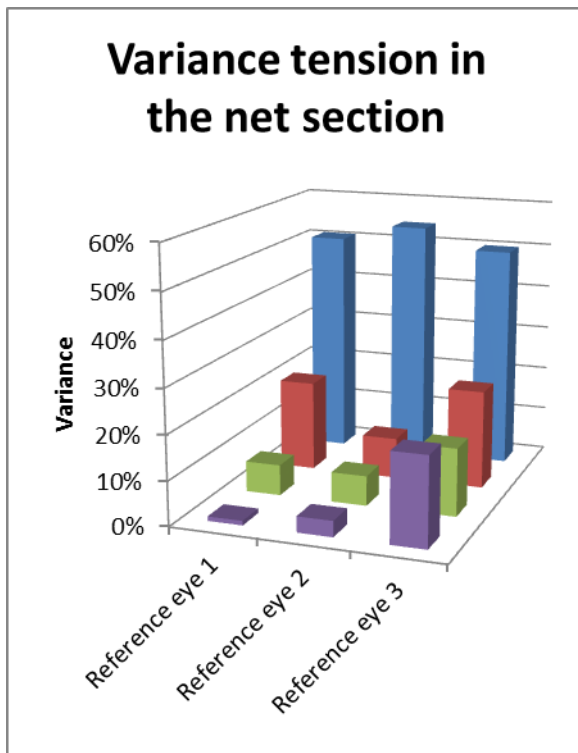


Chart 3-4: Variance tension in the net section

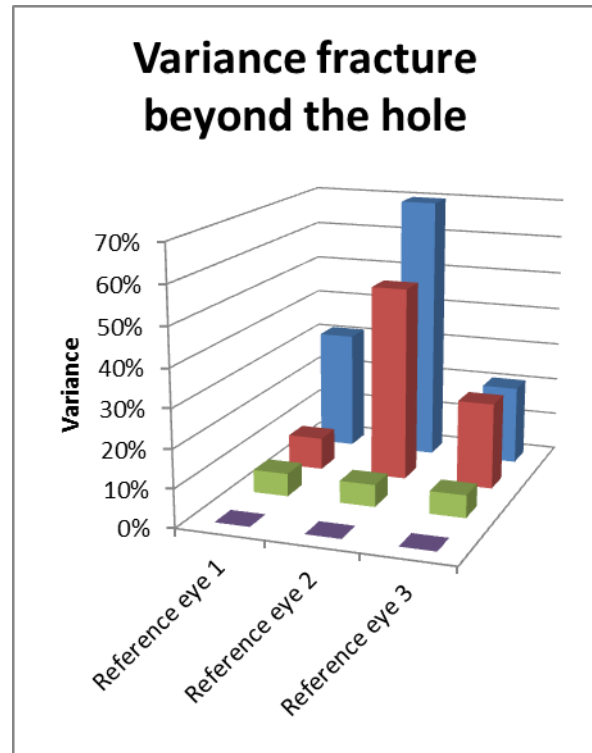
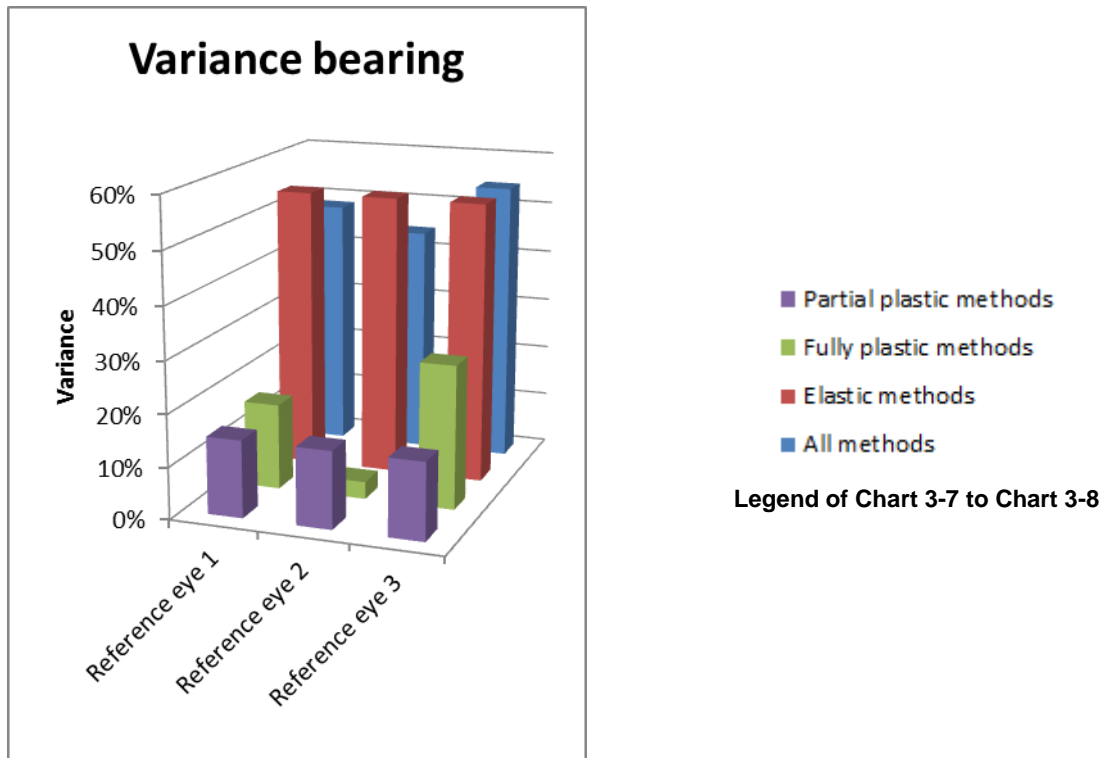


Chart 3-5: Variance fracture beyond the hole



**Chart 3-6: Variance bearing**

It is obvious that for most reference eyes the variance of the separate methods is smaller than the variance of all methods, but that is not always the case. Dividing all methods in different categories still provides a scatter of outcomes, and there are still quite large differences. Also the differences between the methods are different for each reference eye. It can be concluded that the differences between the methods are not only because of the calculation method (elastic behavior, partial plastic behavior or fully plastic behavior). Other assumptions (e.g. load orientation and geometry restrictions) have also influence on the capacities.

In Table C-8 to Table C-16 all averages, standard deviations and variances are listed. In Chart C-13 to Chart C-15, these averages are plotted, including the relative standard deviation as bubble size.

The scatter of outcomes is different for each reference eye. Therefore paragraph 3.2 provides a research of the influence of input parameters.

### 3.2 Parameter influences

All analytical and empirical methods do not provide similar results, and the differences are for some dimensions quite large. It is not clear to compare all methods with each other on parameter influences, because this provides too many results. At Mammoet standards are the common way to check pinned connections. Therefore only the standards are compared in this paragraph.

The parameter influences are based on the input parameters of reference eye 1, see Table C-1. The influence of the eye radius, eccentricity, clearance and steel grade is studied.

In Appendix C.2 the parameter influences for all failure criteria are plotted.

#### 3.2.1 Influence of the eye radius

In Chart 3-9 the capacity is plotted for various input parameters  $R_{eye}$ . All other input parameters are the same as for reference eye 1.

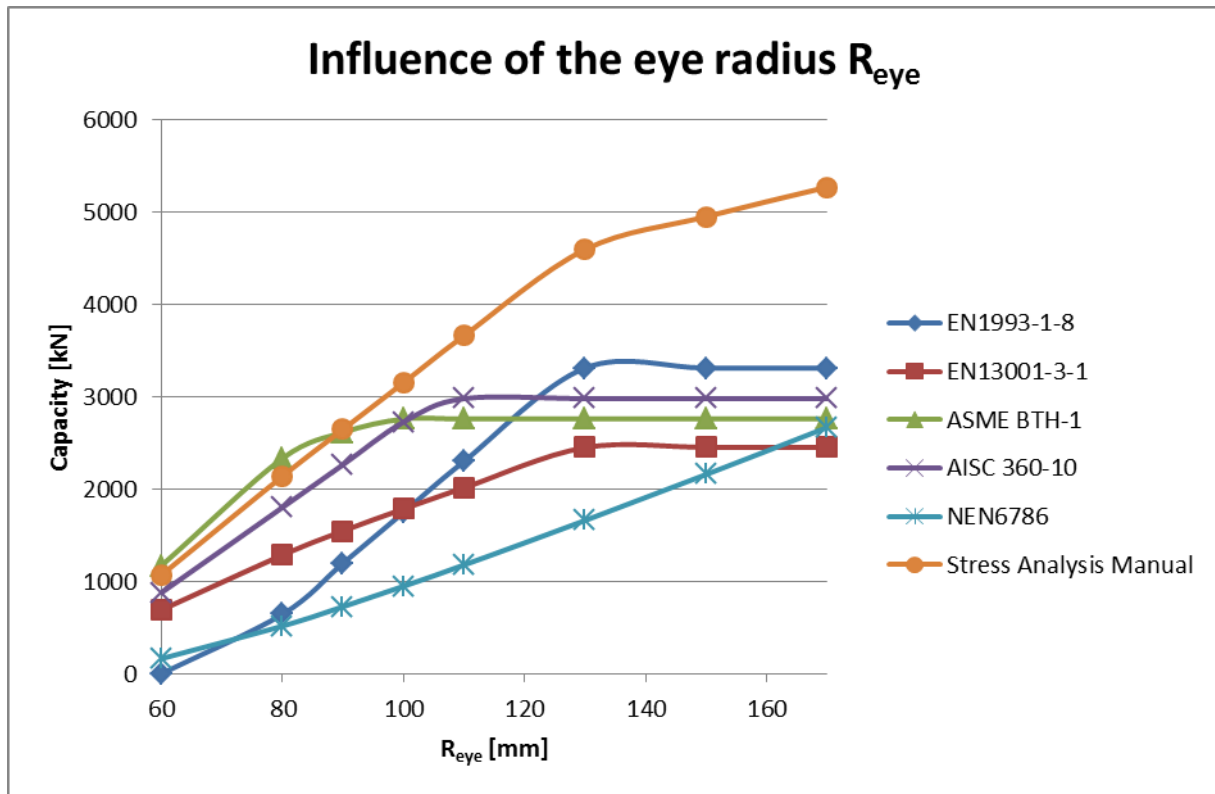


Chart 3-9: Influence of the eye radius R<sub>eye</sub>

From Chart 3-9 can be concluded that for smaller eye radii than 120mm all American<sup>4</sup> standards provide higher capacities. For increasing radii the bearing capacity is critical for all standards, except the NEN6786 which doesn't provide a check for the bearing stress. This is according to reference eye 3 (R<sub>eye</sub> = 150mm), for which bearing is the critical failure mechanism in the EN1993-1-8.

In Chart C-16 to Chart C-20 all capacities for different failure criteria are plotted. From these charts can be observed that for an increasing eye radius:

- The Stress Analysis Manual has an increasing bearing capacity
- The AISC 360-10 limits the tension in the net section capacity while all other standards are more or less linear increasing
- The EN1993-1-8 is most sensitive for various R<sub>eye</sub> values
- For small R<sub>eye</sub> values the EN1993-1-8 provides a negative capacity which is trivial. The minimum capacity is limited to 0 kN
- The NEN6786 provides very conservative capacity

### 3.2.2 Influence of the eccentricity

In Chart 3-10 the capacity is plotted for various eccentricities e. All other input parameters are the same as for reference eye 1.

<sup>4</sup> ASME BTH-1, AISC 360-10 and the Stress Analysis Manual are American standards.

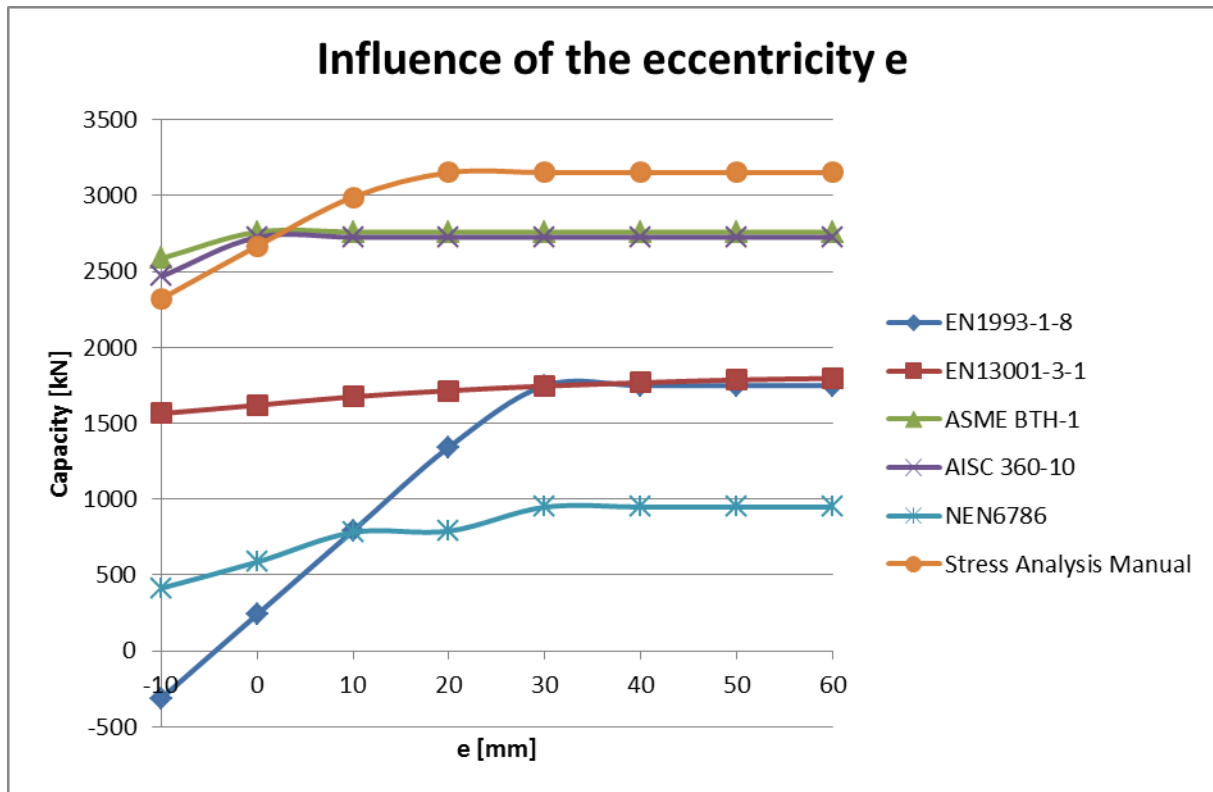


Chart 3-10: Influence of the eccentricity  $e$

From Chart 3-10 can be concluded that again all American standards provide higher capacities. For all standards the influence of the eccentricity is limited. This is because the bearing or tension in the net section becomes critical for higher eccentricities. For relative small eccentricities fracture beyond the hole is the critical failure mechanism. This is in accordance to reference eye 2 ( $e = 0$ mm), for which fracture beyond the hole is critical in the EN1993-1-8.

In Chart C-21 to Chart C-25 all capacities for different failure criteria are plotted. From these charts can be observed that for an increasing eccentricity:

- Only the Stress Analysis Manual has increasing bearing capacity
- The eccentricity has a small influence for tension in the net section in EN13001-3-1
- The NEN6786 has a small “jump” in the capacity because of geometry restrictions
- The EN1993-1-8 is most sensitive for various eccentricities
- For small eccentricities the EN1993-1-8 provides a negative capacity. The minimum capacity is limited to 0 kN
- The NEN6786 provides very conservative capacities

### 3.2.3 Influence of the clearance

In Chart 3-11 the capacity is plotted for various clearances. This is done by vary the pin diameter  $d_p$  (the hole diameter  $d_h$  remains the same). All other input parameters are the same as for reference eye 1.

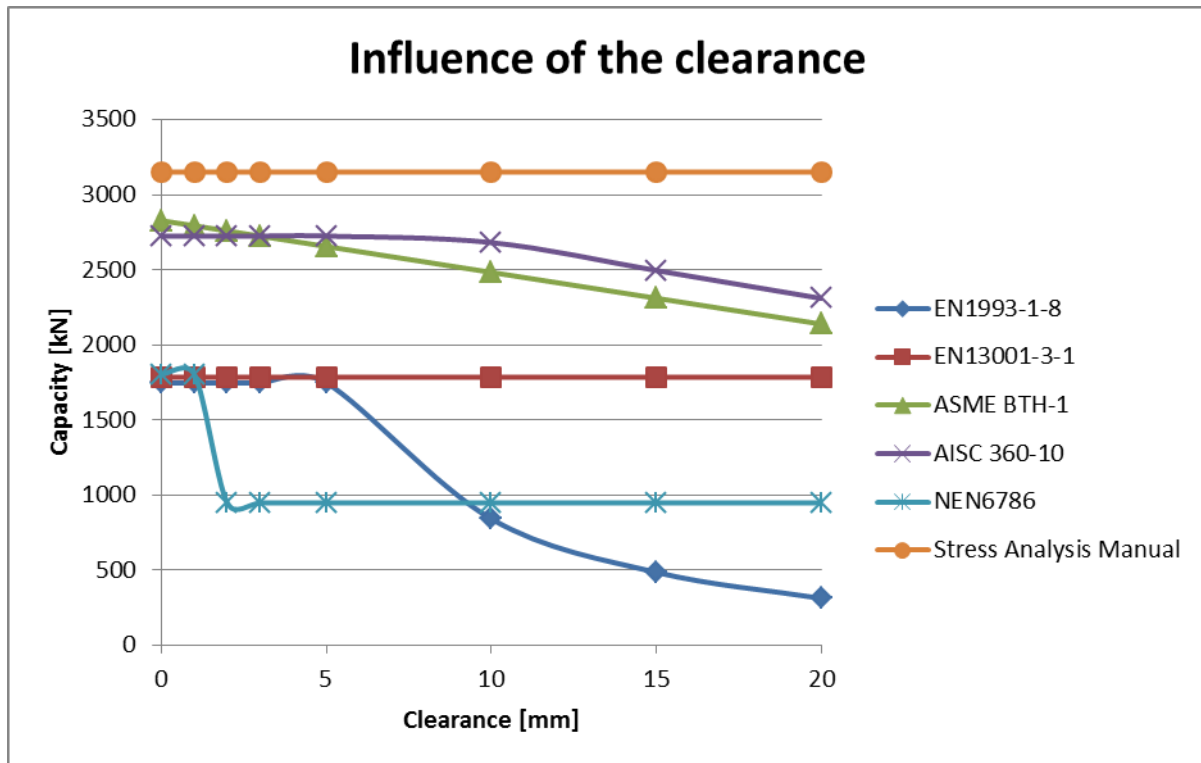


Chart 3-11: Capacity reference eye 1

From Chart 3-11 can be concluded that again all American standards provide higher capacities. The influence of the capacity is relatively small in comparison with the influence of the eye radius and the eccentricity. This is because the clearance has the most influence on the bearing and bearing is not the critical failure mechanism for reference eye 1 (See Chart C-26 to Chart C-30).

In Chart C-26 to Chart C-30 all capacities for different failure criteria are plotted. From these charts can be observed that for an increasing clearance:

- The clearance has no influence on the capacity of the eye in the Stress Analysis Manual
- There is a “jump” in the capacity of the NEN6786 chart between a clearance of 1 and 2mm. This is due to the difference in the calculation method between small and large clearances.
- For clearances higher than 5mm the EN1993-1-8 is most sensitive for various clearances. This is due to the EN1993-1-8 includes a modified Hertz stress formula (equation ( B-113 )), which is very sensitive to clearances.

### 3.2.4 Influence of the steel grade

The compared standards include different factors of steel grade. Most American standards are based on the ultimate tensile stress, while the European standards are based on the yields stress. The difference between the yield stress and the ultimate tensile stress is decreasing for higher steel grades. High strength steel has a relatively small difference between the yield stress and the ultimate tensile stress and low strength steel has a relatively high difference between the yield stress and the ultimate tensile stress. Mammoet requires high quality steel in comparison to the European standards (EN10025). Therefore the material specifications are different at some parts. Common used steel grades with their Mammoet specifications are listed in Table 3-1.

Steel grade	Thickness t [ mm ]	Minimum yield stress $f_y$ [ N/mm <sup>2</sup> ]	Minimum ultimate tensile stress $f_t$ [ N/mm <sup>2</sup> ]	Maximum Ratio $f_y/f_t$ [ - ]	Strain at failure [ % ]
<b>S355</b>	$t \leq 63$	355	510	0.87	22
	$63 < t \leq 150$	325	470	0.87	20
	$150 < t$	300	450	0.87	18
<b>S690</b>	$t \leq 50$	690	770	0.95	15
	$50 < t \leq 100$	690	770	0.95	15
	$100 < t$	650	760	0.95	15
<b>S960</b>	$t \leq 50$	960	980	0.97	12

**Table 3-1: Material properties according to Mammoet**

Since higher steel grades have a higher yield stress and a higher ultimate tensile stress it is hard to give a conclusion just comparing the capacities. All standards provide a similar increase of capacities in Chart 3-12.

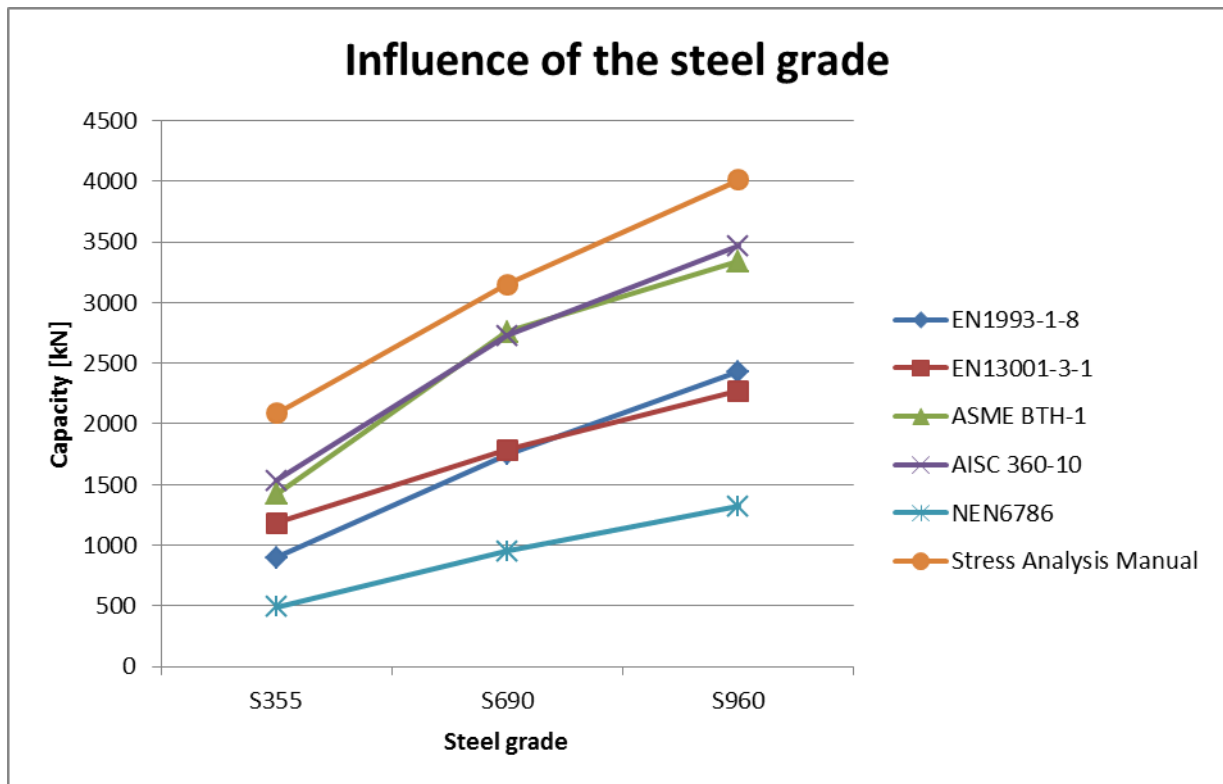


**Chart 3-12: Influence of the steel grade**

To provide a conclusion the capacities are compared with the capacities of steel grade S690. The relative capacity is calculated as follows:

$$Relative\ strength = \frac{Strength\ S###}{Strength\ S690} * \frac{690}{###} \quad (3-4)$$

In which ### is 355 for steel grade S355, and ### is 960 for steel grade S960.

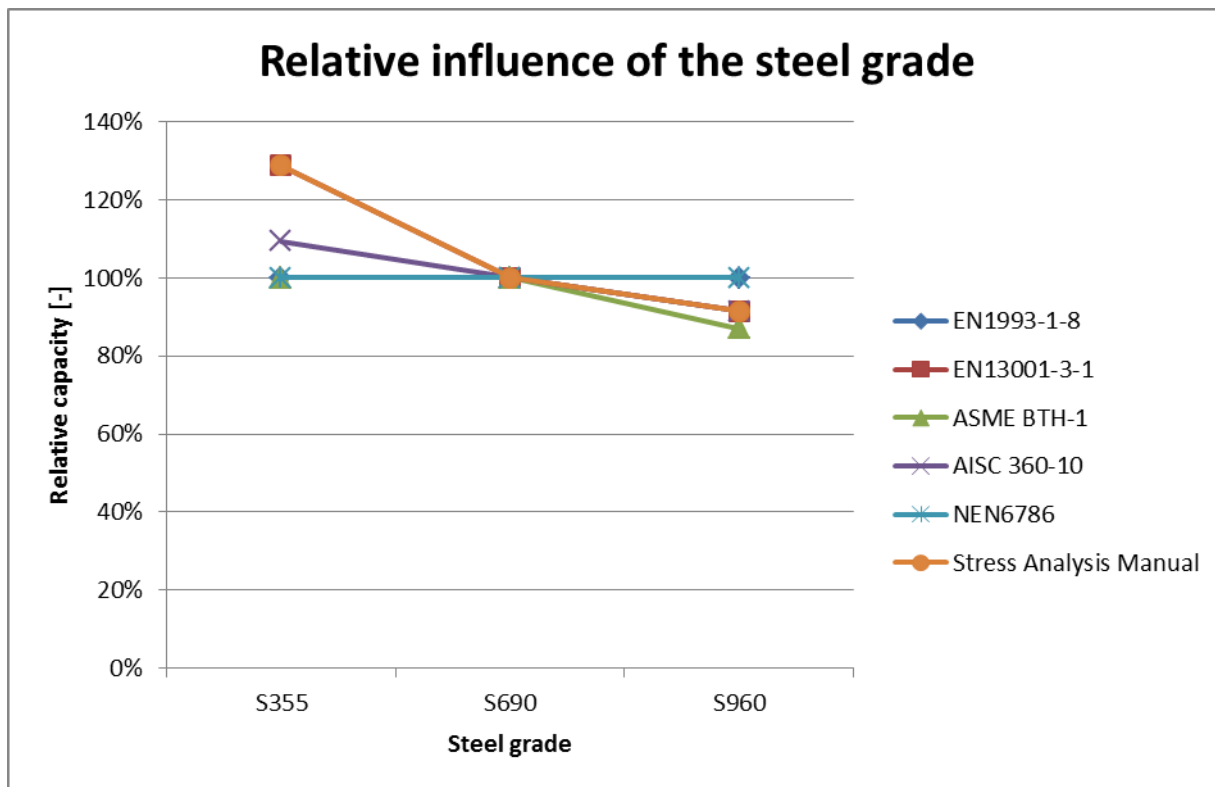


Chart 3-13: Relative influence of the steel grade

From Chart 3-13 can be concluded that an increase of the steel grade gives relative lower capacities in compare to their yield stress. In Chart C-31 to Chart C-40 all capacities and relative capacities for all failure criteria are plotted. From these charts can be observed that for an increasing steel grade:

- The ASME BTH-1 has the highest decrease in relative capacity for tension in the net section
- The EN1993-1-8 has an increase in relative capacity for bearing between steel grade S355 and S690

### 3.2.5 Influence of load angle and tapered eyes

Only the Stress Analysis Manual and the NEN6786 include the effect of different load angles and the Stress Analysis Manual is the only standard which includes the effect of tapered eyes. For clarity are the load angle and eye angle shown in Figure 3-5.

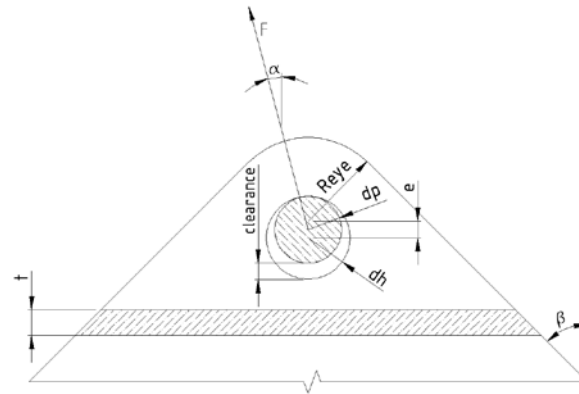


Figure 3-5: Tapered eye geometry with different load angles

From Chart 3-14 and Chart 3-15 the following can be observed for an increasing load angle:

- The NEN6786 provides a linear decrease to the capacity for perpendicular loads
- A load angle of 60° instead of 90° is critical for the Stress Analysis Manual
- Tapered eyes has only influence for oblique loads and the influence is the highest for perpendicular loads
- For 45° tapered eyes the perpendicular capacity is higher than the parallel capacity

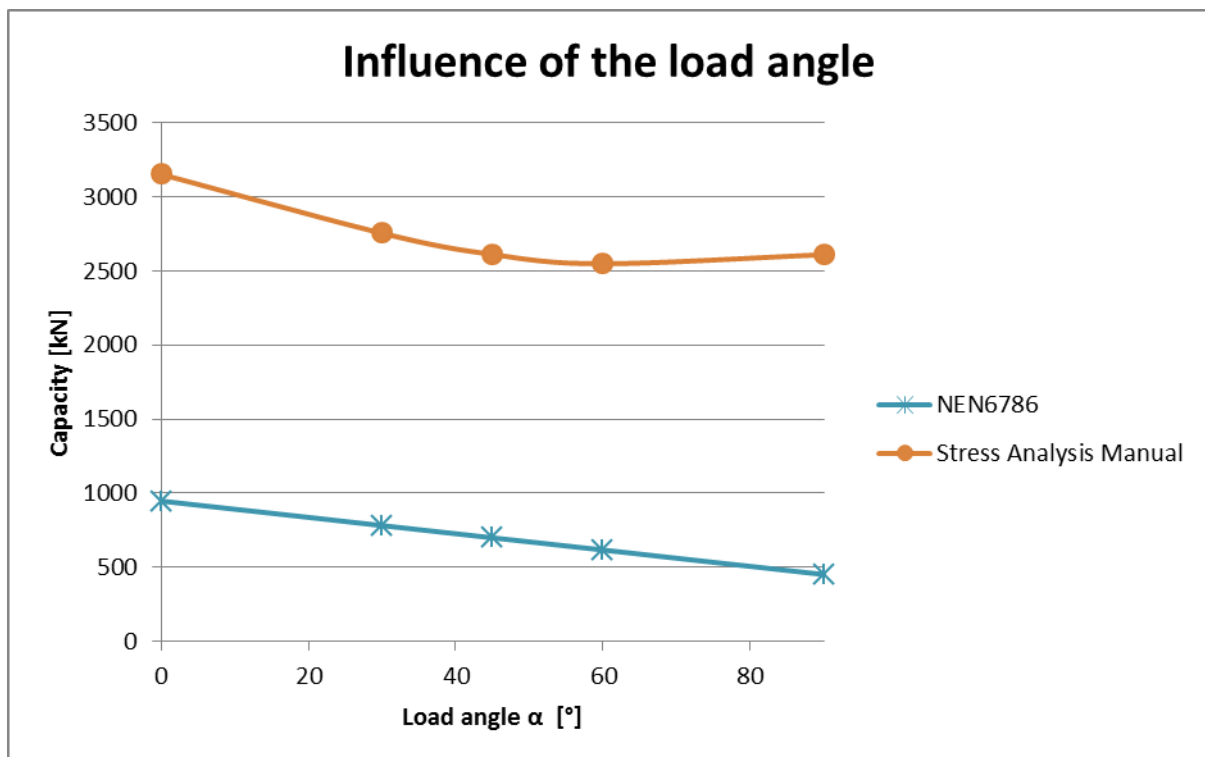


Chart 3-14: Influence of the load angle

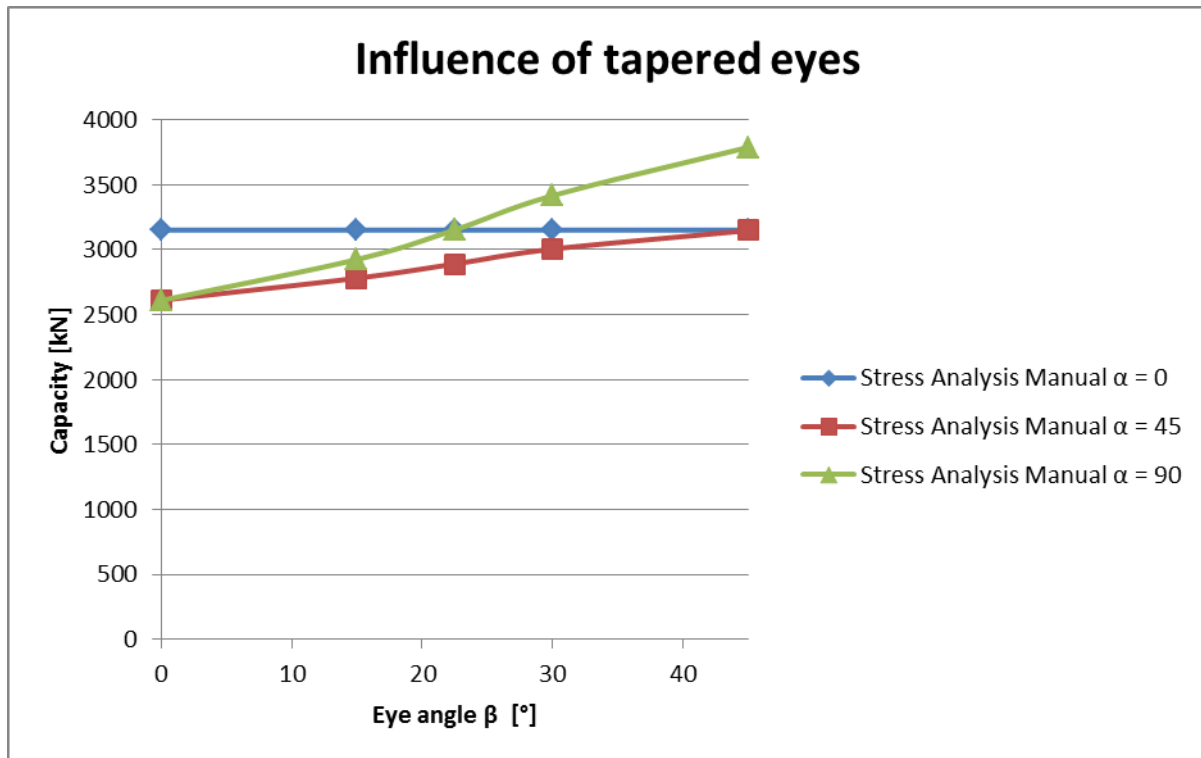


Chart 3-15: Influence of tapered eyes

### 3.3 Design factor influences

There is a difference between the required design factors between the compared standards. In each standard other factors are applied, like load factors, material factors or safety factors.

From paragraph 3.2 can be concluded that for most designs, the American standards provide higher capacities than the European standards. This is because the standards have different backgrounds. In some standards the capacities are based on fully plastic behavior, while others are based on elastic behavior. The difference between the standards could be reduced if all design factors are included. All design factors are listed in Table 3-2.

Standard	Applied factor
EN1993-1-8	<ul style="list-style-type: none"> <li>• Load factor = 1.5</li> <li>• Material factor = 1.0</li> <li>• For the bearing capacity according to ( B-114 ) the load factor = 1.5</li> <li>• For the bearing capacity according to ( B-115 ) the load factor = 1.0</li> </ul>
EN13001-3-1	<ul style="list-style-type: none"> <li>• Load factor = 1.5</li> <li>• General resistance factor = 1.1</li> </ul>
ASME BTH-1	<ul style="list-style-type: none"> <li>• Design factor = 2.4</li> <li>• Design factor for bearing = 2.0</li> </ul>
AISC 360-10	<ul style="list-style-type: none"> <li>• Load resistance factor design (LRFD) = 1/0.75 <ul style="list-style-type: none"> <li>◦ Load factor = 1.5</li> </ul> </li> <li>• Allowable stress factor (ASD) = 2.0 <ul style="list-style-type: none"> <li>◦ Load factor = 1.0</li> </ul> </li> </ul>
NEN6786	<ul style="list-style-type: none"> <li>• Load factor = 1.5</li> <li>• Material factor = 1.2</li> <li>• Material factor = 1.0 for shear and bearing</li> </ul>
Stress Analysis Manual	<ul style="list-style-type: none"> <li>• Load factor = 2.0 (assumed)</li> <li>• Material factor = 1.0</li> </ul>

**Table 3-2: Load, material and design factors**

To incorporate all factors the original capacities are reduced by the design factors, see equation ( 3-5 ) in which  $\gamma$  is the applied load, material or safety factor<sup>5</sup>. Capacity is the capacity without design factors and Capacity  $\gamma$  is the capacity including the design factors.

$$Capacity \gamma = \frac{Capacity}{\gamma} \quad (3-5)$$

In Chart C-43 to Chart C-69 all design capacities incorporating the design factors are plotted. Comparing these results with the results plotted in Chart C-16 to Chart C-42 the following can be concluded:

- All capacities including the design factors are lower
- The difference between the European and the American standards are reduced
- The difference between all standards is not greatly reduced
- The AISC 360-10 provides general the highest capacities

In Chart C-70 to Chart C-77 the variances between the standards are plotted. The solid graphs are without the design factor influences. The dashed graphs include the design factors. All variances are plotted including and excluding the NEN6786 standard because this standard provides very conservative capacities, and has therefore a big influence on the variance. From Chart C-70 to Chart C-77 the following can be concluded:

<sup>5</sup> Load factor, material factor and safety factor are named design factors in this report.

- For some designs and failure criteria there is a great reduction of variance due to the influence of design factors. For some other designs and failure criteria the variance has increased due to the influence of design factors.
- The variance of the capacities is reduced due to the influence of design factors.
- The variances for tension in the net section, fracture beyond the hole and the overall capacities are greatly reduced if the NEN6786 standard is excluded. Nevertheless for some designs the variances are still quite large.

### 3.4 Conclusion/ Recommendation

In paragraph 3.2 and 3.3 a lot of comparisons are made. Several effects and differences are observed. Most interesting and remarkable results are discussed in this paragraph.

#### 3.4.1 Remarkable results

- NEN6786 provides very conservative capacities
  - For almost all designs the NEN6786 provides the lowest capacities. The NEN6786 is a standard for movable bridges. There are general a lot of stress fluctuations in movable bridges. This is mainly due to traffic and opening and closing operations. Fatigue reduces the capacity for an increasing amount of stress fluctuations. In the NEN6786 this effect is already included in the capacity calculations.
- EN1993-1-8 is very sensitive for parameter influences (capacity may be reduced to 0)
  - In the EN1993-1-8 design restrictions are given for the eyes in pinned connections. From these design restrictions the capacity in the net section and the capacity for fracture beyond the hole are derived. These design restrictions are to provide economical connections, in which the use of material is quite effective. To derive capacities from design restrictions might be wrong since the effect of the parameters is too high. These design restrictions should be keep in mind for economical connections. The effect of clearance in the bearing capacity is quite large for clearances higher than 5mm. For high clearances the bearing stress is calculated likewise the theory of Hertz. This is based on elastic stress distributions and definitely doesn't mean failure. Small plastic deformations are reducing the bearing stress. If no plastic deformations are allowable than this bearing capacity can be governing.
- The AISC provides the highest capacities
  - The AISC standard includes design restrictions. Since all these restrictions are not completely fulfilled the capacity might be too progressive. A FEM study should prove this.
- The design factor influences are not reducing the variances between the standards
  - For some failure criteria the standards provide quite similar results. If the design factors are incorporated all variances are reduced, for some designs considerably. For small eccentricities, eye radiuses and for high clearances the variances are quite large. A FEM study should give more knowledge on these criteria. For small clearances, great eccentricities and eye radiuses the variances are relatively small but still around 25%.

#### 3.4.2 Lack of information and recommendation

In none of the compared methods the use of cheek plates are included. The ASME BTH-1 recommends a study on the use of cheek plates. The effect of different thicknesses of the eye and the thicknesses of the cheek plates should be studied.

---

Only the NEN6786 and the Stress Analysis Manual include the effect of different load angles and tapered eyes. A FEM study should point out if these effects give considerable differences in compare to straight eyes and loads.

There are still quite some variances for the failure criteria tension in the net section. The effect of clearance is not included in all standards. Comparing to different analytical methods, the load introductions influences the stress concentration factors. Therefore the clearance effect should be studied. In this study the bearing stresses or plastic deformations should be studied too.

## 4 FEM modeling

### 4.1 Introduction

The Finite Element Method (FEM) divides a structure into a finite amount of parts, named elements. If analytical methods are not sufficient a FEM analysis should be done. Advantage of this method is that more complex structures and shapes can be analyzed like Figure 4-1.

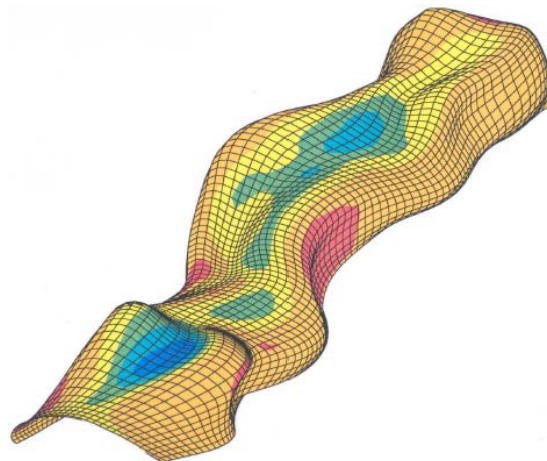


Figure 4-1: Complex shape structure<sup>6</sup>

The positions of engineers, analysts and designers are changed since FEM programs developed to a common practice. The modeling of structures is an important part. Wrong modeling can cause errors and good and smart models can save computing time. But not only modeling is important. Interpretation of the results is also not straightforward. Experience and understanding the model helps the engineer to provide good conclusions of the results.

Before running an analysis several assumptions and choices have to be made to make a good model. Experience with FEM programs involves the capability of making good assumptions and choices.

From chapter 3 can be concluded that there are still a lot of differences between analytical and empirical methods but also different standards provide different capacities for most designs. A pinned connection may be less complex than a structure like Figure 4-1. Nevertheless FEM analysis of pinned connections should provide sufficient results. In this chapter choices and assumptions for FEM modeling and FEM interpretation are discussed. The FEM modelling is done with the program ANSYS [21].

<sup>6</sup> CIE5148 Computational Modeling

## 4.2 Geometry

First the geometry of the pinned connection is determined. The shape and geometry of the pinned connection is different for each design. It is possible to model the pinned connection in 2D or in 3D. 2D modeling has an advantage that there is general only one node over the thickness, so fewer nodes are modelled in compare to 3D modeling in which more nodes over the thickness are modelled. The amount of Degrees Of Freedom (DOF) is a significant factor for the computational time. Choosing between a 2D and 3D model depends on what input and what kind of output is of interesting. If the bending of the pin and out of plane bending of the eye are neglected, a 2D model is sufficient for geometries like Figure 1-1, since there are only in plane stresses. If cheek plates are applied a 3D model is used because in this case the thickness effects are interesting.

To make use of symmetry the amount of nodes and so the computation time can be reduced. In Figure 4-2 to Figure 4-4 the VonMises stresses ( $S_{eqv}$ ) are plotted for the 2D symmetric and non-symmetric model and for the 3D symmetric model. These stresses are based on reference eye 1 (see paragraph 3.1).

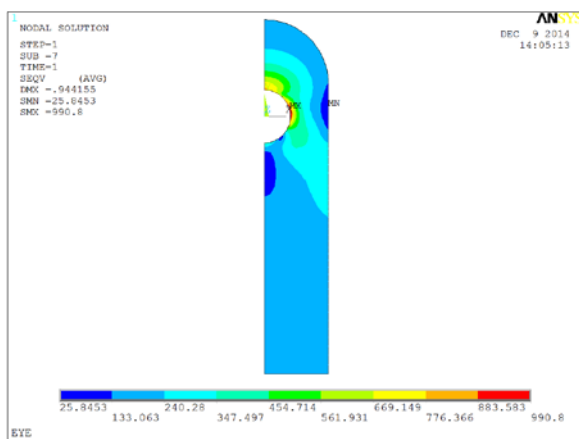


Figure 4-2: 2D  $S_{eqv}$

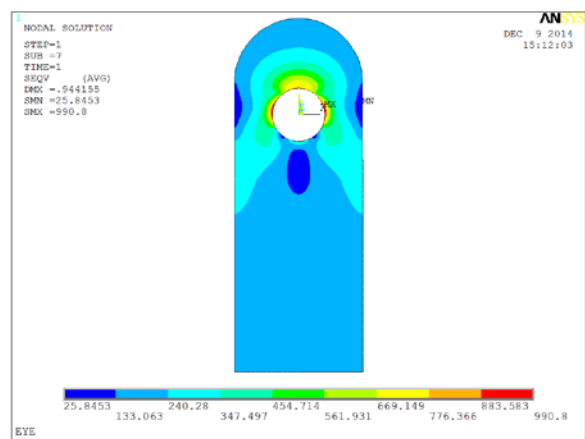


Figure 4-3: 2D Non-symmetric  $S_{eqv}$

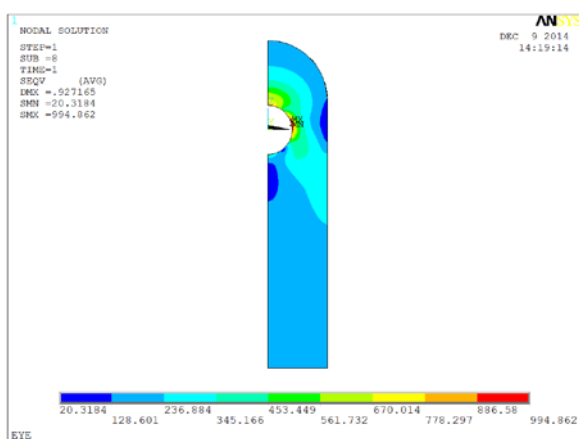


Figure 4-4: 3D  $S_{eqv}$

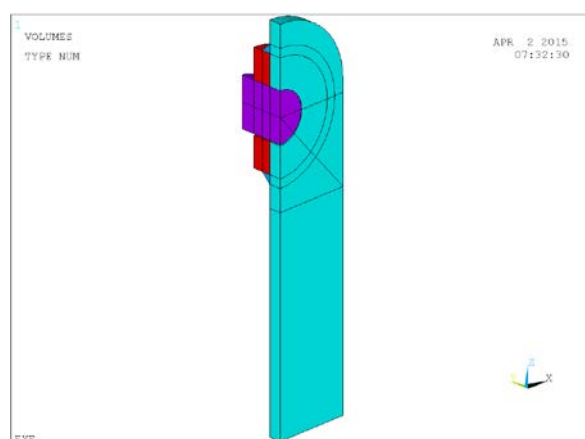


Figure 4-5: Double symmetry if cheekplates are applied

From these models can be shown that the results are quite similar. If the boundary conditions are good applied the results are exact similar in case of symmetry or not. A 3D model provides more or less similar results, but the computation time is much higher for the same element sizes. In case of different load angles symmetry can't be used anymore since the connection is not symmetric due to

the non-symmetric load. For 3D models with cheekplates it is possible to use 2 symmetry planes to save computation time, see Figure 4-5.

## 4.3 Mesh

When the geometry is modelled the FEM program has to divide the geometry into a finite amount of parts, named elements. Each element consists of nodes which have to be in equilibrium. With numerical calculations the equilibrium equations can be derived for all kind of models and solved with numerical iterative methods for all shapes and types of elements.

### 4.3.1 Element type

There are different types of elements which can be modelled, see Figure 4-6. Different properties determine the finite element. Some main properties are listed below:

- Dimension of the shape
  - 0D point mass, 1D straight line, 2D flat shell, 3D curved shell, 3D brick
- Topological dimension
  - 0D point, 1D straight or curved line, 2D quadrilateral or triangle, 3D brick or tetrahedron
- Displacement, strain and stress field
  - Plane strain, plane stress, axial stress, compression and/or tension
- Interpolation of the displacements
  - Linear, quadratic or cubic elements
- Degrees of freedom
  - Displacement directions, rotations
- Solving
  - Full or reduced integration

If geometry of the pinned connection is 3D orientated, 3D shaped elements are needed. Meshes of tetrahedrons are easy to mesh, but tetrahedrons have some disadvantages. These elements are more prone to locking and the elements are generally not orientated in straight lines. Since the geometries are quite simple, the geometry can also be meshed with brick elements. In case of a 3D geometry, brick elements are used. Linear or quadratic brick elements are favorable. Quadratic bricks have 20 nodes per element, while linear bricks have only 8 nodes per element. The accuracy of quadratic elements is generally higher, but the computational costs are higher too. The use of quadratic elements depends on the element size.

If the geometry of the pinned connection is 2D orientated, 2D shaped elements are needed. Likewise for 3D elements, quadrilateral elements are preferred and the order (linear or quadratic) of the element depends on the element size. There are a lot of different elements which are 2D. For a pinned connection two element types are compared:

- 2D plane stress elements allow only stresses in the plane of the element
- Shell elements which include bending of the elements.

Since the geometry is general 2D, and bending of the eye is not of interest (out of plane bending is neglected), 2D plane stress elements are preferred since they have only 2 DOF's per node, and shell elements have 5 or 6 DOF's per node. Another disadvantage of shell elements is that the contact between the pin and the hole is hard to model, since the pin and the eye may "slide" behind each other.

### 4.3.2 Numerical integration

Ansys provides for each element a set of options, named key options. One of these options is the (numerical) integration method, see Figure 4-6. With numerical integration the stiffness matrix of the model is calculated. In certain configurations elements may react to stiff, this is called locking. This is due to the mathematical FEM background. General for (nearly) incompressible materials and for (pure) bending models the reduced integration methods have to be used. For the pinned connections modelled in this report full integration methods are preferred since locking should not occur.

Type of elements which are compared:

- PLANE182: Linear 2D continuum plane stress element. A selective reduced integration method is default to prevent volumetric locking. Since shear locking should not occur, the default integration method is used (KEYOPT 1 = 0).
- PLANE183: Quadratic 2D continuum plane stress element. For higher order elements the default integration method is uniform reduced integration. For PLANE183 elements this is the only integration method which can be chosen.
- SHELL181: Linear 2D shell element. Uniform reduced integration is the default integration method. The use of full integration is limited, for example in out of plane bending problems this can provide errors. For this report the full integration method (KEYOPT 3 = 2) is used, since out of plane bending is not occurring. Shell elements are integrated using 1 to 9 integration points over the thickness. Since out of plane bending does not occur, the default 3 integration points over the thickness are sufficient.
- SHELL281: Quadratic 2D shell element. This element is uniform reduced integrated, with four integration points. This is the default and only option.
- SOLID185: Linear 3D continuum element. This element is fully integrated by default and this is for pinned connections sufficient (KEYOPT 2 = 0).
- SOLID186: Quadratic 2D continuum element. For higher order elements the default integration method is uniform reduced integration. SOLID186 elements provide an option for full integration and this is sufficient (KEYOPT 2 = 1).

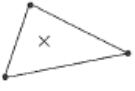
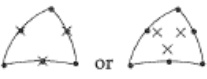
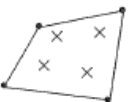
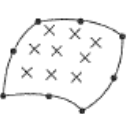
element		integration scheme
two-node bar		1
three-node bar		2
three-node triangle (T3)		1
six-node triangle (T6)		3
four-node quadrilateral (Q4)		2 x 2
eight-node quadrilateral (Q8)		3 x 3

Figure 4-6: Recommended integration schemes for commonly used elements<sup>7</sup>

<sup>7</sup> The Finite Element Method: An Introduction by Dr. Garth N. Wells, Table 4.3

### 4.3.3 Pin-hole contact

The contact between the pin and the hole can be modelled with contact elements. Ansys can model a contact by using contact and target elements. For pinned connections the contact elements are attached to the eye and the target elements are attached to the pin. When the contact surface penetrates the target surface, a surface pressure is generated by the contact stiffness. Analysis of models with contact and target elements is an iterative process, since the contact area and the surface pressure depends on the deformations of the model. Therefore the use of contact elements may increase the number of iterations and therefore the computation time. In Figure 4-7 the contact is plotted between the pin and the hole. Only the elements on the edge are plotted. In Figure 4-8 the whole mesh is plotted.

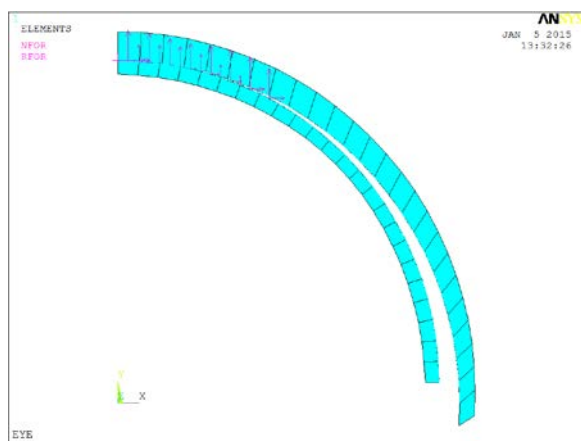


Figure 4-7: Contact reactions between the pin and the hole

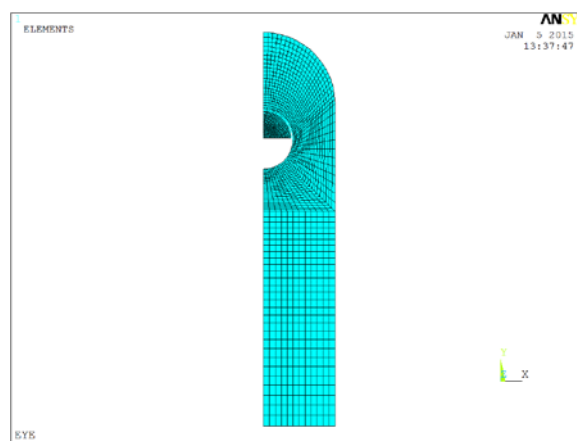


Figure 4-8: Mesh plot using contact elements

Contact elements can be avoided using a holespar. A holespar is a set of elements which connects the center of the hole with the nodes on the edge of the hole. These elements are modelled with compression only 1D elements to model contact behavior. If a holespar is modelled, the computation time is reduced since compression only elements are much simpler than contact and target elements. A disadvantage of the holespar is that a clearance between the pin and the eye is neglected. So only for very small clearances a holespar might be an option.

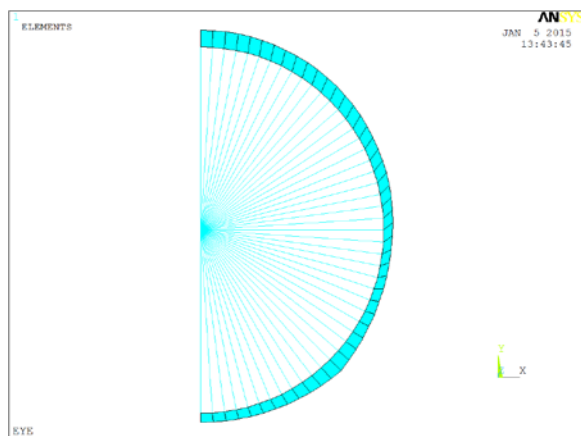


Figure 4-9: holespar model

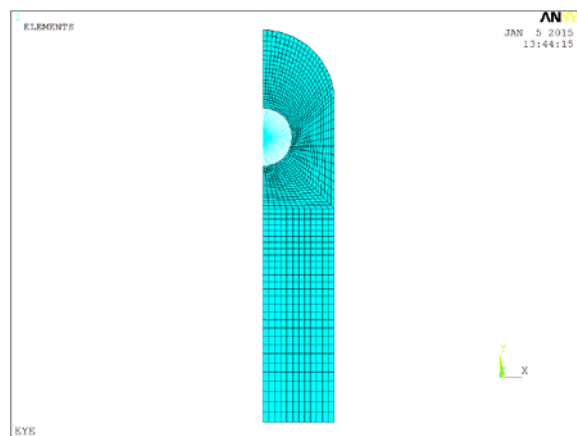


Figure 4-10: Mesh plot using a holespar

### 4.3.4 Element size

Not only the type of elements has influence on the results, the size of elements influences the results as well. The error of the results is general smaller for smaller step sizes. Smaller step sizes means for a FEM analysis smaller elements. The number of elements, nodes and degrees of freedom is larger for smaller elements and so is the computation time. In Figure 4-11 and Figure 4-12 the difference between a rough mesh and a fine mesh is shown.

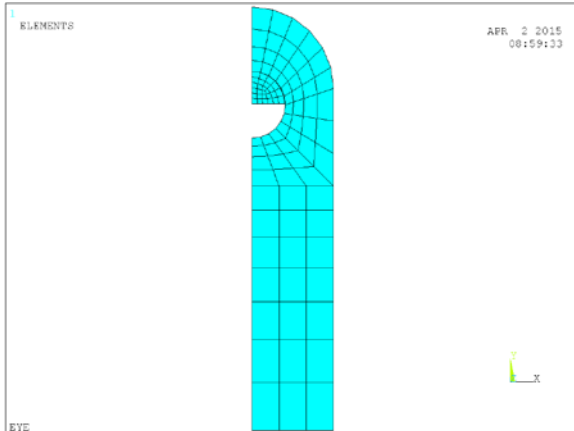


Figure 4-11: Rough mesh

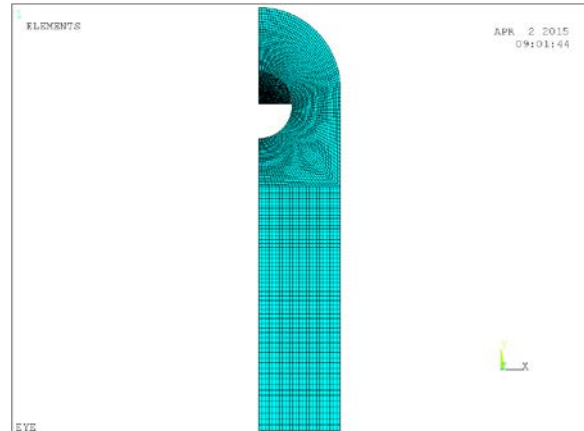


Figure 4-12: Fine mesh

### 4.3.5 Conclusion

In the paragraphs above all different kind of FEM model options are discussed. It is obvious that those options have influence on the results and the computation time. In Table D-1 and Table D-2 the results of different FEM model options are listed. The reference model is with contact/target elements, quadratic brick elements with full numerical integration. In Table D-1 bending of the pin is neglected, while in Table D-2 bending of the pin is included.

If bending of the pin is neglected the following FEM models provide similar results as the reference model:

- Holespar and linear shell elements
- Contact/target and quadratic quadrilateral elements

As already mentioned a model which uses a holespar instead of contact elements neglects the clearance between the pin and the eye. For small clearances the difference between the holespar model and the reference model are small but if the clearance increases, the difference and so the error is quite large, see Chart 4-1. In Chart D-1 the difference between the holespar model and a 3D model including the clearance is plotted for different stress directions. From this chart can be concluded that for some stress directions the clearance has a larger effect than others. This is because only the maximum and minimal values of stress directions are plotted. All differences are dependent on the clearance. At Mammoet a very small clearance (<0.5mm) is not useful because assembling and fitting of components is a common done operation, and is not easy to do with narrow fitting pins. Therefore a model with contact/target and quadratic quadrilateral elements is preferred.

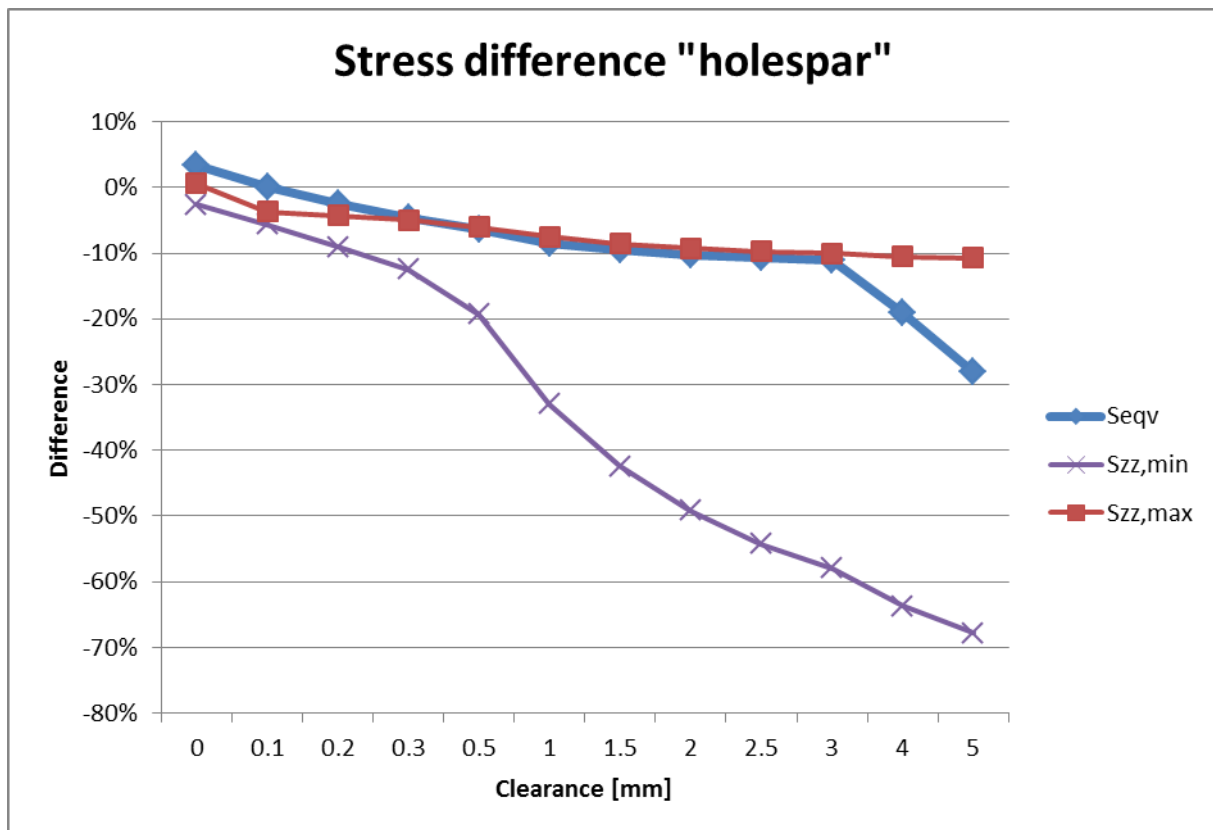


Chart 4-1: Clearance influence<sup>8</sup>

If bending of the pin is included none of the 2D models provide similar results as the reference model. Only the 3D models which include bending provide similar results, but in that case the computation time is not much reduced.

In Table D-3 and Table D-4 all analysis results of different element types and element sizes are listed. If bending of the pin is neglected PLANE183 elements with a relative scale of 1<sup>9</sup>, or SOLID186 elements with a relative scale of 0.5 are preferred. If bending is included SOLID185 elements with a relative scale of 1 or SOLID186 elements with a relative scale of 0.5 are preferred for models which include bending.

In Table D-5 the differences between bending and no bending are listed for different stress directions. From this can be concluded that bending has most influence on the bearing stress ( $S_{zz,min}$  and  $S_{xx,min}$ ), but for other stress directions the difference are smaller but not negligible.

#### 4.4 Analysis types

Not only the geometry and the mesh determine the results of a FEM model. Analysis type to solve the model is important. In contact modeling a geometric non-linear analysis is already required since the stiffness of the contact depends on the displacements. A physical non-linear analysis can include

<sup>8</sup> Note that for small clearances, the VonMises stress ( $S_{eqv}$ ) in the net section is critical, but when the clearance increases, the VonMises stress for bearing becomes critical.  $S_{zz,min}$  is approximately the bearing stress and  $S_{zz,max}$  is approximately the stress in the net section.

<sup>9</sup> Relative scale of 1 is equal to 96 elements over the hole diameter (48 over the half hole diameter due to symmetry).

plasticity of the material. A physical non-linear analysis is general not preferred since the computing time is increased and plasticity is not desirable at Mammoet.

If a linear analysis is done, peak stresses will occur. Peak stresses which are (much) higher than the yield stress can occur in a physical linear analysis. These stresses are not occurring in the real connection since plasticity will redistribute these peak stresses. Therefore peak stresses are general neglected at Mammoet, and only the area of plasticity (where the stresses are higher than the yield stress) is considered. Interpretation of the plastic area is not straightforward but is based on experience and engineering knowledge.

To provide any conclusions about pinned connections and make fair comparisons for all kind of geometries, straight forward checks have to be determined.

#### 4.4.1 Elastic analysis

In an elastic analysis, the stiffness of the material is constant. Different theories are developed to predict failure. Most theories are based on the assumption that failure occurs when a physical variable such as stress, strain or energy reaches a limiting value. These physical variables are a combination of principle variables, like the principle stresses.

There are different failure criteria which check a stress combination with the yield stress, yield strain or yield energy:

- Rankine

$$f_c \leq \sigma_1, \sigma_2, \sigma_3 \leq f_t \quad (4-1)$$

- Saint Venant

$$-\varepsilon_f \leq \varepsilon_1, \varepsilon_2, \varepsilon_3 \leq \varepsilon_f \quad (4-2)$$

$$\varepsilon_f = \frac{1}{E} * (\sigma_1 - \nu(\sigma_2 - \sigma_3)) \quad (4-3)$$

- Tresca

$$\max(|\sigma_1 - \sigma_2|, |\sigma_1 - \sigma_3|, |\sigma_2 - \sigma_3|) \leq f_y \quad (4-4)$$

- Beltrani

$$\sigma_1^2 + \sigma_2^2 + \sigma_3^2 - 2 * \nu(\sigma_1 * \sigma_2 + \sigma_1 * \sigma_3 + \sigma_2 * \sigma_3) \leq f_y^2 \quad (4-5)$$

- VonMises

$$\sqrt{\frac{1}{2} [(\sigma_1 - \sigma_2)^2 + (\sigma_1 - \sigma_3)^2 + (\sigma_2 - \sigma_3)^2]} \leq f_y \quad (4-6)$$

The VonMises criterion is most used for steel designs, and from experiments this criterion seems to fit well with construction steel<sup>10</sup>.

A disadvantage of a physical linear analysis is that it limits the design load due to peak stresses. If the peak stresses are limited to the yield stress a linear analysis provides a good elastic stress field for pinned connections, but the capacities are quite conservative and even lower than the standards.

---

<sup>10</sup> [http://uetmmmsk.weebly.com/uploads/3/6/0/0/3600114/theories\\_of\\_elastic\\_failure.pdf](http://uetmmmsk.weebly.com/uploads/3/6/0/0/3600114/theories_of_elastic_failure.pdf)

Allowing some peak stresses increases the capacity of pinned connections but no clear information about the magnitude of the peak stresses is available. Therefore a plastic analysis is preferred.

#### 4.4.2 Plastic analysis

In a plastic analysis there is a decreased stiffness of the material above the yield stress. A typical stress-strain diagram is shown in Figure 4-13.

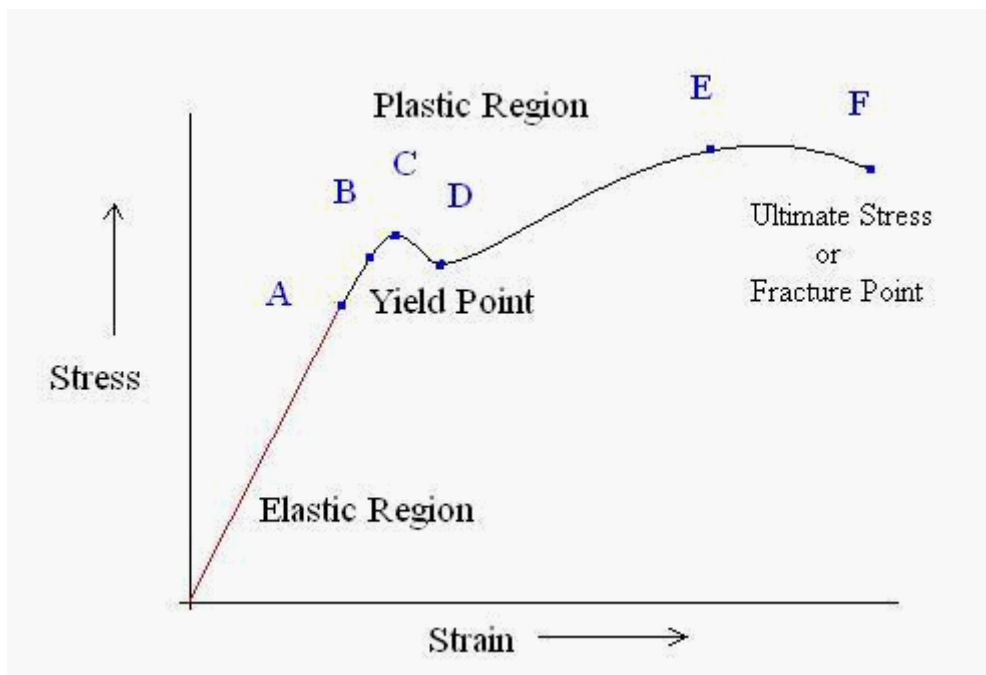


Figure 4-13: Typical Stress-Strain diagram<sup>11</sup>

As opposed to elastic behavior (the Young's modulus is for all steel grades about 210000Mpa), the plastic behavior is more various. Tensile tests of specimens provide more detailed information about plastic behavior and stress-strain diagrams like Figure 4-13.

At Mammoet pinned connections are not loaded until failure, and plastic deformations are not preferable. Prohibit plastic deformations results in conservative capacities, even lower than the standards. Therefore some plasticity is allowed. There are no strict regulations about allowing plasticity in FEM analysis. The EN1993-1-5 Annex C [22] allows 5% plastic strains in the principle directions, but for Mammoet this magnitude of strains and therefore permanent deformations is non desirable.

In EN1993-1-5 different stress-strain curves are recommended. Only the shape of a "true stress-strain curve" is dependent on the steel grade. A disadvantage of this curve is that these are only applicable if the material is tested which is not the case.

Mammoet makes use of different steel grades with different hardening behavior. To incorporate plasticity a bi-linear stress strain behavior is modelled like Figure 4-14. The plastic stiffness is simplified to  $E_2$  which is calculated according equation ( 4-7 ).

$$E_2 = \frac{f_t - f_y}{\epsilon_t - \epsilon_f} \tag{4-7}$$

<sup>11</sup> <http://www.keytometals.com/page.aspx?ID=CheckArticle&site=kts&NM=280> (Figure 1)

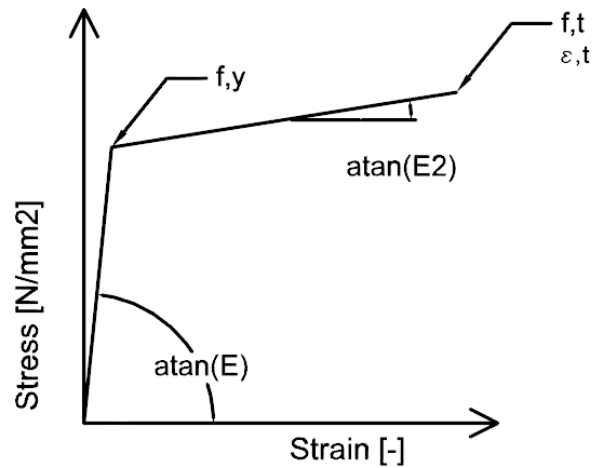


Figure 4-14: Bilinear Stress-Strain behavior

This hardening stiffness is between curve b and c in Figure D-1, but is more precise since the yield stress, ultimate tensile stress and ultimate tensile strain are included.

### 4.4.3 Possible analysis methods

In this sub paragraph some analysis methods are considered but are finally not used in this report.

#### Stefanescu method

M. Dobrescu wrote a Master Thesis [23] about the influence of ductility in the design of (high strength) steel bridges. He developed a method named the Stefanescu Method. This is a method which describes the plastic behavior at stress concentrations.

For this method a linear material behavior is analyzed. Base of this method is that the area of the rectangles from  $\epsilon_{el} * \sigma_{el}$  are equal to the area of the rectangle from  $\epsilon_{pl} * \sigma_{pl}$ .

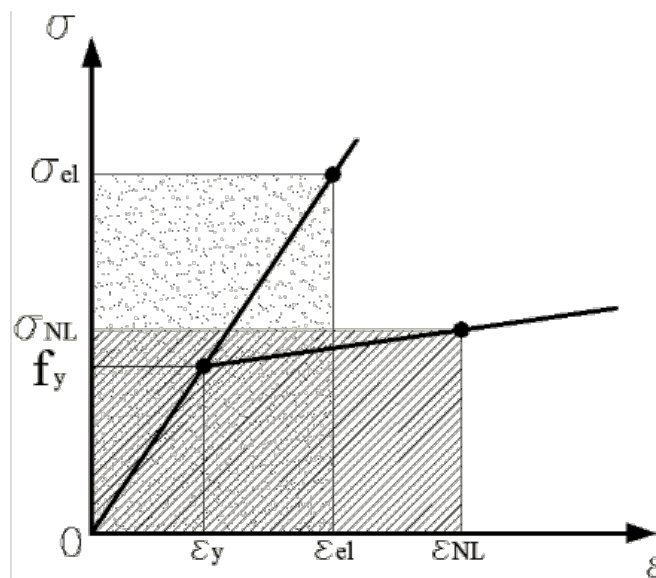


Figure 4-15: Graphical interpretation of the SM method ([23], Fig. 4.1)

With this method the plastic strains can be approximated doing a linear analysis.

Since a non-linear analysis is already needed to model the contact between the pin and the hole, and therefore plasticity is not increasing the computation time that much the Stefanescu method is not used. The linear peak stresses are much depending on the model and therefore not so precise.

### Lemaitre criterion

Ductile failure can occur when the plastic strains become too large. This maximum plastic strain is considered as failure criterion. The maximum allowable plastic strain depends on the material and the stress state (combination of tensile and shear stresses). Lemaitre developed a criterion which decent describes this maximum plastic strain depended on the material and the stress state. Failure occurs when the VonMises plastic strain exceeds the failure strain.

The failure strain is calculated as follows [24]

$$\varepsilon_f^* = \frac{\varepsilon_f}{\frac{2 + 2 * v}{3} + (3 - 6 * v) \left(\frac{\sigma_h}{\sigma_{eq}}\right)^2} \tag{4-8}$$

$$\varepsilon_f = \text{ultimate strain at failure in 1D orientation} \tag{4-9}$$

$$\sigma_h = 1/3 * (\sigma_1 + \sigma_2 + \sigma_3) \tag{4-10}$$

$$\sigma_{eq} = \text{VonMises Stress} \tag{4-11}$$

Lemaitre's failure criterion is visualized in Figure 4-16.

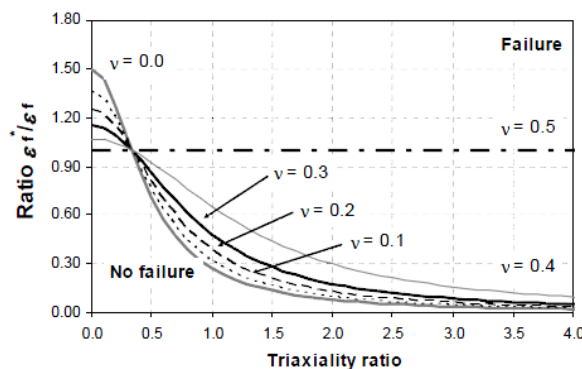


**Figure 4-16: Lemaitre criterion ( [24], Fig. 3)**

By introducing triaxiality, Lemaitres criterion gives a better prediction than a one-dimensional failure criterion. However, to calculate a decent failure load, a real stress-strain relationship should be modelled and a bilinear approximation is not sufficient. Since Mammoet doesn't prefer plasticity and failure is not expected, Lemaitres failure criterion is not used.

### Fatigue Analysis

Fatigue [25] is the mechanism whereby cracks grow in a structure. Growth only occurs under fluctuating stress. Final failure generally occurs in regions of tensile stress when the reduced cross-section becomes insufficient to carry the peak load without rupture. Whilst the loading on the structure is stationary the crack does not grow under normal service temperatures. For example cranes are subjected to fluctuating loads so they might be sensitive to fatigue.

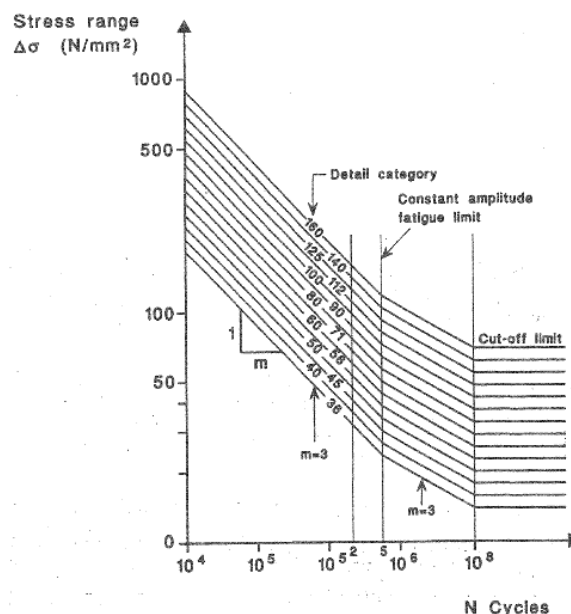


Figure 4-17: Family of design S-N curves ( [25], Lecture 1 Figure 7)

In Figure 4-17 some typical fatigue curves are plotted and it should be noted that these curves start  $10^4$  cycles. At Mammoet this amount of load cycles do generally not occur, and the loads are mostly lower than the capacity. For that reason a fatigue analysis is not included in this report. If fatigue is expected to be governing the conclusions of this report can be used to do a fatigue analysis.

## 4.5 Conclusion

If plasticity is modelled in a FEM analysis, the comparison of elastic stresses between the element types and models may be not useful anymore. With the recommended models (chosen in paragraph 4.3) a plastic analysis<sup>12</sup> is done, based on reference eye 1 without a clearance. These results are plotted in Chart 4-2. From Chart 4-2 can be concluded that the models provide more or less similar results at the plastic strains of 0%, 0.5%, 1%, 5% and 15%. Therefore the model with PLANE183 elements with a relative scale of 1 is recommended because this model includes the clearance effect and has the smallest computation time for precise enough results. The pin is also modelled with the same PLANE183 elements and is fixed in the middle of the section, so therefore only the quarter of the pin is modelled (bottom half is not modelled due to the boundary condition and the left half is not modelled due to symmetry).

<sup>12</sup> Note that only the eye includes plasticity. It is assumed that the pin is made of a higher steel grade than the eye, so yielding only occurs in the eye.

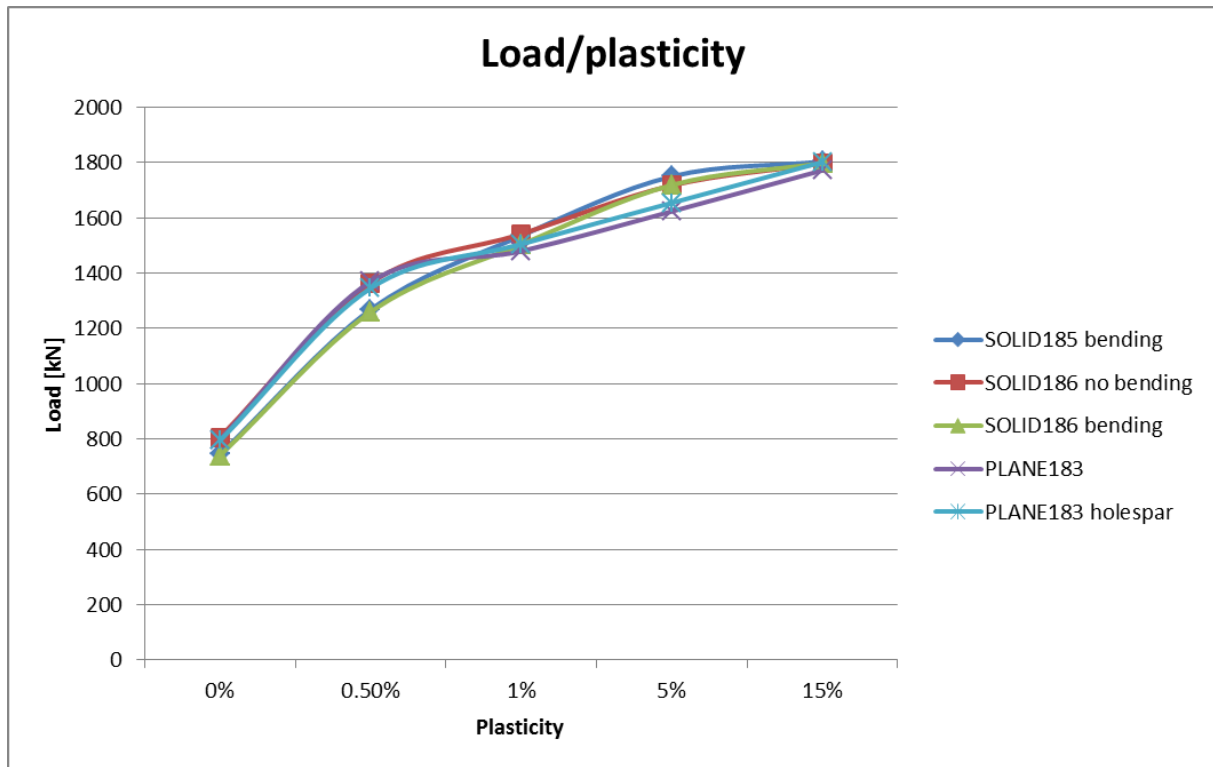


Chart 4-2: Model influences on plastic capacity



## 5 FEM analysis

The Finite Element Model is determined in chapter 4 and is used to analyze all type of pinned connections. There are different ways to study the pinned connections with a FEM program. Basically two different methods are considered.

- Analysis of the results based on the capacity of the standards
- Analysis of the loads based on certain results (stresses/strains)

A graphical interpretation of these methods is shown in Figure 5-1.

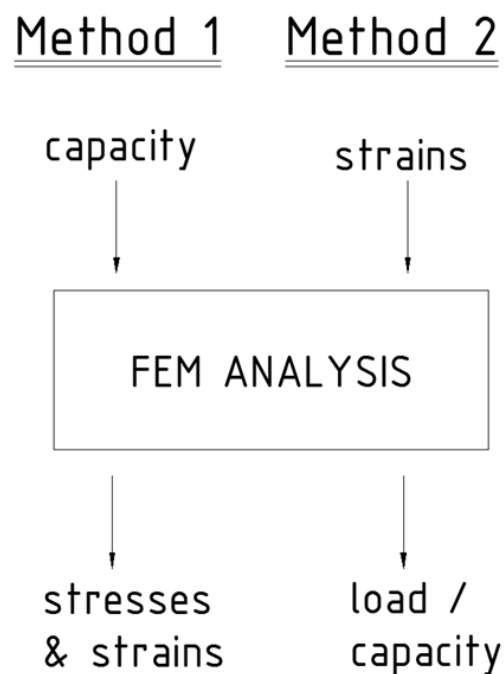


Figure 5-1: Graphical interpretation of the two FEM analysis methods

In paragraph 5.1 the results based on the capacities of the standards are described. The capacities are determined similar as in chapter 3 according to the standards. In paragraph 5.2 the analysis of the loads based on certain results is described.

## 5.1 Analysis of the results based on the capacities of the standards

There are two different capacities which can be used as input. An SLS load or an ULS load can be applied as input load on the FEM model. Both are considered since their difference in safety/load/design factors.

Similar as in chapter 3, the parameters are based on the reference eye 1 (paragraph 3.1). All pinned connections which are considered are made of S690 grade steel.

### 5.1.1 Influence of $R_{eye}$

The influence of  $R_{eye}$  is analyzed by varying the radius from 60mm to 160mm, see Figure 5-2 and Figure 5-3. This is done with and without (similar as reference eye 2) an eccentricity  $e$ .

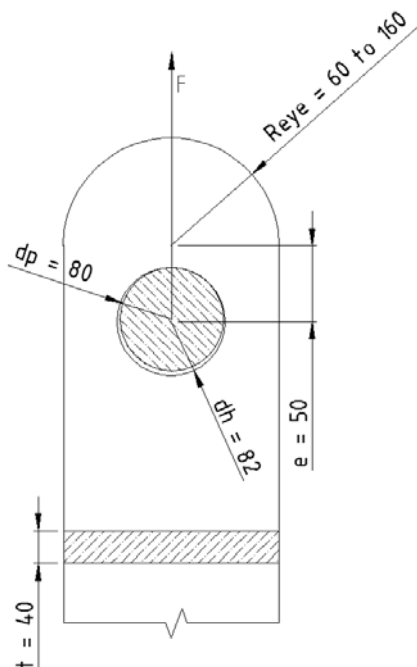


**Figure 5-2: Geometry with varying eye radius with an eccentricity**

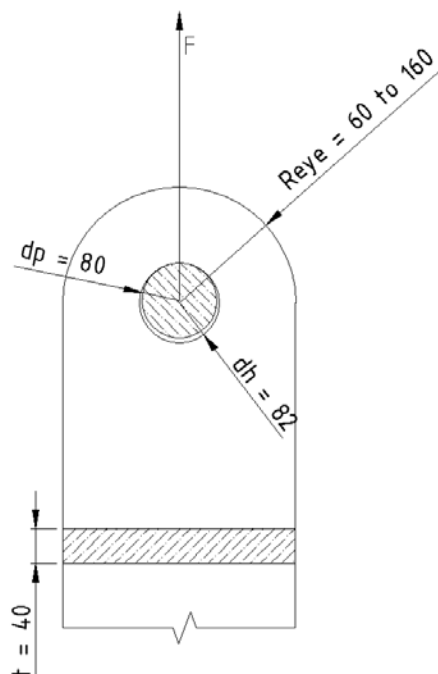


**Figure 5-3: Geometry with varying eye radius without an eccentricity**

From Chart E-1 to Chart E-3 can be concluded that the plastic strains are different not only for each standard, but for each eye radius too.

- Each standard has for certain geometry plastic strains in the net section under SLS loads
- The ASME BTH-1 ULS capacity is based on real empirical results of failure of the connection. Therefore ANSYS doesn't easily find a solution for the ULS load.
- The AISC 360-10 ULS capacities are for some geometry too high for ANSYS to find a solution.

### 5.1.2 Influence of the eccentricity

The influence of the eccentricity is studied by varying the eccentricity from -25mm to 50mm with an eye radius of 80mm and an eye radius of 100mm, see Figure 5-4.

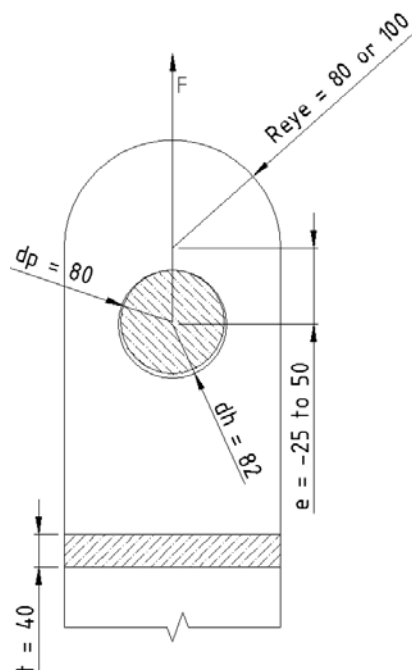


Figure 5-4: Geometries with a varying eccentricity

From Chart E-4 and Chart E-5 can be concluded that the eccentricity has an influence on the plastic strains in the net section although only the EN13001-3-1 standard includes this effect. For larger eccentricities the plastic strains in the net section are reduced. Even for the EN13001-3-1 standard which already includes the effect of the eccentricity.

The eccentricity has an influence for the fracture beyond the hole strains/stresses too. Each standard includes the effect of eccentricity for checking the fracture beyond the hole or for the shear criteria. Since the plastic shear strains are hardly notable (see Figure 5-14) by a FEM analysis, only the strains/stresses in the top of the eye are useful to compare with each other.

In Chart E-4 to Chart E-9 all stresses (or plastic strains if they occur) are plotted for different eccentricities, SLS and ULS loads as input, for an eye radius of 80mm and 100mm. From these charts can be concluded that all standards provide different stress/strains and the effect of different eccentricities is different for each standard. Only the EN1993-1-8 standard has a critical unity check for fracture beyond the hole and or shear for positive eccentricities. For the other standards this becomes critical only for negative eccentricities which are not used at Mammoet.

### 5.1.3 Influence of the clearance

The influence of the clearance is studied by varying the pin diameter from 62mm to 82mm. This means a varying clearance from 0mm to 20mm. This is done with a geometry based on reference eye 3, see Figure 5-5.

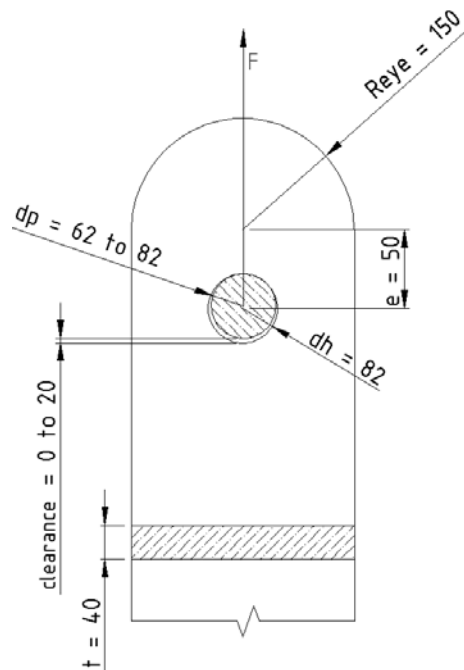


**Figure 5-5: Geometry with a varying clearance**

The influence of the clearance has most influence on the bearing stress/strain. For the chosen geometries in Figure 5-5 bearing is the governing criteria for all compared standards. In Chart E-10 and Chart E-11 the plastic bearing strains are plotted for different clearances. From these charts can be concluded that the plastic strains are increasing for larger clearances. Even for SLS loads there appear already quite large plastic strains (above 5%), although these strains are only present on a very small part of the connection (see Figure 5-6).

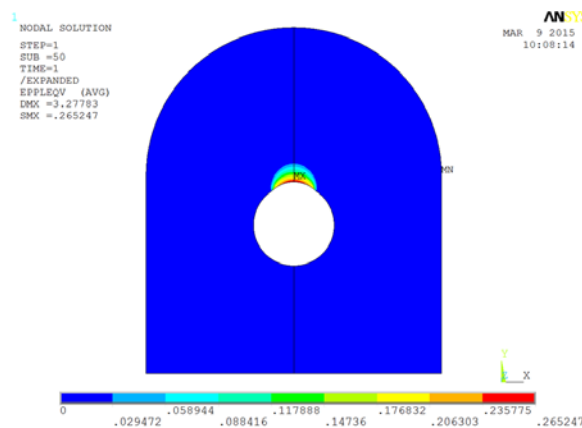


**Figure 5-6: Plastic bearing strains<sup>13</sup>**

All standards calculate the bearing capacity on a similar way. The load is distributed over an area which is equal to the pin diameter times the thickness. This stress may not exceed a certain value. The assumption of this “contact” area is quite rough because the contact area is also depended on the clearance between the pin and the hole.

<sup>13</sup> Note that symmetry in the model is applied, but for presentation reasons only the results are mirrored.

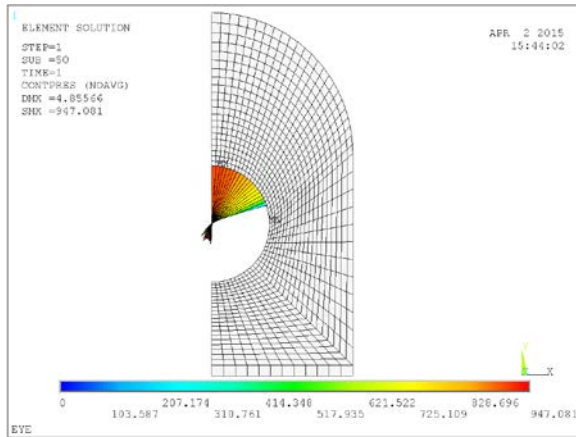


Figure 5-7: Contact pressure with a small clearance

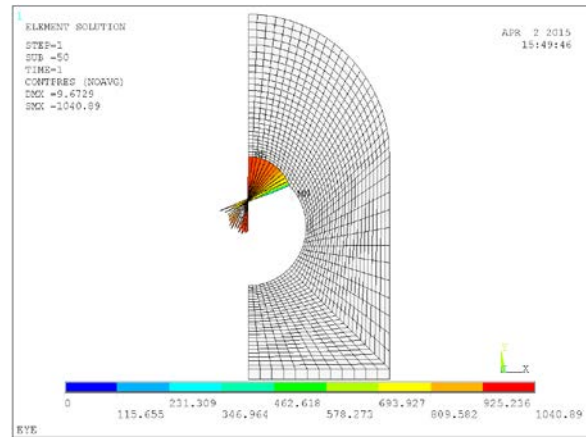


Figure 5-8: Contact pressure with a large clearance

Only the EN1993-1-8 takes this into account with a formula (equation: ( B-114 )) which is a customized “Hertz stress” formula (equation: ( B-1 )). In Chart E-10 and Chart E-11 this effect is notable from clearances which are higher than 3mm.

### 5.1.4 Conclusion

The compared standards (EN1993-1-8, EN13001-3-1, AMSE BTH-1 and AISC 360-10) are providing SLS and ULS capacities, based on a governing unity check of 1.0 for any criteria. The amplitude of these loads is different, but the sensibilities on different geometry parameters are different too. Although all standards provide another calculation to check a pinned connection, none of them provide similar results (e.g. stresses/plastic strains) for all kind of geometries. Therefore it is hard to give any conclusion on allowable strains/stresses according to a certain standard.

Not all geometries which are compared are really used at Mammoet. Negative eccentricities and very small eye radii compared to the hole diameter are not used. With the following defined parameters, the geometries are restricted to certain boundaries. The graphical interpretations of these boundaries are shown in Figure 5-9.

$$0.25 \leq G = \frac{R_{eye} - d_h/2}{R_{eye} + d_h/2} \leq 0.6 \tag{5-1}$$

$$0 \leq E = \frac{e}{e + R_{eye}} \leq 0.45 \tag{5-2}$$

$$0 \leq clear = \frac{d_h - d_p}{d_h} \leq 0.25 \tag{5-3}$$

The geometries which are fulfilling these restrictions are compared and listed in Table 5-1.

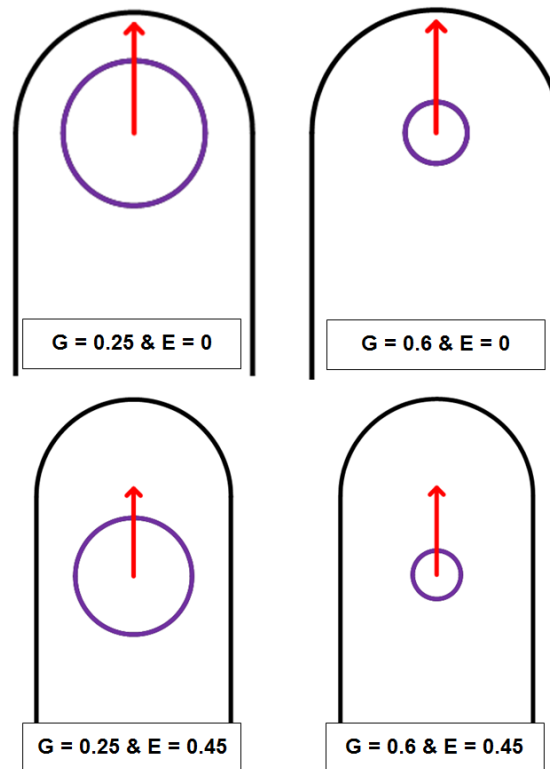


Figure 5-9: Graphical interpretation boundaries of the geometric restrictions

Max stress [N/mm <sup>2</sup> ]/plastic strain [-]	EN1993-1-8	EN13001-3-1	ASME BTH-1	AISC 360-10
Failure criteria				
1 SLS	0.20%	0.00% (0.19%)	0.46%	0.53% (1.19%)
2 SLS	293 N/mm <sup>2</sup>	203 N/mm <sup>2</sup> (0.02)	0.12%	388 N/mm <sup>2</sup> (0.31%)
3 SLS	10.94%	0.00% (14.94%)	13.62%	2.36% (20.46%)
1 ULS	0.43%	1.19% (1.94%)	-	-
2 ULS	688 N/mm <sup>2</sup>	308 N/mm <sup>2</sup> (0.31%)	-	-
3 ULS	28.52%	5.45% (26.14%)	-	-

Table 5-1: Max stress/plastic strain according to SLS and ULS capacities<sup>14</sup>

<sup>14</sup> The EN13001-3-1 and the AISC 360-10 have limited the clearance of reference eye 1 to 0.5mm and 1mm. Since most parameter studies do not fulfill these restrictions the results may be not reliable. The values between the brackets do not fulfill these restrictions. It is recommended to use the values between the brackets for failure criteria 1 and 2. For bearing it is recommended to use the value before the brackets (which fulfill the clearance criteria).

The ASME BTH-1 and the AISC 360-10 provide for some geometry that large ULS capacities that ANSYS can't find a solution for these loads (it is close to the failure load). For that reason these results are not listed.

## 5.2 Analysis of the loads based on plastic strains

The FEM model calculates under a certain load all kind of output, like stresses and strains. In this paragraph is studied under what conditions (Load) the FEM model provides certain strains on specific locations (failure criteria), see Figure 5-10. Under different geometry parameters the loads which provide 0%, 0.5%, 1%, 5% and 15% plastic strain for each failure criteria are noticed. Also the loads which provide plastic strains trough a whole section is noticed, see Figure 5-11. This phenomenon is named yielding in this report.

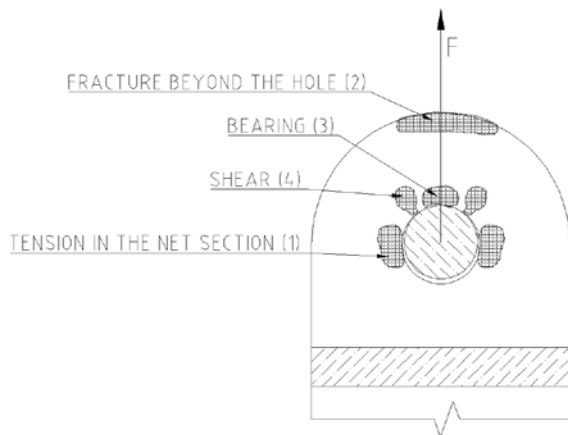


**Figure 5-10: Specified failure locations**

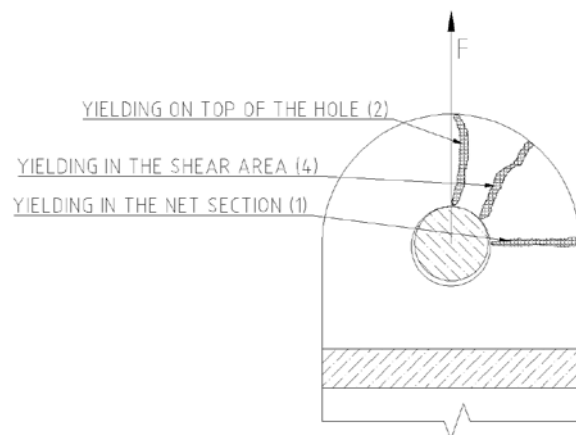


**Figure 5-11: Specified yielding locations**

Similar as in paragraph 5.1 the influences of different parameters are considered. All results are listed in appendix F.1.

### 5.2.1 Influence of $R_{eye}$

The influences of  $R_{eye}$  are analyzed with and without an eccentricity, see Figure 5-2 and Figure 5-3.

In Figure 5-12 and Figure 5-13 two different yield contours are plotted. Only in the colored part the eye is yielding. For a relative larger eye radius, yielding is occurring for shear/ fracture beyond the hole (see Figure 5-13), while for a smaller eye radius yielding through the eye is occurring in the net section (see Figure 5-12). This is because the relative eccentricity  $E$  (see equation ( 5-2 )) is decreasing for larger eye radii.

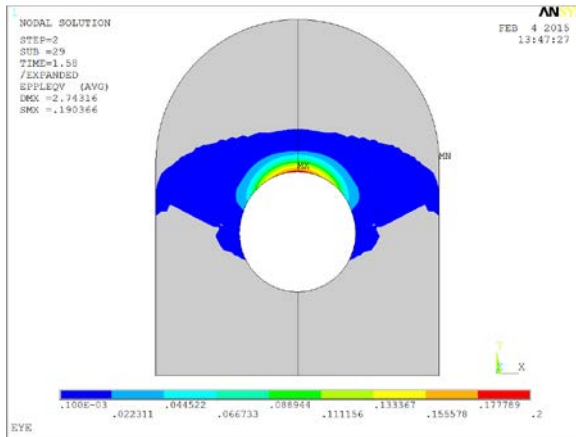


**Figure 5-12: Yielding in the net section ( $R_{eye} = 100\text{mm}$ )**

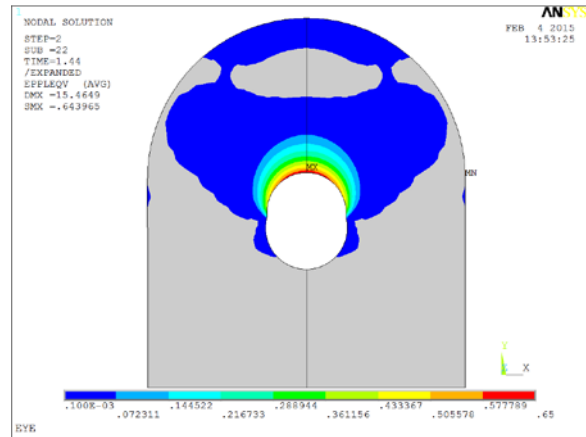


**Figure 5-13: Shear /Fracture beyond the hole yielding ( $R_{eye} = 160\text{mm}$ )**

In Chart E-12 to Chart E-14 the loads which cause 0%, 0.5%, 1%, 5% and 15% plastic VonMises strain are plotted for all different failure criteria for various eye radii with an eccentricity. For a relative large eye radius, bearing instead of tension in the net section is normative. Not for all  $R_{eye}$  values plastic strains occurring for each failure mechanism. A clear plastic strain development is hardly notable for the shear criteria (see Figure 5-14) and therefore the plastic strains in the shear area are not discussed.

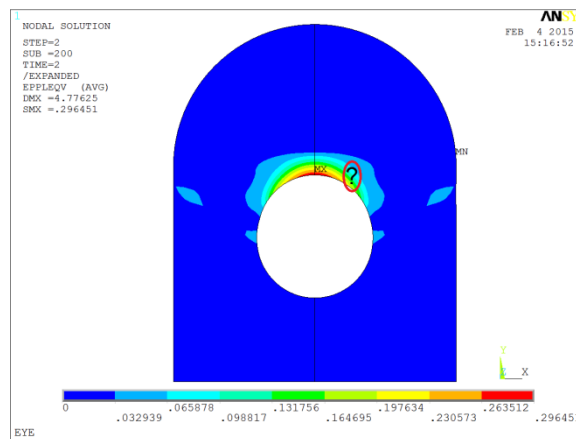


**Figure 5-14: Non notable plastic strain in the shear criteria ( $R_{eye} = 130\text{mm}$ ,  $e = 50\text{mm}$ ,  $F = 3000\text{kN}$ )**

From these charts can be observed that:

- The 0% strain plot for tension in the net section is increasing from 500kN to 1600kN although the slope is decreasing. This means that the stress concentration factor is decreasing for a larger eye radius, or a relative smaller effective width of the eye. All other plastic strain plots are more or less linear increasing.
- Between eye radii 100mm and 110mm there is a “jump” in the 0.5% plastic strain plot for tension in the net section. This is due to the area at which the plastic strains occur is increasing, but the magnitude of the plastic strains are not. This is shown in Figure 5-15 and Figure 5-16.

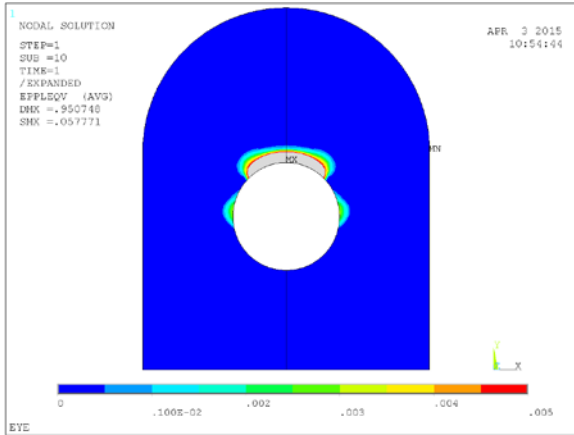


Figure 5-15: Plastic strains before "jump" in 0.5% plastic strain plot

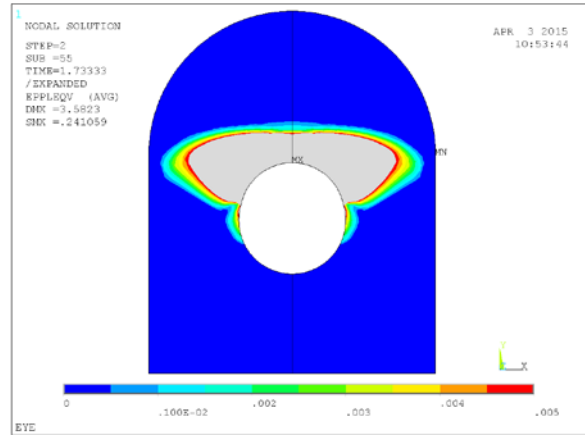


Figure 5-16: Plastic strains after "jump" in 0.5% plastic strain plot

- Only for an eye radius larger than 120mm the top of the eye starts to yield on top of the eye.
- All strain plots for fracture beyond are more or less linear increasing.
- For a small eye radius an increasing eye radius has a negative effect on the bearing strains. This is because for an increasing eye radius, the eye becomes stiffer.
- For an eye radius larger than 100mm the stiffness of the eye remains constant and the influence of an increasing  $R_{eye}$  is negligible for bearing strains.

In Chart E-15 to Chart E-17 the loads which cause 0%, 0.5%, 1%, 5% and 15% plastic VonMises strain are plotted for all different failure criteria for various eye radii without an eccentricity. For a relative large eye radius, bearing instead of tension in the net section is normative. Not for all  $R_{eye}$  values plastic strains occurring for each failure mechanism. From these charts can be observed that:

- For fracture beyond the hole, the plastic strains are now occurring for small eye radii too.
- The 0% strain plot for fracture beyond the hole is increasing from 250kN to 1500kN although the slope is decreasing. These loads are lower than the eyes with an eccentricity.
- Yielding occurs now for fracture beyond the hole/shear, see Figure 5-17.

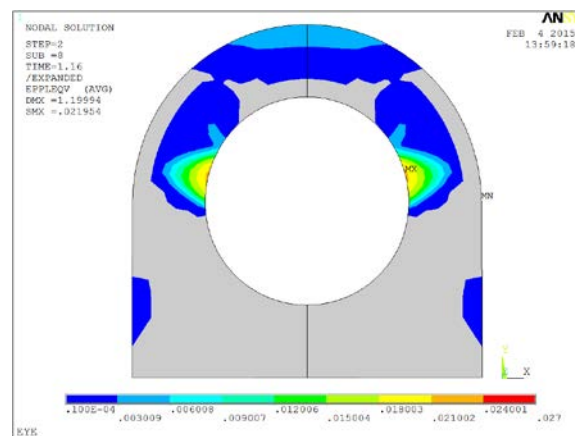


Figure 5-17: Yield contour ( $R_{eye} = 70\text{mm}$ )

- Only the 0% plastic strain for fracture beyond the hole loads are lower than the yield load. The 0.5%, 1%, 5% and 15% are above the yield load, and are very close to each other. This means that if the eye is totally yielding through a section, the strains increase much faster.

- Only for the small  $R_{eye}$  values the 1%, 5% and 15% plastic strains in the net section are notable. This is because other failure criteria are normative for a larger eye radius, and the plastic strains in the net section are not notable or occurring.

### 5.2.2 Influence of the eccentricity

The influence of the eccentricity is studied by varying the eccentricity from -25mm to 50mm with an eye radius of 80mm and an eye radius of 100mm, see Figure 5-4.

The location where the eye is yielding through a whole section is dependent on the eccentricity. In Figure 5-18 and Figure 5-19 two different yield failures are shown for a small and a large eccentricity.

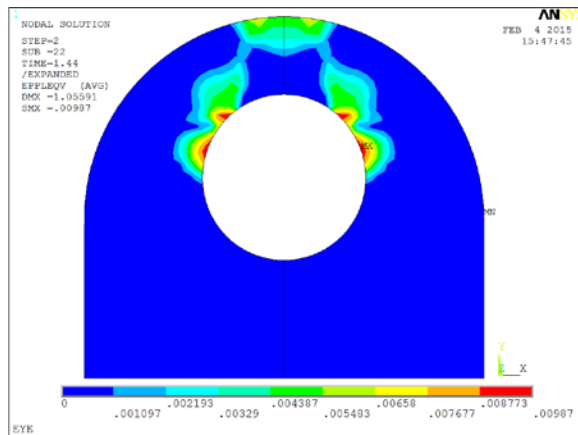


**Figure 5-18: Yield failure in shear/ fracture beyond the hole with a small (negative) eccentricity**

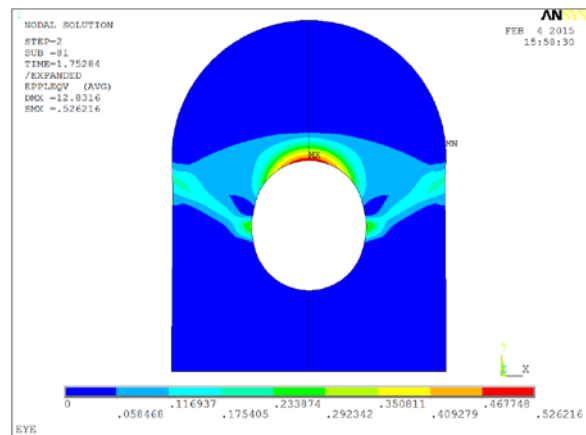


**Figure 5-19: Yield failure tension in the net section with a large eccentricity**

In Chart E-18 to Chart E-20 the loads which cause 0%, 0.5%, 1%, 5% and 15% plastic VonMises strains are plotted for all failure criteria.

- It is shown that not only the eye radius has an influence for tension in the net section but the eccentricity has influence too. This is in accordance to the EN13001-3-1 which also incorporates this effect. The influence is limited for very large eccentricities ( $\pm e$  is larger than 50mm).
- The eccentricity has more or less a linear influence for fracture beyond the hole.
- Likewise for the eye radius, the eccentricity has a small effect on the bearing strains. For a small eccentricity the 0%, 0.5%, 1% and the 5% bearing are on the same level, which indicates brittle failure. These values are reached above the yield load, so another failure criterion is critical. For larger eccentricities an increasing eccentricity is negative for the bearing strains, because the eye becomes stiffer. Only for the 15% plastic strain the larger eccentricity has a positive effect, but this effect is also limited. For the small eccentricities the bearing loads are increasing because other effects, such like fracture beyond the hole are critical, and these stresses also have influence on the bearing area. For an increasing eccentricity these side effects are much smaller, and therefore these loads are increasing until a certain level.

### 5.2.3 Influence of the clearance

The influence of the clearance is studied for different geometries. The clearance has not only effect on the bearing strains, but also has influence on the other failure criteria. For different geometries which have different governing failure criteria the effect of the clearance is discussed.

The influence of the clearance with an eye radius of 100mm is analyzed with an eccentricity of -10mm, 20mm or 50mm. The pin diameter is varying from 62mm to 82mm. The hole diameter is constant 82mm so the clearance is increasing from 0mm to 20mm, see Figure 5-20.

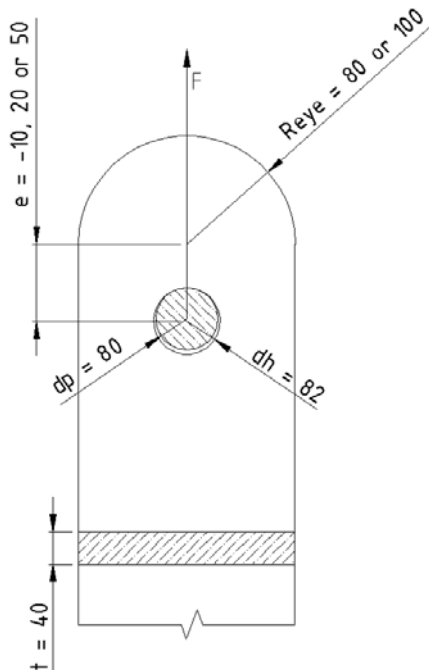


Figure 5-20: Geometry with a varying clearance with an Reye of 100mm and an eccentricity of -10mm, 20mm or 50mm

**Influence of the clearance for tension in the net section**

In Figure 5-21 and Figure 5-22 two yield contours are plotted with no clearance and a large clearance (10mm). Both are yielding in the net section, although the maximum strains are much higher for the geometry with the large clearance.

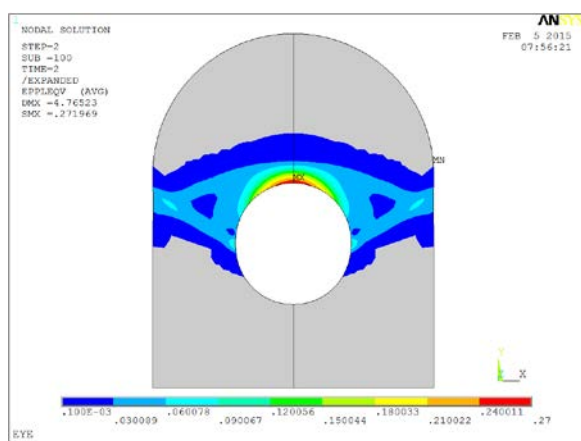


Figure 5-21: Yielding in the net section (Clearance = 0mm, F = 3000kN)

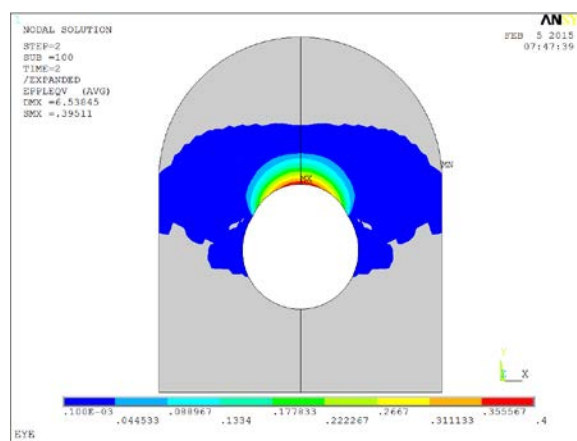


Figure 5-22: Yielding in the net section (Clearance = 10mm, F = 3000kN)

In Chart E-22 and Chart E-23 the loads which cause 0%, 0.5%, 1%, 5% and 15% plastic VonMises strains are plotted for tension in the net section.

- For larger eccentricities the effect of clearance on the net section is getting smaller. The clearance effect is only notable for small clearances. For larger clearances the loads remain more constant.

- For a smaller eye radius the effect of eccentricities is also larger, see Chart E-21 and Chart E-24. The eccentricity and eye radius have more or less the same influence on the effect of different clearances.

**Influence of the clearance for fracture beyond the hole**

In Figure 5-23 and Figure 5-24 two yield contours are plotted with no clearance and a large clearance (20mm). Both are yielding beyond the hole, although the maximum strains are much higher for the geometry with the large clearance, while this load is smaller.

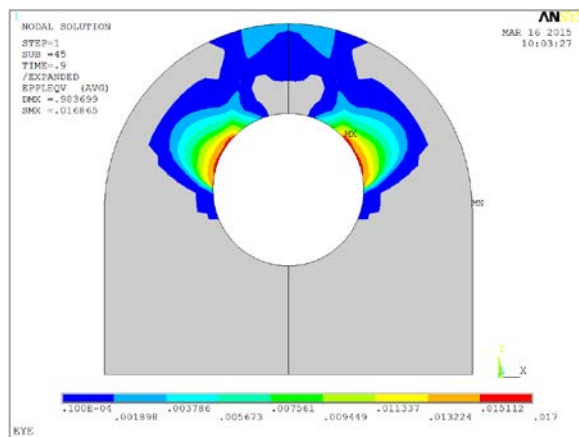


**Figure 5-23: Yielding beyond the hole (Clearance = 0mm, F = 2000kN)**

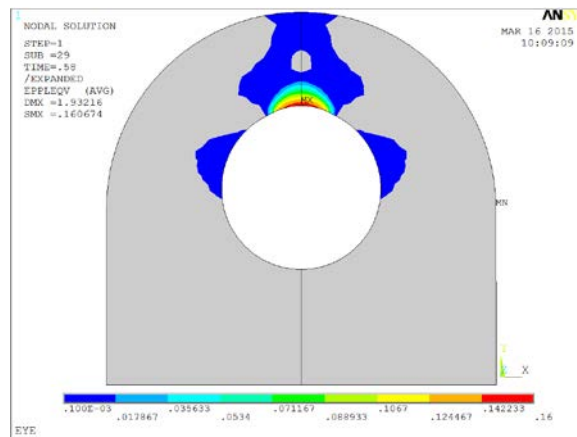


**Figure 5-24: Yielding beyond the hole (Clearance = 20mm, F = 1300kN)**

In Chart E-25 and Chart E-26 the loads which cause 0%, 0.5%, 1%, 5% and 15% plastic VonMises strains are plotted for fracture beyond the hole. From these charts can be observed that:

- The clearance effect is notable for all clearances. For larger clearances the varying clearance has most effect on the larger strain plots (5% and 15%), while for smaller clearances the varying clearance has most effect on the smaller strain plots (0% and 0.5%).

**Influence of the clearance for bearing**

In Chart E-27 to Chart E-29 the loads which cause 0%, 0.5%, 1%, 5% and 15% plastic VonMises strains are plotted for bearing. From these charts can be observed that:

- For the 0% strain plot a small clearance has a positive effect compared to a perfectly fitting pin. This might be due to a “clamping” effect for a perfect fitting pin. In that case the strains in the bearing area are not only because of bearing but due to a “clamping” effect too. This effect is negligible for the larger strain plots.
- Bearing strains are very sensitive for clearances. This is because the contact area is reduced for larger clearances. Also can be concluded that the magnitude of the strain plots have some small differences for different geometries (eye radii and eccentricities). The shape of the strain plots are more or less the same for different geometries.

**5.2.4 Conclusion**

Plastic strains in the net section are almost in all cases larger than plastic strains for fracture beyond the hole. Even when total yielding through the eye is in the shear/ fracture beyond the hole area, the plastic strains are higher in the net section.

The bearing is very sensitive for clearances. Although the shapes of the bearing plots are more or less similar, the magnitude of the loads might be also dependent on the model. With a 3D FEM analysis, or a refined mesh the magnitude of these strains may be different.

All geometry parameters (eye radius, eccentricity, pin diameter, hole diameter and thickness) have effect for each failure criteria. The formulas which are used in the standards don't include all these effects but are not so complicated.

### 5.3 Cheek plates

At Mammoet cheekplates (Figure 1-2 and Figure 1-3) are commonly used to strengthen a pinned connection. No research is done about applying cheekplates in the past which provided clear conclusions. If cheekplates are applied new geometry parameters are introduced for the cheekplates so the behavior of the pinned connections is more complex.

D. Duerr [18] recommends a further research about applying cheekplates. He did two assumptions to calculate the load distribution between the main plate and the cheekplates.

- Calculate the capacities of the individual plates and the summation is the capacity of the connection
- Load is distributed between the pin and the plate as uniform bearing. Using this approach, the calculated capacity of each plate is compared to the applied load on each plate.

In this paragraph the load distribution between the cheek plates and the main plate is studied. Similar as in paragraph 5.2 the loads which provides 0%, 0.5%, 1%, 5% and 15% plastic strain on specific locations (see Figure 5-10), are noticed too. For cheekplates some additional failure criteria are introduced, see Figure 5-25. Also the loads which provide plastic strains trough a whole section (yielding) is noticed, see Figure 5-11. It is assumed that yielding in the cheek plate doesn't provide large plastic deformations, because in that case the cheek plate is "hold together" by the main plate. Only yielding in the main plate is noticed because in that case the cheek plates yield too.

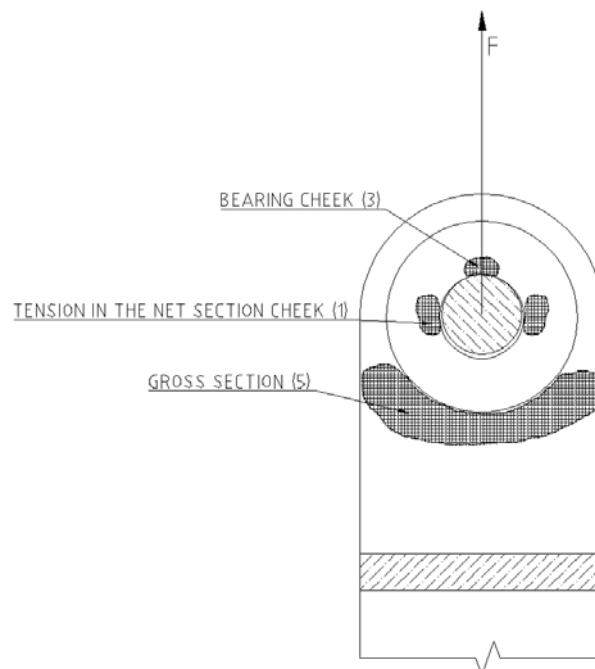


Figure 5-25: Additional failure criteria for applying cheekplates

#### 5.3.1 Load distribution between the cheek plates and the mid plate

The load distribution is studied for different eye radii, eccentricities, thicknesses, cheek plate radii, cheek plate thicknesses and weld throats. These results are plotted in Chart E-30 to Chart E-33. From these charts can be concluded that:

- For all studied geometries more load is transferred via the mid plate than calculated with the thickness ratio
- The weld throat size has a small effect on the load distribution. For larger weld throats, more load is transferred via the cheek plates.
- The eccentricity has no influence on the load distribution
- The cheek plate radius has an influence on the load distribution. For smaller cheek plate radii, more load is transferred via the mid plate.

With these conclusions some additional geometry parameters are introduced. It is assumed that the load distribution is dependent from the following geometry parameters:

- $G_g$ , see equation ( 5-6 ), describes the difference in cheek plate stiffness and mid plate stiffness based on their shape parameters  $G$ . Stiff elements generally attract more forces than non-stiff elements.
- $T_t$ , see equation ( 5-7 ), describes the thickness ratio between the cheek plate and the mid plate. From this study can be concluded that the load distribution between the cheek plates and the mid plate is not simply linear dependent on the thickness ratio.
- $W$ , see equation ( 5-8 ), describes the effect of the weld between the cheek plates and the main plate. The weld strength and stiffen the cheek plate. If the weld is (too) small the cheek plates can bend away from the mid plate, see Figure 5-26.

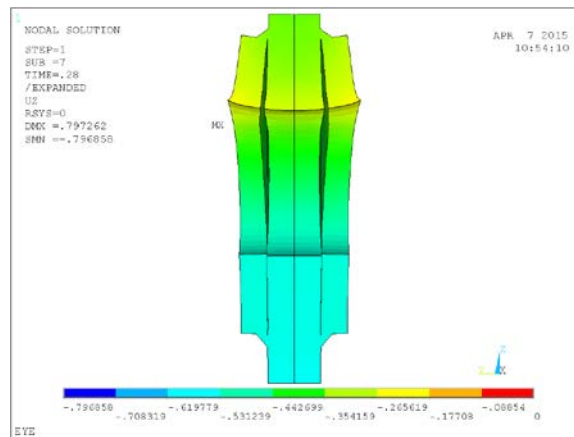


Figure 5-26: Out of plane bending of the cheek plate

$$G = \frac{R_{eye} - d_h/2}{R_{eye} + d_h/2} \quad (5-4)$$

$$G_{cheek} = \frac{R_{cheek} - d_h/2}{R_{cheek} + d_h/2} \quad (5-5)$$

$$G_g = \frac{G}{G_{cheek}} = \frac{(R_{eye} - d_h/2) * (R_{cheek} + d_h/2)}{(R_{eye} + d_h/2) * (R_{cheek} - d_h/2)} \quad (5-6)$$

$$T_t = \frac{T_{cheek}}{T} \quad (5-7)$$

$$W = \frac{a_{weld}}{T_{cheek}} \quad (5-8)$$

The load distribution is calculated with a load which is equal to the yield load. In Chart E-34 the load distribution is plotted for different load magnitudes. From Chart E-34 can be concluded that the load magnitude has no influence on the load distribution.

### FEM method to determine the load distribution

To list the load distribution some additional steps are done in Ansys [21] to list these distributions. Between the cheek plate and mid plate only normal contact (pressure only) is modelled without friction. So all forces can only transfer via the weld from the cheek plate to the mid plate.

The nodes are general in equilibrium if all elements around the nodes are selected, for example in Figure 5-27 ( $F_{weld} - F_{mid\ plate} = 0$ ). If only the nodes on the mid plate which attach the weld are selected, and the elements in the weld which attach these nodes are selected, the summation of nodal forces is not zero anymore ( $F_{weld} - F_{mid\ plate} \neq 0$ ). A summation of all these nodes provide exactly the load which is going through the weld, and so the load distribution between the cheek plates and the mid plate.

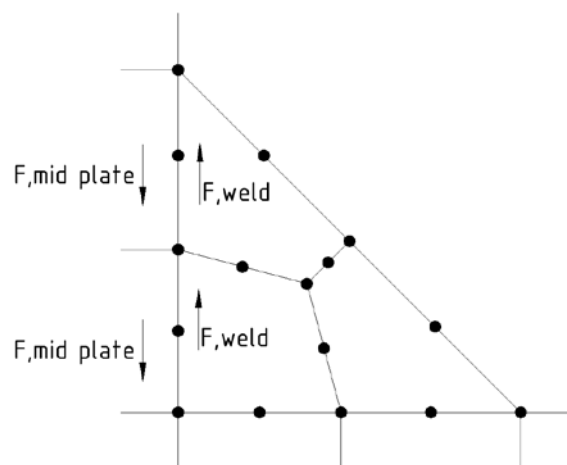


Figure 5-27: Nodal equilibrium

### 5.3.2 Other effects

More than just the load distribution is studied by applying cheek plates. Similar as in paragraph 5.2 the loads which result in 0%, 0.5%, 1%, 5% and 15% plastic strains and section yielding are listed. This is done for the mid plate and the cheek plates, see Figure 5-10, Figure 5-11 and Figure 5-25. To compare all these loads the load is split in a load via the mid plate ( $F_{mid\ plate}$ , see equation ( 5-9 )) and a load via the cheek plate ( $F_{cheek\ plate}$ , see equation ( 5-10 )). The load via the cheek plate is normalized to compare different cheek plate thicknesses.

$$F_{mid\ plate} = F * F_{ratio} \tag{ 5-9 }$$

$$F_{cheek\ plate} = F * \frac{(1 - F_{ratio})}{2} * \frac{10}{T_{cheek}} \tag{ 5-10 }$$

From Chart E-35 to Chart E-39 can be concluded that  $F_{mid\ plate}$  is for some strains independent<sup>15</sup> of the cheek plate parameters, and  $F_{cheek\ plate}$  is for some strains independent of the mid plate parameters.

Unfortunately bearing strains in the mid plate and cheek plate are not independent from each other, see Chart 5-1. Also the normalized load (which normalizes different cheek plate thicknesses) is various for different cheek plate thicknesses.

<sup>15</sup> The loads are within a range of 10%.

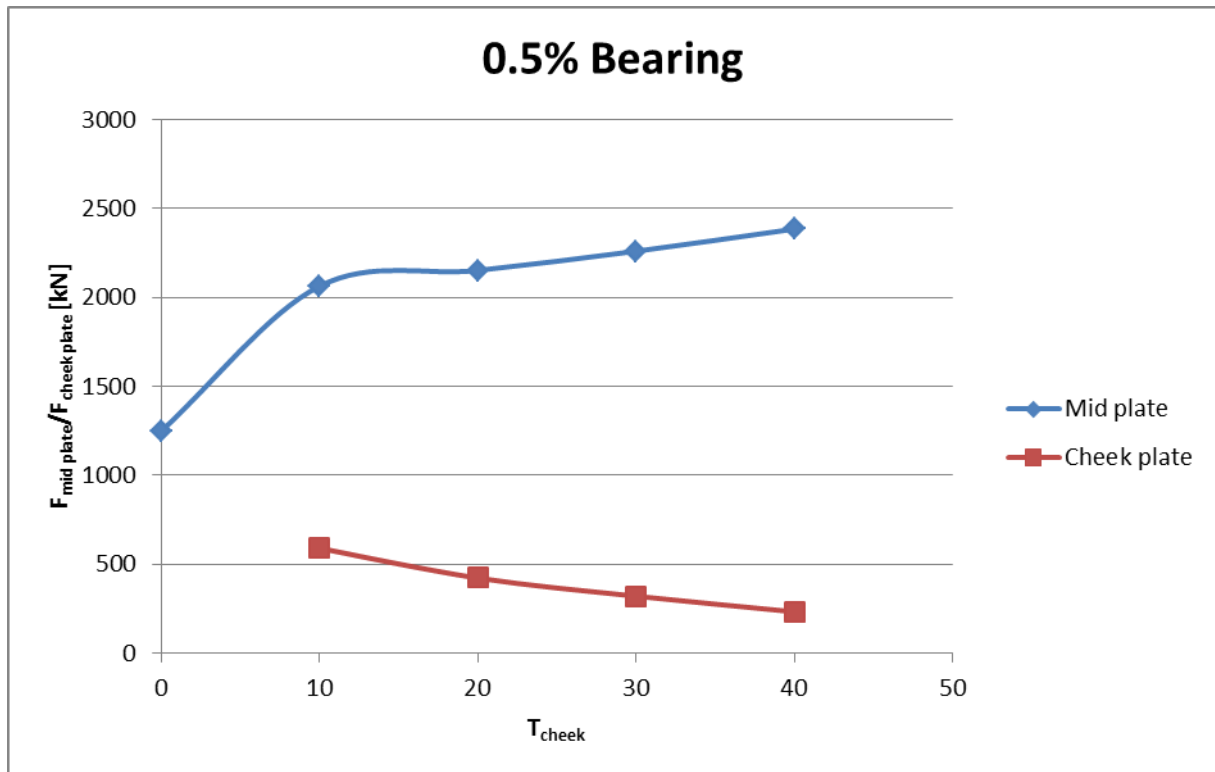


Chart 5-1: 0.5% Bearing strains (Reye = 100mm, e = 0, T = 40mm, Rcheek = 80mm, aweld = 6mm, dh = 82mm, dp = 80mm)

**Welds**

The stresses/strains at the cheek plates and mid plate at the location of the weld have influence on the stresses/strains in the weld, see Figure 5-28. So the weld is not just loaded on shear and bending (Figure 5-29) to transfer the load from the cheek plates to the mid plate.

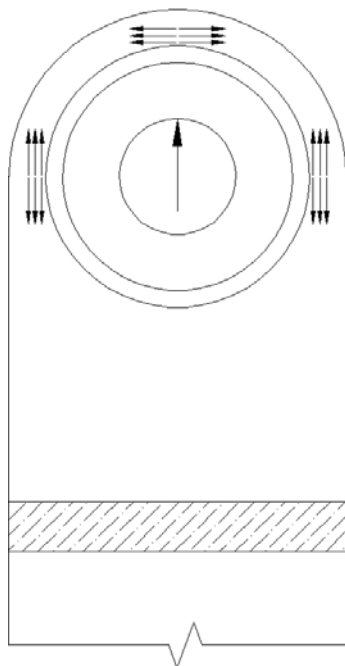


Figure 5-28: Stresses/strains of mid plate and cheek plate have influence on the weld

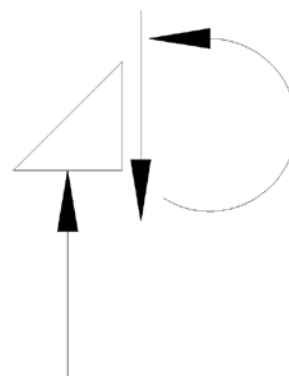


Figure 5-29: Stress assumption welds

The stresses/strains in the weld are not so straightforward to describe since they are not only loaded to transfer the load between the cheek plates and the mid plate. However EN1993-1-8 [3] states that the distribution of forces in a welded connection may be calculated on the assumption of either elastic or plastic behavior. It is acceptable to assume a simplified load distribution within the weld.

By using simplified load distributions it is easier to describe the capacity of the welds, instead of the complex stress/strain orientations according to a FEM analysis. For that reason, the stresses/strains within the welds are excluded from this report.



## 6 Comparison FEM versus theory

In this chapter the agreements and differences between the standards and the FEM analysis are briefly discussed.

Standards provide relative simple unity checks to calculate the capacity of pinned connections. Chapter 3 shows that all standards are somehow sensitive for different geometry parameters. The geometry parameters which have most influence on the capacity of failure criteria are included in the unity checks.

- Eye radius, hole diameter and thickness for tension in the net section
- Eye radius, eccentricity, hole diameter and thickness for fracture beyond the hole
- Pin diameter and thickness for bearing

In paragraph 5.2 is shown that the same geometry parameters have most influence on these capacities, although the influences are different. Most capacities from the standards are linear dependent on the geometry parameters (Figure 6-1), while from paragraph 5.2 can be concluded that it is more complex (Figure 6-2).

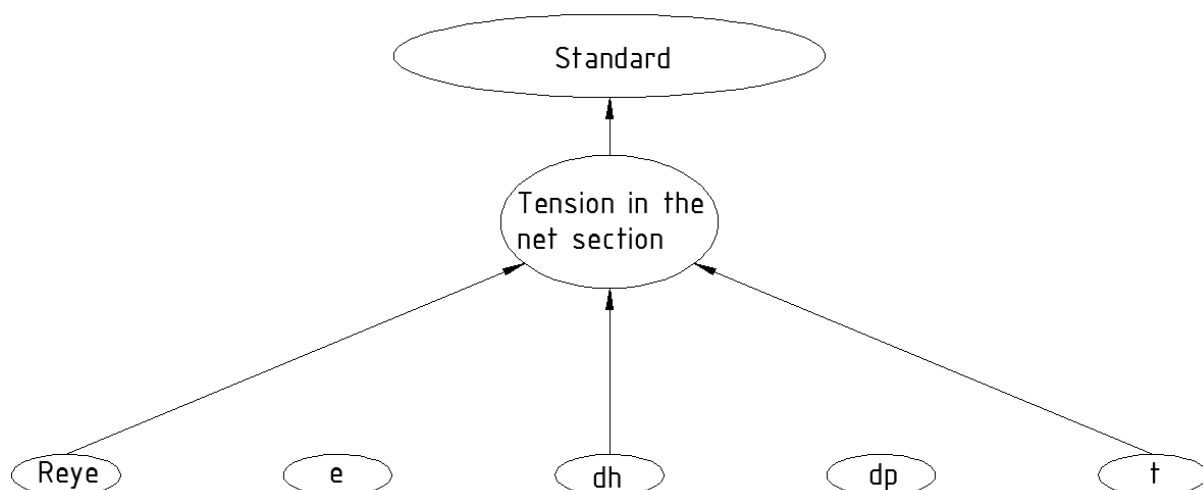
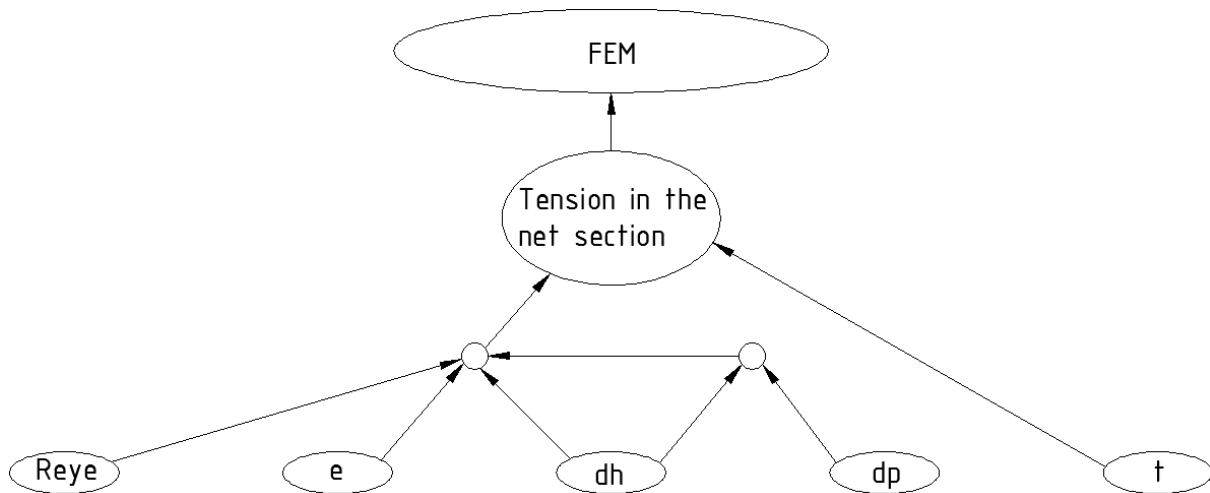


Figure 6-1: Influence of the geometry parameters for tension in the net section according to standards



**Figure 6-2: Influence of the geometry parameters for tension in the net section according to FEM**

In Figure 6-1 is shown that the tension in the net section capacity is linear dependent on the eye radius, hole diameter and thickness. With these parameters the capacity is relative simple to determine.

In Figure 6-2 is shown that the tension in the net sections capacity is nonlinear dependent on the eye radius, eccentricity, hole diameter and pin diameter. Only the thickness influence is linear. The combinations of the geometry parameters determine the capacity, which is more complex.

These figures are plotted for tension in the net section, but for the other failure criteria the conclusions are similar.

Another difference between the standards and the FEM analysis is that standards provide the capacity with a simple unity check. The FEM analysis provides a load when a certain plastic strain will occur. It doesn't provide the capacity if there are no limitations about the plastic strains.

In paragraph 5.1 the SLS and ULS capacities are used in the FEM model to determine the plastic strains. From all these results can be concluded that there are various strains acceptable for various geometries. In Table 5-1 all maximum strains are listed, so it is assumed that those should be acceptable.

Paragraph 5.2 provides a study on loads which provide 0%, 0.5%, 1%, 5% and 15% plastic strain. To make a comparison between the standards and the FEM analysis, those strains should be precisely described. Since not all strains for all failure criteria are of interest (they are not close to the SLS/ULS capacity according to the standards), the following strain formulas are precisely determined in chapter 7:

- 0% strain in the net section
- 0.5% strain in the net section
- 0% strain for fracture beyond the hole
- 0.5% strain for fracture beyond the hole
- 5% strain for bearing
- 15% strain for bearing
- Yielding
- Load distribution for applying cheek plates

# 7 Post processing FEM results

In this chapter the results of paragraph 5.2 and paragraph 5.3 are approximated by formulas. The assumptions and methods to find these formulas are detailed described.

## 7.1 Assumptions

The results of paragraph 5.2 are determined with an accuracy of 2kN. To determine a formula which describes these results, an accuracy of 10% is preferred. All FEM results, formula results and a comparison between both results are listed in Table F-1 to Table F-30 in appendix F.1.

The following additional parameters (similar as equation ( 5-1 ) to equation ( 5-3 )) are used to determine the formulas. These parameters are restricted since the formulas are not precisely enough out of these boundaries. Note that for common designs at Mammoet and economical designs the geometry parameters are always covered by these formulas. (The restrictions are wide.)

$$0.25 \leq G = \frac{R_{eye} - d_h/2}{R_{eye} + d_h/2} \leq 0.6 \quad (7-1)$$

$$0 \leq E = \frac{e}{e + R_{eye}} \leq 0.45 \quad (7-2)$$

$$0 \leq clear = \frac{d_h - d_p}{d_h} \leq 0.25 \quad (7-3)$$

A formula which covers all results within the scope is quite complex. General polynomial equations can approximate a wide set of results, if the order of the polynomial is large enough. The resulting formula is general a multiplication of a shape function (all results with the same clearance) with a clearance function (including the clearance effect).

## 7.2 Formulas

### 7.2.1 Tension in the net section

#### 0%

It is possible to approximate the results accurate enough with a polynomial equation of the 3<sup>rd</sup> order for the shape function, see equation ( 7-4 ). In Chart 7-1 the solution of this function is plotted for various eye radii and eccentricities.

$$F_{shape} = c_1 + c_2 * G + c_3 * G^2 + c_4 * E + c_5 * G * E + c_6 * G^2 * E + c_7 * E^2 \quad (7-4)$$

The clearance effect is assumed to be an exponential function. To describe all results with a clearance of 2mm ( $d_h = 82\text{mm}$  and  $d_p = 80\text{mm}$ ) the factor  $\beta^2$  is added. In Chart 7-2 the clearance function is plotted for various G and clear values.

$$F_{clear} = 1 - \alpha * (\beta^2 - \beta^{clear*82}) \quad (7-5)$$

$$\alpha = 0.435 * 0.221^{G+E} \quad (7-6)$$

$$\beta = 0.3 \quad (7-7)$$

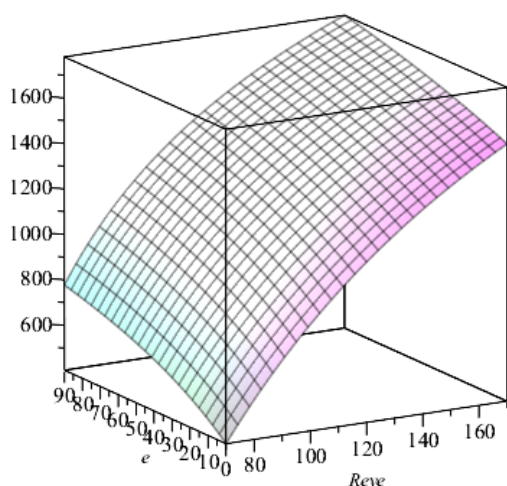


**Chart 7-1: 3D plot of 0% plastic strain tension in the net section shape functions ( $t = 40\text{mm}$ ,  $d_h = 82\text{mm}$  and  $d_p = 80\text{mm}$ )**

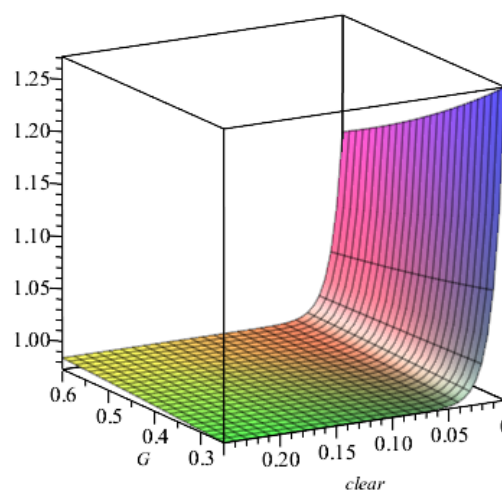


**Chart 7-2: 3D plot of 0% plastic strain tension in the net section clearance functions ( $E = 0$ )**

The multiplication of the shape function and the clearance function provides a (complex) formula which describes all results from the FEM analysis.

**0.5%**

It is possible to approximate the results accurate enough with a polynomial equation of the 3<sup>rd</sup> order for the shape function, see equation ( 7-8 ).

$$F_{shape,1} = c_1 + c_2 * G + c_3 * G^2 + c_4 * E + c_5 * G * E + c_6 * G^2 * E + c_7 * E^2 + c_8 * G * E^2 \quad (7-8)$$

$$F_{shape,2} = d_1 + d_2 * G + d_3 * G^2 + d_4 * E + d_5 * G * E \quad (7-9)$$

As already mentioned in paragraph 5.2, there is a “jump” in the strain plot due to stress distributions. Therefore the shape function is split in a function which approximate the results before the “jump” (equation ( 7-8 )) and a function which approximate the results after the “jump” (equation ( 7-9 )).

The geometries before and after the “jump are shown in Chart 7-3.

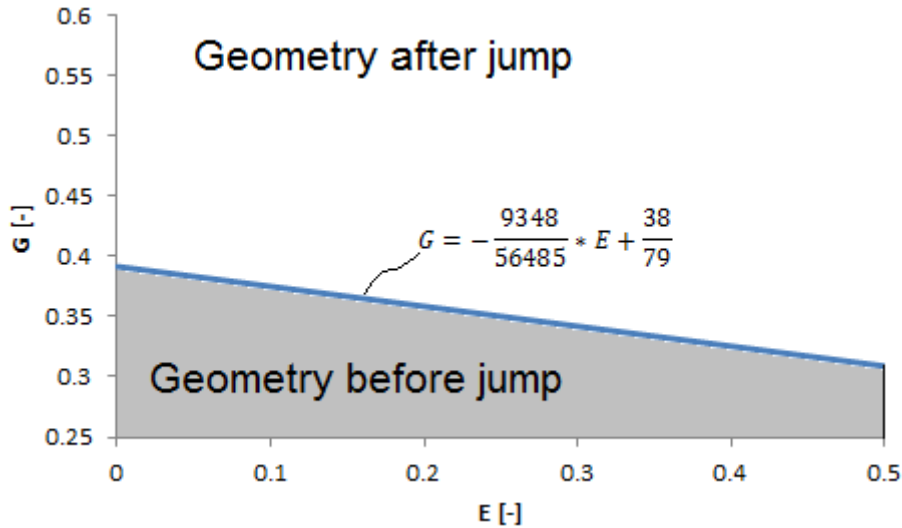


Chart 7-3: Geometry boundaries of 0.5% plastic strain jump

With these boundaries the  $F_{shape}$  formula is plotted for various  $R_{eye}$  and  $e$  values in Chart 7-4, in which the “jump” is easy to see.

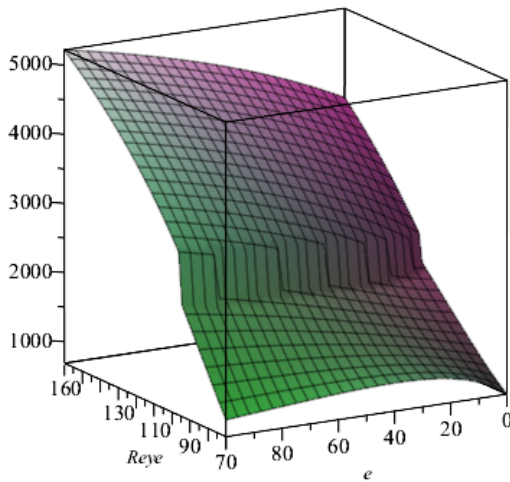


Chart 7-4: 3D plot of 0.5% plastic strain tension in the net section shape functions ( $t = 40\text{mm}$ ,  $d_h = 82\text{mm}$  and  $d_p = 80\text{mm}$ )

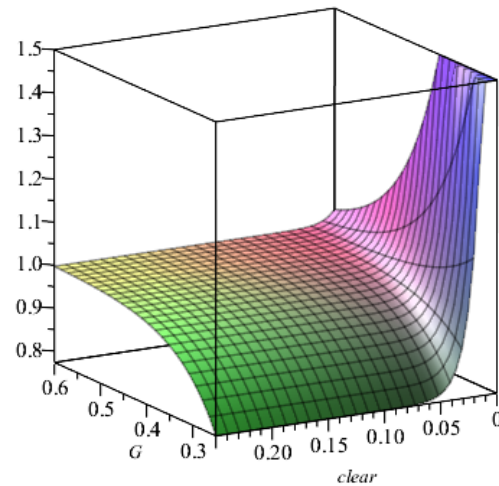


Chart 7-5: 3D plot of 0.5% plastic strain tension in the net section clearance functions ( $E = 0$ )

The clearance effect is assumed to be an exponential function. To describe all results with a clearance of 2mm ( $d_h = 82\text{mm}$  and  $d_p = 80\text{mm}$ ) the factor  $\beta^2$  is added. The clearance effect is limited to 1.5, to give a boundary on the positive effect of small clearances. The clearance function is plotted in Chart 7-5 for various  $G$  and  $clear$  values.

$$F_{clear} = 1 - \alpha * (\beta^2 - \beta^{clear*82}) \leq 1.5 \tag{7-10}$$

$$\alpha = 53.51 * e^{-3.811 * E - 12.228 * G} \tag{7-11}$$

$$\beta = 0.3 \tag{7-12}$$

The multiplication of the shape function and the clearance function provides a (complex) formula which describes all results from the FEM analysis.

### 7.2.2 Fracture beyond the hole

#### 0%

It is possible to approximate the results accurate enough with a polynomial equation of the 4<sup>th</sup> order for the shape function, see equation ( 7-13 ). In Chart 7-6 the solution of this function is plotted for various eye radii and eccentricities.

$$F_{shape} = c_1 + c_2 * G + c_3 * G^2 + c_4 * E + c_5 * G * E + c_6 * G^2 * E + c_7 * E^2 + c_8 * G * E^2 + c_9 * G^3 * E \quad (7-13)$$

The clearance effect is assumed to be an exponential function. To describe all results with a clearance of 2mm ( $d_h = 82\text{mm}$  and  $d_p = 80\text{mm}$ ) the factor  $\beta^2$  is added. The clearance effect is limited to a clearance of 0.005 (0.5mm gap on a hole of 100mm) to give a boundary on the positive effect of small clearances. In Chart 7-7 the clearance function is plotted for various E and clear values.

$$F_{clear} = 1 - \alpha * (\beta^2 - \beta^{clear*82}) \quad (7-14)$$

$$clear \geq 0.005 \quad (7-15)$$

$$\alpha = 0.598 - 2.088 * E \geq 0 \quad (7-16)$$

$$\beta = 0.65 \quad (7-17)$$

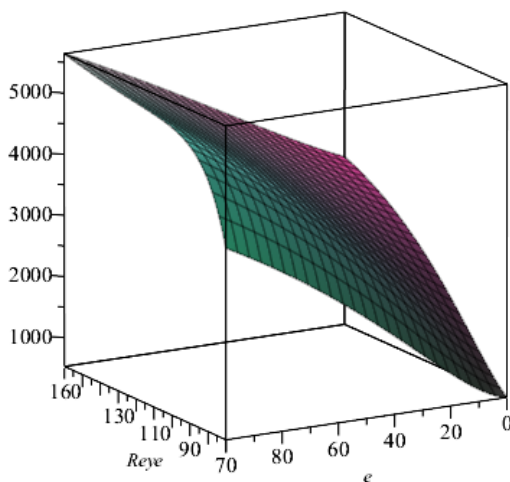


Chart 7-6: 3D plot of 0% plastic strain fracture beyond the hole shape functions ( $t = 40\text{mm}$ ,  $d_h = 82\text{mm}$  and  $d_p = 80\text{mm}$ )

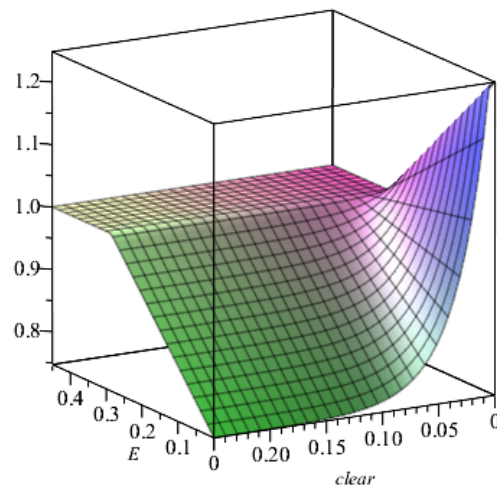


Chart 7-7: 3D plot of 0% plastic strain fracture beyond the hole clearance functions

The multiplication of the shape function and the clearance function provides a (complex) formula which describes all results from the FEM analysis.

**0.5%**

It is possible to approximate the results accurate enough with a polynomial equation of the 3<sup>rd</sup> order for the shape function, see equation ( 7-18 ). In Chart 7-8 the solution of this function is plotted for various eye radii and eccentricities.

$$F_{shape} = c_1 + c_2 * G + c_3 * G^2 + c_4 * E + c_5 * G * E + c_6 * G^2 * E + c_7 * E^2 \tag{7-18}$$

The clearance effect is assumed to be an exponential function. To describe all results with a clearance of 2mm ( $d_h = 82\text{mm}$  and  $d_p = 80\text{mm}$ ) the factor  $\beta^2$  is added. The clearance effect is limited to a clearance of 0.005 (0.5mm gap on a hole of 100mm) to give a boundary on the positive effect of small clearances. In Chart 7-9 the clearance function is plotted for various E and clear values.

$$F_{clear} = 1 - \alpha * (\beta^2 - \beta^{clear*82}) \tag{7-19}$$

$$clear \geq 0.005 \tag{7-20}$$

$$\alpha = 0.398 - 0.828 * E \geq 0 \tag{7-21}$$

$$\beta = 0.82 \tag{7-22}$$

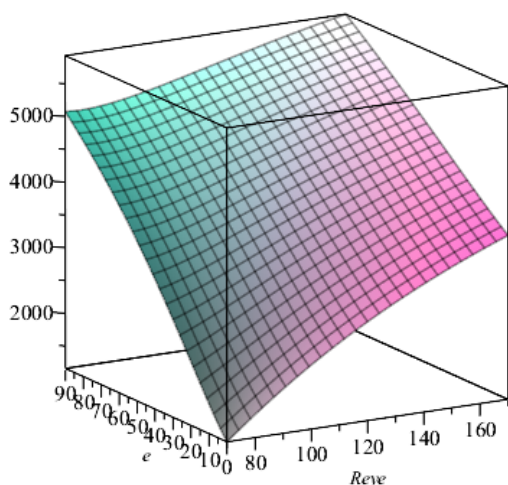


**Chart 7-8: 3D plot of 0.5% plastic strain fracture beyond the hole shape functions (t = 40mm, dh = 82mm and dp = 80mm)**

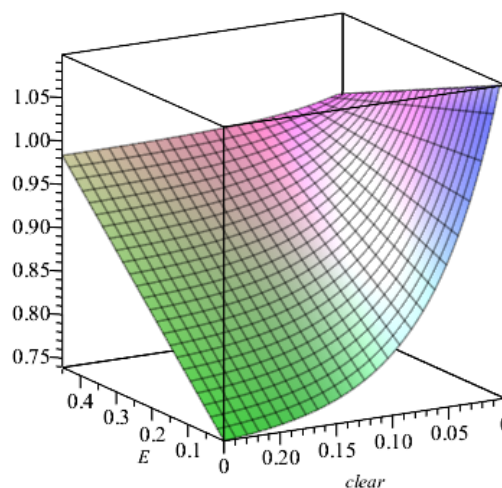


**Chart 7-9: 3D plot of 0.5% plastic strain fracture beyond the hole clearance functions**

The multiplication of the shape function and the clearance function provides a (complex) formula which describes all results from the FEM analysis.

**7.2.3 Bearing**

**5%**

It is possible to approximate the results accurate enough with a polynomial equation of the 2<sup>nd</sup> order for the shape function, see equation ( 7-23 ). In Chart 7-10 the solution of this function is plotted for various eye radii and eccentricities. These shape function is restricted to limit the positive effect of very small eye radii and eccentricities, and the negative effect of very large eye radii and eccentricities.

$$1880 \leq F_{shape} = c_1 + c_2 * G + c_4 * E + c_5 * G * E \leq 2050 \quad (7-23)$$

The clearance effect is assumed to be an exponential function. To describe all results with a clearance of 2mm ( $d_h = 82\text{mm}$  and  $d_p = 80\text{mm}$ ) the factor  $\beta^2$  is added. In Chart 7-11 the clearance function is plotted for various clearances.

$$F_{clear} = 1 - \alpha * (\beta^2 - \beta^{clear*82}) \quad (7-24)$$

$$clear \geq 0.005 \quad (7-25)$$

$$\alpha = 0.9 \quad (7-26)$$

$$\beta = 0.78 \quad (7-27)$$

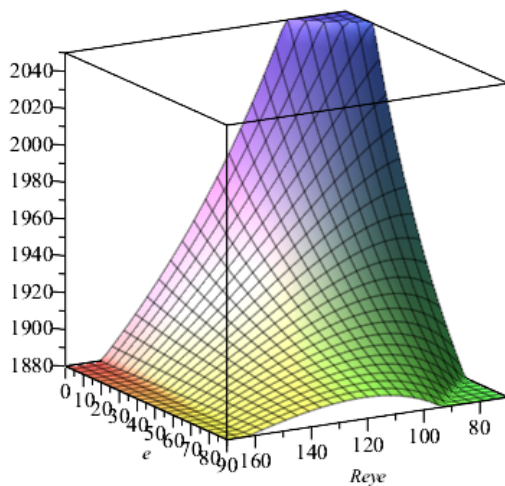


**Chart 7-10: 3D plot of 5% plastic strain bearing shape functions ( $t = 40\text{mm}$ ,  $d_h = 82\text{mm}$  and  $d_p = 80\text{mm}$ )**

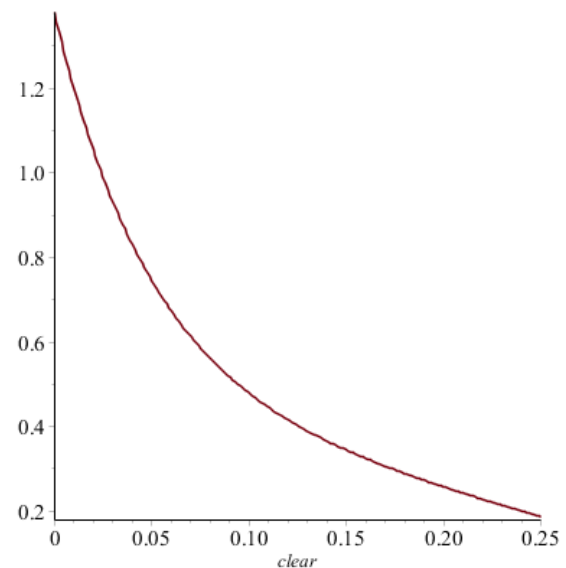


**Chart 7-11: 2D plot of 5% plastic strain bearing clearance functions**

The multiplication of the shape function and the clearance function provides a (complex) formula which describes all results from the FEM analysis.

### 15%

It is possible to approximate the results accurate enough with a polynomial equation of the 2<sup>nd</sup> order for the shape function, see equation ( 7-28 ). In Chart 7-12 the solution of this function is plotted for various eye radii and eccentricities.

$$F_{shape} = c_1 + c_2 * G + c_4 * E + c_5 * G * E \quad (7-28)$$

The clearance effect is assumed to be an exponential function. To describe all results with a clearance of 2mm ( $d_h = 82\text{mm}$  and  $d_p = 80\text{mm}$ ) the factor  $\beta^2$  is added. In Chart 7-13 the clearance function is plotted for various clearances.

$$F_{clear} = 1 - \alpha * (\beta^2 - \beta^{clear*82}) \quad (7-29)$$

$$clear \geq 0.005 \quad (7-30)$$

$$\alpha = 0.47 \tag{7-31}$$

$$\beta = 0.88 \tag{7-32}$$

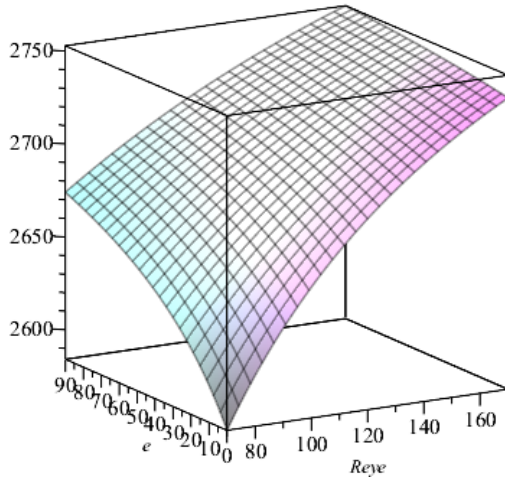


Chart 7-12: 3D plot of 15% plastic strain bearing shape functions ( $t = 40\text{mm}$ ,  $d_h = 82\text{mm}$  and  $d_p = 80\text{mm}$ )

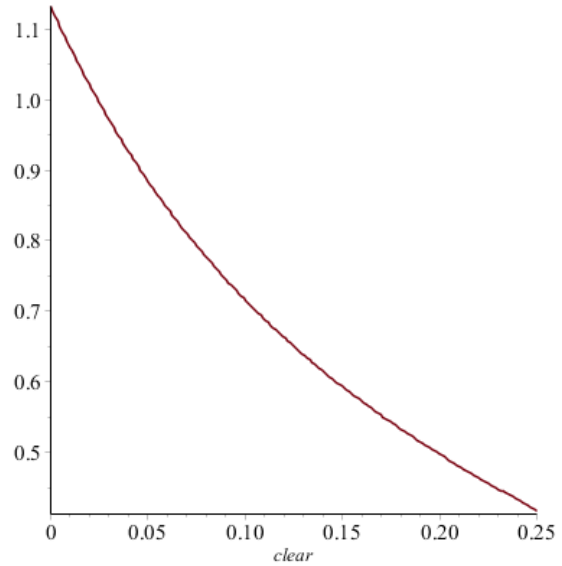


Chart 7-13: 2D plot of 15% plastic strain bearing clearance functions

The multiplication of the shape function and the clearance function provides a (complex) formula which describes all results from the FEM analysis.

### 7.2.4 Yielding

#### Yielding in the net section

The results of yielding in the net section are approximated with two formulas, one for lower  $G$  values ( $G < 59/141$ ) and one for larger  $G$  values ( $G > 59/141$ ), see equation ( 7-33 ) and equation ( 7-34 ). Both formulas have an equal value at  $G = 59/141$ , and have the same derivative ( $\frac{\partial F_{shape,low}}{\partial G} = \frac{\partial F_{shape,high}}{\partial G}$ ) at  $G = 59/141$ . In Chart 7-12 the solution of this function is plotted for various eye radii and eccentricities. The clearance has now effect on the yield load in the net section.

$$F_{low} = d_1 + d_2 * G + d_3 * G^2 + d_4 * \left( \frac{59}{141} - G \right) * E + d_4 * \left( \left( \frac{59}{141} \right)^2 - G^2 \right) * E \tag{7-33}$$

$$F_{high} = c_1 + c_2 * G + c_4 * G^2 \tag{7-34}$$

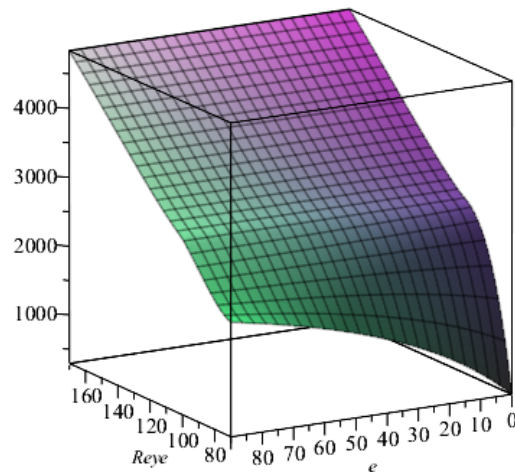


Chart 7-14: 3D plot of yielding in the net section function ( $t = 40\text{mm}$ ,  $d_h = 82\text{mm}$  and  $d_p = 80\text{mm}$ )

**Yielding in shear/fracture beyond the hole**

The results of yielding in shear/fracture beyond the hole is approximated with a polynomial function of the 3<sup>rd</sup> order, see equation ( 7-35 ). In Chart 7-15 the solution of this function is plotted for various eye radii and eccentricities.

$$F_{shape} = c_1 + c_2 * G + c_3 * G^2 + c_4 * E + c_5 * G * E + c_6 * G^2 * E + c_7 * E^2 \tag{ 7-35 }$$

In contradiction to yielding in the net section, the clearance has an effect for yielding in shear/fracture beyond the hole. The clearance effect is assumed to be an exponential function. To describe all results with a clearance of 2mm ( $d_h = 82\text{mm}$  and  $d_p = 80\text{mm}$ ) the factor  $\beta^2$  is added. In Chart 7-16 the clearance function is plotted for various E and clear values.

$$F_{clear} = 1 - \alpha * (\beta^2 - \beta^{clear*82}) \tag{ 7-36 }$$

$$clear \geq 0.005 \tag{ 7-37 }$$

$$\alpha = 0.364 - 0.684 * E \tag{ 7-38 }$$

$$\beta = 0.83 \tag{ 7-39 }$$

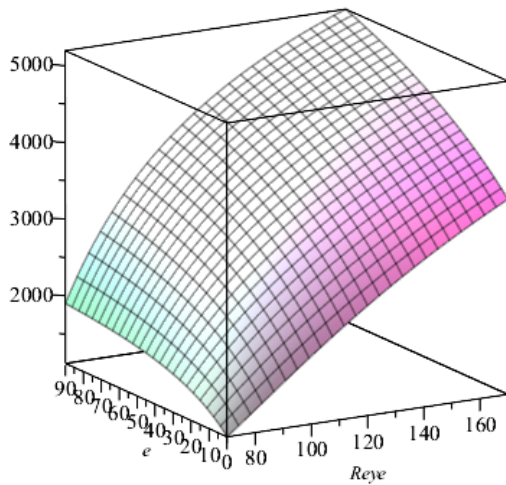


Chart 7-15: 3D plot of yielding in shear/fracture beyond the hole shape functions ( $t = 40\text{mm}$ ,  $d_h = 82\text{mm}$  and  $d_p = 80\text{mm}$ )

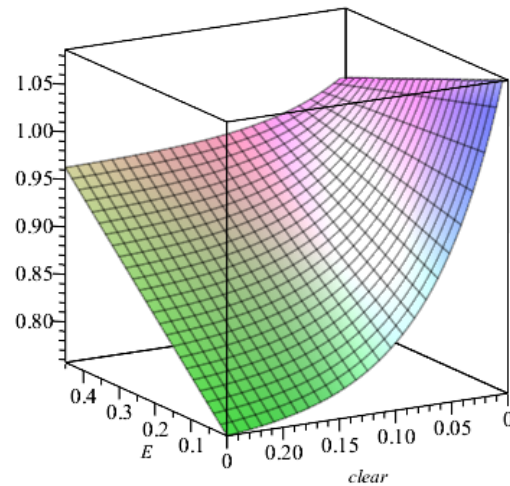


Chart 7-16: 3D plot of yielding in shear/fracture beyond the hole clearance functions

### 7.2.5 Dishing

If cheek plates are applied the connection is more sensitive to dishing, because cheek plates have commonly a reduced thickness. D. Duerr [18] already did research about this phenomenon which includes all geometry parameters. For that reason a further detailed study is not included in this report. Those formulas are listed in Appendix B.2. In equation ( B-97 ) to equation ( B-106 ) the formulas to calculate dishing capacity are listed. Duerr also recommends a “minimal” thickness of the plates when dishing cannot occur, equation ( B-107 ).

### 7.2.6 Load distribution for applying cheek plates

The load distribution between the mid plate and the cheek plates is studied in paragraph 5.3. This load distribution is approximated with a linear function, see equation ( 7-40 ).

In Chart 7-17 the solution of this function is plotted for  $G_g$  and  $T_t$  values.

$$F_{midplate} = 0\% \leq c_1 * \frac{t}{t + 2 * t_{cheek}} + c_2 + c_3 * G_g + c_4 * T_t + c_5 * W \leq 100\% \quad (7-40)$$

$$0.25 \leq G_{cheek} = \frac{R_{cheek} - d_h/2}{R_{cheek} + d_h/2} \leq 0.6 \quad (7-41)$$

$$G_g = \frac{G}{G_{cheek}} = \frac{(R_{eye} - d_h/2) * (R_{cheek} + d_h/2)}{(R_{eye} + d_h/2) * (R_{cheek} - d_h/2)} \quad (7-42)$$

$$0 \leq T_t = \frac{T_{cheek}}{T} \leq 1 \quad (7-43)$$

$$W = \frac{a_{weld}}{T_{cheek}} \quad (7-44)$$

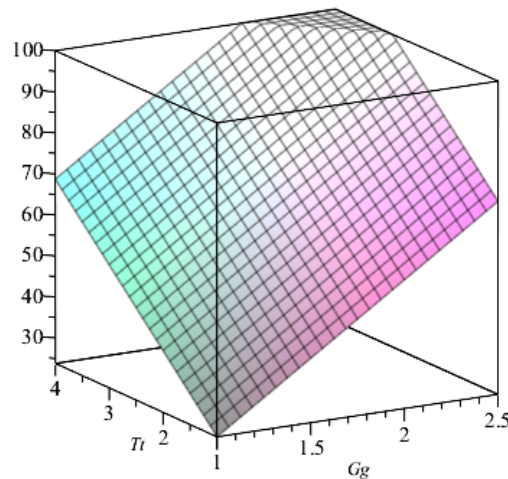


Chart 7-17: 3D plot of the load percentage through the mid plate for applying cheek plates ( $W = 0.7$ )

### 7.3 Use of formulas

In paragraph 7.2 is explained which functions are used to describe the results of the FEM analysis. The (3D) charts show the general behavior of those functions. It should be noticed that the result of these functions are quite complex and may be hard to use compared to the standards. Although, when the functions are once programmed in a spreadsheet, they are easy to use. The final formulas are listed in appendix F.2.

All capacities according to the standards can easily be compared with the results of the FEM analysis by using a programmed spreadsheet, see appendix G. Because standards are based on legislations and regulations they cannot be rejected. As already mentioned, analyzing FEM results provide some engineering judgment and experience. For that reason the results should not overwrite the capacities according to the standards, but provide more clarity about the allowable plastic strains in the connection.

Most standards include geometry restrictions, but these are not always fulfilled. If the geometry is not covered by the standard, but within the scope of the FEM results, the FEM results provide clarity about the design and capacity. A geometry which is covered by a standard and is close to the “real” geometry can be compared with the “real” geometry via the FEM results. For example:

- If the clearance is not fulfilling the clearance restriction, the design is not according to a standard. For this case the FEM results can validate or reject a design with their capacity.
- If cheek plates are used, the FEM results provide information about the stress distribution which can be used as input in a standard.

#### 7.3.1 Method to determine additional capacities

The formulas which predict the FEM results can be used to determine capacities for designs which are not fulfilling the requirements of a specified standard. If the geometry is not according to a specified standard, the following scheme can be used to determine the capacity.

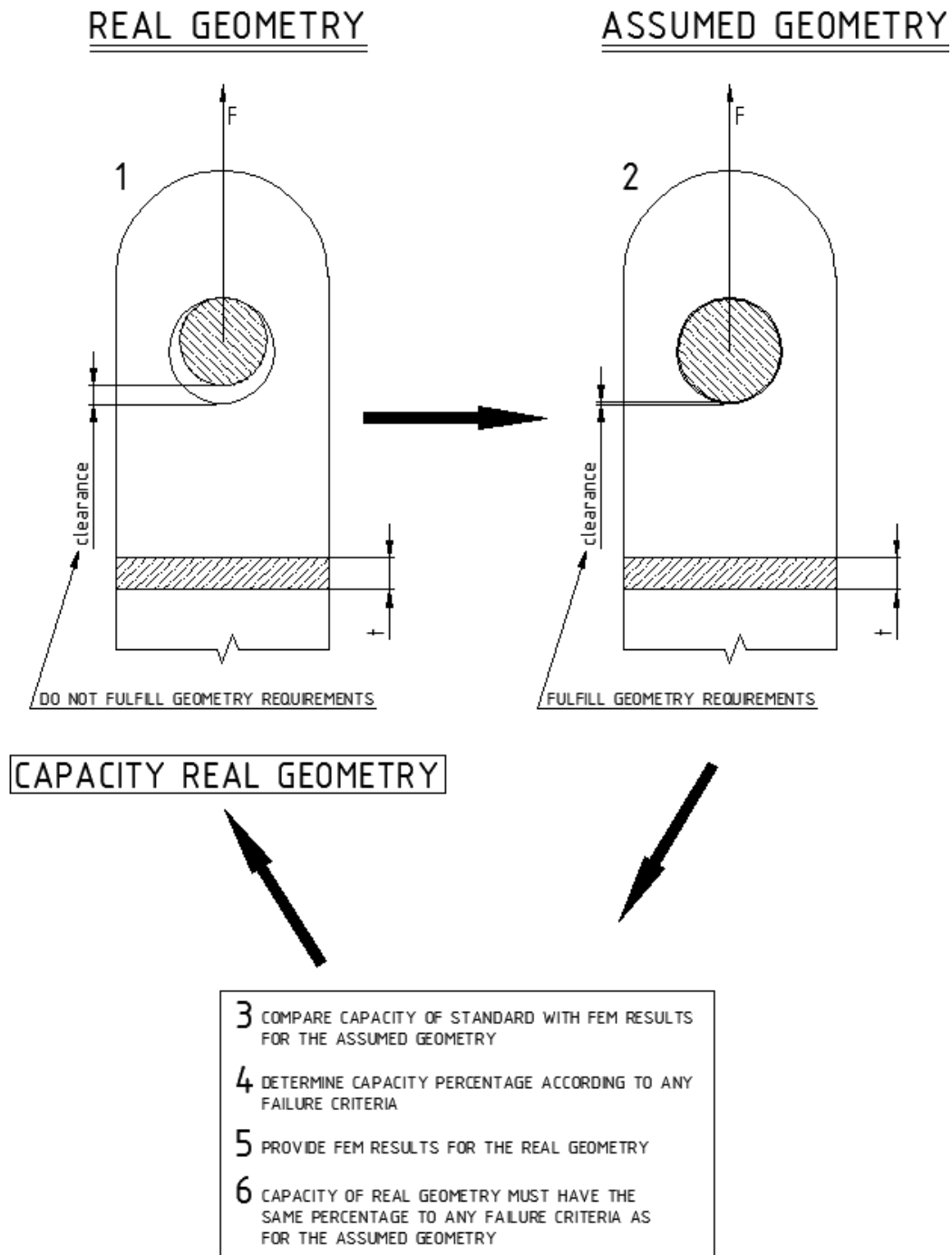


Figure 7-1: Method to determine capacity using FEM analysis

The following steps are taken to determine an additional capacity.

- 1 Determine the real geometry with their geometry parameters like in Figure 1-1.
- 2 Assume geometry which is close to the real geometry which fulfills the geometry requirements of the standard
- 3 Compare the capacity of the standard with the FEM results for the assumed geometry
- 4 Determine the capacity percentage according to any failure criteria of the FEM results for the assumed geometry
- 5 Provide FEM results of the real geometry
- 6 Capacity of real geometry must have the same percentage to any failure criteria as for the assumed geometry

The FEM results can also be used to improve the capacity by interpret the plastic strains since the FEM results provide additional information about the plastic strains. A competent person has to interpret if these strains are acceptable or not.

The formulas can be expanded for other steel grades using the yield stress, the ultimate tensile stress and the critical plastic strain.

$$F_{####,x\%} = F_{S690,0\%} * \frac{f_{y####}}{f_{yS690}} + (F_{S690,x\%} - F_{S690,0\%}) * \frac{E_{2,####}}{E_{2,S690}} \quad (7-45)$$

In equation ( 7-45 ) is #### the steel grade and x the plastic strain magnitude.  $E_2$  is the hardening stiffness according to equation ( 4-7 ). Note that such expansion is quite rough, and it is recommended to do additional research for other steel grades. For steel grades smaller than S690 this expansion is safe, while for higher steel grades this expansion might be too progressive.

## 8 Conclusion and recommendation

### 8.1 Conclusion

A lot of research about pinned connections is already done in the past, which resulted into different standards. Each standard has different design factors, restrictions and calculation rules and provide different capacities. The EN13001-3-1 [4] and the ASME BTH-1 [5] include unity checks which are dependent on most geometry parameters and seem to be most accurate compared to the FEM results.

Pinned connections can be modelled in different ways in a FEM program. To save time a 2D FEM model is already accurate enough to determine the internal stresses/strains. Only for very small clearances ( $< 0.5\%$ ) between the hole and pin a holespar can be applied to save time. For larger clearances a holespar model can provide to optimistic results. In that case the pin - hole contact should be modelled with contact elements which include the clearance. Elastic analysis shows that the peak stress in the model is sensitive for different element types and mesh sizes. Plastic analysis provides more similar results for different element types and mesh sizes and is therefore preferred. Only the bearing strains are still various for different type of models.

Standards include straightforward unity checks, but do not provide information about the stress/strain distribution within the connection. With a FEM analysis these stress/strain distributions are calculated and can be plotted. The capacities according to the standards results in different magnitude of stresses and strains. This is due to the simplified unity check formulas, which don't include all geometry effects. From this can be concluded that the FEM results do not automatically agree with the capacities according to the standards.

All geometry parameters (eye radius, eccentricity, pin diameter, hole diameter and thickness) have effect for each failure criteria. The formulas which include all these effects are quite complicated compared to the unity checks of the standards. These formulas predict FEM results with an accuracy of 10%, without doing a (time consuming) FEM analysis, and can be used additional to the standards. An advantage of these formulas is their wide range of applicability, so they provide additional information when geometry restrictions of a standard are not fulfilled.

Currently the load distribution between cheek plates and the mid plate is assumed to be dependent on the thicknesses. From FEM analysis can be concluded that this simple load distribution is not accurate because it is also dependent on the stiffness differences between the cheek plate, the mid plate and the stiffness of the welds between them. General a higher percentage of the load is transferred through the mid plate (which can be unsafe) and a smaller percentage is transferred through the cheek plates (which is safe), compared to the thickness ratio.

---

## 8.2 Recommendation

The current work is done to provide more information and clarity about the standards and FEM results of pinned connections at the Mammoet Solutions Department. This report can be used additional to the standards to verify designs which are not totally covered by a standard.

To improve this report some additional work is recommended. Some simplifications and unaddressed issues deserve more detailed investigation.

- Validate the results for other steel grades than S690, to prove the expansion of the FEM results of steel grade S690
- Study the effect of tapered eyes
- Study the effect of oblique and perpendicular loads
- Study the effect of various clearances for the load distribution between the cheek plates and the mid plate

---

# Bibliography

## General references

- [1] Bleich, Dr. Ing. F, "Theorie und beruchnung der eisernen brücken," Julius Springer, Berlin, 1924.
- [2] Poócza, A., "Zur Festigkeitsberechnung geschlossener Stangenköpfe," Springer, Berlin, 1967.
- [7] Boake, T.M. and Hui, V., "Fun is in the Details: Innovation in Steel Connections," Steel Structures Education foundation, [Online]. Available: [tboake.com/SSEF1/pin.shtml](http://tboake.com/SSEF1/pin.shtml). [Accessed 16 10 2014].
- [8] Bohny, F., "Theorie und Konstruktion versteifter Hängebrücken," Engelmann, Darmstadt, 1905.
- [9] Schaper, G., Eisenen Brücke, Berlin: Verlag Wilhelm Ernst & Sohn Berlin, 1908.
- [10] Reissner, H. and Strauch, F, "Ringplatte und Augenstab," *Ingenieur-Archiv*, vol. IV, p. 481, 1933.
- [11] Reidelbach, W., "Der Spannungszustand in einem durchbohrten, durch eine Bolzenkraft auf Zug beanspruchten Stangenkopf," *Das Industrieblatt* Bd.62, Nr.11, Berlin, 1962.
- [12] Hertz, H. R., Über die Berührung elastischer Körper, Berlin: Miscelaneous Papers, 1882.
- [13] Pilkey, W. D., Petersons Stress Concentration Factors, New York: John Wiley & Sons, Inc., 1997.
- [14] Ekvall, J.C., "Static Strength Analysis of Pin-Loaded Lugs," *Journal of Aircraft*, pp. 438-443, May 1986.
- [15] Petersen, C, "Verbindungstechnik III: Bolzenverbindungen mit Augenlaschen," in *Stahlbau*, Braunschweig, Friedr. Vieweg & Sohn Verslagsgesellschaft mbH, 1988, pp. 517,528.
- [16] Dietz, P. and Rothe, F, "Berechnung und Optimierung von Bolzen-Lasch-Verbindungen," IMW Institutsmitteliung, 1994.
- [17] Guo-Geruschkat, Dipl. Ing. Z. N., "Augenstab-Bolzen-Verbindungen unter Berücksichtigung der

Reibung," Universität Hannover, Hannover, 2001.

[18] Duerr, D., "Pinned Connection Strength and Behavior," Journal of Structural Engineering, 2006.

[21] ANSYS, *Mechanical APDL v.14.0*.

[23] M. Dobrescu, "Influence of ductility in the design of (high strength) steel bridges," <http://repository.tudelft.nl/>, Delft, 2014.

[24] Ana M Girao Coleho, Frans S. K. Bijlaard, "Finite element evaluation of the rotation capacity of partial strength steel joints," 2010.

[25] D. M. Kolstein, *Fatigue*, Delft: Faculty of Civil Engineering and Geosciences, 2007.

### Normative references

[3] NEN-EN 1993-1-8, „Eurocode 3: Design of steel structures - Part 1-8: Design of joints,” European committee for standardization, Brussels, 2006.

[4] NEN-EN 13001-3-1, „Normcommissie 345002 "Hijswerktuigen",” Nederlands Normalisatie-instituut, Delft, 2012.

[5] ASME BTH-1-2011, „Design of Below-the-Hook Lifting Devices,” The American Society of Mechanical Engineers, New York, 2012.

[6] NEN 6786, „Voorschriften voor het ontwerpen van beweegbare bruggen (VOBB),” Normcommissie 351062 "Beweegbare bruggen", Delft, 2001.

[19] AISC 360-10, *Specification for Structural Steel Buildings*, Chicago: American Institute of Steel Construction, 2010.

[20] Maddux, G.E., „Stress Analysis Manual,” Technology Incorporated, Dayton, 1969.

[22] NEN-EN 1993-1-5+C1, „Eurocode 3: Ontwerp en berekening van staalconstructies - Deel 1-5: Constructieve plaatvelden,” European Committee for Standardization, Brussel, 2012.

# Appendices

# A Literature study

## A.1 Introduction

During the Bachelor Civil Engineering and Master Structural Engineering at Delft mechanical and structural topics are educated. All this information and knowledge earned gives a good technical background to understand other topics such like pinned connections. The steel topic courses already provide some basic knowledge about steel properties and steel connections. To gain more specific information about pinned connections a literature study is done, which is summarized in this chapter.

The main goal of this literature study is to give an overview of different standards and theories. In this overview the differences, the similarities and the design restrictions are stated.

Mammoet is a worldwide operating company and is therefore required to use different standards for different countries. Currently there are various standards which may be used at Mammoet.

Unfortunately all these standards are different and give different results. This is due the fact that the standards have limited design variables, different safety levels and methods to check the connections.

Technical background of pinned connections should give more clearance about differences in the standards. Therefore the analytical and empirical backgrounds of pinned connections are studied.

To collect literature, a TU-Delft campus license is used to get access to more publications. Also the TU-Delft library provides many articles about pinned connections. For this study the following kind of information is studied about pinned connections:

- General information
- Analytical background
- Empirical background
- Standards

The analytical background, empirical background and standards are studied on the theories used, failure criteria, design restrictions and strength calculations. All strength calculations are described in Appendix B.

## A.2 Pinned connections

### A.2.1 General

Pinned connections are one of the simplest steel to steel connections. They are easy to fabricate, and easy to assemble or disassemble. Pinned connections allow uniaxial rotations, thus preventing

---

bending moments. A pinned connection has only one pin (or bolt, axle) going through a lapped type connection, like pad eyes or eye bars.

A pinned connection allows rotation and only transfers shear forces through the pin. The design load will determine the dimensions of the connection. Pinned connections are often used to simplify construction. If there are slight differences in angles of construction elements pinned connections prevent high internal stresses since they are statically determined. In Figure A-1 to Figure A-7 some general applications of pinned connections are shown according to [7].

Pinned connections can be used as column base like in Figure A-1 and Figure A-2. Bending moments and shear forces in the pin are dependent on the type of connection and the clearances between the connected parts.



**Figure A-1: Typical 2-1 connection (one part at the foundation, two parts at the column)**



**Figure A-2: Typical 2-2 connection (two parts at the foundation and two parts at the column)**

Pinned connections can also be a part of a bracing system. It might connect even more than just two members, for example three shown in Figure A-3.



**Figure A-3: Connection with more than two members**



**Figure A-4: Bracing system**

Advantages of pinned connections in bracing systems are that connected members are statically determined and only transfer axial loads, and therefore the dimensions can be reduced. In Figure A-5 is shown how pinned members can be fabricated. Eyes are often welded to the main members, and further detailing improves the smoothness of the connection, see Figure A-6. In this case cheekplates are welded on the eye, to improve the strength of the connection.



**Figure A-5: Fabrication of a pinned member**



**Figure A-6: Finished pinned member**

Pinned connections might even be aesthetic connections, see Figure A-7, in which the impression of movement is indicated.



**Figure A-7: Aesthetic connection**

### **A.2.2 Mammoet**

Pinned connections are commonly used at Mammoet for all different type of equipment. Assembly and disassembly of components are forming equipment. This is a frequently occurring operation at Mammoet and is easy with pinned connections.

Equipment of Mammoet is often disassembled in “small” components (Figure A-8) which can be transported in/on containers (Figure A-9 and Figure A-10). This is called containerization in Mammoet terms.



**Figure A-8: Disassembled parts which can be transported on containers**



**Figure A-9: Different type of containers which are used by Mammoet**



**Figure A-10: Disassembled part on container**

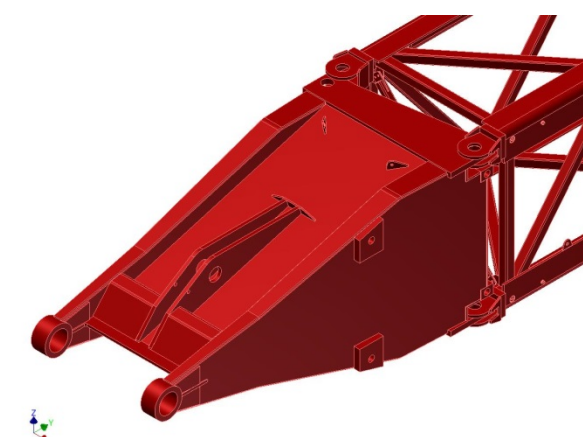


**Figure A-11: Model of two assembled parts**

After transport the disassembled components can be connected on site (Figure A-11). Depending on the size and application of the connection this can be done by hand or with hydraulic tools. Clearances in connections are also dependent on the application of the connection. Some connections are not only designed to connect components, but are the center of rotation (pivot) of the equipment (Figure A-12 and Figure A-13).



**Figure A-12: Pivot application**

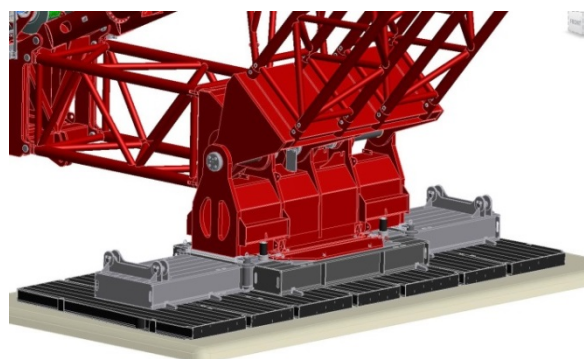


**Figure A-13: Pivot application for main boom**

In application of equipment the use of pinned connections are still easy to see. In Figure A-14 one might see the pivots of the booms of a crane. In a detailed look in Figure A-15 one might also see the connections of the braced parts (white painted in booms of the crane).

Mammoet does not use pinned connections only for main pivots and assemble components. Some typical members which have pinned connections are shown in Figure A-15.



Figure A-14: Application of equipment



Figure A-15: Typical members for pinned connections

### A.2.3 History

In the end of the 19<sup>th</sup> century and the beginning of the 20<sup>th</sup> century some bridge designers started to make standards for pinned connections. The first bridge type that was developed was the suspension bridge like Figure A-17, where the suspension “cable” was composed of “eye bars” (Figure A-16) or “link plates” [8].

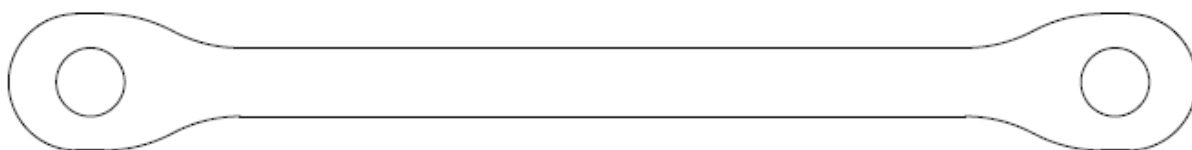


Figure A-16: Typical eye bar

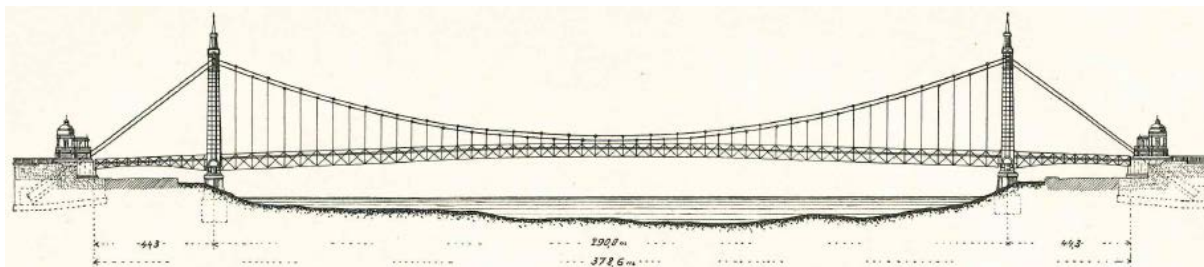


Figure A-17: Elisabeth Bridge in Budapest (Bohny (1905), Fig. 41.)

There was hardly any information about stress distribution in the eye at that time. With rough approximations, experimental results and experience the first connections were designed depending on the width of the bar and/or the diameter of the hole, see Figure A-18. In Table A-1 a list of some designs for pinned connections are shown. In Table A-1 parameter  $b$  is similar as  $L_{gross}$ , parameter  $a$  is the width in the net sections, parameter  $c$  is the height above the hole and  $d$  is the hole diameter. Figure A-18 show these different designs.

Project/ Engineer	a=	c=
Elisabeth Bridge (Budapest, Hungary)	$0.58b (d=2b/3)$	$0.75b$
Winkler (Wien, Austria)	$0.5b + 0.333d$	$0.5b + 0.667d$
Häseler (Germany)	$0.5b + 0.167d$	$0.5b + 0.625d$
Gerber (Germany)	$0.55b$	$0.75b$
Pencoyd-Works (USA)	$0.665b$	$0.665b$
Baltimore Bridge- company (USA)	$0.75b$	$0.75b$
Yale University (USA)	$0.645b + 0.125d$	$0.645b + 0.125d$

Table A-1: Standard geometries in the late 19<sup>th</sup> century/ early 20<sup>th</sup> century

It is interesting that the recommendation of Winkler is the basis of the currently used standard EN-1993-1-8 [3].

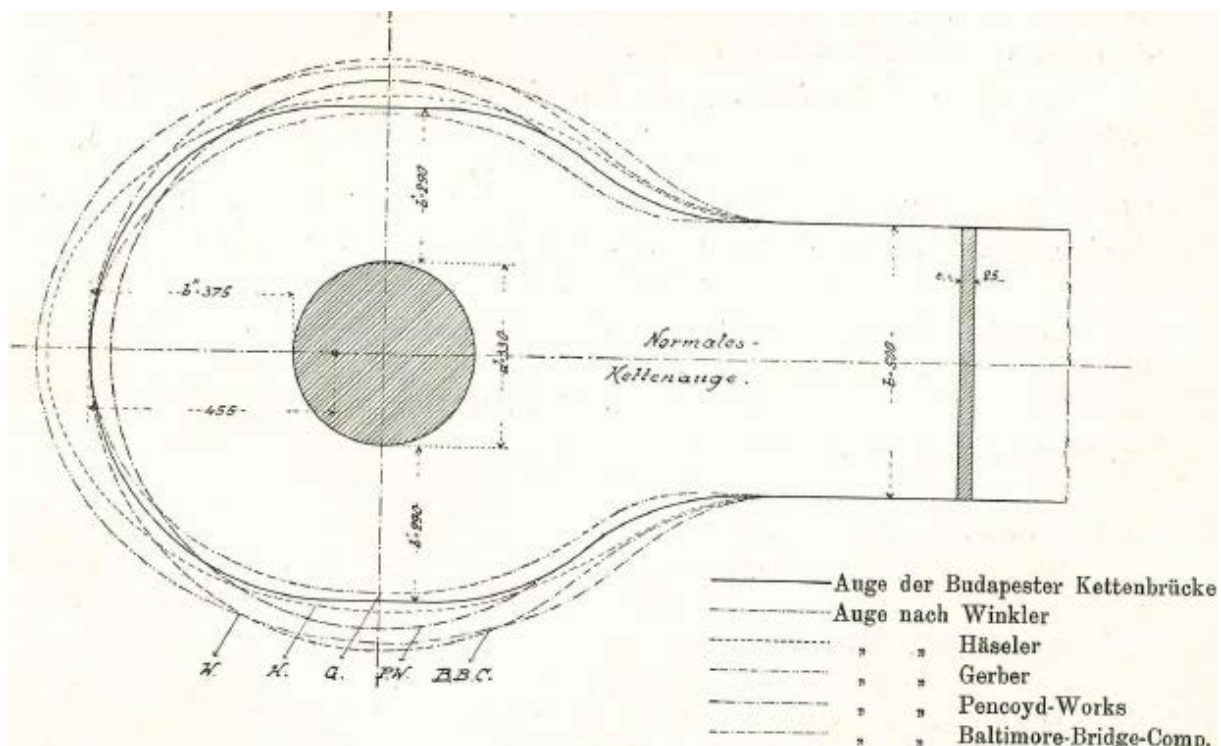
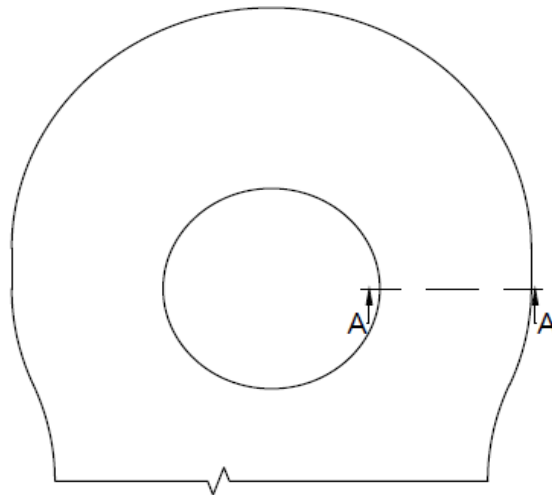


Figure A-18: Standard geometries in the late 19th century/ early 20th century (Bohny (1905), Fig. 69.)

The U.S.A. had the most experience in pinned connections at that time and it is remarkable that the connections designed in the U.S.A. were bigger than connections designed in Europe. It was not well known how high the internal stresses in the connections would be and it was not allowed that the bar would fail at the eye.



**Figure A-19: Failure section A-A of the eye**

For the design of suspension bridges in Europe the maximum allowable stress was half of the yield stress. It was already expected that the maximum stress was in section A-A at the edge of the hole, see Figure A-19. In the beginning of the 20<sup>th</sup> century nothing was said about the stress distribution in that section. With experimental results of a reference eye the first stress concentration factors were derived for the design of pinned connections. To improve the design of pinned connection researchers did a lot of research and experiments for more detailed calculations of pinned connections. More failure mechanisms were derived, which are shown in Figure A-20 to Figure A-23.

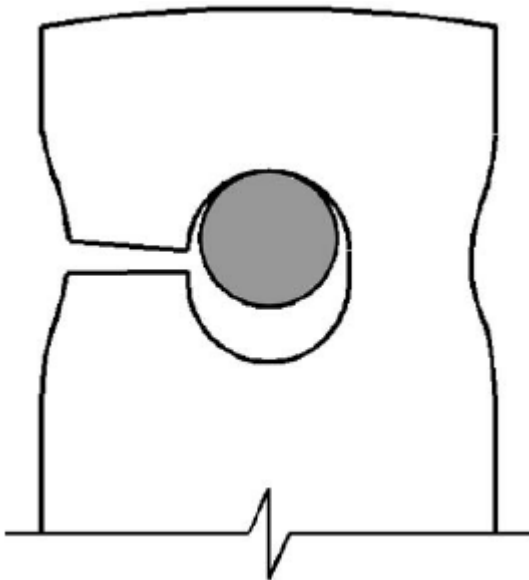


**Figure A-20: Tension in net section**

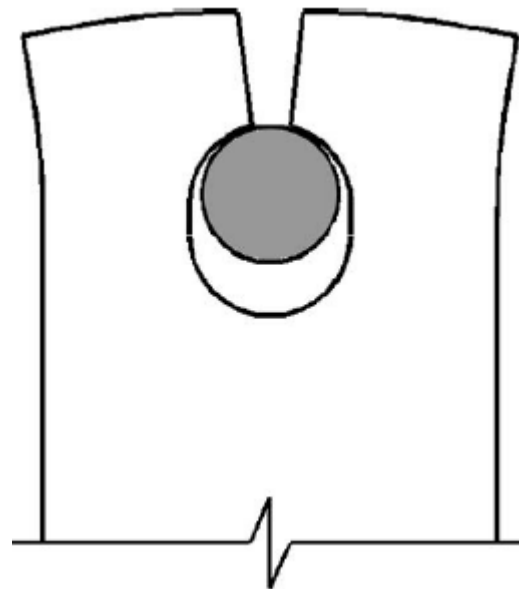


**Figure A-21: Fracture beyond the hole**

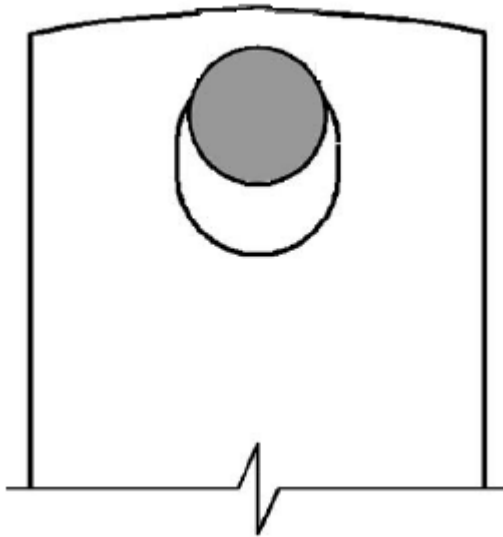


Figure A-22: Bearing failure

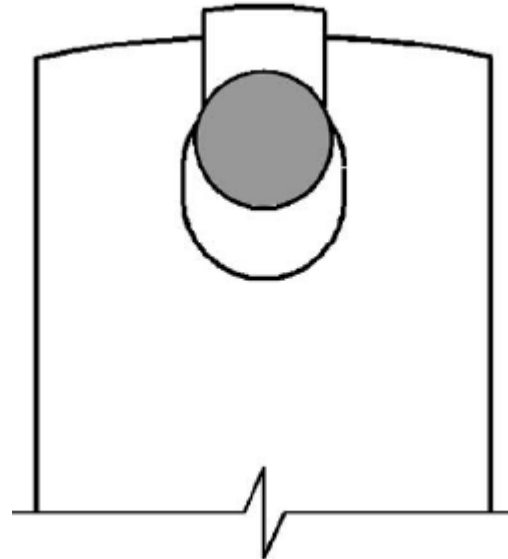


Figure A-23: Double shear plane

In the beginning of the 20<sup>th</sup> century the first theories were derived with mathematics. In the end of the 20<sup>th</sup> century and the beginning of the 21<sup>st</sup> century most research is done with finite element programs. Paragraph A.3 and A.4 chronically state these theoretical and empirical findings. With these theories and experiments some design standards are developed which are stated in paragraph A.5. In chapter 2 all these theories and standards are compared.

### A.3 Analytical background

Several researches derived theories about stress distributions in pinned connections. These theories are based on different assumptions following by different results. In this paragraph the following theories are summarized:

- Hertz
- Schaper
- Bleich
- Reissner and Strauch
- Reidelbach
- Poócza

#### Hertz

Heinrich Hertz did research [12] to contact stress when two surfaces are in contact. Nowadays his theory is still useful to calculate surface stresses between two elastic bodies. This theory is only valid for elastic strains/stresses.

#### Schaper

G. Schaper [9] assumed that for small clearances the bearing load on the eye is just radial orientated. By integration from C' to A' or B' the resultant vertical force should be equal to half of F (the tension force P in Figure A-24).

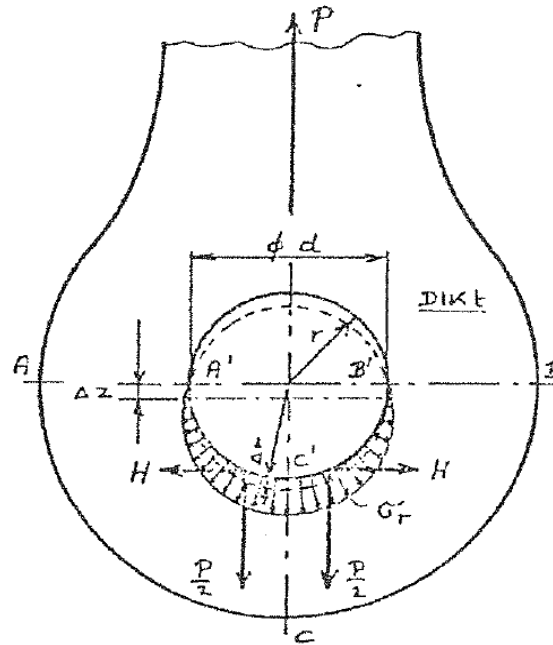


Figure A-24: Eye geometry for Schaper theory

Schaper assumed that the maximum bearing stress is equal to:

$$\sigma_{b,Ed} = \frac{4}{\pi} * \frac{F}{d_p * t} \tag{A-1}$$

The distributed bearing stress is simplified to two point loads, with a vertical force of

$$V = F/2 \tag{A-2}$$

and a horizontal force of

$$H = F/\pi \tag{A-3}$$

**Bleich**

Dr. Ing. F. Bleich [1] derived a set of equations from which the stress concentration factors could be derived. As basis he analyzed an eye like Figure A-25. To derive equilibrium equations, Bleich made the following assumptions:

- The eye is analyzed as an strong curved beam with a constant cross section
- The yield stress is never exceeded
- The radial eye sections remain flat after deformations
- The bearing force is calculated without a clearance and is radial orientated and taken as:

$$p = -p_0 * \cos \psi \tag{A-4}$$

$$p_0 = \frac{-4 * F}{\pi * d_h} \tag{A-5}$$

- The normal stress under the eye is even distributed and its integral is equal to F.

With these assumptions the eye is schematized as Figure A-25 and Figure A-26. From Figure A-26 a set of equilibrium equations is derived, and with these equations all section stresses can be derived.

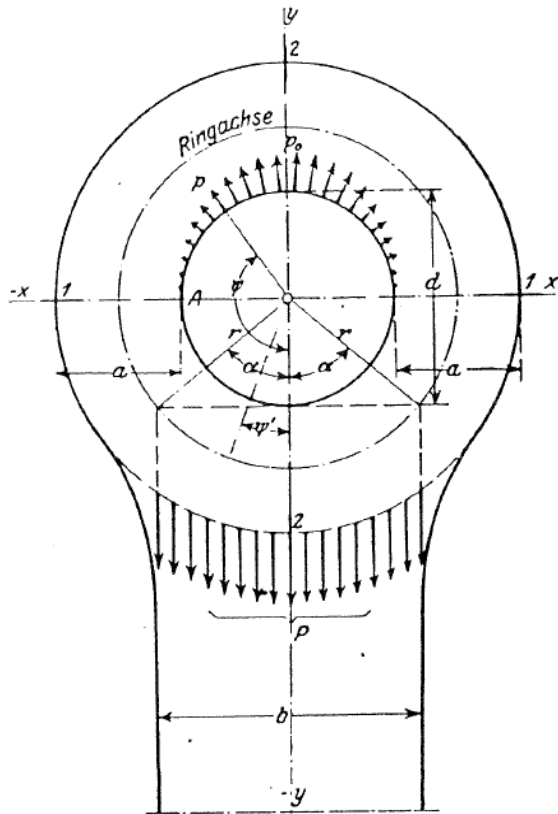


Figure A-25: Schematized eye (Theorie und berechnung der eisernen brücken (1924), Abb. 201)

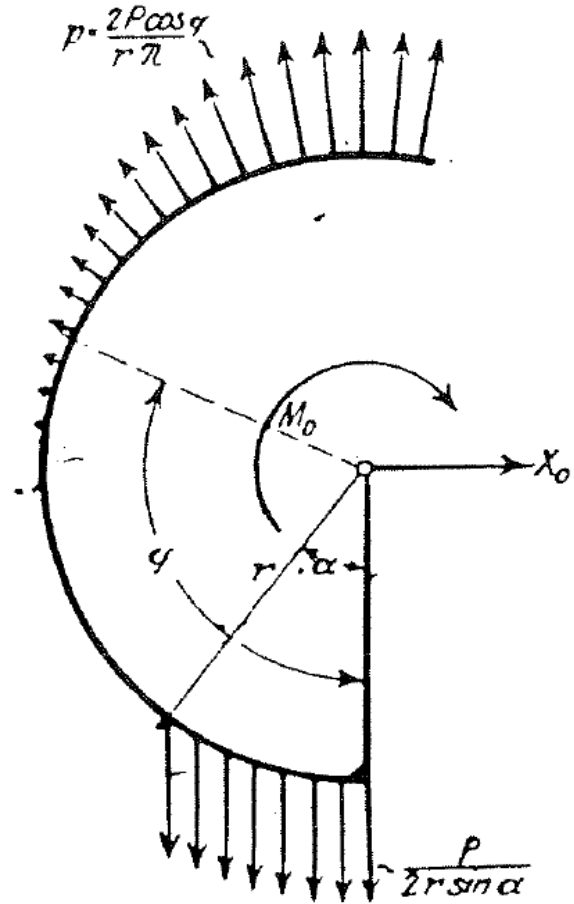


Figure A-26: Schematized eye (Theorie und berechnung der eisernen brücken (1924), Abb. 203)

Guo-Gerschkat [17] found out that the theory derived by Bleich is only useful for

$$0.6 \leq \frac{d_h}{R_{eye}} \leq 1 \quad (A-6)$$

because for smaller ratios the rope effect is neglected, and for higher ratios the Bernoulli theory is less applicable.

### Reissner

H. Reissner and F. Strauch [10] also used the elasticity and deformations theory but made another assumption than Bleich [1].

- The normal stress under the eye is sinusoidal distributed and radial orientated

With these assumptions they derived a formula to calculate the maximum stress for tension in the net section (Figure A-27).

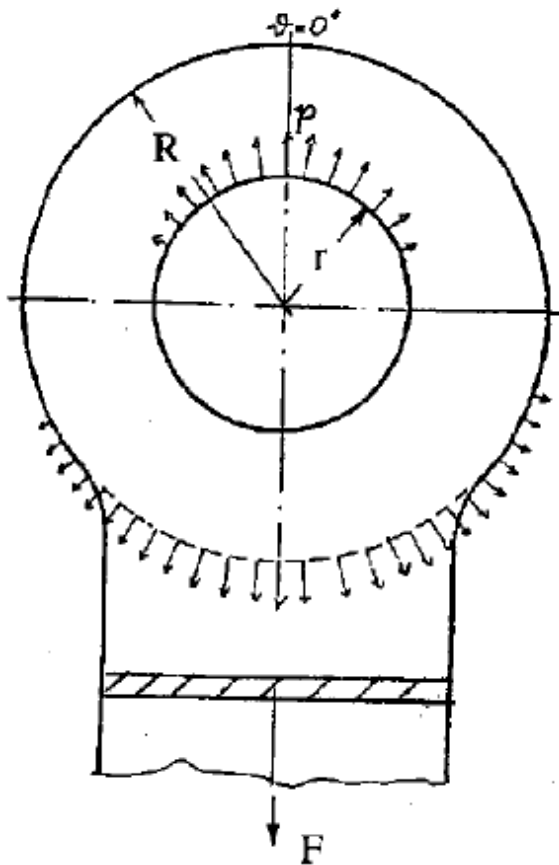


Figure A-27: Stress distribution according to Reissner and Strauch

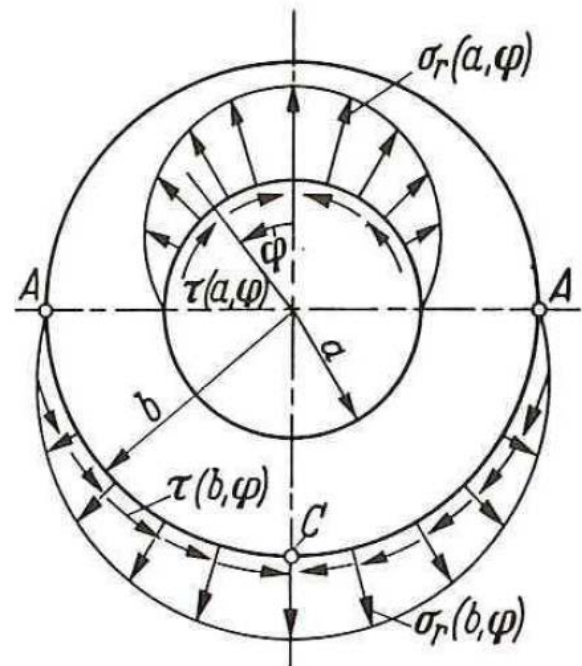


Figure A-28: Stress assumption in according to Reidelbach (1967), Bild 3)

### Reidelbach

In contrast to H. Reissner and Fr. Strauch [10], W. Reidelbach [11] made the assumption that there is not only a normal stress but also a shear stress in the section under the eye (Figure A-28). With elasticity theory and mathematics he derived a set of equations to calculate stress concentration factors.

Reidelbach also derived stress concentration factors in the section beyond the hole. He did this for two sets of assumptions.

1. Radial and shear stress are sinusoidal distributed
2. Radial and shear stress are sinusoidal quadratic distributed

Stress concentration factors for two eye geometries are shown in Table A-2. For explanation of the inner and outer edge, see Figure A-29.

$K_t$	Inner edge		Outer edge	
	Sinusoidal	Sinusoidal quadratic	Sinusoidal	Sinusoidal quadratic
$R=d_h$	-1.54	-3.22	3.33	4.07
$R=4/3d_h$	-0.84	-1.83	1.54	1.90

Table A-2:  $K_t$  for section beyond the hole in according to Reidelbach

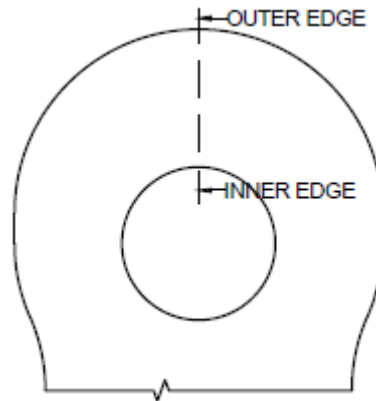
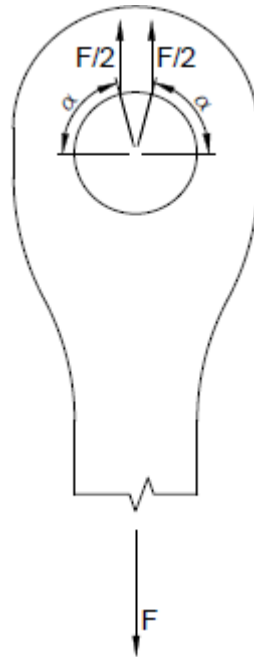


Figure A-29: Inner and outer edge on section beyond the hole

**Poócza**

Dipl.-Ing. Antal Poócza [2] made the following assumptions to calculate nominal stresses in the eye:

- Thickness is constant
- Stress over the thickness is constant
- No supports/ effect from bearings to the strength of the eye
- Eye geometry is symmetric
- The deformation of the eye under a certain load, doesn't change the interaction between the pin and the eye (2<sup>nd</sup> order effect is neglected)
- The eye is loaded in accordance to Figure A-30



**Figure A-30: Connection loading according to Poócza**

With these base assumptions Poócza derived a set of equations to calculate the nominal stresses in an eye. Therefore he used the 2<sup>nd</sup> theory of Castigliano:

$$\frac{\partial A}{\partial M_0} = 0 \tag{A-7}$$

The deformation work A is dependent on the moment of inertia of all cross-sections through the eye, and all bending moments through the eye. Therefore all cross-sections of the eye need to be described. Poócza described the geometry of the eye as a strong curved beam with variable section heights. (This is in contrast to the theory of Bleich [1].)

To solve the equation of deformation work this equation is simplified by approximating an upper- and a lower bound.  $\alpha$  (see Figure A-30) should be taken as 75°.

**Conclusion**

All analytical backgrounds are bases on stress distributions in pinned connections. These stress distributions are based on elastic material behavior. Differences in outcome of these theories are because of other assumptions and simplifications.

**A.4 Empirical background**

Since all analytical theories give different results, there are still uncertainties about the validity of the analytical theories. To give more value and clarity many engineers did research and experiments on pinned connections. Much of data is gained from experiments and later on most data is gained from FEM analysis. In this paragraph the following empirical studies are summarized:

- Peterson
- Ekvall
- Petersen
- Dietz
- Guo-Geruschkat
- Duerr

## Peterson

Peterson derived with experiments stress concentration factors for all kind of shapes and structures, and published his findings in 1953. Walter D. Pilkey republished these findings in 1997 [13]. Part of this book is about pinned connections. Stress concentration factors are derived around the perimeter of the hole. The effect of clearance between the pin and the hole is included in these factors.

## Ekvall

J.C. Ekvall [14] studied various experiments to derive the design strength for different type of pinned connections. He provides a manual with different type of graphs to calculate the design strength. Ekvall did not only study straight lugs but also tapered ( $\beta \neq 0$ ) lugs with a load angle  $\alpha$  between 0 and 90. Also the effect of eccentricity is included in these calculations.

## Petersen

C. Petersen [15] summarized and analyzed a lot of literature and experiments about pinned connections. He compared different stress concentration factor studies, from which he derived the following formula:

$$K_t = 3.4 * \left(\frac{c}{a}\right)^{0.2} * \left(\frac{c}{d}\right)^{0.5}, \text{ if } 0.8 < \frac{c}{a} < 1.1 \text{ \& } 0.6 < \frac{c}{d} < 1.3 \quad (\text{A-8})$$

Petersen also derived the safety checks for failure in the net section and fracture beyond the hole (Figure A-20 and Figure A-21) which are the basis of the EN-1993-1-8 [3] and are frequently used at Mammoet.

## Dietz

Dietz [16] did research about the following issues:

- Surface pressure between pins and holes
  - Contact angle
  - Surface pressure over the hole
  - Surface pressure over the thickness
- Calculation of the stresses in section beside the hole
  - Influence load introduction
  - Structural calculation method (influence on support effects)
  - Stress analysis
- Eye optimization

Most useful for this thesis is about his research the surface pressure between the pin and the hole.

## Guo-Geruschkat

Dip. Ing. Z. Guo-Geruschkat did PhD [17] on pinned connections at the University of Hannover (Germany). He compared several parameter studies for different eye geometries.

He analyzed the following influence with a 2D FEM analysis with plain strain elements:

- Hole clearance
- Friction between pin and eye
- Geometry parameters
- Applied load

He compared some results of the 2D FEM analysis with a 3D FEM analysis with solid elements. Only stresses in the eyes are analyzed. The pin is just modelled for input of the analysis. He compared his findings with DIN22261 Part2 and recommended some simple and safe stress concentration factors in

addition to DIN 22261. These stress concentration factors are only valid for eye geometries which are in according to

$$0.3 \leq g = \frac{R - r}{R + r} \leq 0.5 \quad (\text{A-9})$$

in which  $g$  is a ratio of the eye radius and the hole diameter.

Other restrictions to his research are a friction between the pin and the hole of 0.3, a clearance smaller than 0.4mm and a nominal stress in the net section of at least 25 N/mm<sup>2</sup>. For Mammoet applications the clearance between the pin and hole will be usually higher than 0.4mm.

### Duerr

David Duerr [18] compared and summarized different theoretical and experimental studies (since ± 1940). First issue of his article is the stress concentration factor for tension for elastic behavior in the net section. Comparing experimental results he derived this factor as:

$$k = 1.5 + 2.5 * \frac{c}{d_h} - 0.27 * \left(\frac{c}{d_h}\right)^2 \quad (\text{A-10})$$

This equation is valid for small or no clearance between the pin and hole. Beside this elastic stress distribution, Duerr did also research to the following failure mechanisms of pinned connections:

- Bearing stress and deformation
- Tension in the net section through the hole
- Splitting on a single plane beyond the hole
- Shear on two planes beyond the hole
- Out of plane instability
- Shear of the pin
- Bending of the pin

All these failure mechanisms are verified with experimental data. These failure criteria are the base of the ASME BTH-1 standard [5]. Duerr mentioned that cheek plates can be applied and that the strength of the connection becomes as strong as the summation of the strength of the mid plate and cheek plates. This is in agreement with some experimental data, but to give clear conclusions Duerr recommended more research must be provided. Another approach is to divide the bearing load over the different plates, and calculate the critical strength versus the bearing load per plate.

### Conclusion

Like all analytical backgrounds, most empirical background is based on stress concentration factors in the net section based on elastic material behavior. The ultimate strength includes plasticity and therefore stress redistributions occur. Ekvall, Petersen and Duerr studied the ultimate strengths of pinned connections.

## **A.5 Standards**

As mentioned Mammoet is a worldwide operating company which have to deal with different regulations and legislations. Therefore different standards are currently used at Mammoet. These standards have different ways to check the strength, and also have different design restrictions. Because none of these standards cover all design criteria which are applied at Mammoet, it is currently not very clear which standard one should use. The following standards are used at Mammoet:

- DIN18800 Part 1
- NEN6772
- EN1993-1-8
- EN13001-3-1
- ASME BTH-1
- AISC

Because Eurocode (EN) standards overrule national standards like NEN (in the Netherlands) and DIN (in Germany) standards, DIN 18800 Part 1 and NEN6772 are neglected.

In this literature study also two other standards (NEN6786 and the Stress Analysis Manual) are included which are not used at Mammoet. These standards might be valuable because they have other design and geometry restrictions.

The following standards are stated:

- EN1993-1-8
- EN13001-3-1
- ASME BTH-1
- AISC 360-10
- NEN6786
- Stress Analysis Manual

### **EN1993-1-8**

#### **General:**

This European standard [3] describes the calculation rules for all type of connections, including pinned connections. Resistance of a joint should be determined on the basis of the resistances of its basic components. Linear-elastic or elastic-plastic analysis may be used in the design of joints.

#### **Loads:**

Applied forces at the ultimate limit state should be determined according to the principles in EN 1993-1-1. Fatigue loads must satisfy the principles given in EN1993-1-9.

Loads are commonly multiplied with load factors  $\gamma_F$  to get the design load  $F_{Ed}$ .

#### **Design validity:**

Standard covers steel grades S235 up to S700 (steel grades higher than 460 are in accordance to EN1993-1-12). Only a particular geometry is covered for the design of pinned connections. The geometry parameters are dependent on each other. Nothing is stated about other than the described geometries, nothing is stated about cheek plates and nothing is stated about loads in other directions.

#### **Static strength checks:**

Only describes the strength of the pin. The strength of the eye can be derived from the geometry specifications. Strength is divided by a material factor  $\gamma_m$  which is separated in  $\gamma_{m,2}$  and  $\gamma_{m,6,ser}$ .

Safety checks:

- Pin bearing
  - Pin bending
  - Pin shear
  - Pin combined bending + shear
  - Eye fracture beyond the hole
  - Eye strength in the net section
-

- Eye bearing strength

**Background information:**

No background about pinned connections is stated in the standard. This literature study pointed out that C. Petersen derived some equations which are the same as in this standard. The geometry restrictions are actually the same as Winkler derived more than hundred years ago.

**EN13001-3-1**

**General:**

This European Standard [4] is to be used together with EN13001-1 and EN13001-2 and as such they specify general conditions, requirements and methods to prevent mechanical hazards of cranes by design and theoretical verification. Plasticity is not allowed.

**Loads:**

Applied forces at the ultimate limit state should be determined according to EN13001-1 and EN13001-2. Fatigue loads must satisfy the principles given in chapter 6 of the EN13001-3-1.

**Design validity:**

The ratio of the ultimate tensile stress and the yield stress should be in accordance to:

$$\frac{f_u}{f_y} \geq 1.05 \quad (\text{A-11})$$

Several (more than in the EN1993-1-8) geometries are covered. This standard allows the use of hollow pins. Nothing is stated about cheek plates and nothing is stated about loads in other directions.

**Static strength checks:**

Standard describes the strength of the pin and the strength of the eyes. Strength is divided by several factors including a stress concentration factor and material factor  $\gamma_m$ .

Safety checks:

- Pin bearing
- Pin bending
- Pin shear includes factor for hollow pins
- Eye strength in the net section
- Eye shear beyond the hole parallel to load direction
- Eye bearing strength

**Background information:**

No background about pinned connections is stated.

**ASME BTH-1**

**General:**

This standard [5] provides minimum structural and mechanical design and electrical component selection criteria for ASME B30.20, Below-the-Hook Lifting Devices. Pinned connections are defined as a nonpermanent connection.

**Loads:**

Applied forces at the ultimate limit state should be determined. This standard describes a structural analysis method for the strength calculation. Fatigue loads and resistance should be calculated as described in paragraph 3.4 of the standard.

**Design validity:**

Only covers load in the eye direction. Nothing is stated about cheek plates and nothing is stated about loads in other directions.

**Static strength checks:**

This standard is based on failure strength (including plastic deformations and ultimate tensile stresses), and multiplied with certain design and load factors to give safe design provisions. Standard includes a design category A and B (in accordance to paragraph 3.1.3), which lower the strength with factor  $N_D$ . This design factors are based on the variance and reliability of the load and strength. All checks are based on a reduction of the strength.

Safety checks:

- Eye strength in the net section
- Eye fracture beyond the hole
- Eye shear strength
- Eye bearing
- Pin bearing
- Pin bending
- Pin shear includes factor for hollow pins

**Background information:**

[18] (D. Duerr)

**AISC 360-10****General:**

This American standard [19] is a specification for structural steel buildings. Part of this standard is about the design of pinned connections.

**Loads:**

Applied forces at the ultimate limit state should be determined. This standard describes a structural analysis method for the strength calculation.

**Design validity:**

Only covers load in the eye direction. Clearance of the hole should be in accordance to:

$$d_h - d_p \leq 1mm \quad (\text{A-12})$$

Nothing is stated about cheek plates and nothing is stated about loads in other directions.

**Static strength checks:**

This standard is based on failure strength (including plastic deformations and ultimate tensile stresses). All checks are based on a reduction of the yield or ultimate tensile stress. These calculated strengths are multiplied with given safety factors to calculate the design strength.

Safety checks:

- Eye strength in the net section
-

- Eye shear strength
- Eye bearing strength
- Eye gross section of the eye bar

### **NEN 6786**

#### **General:**

This Dutch standard [6] describes technical provisions about the design of mechanical equipment and electrical installations of all types of moveable bridges for road and rail transport. This standard is not used at Mammoet. Because the load direction perpendicular to the eye geometry is included in this standard, it is valuable for comparison with FEM results.

#### **Loads:**

Applied load is design force  $F_{Ed}$ . This design load is already including load factors in accordance to the described standard. Loads may be applied in the eye direction or perpendicular to the eye geometry.

#### **Design validity:**

Covers low and higher clearances between the pins and holes. Nothing is stated about cheek plates.

#### **Static strength checks:**

Standard describes how to calculate stress in the eyes. Stresses are multiplied with a stress concentration factor  $k$ , depending on the geometry. These design stresses should be compared with the maximum allowable stresses.

#### **Safety checks:**

- Eye strength in the net section
- Eye fracture beyond the hole
- Eye shear strength

### **Stress Analysis Manual**

#### **General:**

In 1969 the American Airforce developed a manual about Structural Analysis Methods. This results in the Stress Analysis Manual [20]. This manual is developed by the American Airforce, and is therefore a manual for aerospace engineers. Part of this manual is about pinned connections. Chapter 9 of this manual presents methods of analyzing eyes (lugs) and their pins and bushings under various loading angles. This standard is not used at Mammoet. Because this standard includes oblique and perpendicular loads, it is valuable for comparison.

#### **Loads:**

Input for the strength calculations and unity checks should be the design load. The direction of this load may be oblique or perpendicular to the eye geometry. Nothing is stated about any load factor.

#### **Design validity:**

All strength calculations are based on ultimate material strength.

#### **Static strength checks:**

- Eye strength in the net section
- Eye fracture beyond the hole
- Eye bearing strength
- Pin bending strength

- Pin shear strength
- Pin combined bending + shear

### **Conclusion**

Standards provide obviously ways to calculate the strength of pinned connections. The calculations are relatively simple since all analytical theories and/or empirical background are simplified to small formulas or charts. Unfortunately all standards provide different strength calculations. Also the outcome of the standards is different. One provides design stress under loading, while others provide ultimate strengths of the connection. Also different standards include different safety levels. To compare the standards with each other these safety factors (load factors and material factors) must be set to an identical magnitude. The American standards are mostly based on plastic behavior, while the European standards are based on elastic/plastic behavior.

### **A.6 Comparison / summary**

It is clear that already a lot of research is done about pinned connections. Unfortunately all this research did not provide a clear standard for all type of pinned connections. The use of for example cheek plates and oblique loads is not mentioned in most references. Nowadays some different standards are used at Mammoet with different design restrictions. To develop a clear calculation method for Mammoet, all references are compared by a numerical analysis. A FEM analysis with the program ANSYS [21] should validate and complement the compared references.

In Table A-3 all backgrounds and standards are summarized in a table with possible strength criteria. It is clear that most literature is about tensile in the net section of the eye (Figure A-20). This failure mechanism provides most uncertainties and questions. Bearing and shear stress in the eye, and stress distributions in the pin are less mentioned in the literature because it's more clear how these stresses are distributed. A comparative study in chapter 2 will indicate the differences of the backgrounds and the standards.

	Possible failure criteria							
	Background	Tensile in net section	Fracture beyond hole	Bearing	Shear	Bending pin	Shear pin	Extra info, influence parameters
Hertz	A			x				Clearance
Schaper	A			x				
Bleich	A	x	x	x				
Reissner	A	x						
Reidelbach	A	x						
Poócza	A	x	x					
Peterson	E	x						Clearance
Ekvall	E	x						Tapered eyes and oblique loads
Petersen	E	x	x			x	x	
Dietz	N	x		x				Clearance
Guo-Geruschkat	N	x						Clearance, tapered eyes and oblique loads
Duerr	E	x	x		x			Clearance and tapered eyes
EN1993-1-8	S	x	x	x		x	x	Clearance, geometry restrictions
EN13001-3-1	S	x		x	x	x	x	
ASME BTH-1	S	x	x	x	x	x	x	Clearance
AISC 360-10	S	x		x	x			Geometry restrictions
NEN6786	S	x	x					Clearance, and oblique loads
Stress Analysis Manual	S	x	x	x		x	x	Tapered eyes and oblique loads

Table A-3: Possible strength criteria

# B Capacity calculations

## B.1 Analytical background

### Hertz

$$\sigma_b = \sqrt{\frac{2 * F}{\pi * t} * \left(\frac{1}{d_p} - \frac{1}{d_h}\right) * \left(\frac{(1 - \nu_1^2)}{E_1} + \frac{(1 - \nu_2^2)}{E_2}\right)^{-1}} \leq f_y \quad (\text{B-1})$$

$$F_{Rd,b} = \frac{\pi * t * f_y^2 * \left(\frac{(1 - \nu_1^2)}{E_1} + \frac{(1 - \nu_2^2)}{E_2}\right)}{2 * \left(\frac{1}{d_p} - \frac{1}{d_h}\right)} \quad (\text{B-2})$$

### Schaper

$$\sigma_b = \frac{4}{\pi} * \frac{F}{d_p * t} \leq f_y \quad (\text{B-3})$$

$$F_{Rd,b} = \frac{f_y * \pi * d_p * t}{4} \quad (\text{B-4})$$

### Bleich

$$\sigma_b = \frac{4}{\pi} * \frac{F}{d_p * t} \leq f_y \quad (\text{B-5})$$

$$F_{Rd,b} = \frac{f_y * \pi * d_p * t}{4} \quad (\text{B-6})$$

$$r_a = \frac{R_{eye} + d_h/2}{2} \quad (\text{B-7})$$

$$Z = r_a^2 * \left[ r_a * \ln\left(\frac{r_a + c/2}{r_a - c/2}\right) - c \right] \quad (\text{B-8})$$

$$\alpha = \sin^{-1} \left[ \min \left( \frac{L_{gross}/2}{r_a}; 1 \right) \right] \quad (\text{B-9})$$

$$\beta = \frac{\frac{\alpha}{\sin(\alpha)} - \cos(\alpha) + (\pi - \alpha) * \sin(\alpha)}{8 * \pi * \left( 1 + \frac{c * r_a^2}{Z} \right)} - \quad (\text{B-10})$$

$$\frac{r_a^2}{Z} * \left[ \frac{\alpha}{\sin(\alpha)} + 3 * \cos(\alpha) - 2 * (\pi - \alpha) * \sin(\alpha) + \frac{16}{\pi} \right]$$

$$8 * \pi * \left( \frac{1}{c} + \frac{r_a^2}{Z} \right)$$

$$\lambda = \frac{1}{2 * \pi} * \left[ \frac{1}{2} - \frac{\sin^2(\alpha)}{3} \right] \quad (\text{B-11})$$

$$\mathfrak{R} = \frac{\sin(\alpha)}{4} - \beta \quad (\text{B-12})$$

$$M_1 = r_a * \left( \frac{1}{2} + \beta - \frac{\sin(\alpha)}{4} \right) \quad (\text{B-13})$$

$$M_2 = r_a * \left( \frac{\sin(\alpha)}{4} + \lambda - \beta - \frac{1}{\pi} \right) \quad (\text{B-14})$$

$$k_{1,in} = \frac{\mathfrak{R}}{c} + \frac{M_1 * c/2}{Z} * \frac{r_a}{r_a - c/2} \quad (\text{B-15})$$

$$k_{1,out} = \frac{\mathfrak{R}}{c} - \frac{M_1 * c/2}{Z} * \frac{r_a}{r_a + c/2} \quad (\text{B-16})$$

$$k_{2,in} = \frac{\mathfrak{R}}{c} + \frac{M_2 * c/2}{Z} * \frac{r_a}{r_a - c/2} \quad (\text{B-17})$$

$$k_{2,out} = \frac{\mathfrak{R}}{c} - \frac{M_2 * c/2}{Z} * \frac{r_a}{r_a + c/2} \quad (\text{B-18})$$

From these stress concentration factors k, the strength  $F_{Rd}$  can be calculated as follows:

Net section

$$F_{Rd,t} = \frac{f_y * t}{\max \left( \text{abs}(k_{1,in}); \text{abs}(k_{1,out}) \right)} \quad (\text{B-19})$$

Fracture beyond the hole

$$F_{Rd,t} = \frac{f_y * t}{\max \left( \text{abs}(k_{2,in}); \text{abs}(k_{2,out}) \right)} \quad (\text{B-20})$$

## Reissner

$$v_{\delta} = 4.21 + 0.09 * R_{eye} / d_h \quad (\text{B-21})$$

$$\sigma_t = v_{\delta} * \frac{8 * F}{\pi^2 * R_{eye} * t} \leq f_y \quad (\text{B-22})$$

$$F_{Rd,t} = \frac{f_y * \pi^2 * R_{eye} * t}{v_{\delta} * 8} \quad (\text{B-23})$$

## Reidelbach

$$cr = d_h / (2 * R_{eye}) \quad (\text{B-24})$$

$$K_t = \frac{3 * (1 - cr)}{2 * (1 - cr^2)^2} * \left( \frac{1 + 3 * cr^2}{2 * cr} + \frac{1 + 2 * cr^2 - 2 * cr^4 + 5 * cr^6}{1 + 2 * cr^2} \right) \quad (\text{B-25})$$

$$\sigma_t = K_t * \frac{F_{Ed}}{2 * c * t} \leq f_y \quad (\text{B-26})$$

$$F_{Rd,t} = \frac{f_y * 2 * c * t}{K_t} \quad (\text{B-27})$$

## Póócza

$$a_1 = \frac{1}{(a/c)^3 - 1} \quad (\text{B-28})$$

$$a_2 = \frac{\pi * a_1}{2} \quad (\text{B-29})$$

$$r_a = \frac{R_{eye} + d_h/2}{2} \quad (\text{B-30})$$

$$\delta_0 = \frac{R_{eye} - d_h/2}{R_{eye} + d_h/2} \quad (\text{B-31})$$

$$J_{\varphi,1} = 1 + \frac{\sin \varphi}{a_1} \quad (\text{B-32})$$

$$J_{\varphi,2} = 1 + \frac{\varphi}{a_2} \quad (\text{B-33})$$

$$J_{a,i} = \int \frac{1}{J_{\varphi,i}} d\varphi \quad (\text{B-34})$$

$$J_{b,i} = \int \frac{\cos \varphi}{J_{\varphi,i}} d\varphi \quad (\text{B-35})$$

$$\alpha = 75^\circ \quad (\text{B-36})$$

$$\Phi_i = \frac{[J_{a,i}]_0^{\pi/2} - \cos(\alpha) * [J_{a,i}]_\alpha^{\pi/2} - [J_{b,i}]_0^\alpha}{2 * [J_{a,i}]_0^{\pi/2}} \quad (\text{B-37})$$

$$\lambda_1 = \frac{\Phi_1}{1 + \frac{(a/c - 1) * \delta_0}{[J_{a,1}]_0^{\pi/2}}} \quad (\text{B-38})$$

$$\lambda_2 = \frac{\Phi_2}{1 + \frac{(a/c - 1) * 2 * \delta_0}{\pi * a_1 * \ln\left(\frac{a_1 + 1}{a_1}\right)}} \quad (\text{B-39})$$

$$\lambda = \frac{\lambda_1 + \lambda_2}{2} \quad (\text{B-40})$$

Tension in the net section

$$k = 1 - 2 * \lambda * \left(1 + \frac{2 * \delta_0^2}{\left(\ln\left[\frac{1 + \delta_0}{1 - \delta_0}\right] - 2 * \delta_0\right) * (\delta_0 - 1)}\right) \quad (\text{B-41})$$

$$\sigma_t = \frac{k * F}{2 * t * c} \leq f_y \quad (\text{B-42})$$

$$F_{Rd,t} = \frac{f_y * 2 * c * t}{k} \quad (\text{B-43})$$

Fracture beyond the hole

$$M_{\pi/2} = F * r_a * (\lambda - 0.5 + 0.5 * \cos(\alpha)) \quad (\text{B-44})$$

$$W_{\pi/2} = \frac{t * a^2}{6} \quad (\text{B-45})$$

$$\sigma_{\pi/2} = \frac{M_{\pi/2}}{W_{\pi/2}} \leq f_y \quad (\text{B-46})$$

$$F_{Rd,t} = \text{abs}\left(\frac{f_y * W_{\pi/2}}{r_a * (\lambda - 0.5 + 0.5 * \cos(\alpha))}\right) \quad (\text{B-47})$$

## B.2 Empirical background

### Peterson

$$c = R_{eye} + e \quad (\text{B-48})$$

$$d = d_h \quad (B-49)$$

$$h = t \quad (B-50)$$

$$H = L_{gross} \quad (B-51)$$

If there is a clearance between the pin and the hole the maximum stress concentration factor is not in points A of Figure B-1, but at points B, with  $10^\circ \leq \theta \leq 30^\circ$ .

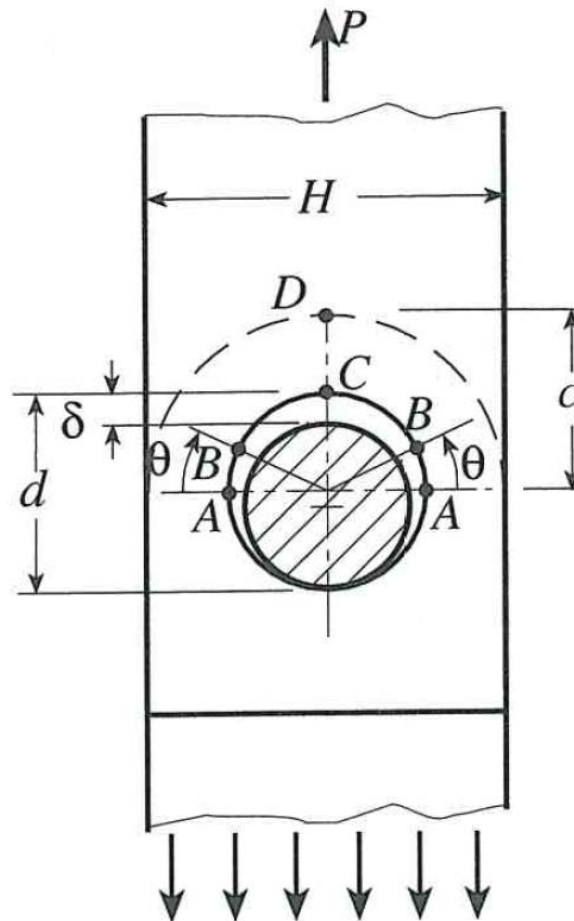


**Figure B-1: Geometry in accordance to Petersons Stress Concentration Factors (Petersons Stress Concentration Factors (1997), Figure 5.10 b)**

$K_{te}$  factor can be derived in accordance to Figure B-2 in which  $K_{te}$  is plotted for  $c/H = 0.4, 0.5, 0.6$  and  $\infty$

$K_{te}$  may be used for ratio  $h/d$  is smaller than 0.5. If  $h/d$  is greater than  $K'_{te}$  must be used, which can be derived with Figure B-3.

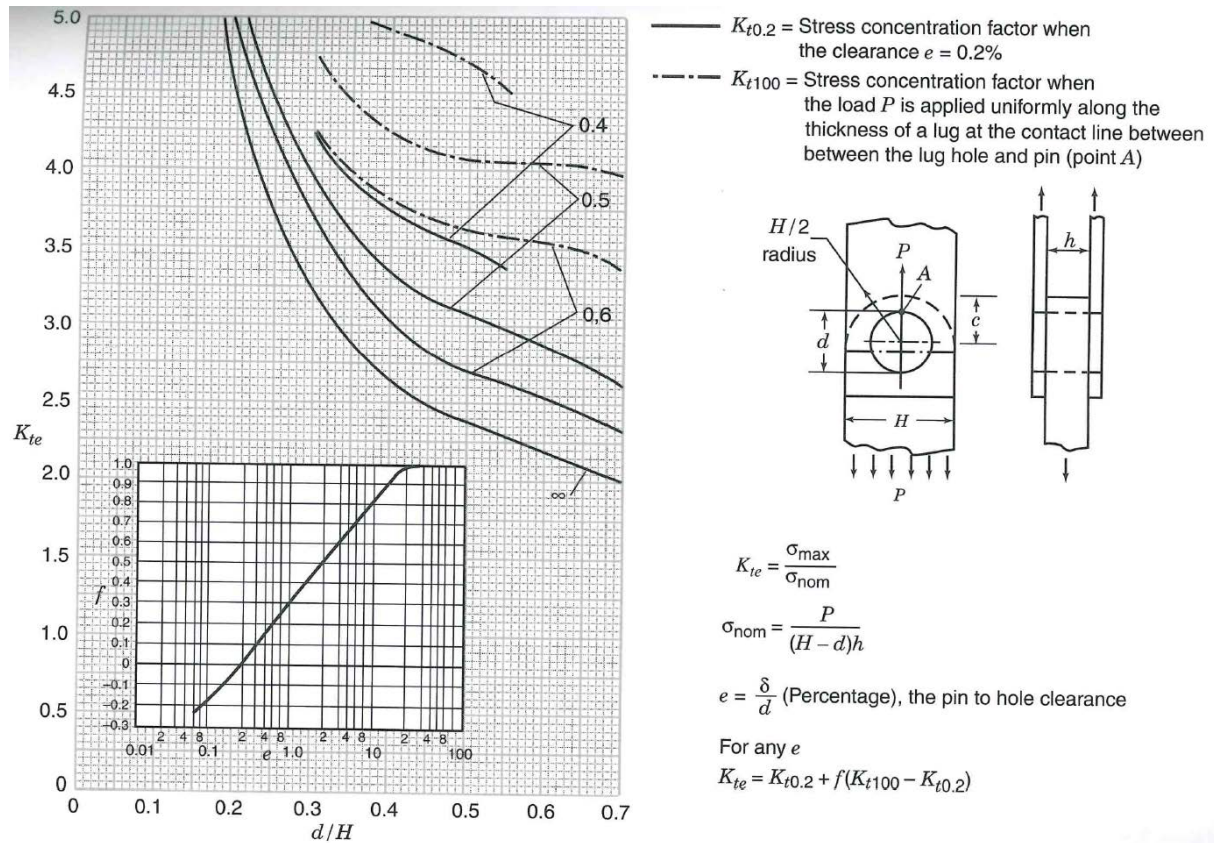


**Figure B-2: Stress concentration factor  $K_{te}$  according to Peterson's Stress Concentration Factors (Peterson's Stress Concentration Factors (1997), Chart 5.12)**

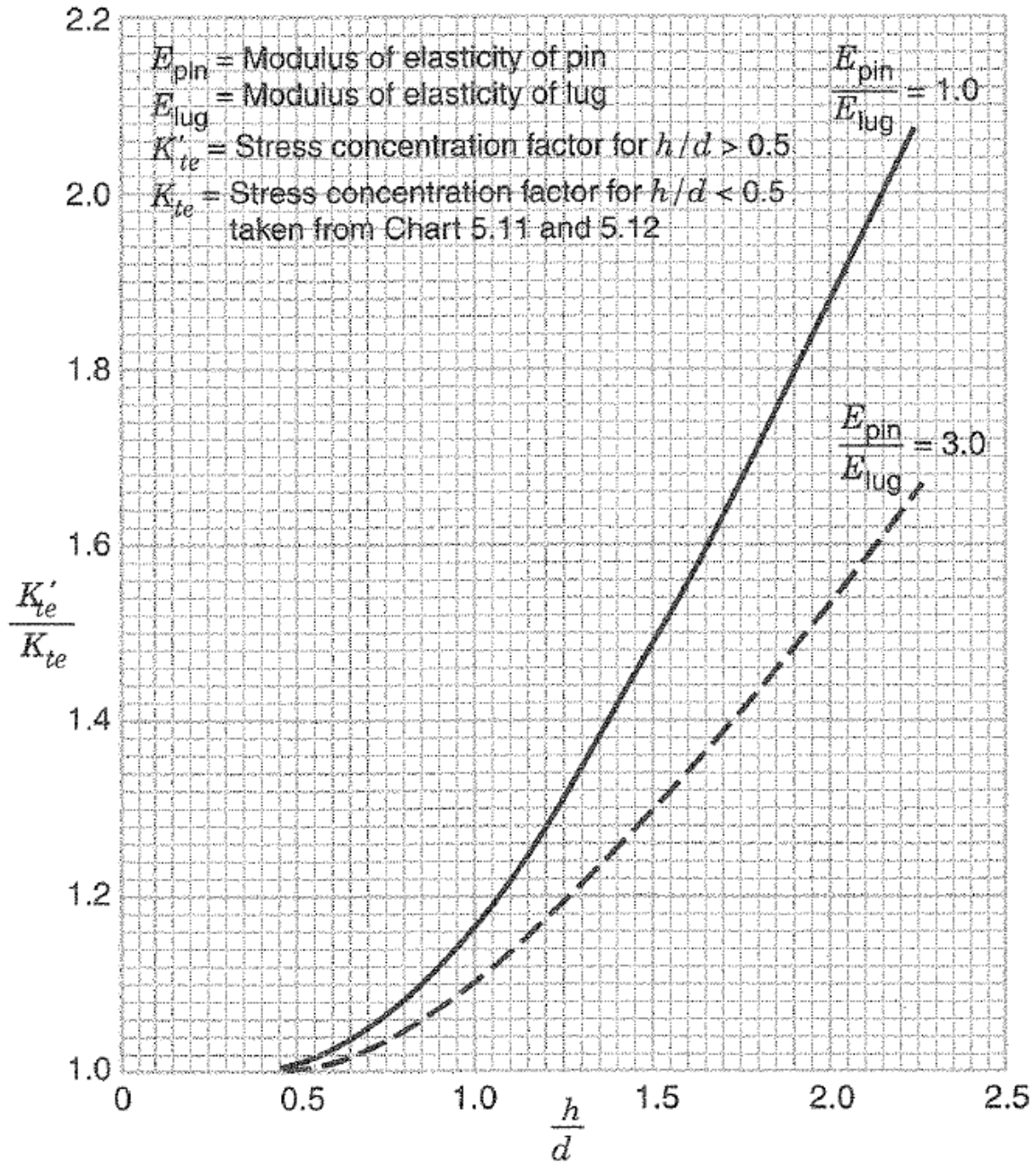


Figure B-3: Stress concentration factor  $K'_{te}$  according to Petersons Stress Concentration Factors (Petersons Stress Concentration Factors (1997), Chart 5.13)

$$\sigma_{max} = \frac{K'_{te}}{K_{te}} * K_{te} * \frac{F}{H-d} \leq f_y \tag{B-52}$$

$$F_{Rd,t} = \frac{f_y * (H-d)}{\frac{K'_{te}}{K_{te}} * K_{te}} \tag{B-53}$$

**Ekvall**

$$R_o = R_{eye} \tag{B-54}$$

$$W = 2 * R_{eye} \tag{B-55}$$

$$D = d_h \quad (\text{B-56})$$

$$a = R_{eye} + e \quad (\text{B-57})$$

$$\beta = \beta/2 \quad (\text{B-58})$$

$$\theta = \alpha \quad (\text{B-59})$$

### Straight lugs

1. Determine  $K_{tb,s}$  with Figure B-4 and use linear interpolation for load angles between  $0^\circ$  and  $90^\circ$ .
2. Use Figure B-5 to determine the eccentricity factor and determine  $K_{tb,e}/K_{tb,s}$

### Tapered lugs

1. Determine  $K_{tb,s}$ 
  - a. For  $\beta = 45^\circ$  use Figure B-6 to determine  $K_{tb,s}$
  - b. For  $0^\circ < \beta < 45^\circ$  and  $\theta = 0^\circ$  use equation ( B-60 )

$$K_{tb} = \left(2.75 - \frac{\beta}{135}\right) * \left(\frac{2 * R_0}{D} - 1\right)^{-(0.675 - \beta/1000)} \quad (\text{B-60})$$

- c. For all other cases:
  - i. Use Figure B-4 to determine  $K_{tb,\theta_1}$  (for straight lugs ( $\beta = 0^\circ$ ))
  - ii. Determine  $K_{tb,\theta_2}$ 
    1. Determine  $K_{tb,0}$  with equation ( B-61 )

$$K_{tb,0} = 2.417 * \left(\frac{2 * R_0}{D} - 1\right)^{-0.63} \quad (\text{B-61})$$

2. If  $\theta \neq 0^\circ$  calculate  $K_{tb,\theta}/K_{tb,0}$  by equation ( B-62 ) to determine  $K_{tb,\theta_2}$ , otherwise  $K_{tb,\theta_2} = K_{tb,0}$  (for tapered lugs with  $\beta = 45^\circ$ )

$$\frac{K_{tb,\theta}}{K_{tb,0}} = 1 + 6.33 * 10^{-3} \theta - 8.15 * 10^{-5} \theta^2 \quad (\text{B-62})$$

$$K_{tb,\theta_2} = \frac{K_{tb,\theta}}{K_{tb,0}} * K_{tb,0} \quad (\text{B-63})$$

3. Use linear interpolation between  $K_{tb,\theta_1}$  ( $\beta = 0^\circ$ ) and  $K_{tb,\theta_2}$  ( $\beta = 45^\circ$ ) to determine  $K_{tb,s}$

2. Use Figure B-5 to determine the eccentricity factor and determine  $K_{tb,e}/K_{tb,s}$ . Let  $2a/W = a/R_0$

Tension in the net section

$$F_{Rd,t} = K_{tb,s} * \frac{K_{tb,e}}{K_{tb,s}} * d_h * t * f_u \quad (\text{B-64})$$

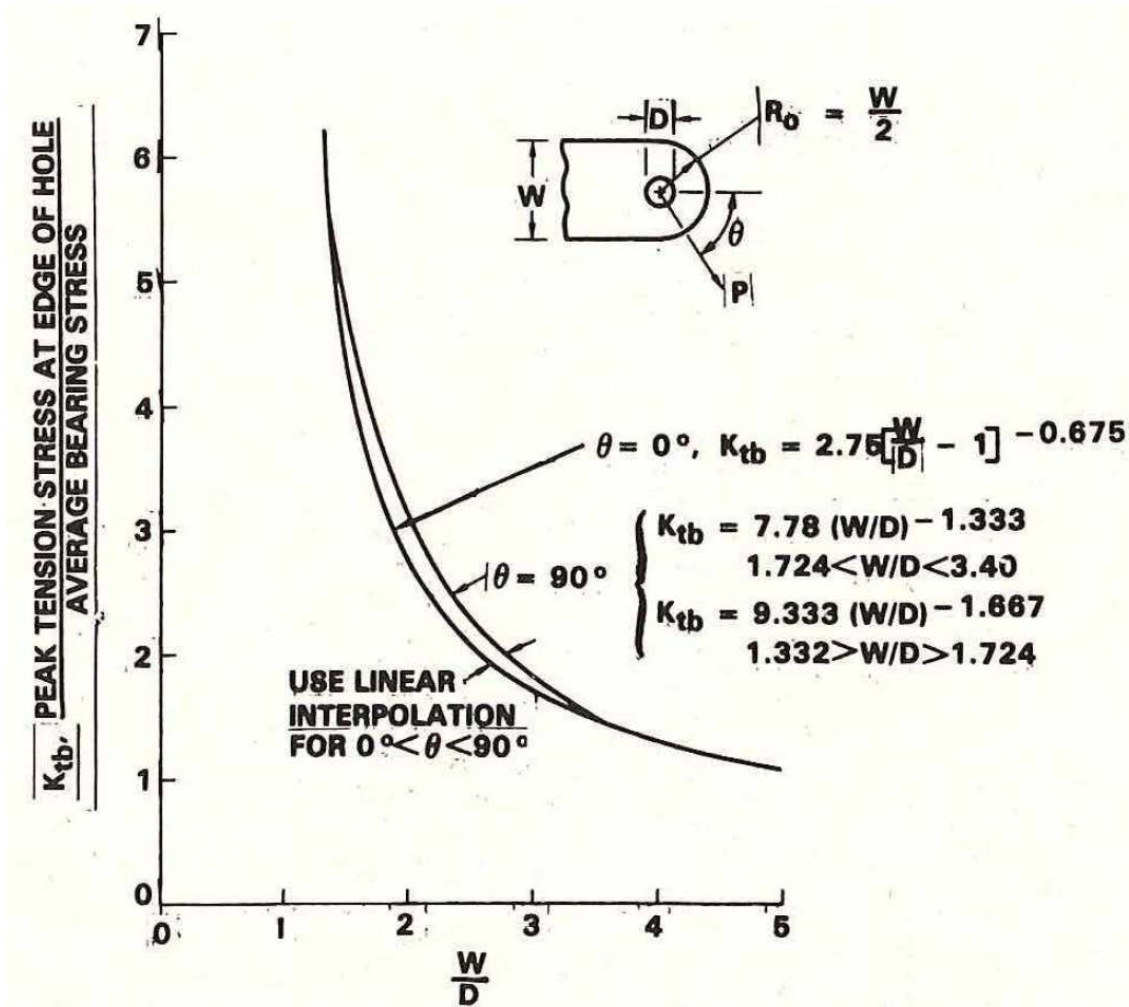


Figure B-4:  $K_{tb}$  for straight lugs (Static Strength Analysis of Pin-Loaded Lugs (1986), Fig. 5)

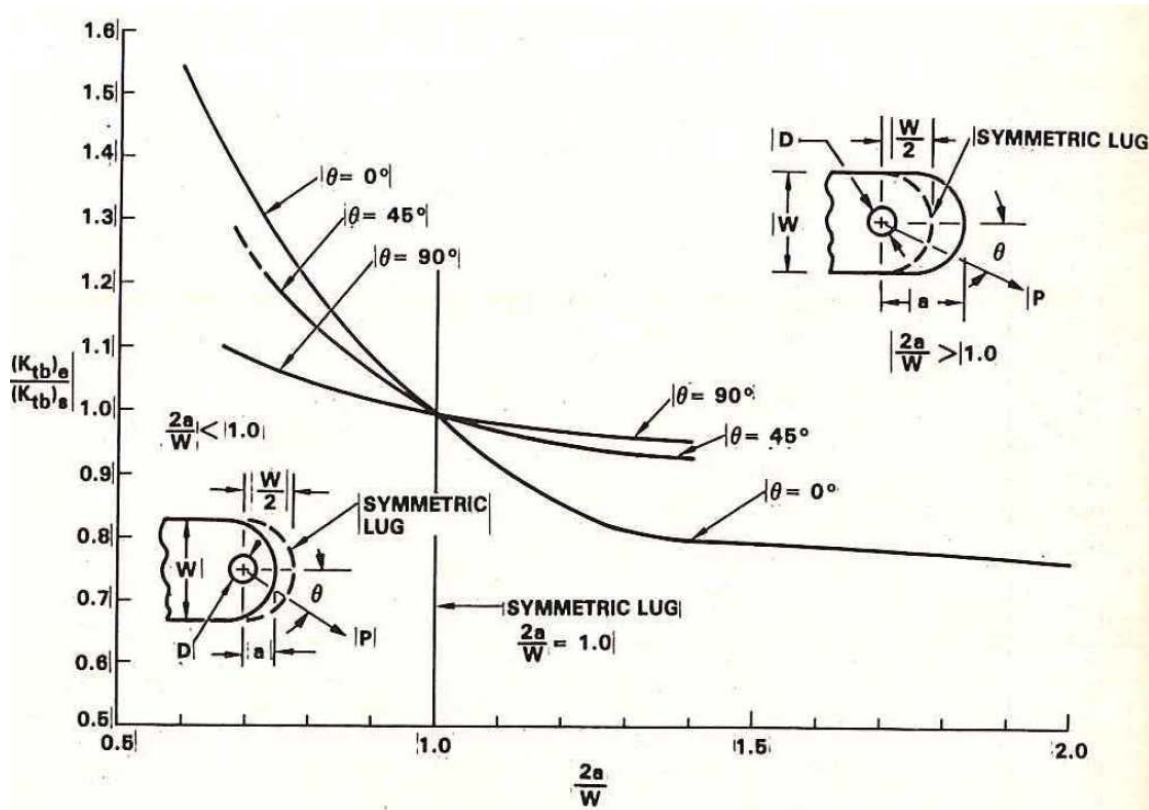


Figure B-5: Eccentricity factor (Static Strength Analysis of Pin-Loaded Lugs (1986), Fig. 6)

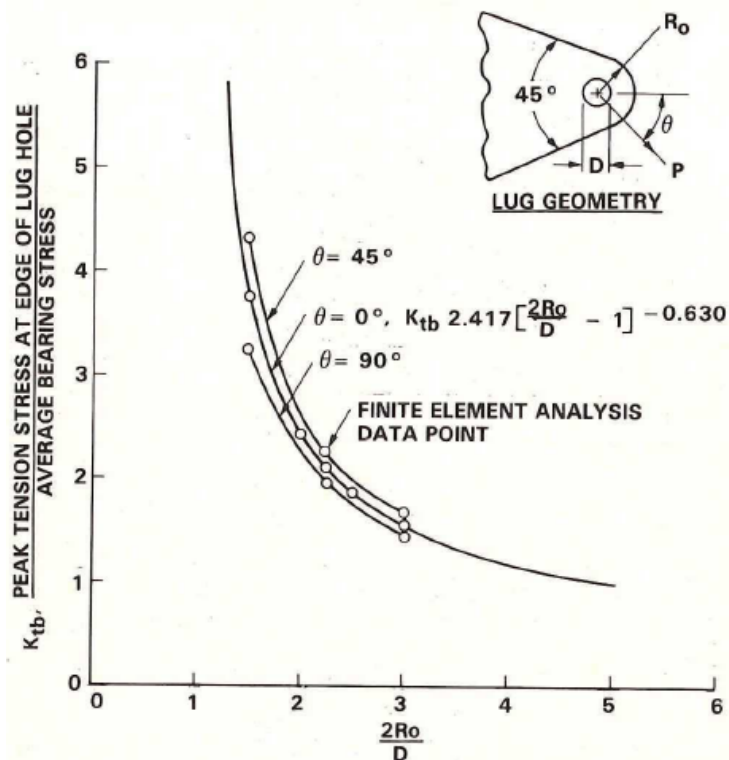


Figure B-6:  $K_{tb}$  45° tapered lugs loaded with an angle of 0°, 45° and 90° (Static Strength Analysis of Pin-Loaded Lugs (1986), Fig. 2)

**Petersen**

$$a_p = t + t_2 + 2 * s \tag{B-65}$$

Bending strength of the pin

$$M = F * \frac{t + 2 * t_2 + 4 * s}{8} \quad (\text{B-66})$$

$$W = \frac{\pi * d_p^3}{32} \quad (\text{B-67})$$

$$\sigma_{max} = \frac{M}{W} + \frac{2}{3} * 1.27 * \frac{F}{t * d_p} * \tan^{-1} \left( 0.42 \frac{t}{d_p} \right) \leq f_y \quad (\text{B-68})$$

$$F_{Rd,b} = \frac{f_y}{\frac{t + 2 * t_2 + 4 * s}{8 * W} + \frac{2.54}{3 * t * d_p} * \tan^{-1} \left( 0.42 \frac{t}{d_p} \right)} \quad (\text{B-69})$$

Shear strength of the pin

$$A = \frac{\pi * d_p^2}{4} \quad (\text{B-70})$$

$$\tau_{max} = \left( 1.1 + 0.02 * \left( \frac{d_p}{a_p} \right)^2 + \frac{1}{4} * \tan^{-1} \left( \frac{a_p}{d_p} \right) \right) * \frac{F}{2 * A} \leq f_y / \sqrt{3} \quad (\text{B-71})$$

$$F_{Rd,\tau} = \frac{f_y * 2 * A}{\sqrt{3} * \left( 1.1 + 0.02 * \left( \frac{d_p}{a_p} \right)^2 + \frac{1}{4} * \tan^{-1} \left( \frac{a_p}{d_p} \right) \right)} \quad (\text{B-72})$$

Tension in the net section

$$F_{Rd,t} = (c - 1/3 * d_h) * 2 * t * f_y \quad (\text{B-73})$$

Fracture beyond the hole

$$F_{Rd,t} = (a - 2/3 * d_h) * 2 * t * f_y \quad (\text{B-74})$$

## Dietz

Tension in the net section

$$k = \frac{9}{5} + \left( \frac{2 * R_{eye}}{d_h} - \frac{6}{5} \right) * \left( \frac{9}{5} - \frac{R_{eye} + e}{2 * R_{eye}} \right) \quad (\text{B-75})$$

$$F_{Rd,t} = \frac{f_y * 2 * c * t}{k} \quad (\text{B-76})$$

Bearing strength

$$s = \frac{d_h - d_p}{d_h} \quad (\text{B-77})$$

$$\varphi_{max} = \sin^{-1}(1 - s) \quad (\text{B-78})$$

$$c = 10^{-6} \tag{B-79}$$

$$q = \frac{F}{d_h * t} \tag{B-80}$$

$$\varphi_k = \varphi_{max} * \left(1 - e^{\left(\frac{-c * q}{s}\right)}\right) \tag{B-81}$$

$$\sigma = \frac{q}{\cos(\varphi_k)} * \left(\frac{\pi}{2 * \varphi_k} - \frac{2 * \varphi_k}{\pi}\right) \tag{B-82}$$

Dietz assumed that the bearing stress have the following distribution over the thickness of the eye (Figure B-7). The maximum thickness factor is cutoff at 2.35.

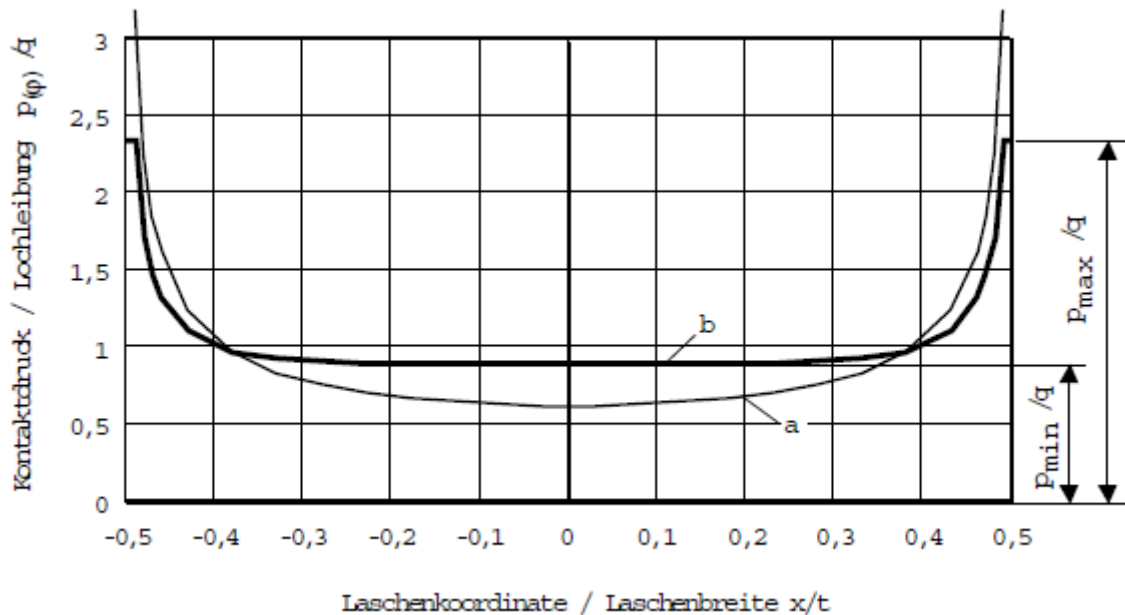


Figure B-7: Contact pressure over the thickness in accordance to Dietz (Berechnung und Optimierung von Bolzen-Lasche-Verbindungen (1994), bild 3.6)

The maximum bearing stress is

$$\sigma_{max} = 2.35 * \sigma \leq f_y \tag{B-83}$$

Calculation of the maximum bearing load is an iterative process.

**Guo-Geruschat**

For eye geometry like Figure 1-1:

$$k = 4.3 \tag{B-84}$$

For eye geometry with a reduced gross sections:

$$k = 5.6 \tag{B-85}$$

For a tapered eye:

$$g = \frac{d_h/2}{R_{eye}} \quad (\text{B-86})$$

$$\beta \geq 30^\circ \quad (\text{B-87})$$

$$k = \frac{9.2 * g}{4 * g + \tan(\beta)} + 2 \leq 3.4 \quad (\text{B-88})$$

Tension in the net section

$$F_{Rd,t} = \frac{f_y * 2 * c * t}{k} \quad (\text{B-89})$$

### Duerr

$$C_r = 1 - 0.275 * \sqrt{1 - \frac{d_p^2}{d_h^2}} \quad (\text{B-90})$$

$$b_{eff} = c * 0.6 * \frac{f_u}{f_y} * \sqrt{\frac{d_h}{c}} \leq c \quad (\text{B-91})$$

Tension in the net section

$$F_{Rd,t} = C_r * f_u * 2 * t * b_{eff} \quad (\text{B-92})$$

Fracture beyond the hole

$$F_{Rd,t} = C_r * f_u * \left( 1.13 * a + \frac{0.92 * c}{1 + c/d_h} \right) * t \quad (\text{B-93})$$

Shear

$$\phi = 55 * \frac{d_p}{d_h} \quad (\text{B-94})$$

$$A_{eff} = \left( a + \frac{d_p}{2} * (1 - \cos \phi) - \left( R_{eye} - \sqrt{R_{eye}^2 - \left( \frac{d_p}{2} * \sin \phi \right)^2} \right) \right) * t \quad (\text{B-95})$$

$$F_{Rd,v} = 0.7 * f_u * 2 * A_{eff} \quad (\text{B-96})$$

### Dishing according to Duerr

$$a = R_{eye} + e - d_h/2 \quad (\text{B-97})$$

$$b_e = R_{eye} - d_h/2 \quad (\text{B-98})$$

$$K = 2 * \sqrt{b_e/a} \quad (\text{B-99})$$

$$i = \frac{K * a * \sqrt{12}}{t} \quad (\text{B-100})$$

$$C_c = \sqrt{\frac{2 * \pi * E}{f_y}} \quad (\text{B-101})$$

$C_c < i \rightarrow$  plastic buckling, otherwise elastic buckling (B-102)

$$F_{plastic} = \left( \frac{1 - 0.5 * i^2 / C_c^2}{1 - \nu^2} \right) * f_y \quad (\text{B-103})$$

$$F_{elastic} = \frac{\pi^2 * E}{i^2 * (1 - \nu^2)} \quad (\text{B-104})$$

$$W_{eff} = \min(d_p + a, d_h + 1.25 * b_e) \quad (\text{B-105})$$

$$P = W_{eff} * t * F \quad (\text{B-106})$$

$$t > \frac{a * d_h}{0.19 * d_p} * \sqrt{\frac{f_y}{E}} \quad (\text{B-107})$$

## B.3 Standards

### EN1993-1-8

#### Design restrictions

$$a \geq \frac{F}{2 * t * f_y} + \frac{2 * d_h}{3} \quad (\text{B-108})$$

$$c \geq \frac{F}{2 * t * f_y} + \frac{d_h}{3} \quad (\text{B-109})$$

$$d_h \leq 2.5 * t \quad (\text{B-110})$$

#### Strength calculations

Tension in the net section

$$F_{Rd,t} = \left( c - \frac{d_h}{3} \right) * 2 * t * f_y \quad (\text{B-111})$$

Fracture beyond the hole

$$F_{Rd,t} = \left( a - \frac{2 * d_h}{3} \right) * 2 * t * f_y \quad (\text{B-112})$$

Bearing strength

$$\sigma_{h,Ed} = 0.591 * \sqrt{\frac{E * F * (d_h - d_p)}{d_p^2 * t}} \leq f_{h,Ed} = 2.5 * f_y \quad (\text{B-113})$$

$$F_{Rd,b,1} = \left(\frac{2.5 * f_y}{0.591}\right)^2 * \frac{d_p^2 * t}{E * (d_h - d_p)} \quad (\text{B-114})$$

$$F_{Rd,b,2} = 1.5 * d_p * t * f_y \quad (\text{B-115})$$

$$F_{Rd,b} = \min(F_{Rd,b,1}; F_{Rd,b,2}) \quad (\text{B-116})$$

Pin bending

$$M = F * \frac{t + 2 * t_2 + 4 * s}{8} \quad (\text{B-117})$$

$$W = \frac{\pi * d_p^3}{32} \quad (\text{B-118})$$

$$F_{Rd,pb} = 0.8 * \frac{8 * f_y * W}{t + 2 * t_2 + 4 * s} \quad (\text{B-119})$$

Pin shear

$$A = \frac{\pi * d_p^2}{4} \quad (\text{B-120})$$

$$F_{Rd,pv} = 1.2 * A * f_u \quad (\text{B-121})$$

Pin combined

$$F_{Rd,pc} = \frac{1}{\sqrt{\left(\frac{t_2 + s}{\frac{t}{4} + \frac{s}{2}}\right)^2 + \left(\frac{1}{1.2 * A * f_u}\right)^2}} \quad (\text{B-122})$$

### **EN13001-3-1**

In the EN13001-3-1 some parameters have other symbols, this is stated in equations ( **B-123** ) and ( **B-124** ).

$$c = a \quad (\text{B-123})$$

$$b = c \quad (\text{B-124})$$

Stress concentration factor k can be derived with Figure B-8.

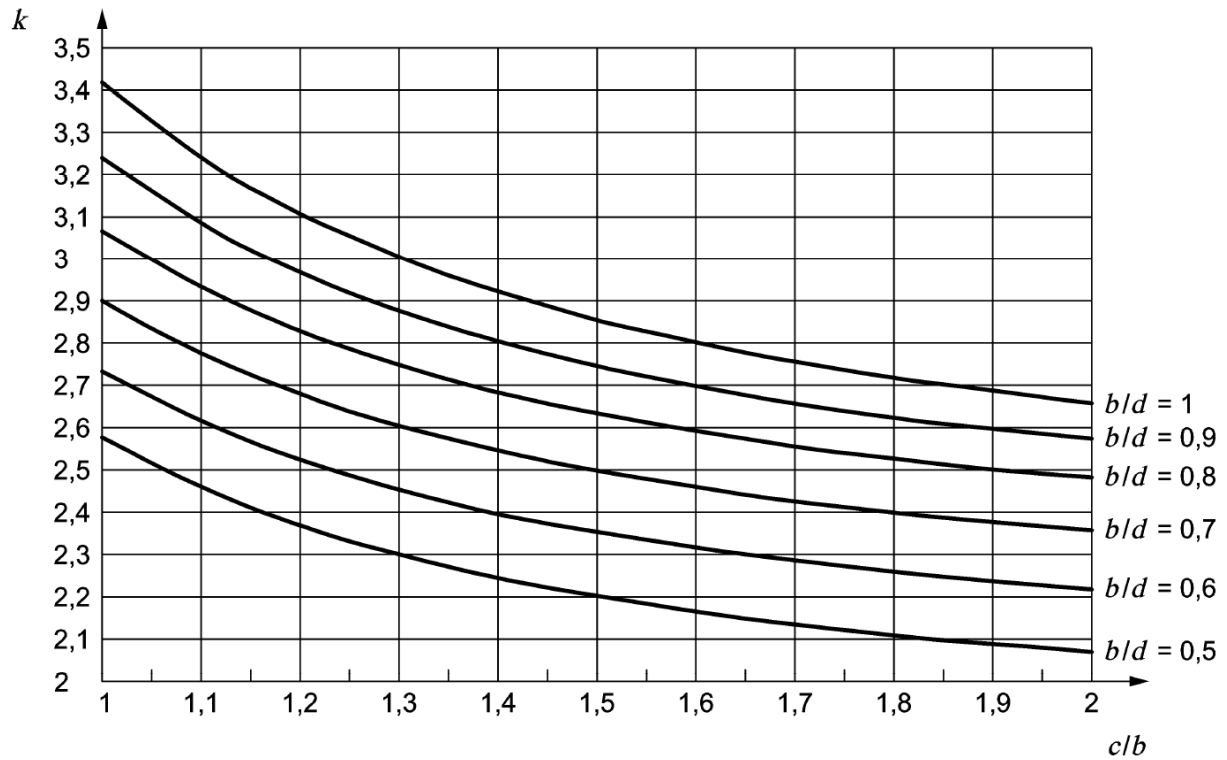


Figure B-8: Stress concentration factor according to EN13001-3-1

$$\gamma_{spt} = \frac{0.95}{\sqrt{k}} * \frac{1.38 * f_y}{f_u} \quad (\text{B-125})$$

Tension in the net section

$$F_{Rd,t} = \frac{2 * b * t * f_y}{k * \gamma_{spt}} \quad (\text{B-126})$$

Bearing strength

$$F_{Rd,b} = \frac{d_p * t * f_y}{0.9} \quad (\text{B-127})$$

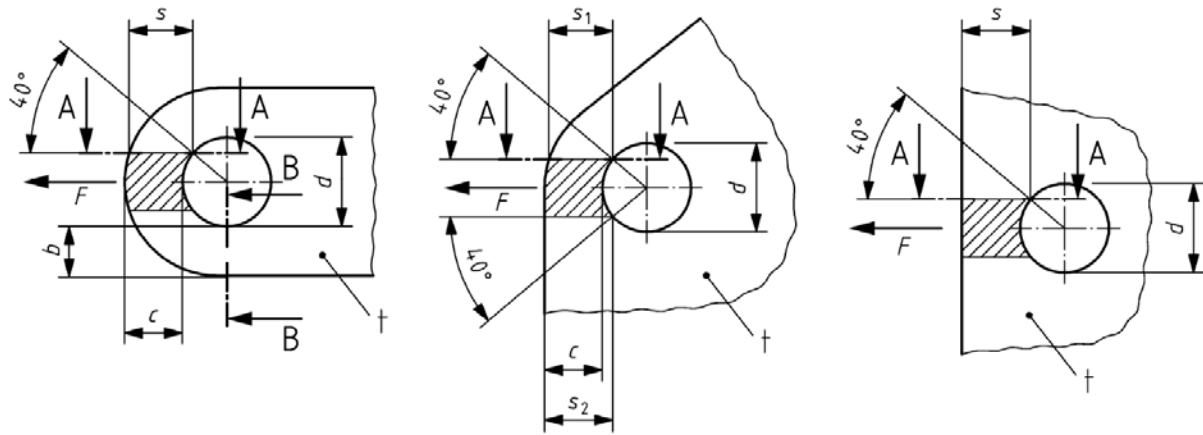
Shear strength

$$A_{eff} = 2 * s * t, \quad \text{for Figure B9, a) and c)} \quad (\text{B-128})$$

$$s_1 \geq c, \quad s_2 \geq c \quad (\text{B-129})$$

$$A_{eff} = 2 * (s_1 + s_2) * t, \quad \text{for Figure B9, b)} \quad (\text{B-130})$$

$$F_{Rd,v} = \frac{A_{eff} * f_y}{\sqrt{3}} \quad (\text{B-131})$$



a) type I

b) type II

c) type III

**Figure B-9: Geometry connected parts in accordance to EN13001-3-1 (EN13001-3-1 (2012), Figure 6)**

Pin bending

$$M = F * \frac{t + 2 * t_2 + 4 * s}{8} \quad (\text{B-132})$$

$$W = \frac{\pi * d_p^3}{32} \quad (\text{B-133})$$

$$F_{Rd,pb} = \frac{8 * f_{yp} * W}{t + 2 * t_2 + 4 * s} \quad (\text{B-134})$$

Pin shear

$$u = 4/3, \quad \text{for solid pins} \quad (\text{B-135})$$

$$v_D = \frac{d_p - t_p}{d_p} \quad (\text{B-136})$$

$$u = 4/3 * \frac{1 + v_D + v_D^2}{1 + v_D^2}, \quad \text{for hollow pins (pipes)} \quad (\text{B-137})$$

$$A = \frac{\pi * d_p^2}{4} \quad (\text{B-138})$$

$$F_{Rd,pv} = \frac{2}{u} * \frac{A * f_{yp}}{\sqrt{3}} \quad (\text{B-139})$$

### **ASME BTH-1**

$$C_r = 1 - 0.275 * \sqrt{1 - \frac{d_p^2}{d_h^2}}, \quad C_r = 1 \text{ if } \frac{d_p}{d_h} > 0.9 \quad (\text{B-140})$$

$$b_{eff} = \min \left( 4 * t; c * 0.6 * \frac{f_u}{f_y} * \sqrt{\frac{d_h}{c}} \right) \leq c \quad (\text{B-141})$$

Tension in the net section

$$F_{Rd,t} = C_r * f_u * 2 * t * b_{eff} \quad (\text{B-142})$$

Fracture beyond the hole

$$F_{Rd,t} = C_r * f_u * \left( 1.13 * a + \frac{0.92 * c}{1 + c/d_h} \right) * t \quad (\text{B-143})$$

Bearing

$$F_{Rd,b} = 1.25 * f_y * t * d_p \quad (\text{B-144})$$

Shear

$$\phi = 55 * \frac{d_p}{d_h} \quad (\text{B-145})$$

$$A_{eff} = \left( a + \frac{d_p}{2} * (1 - \cos \phi) - \left( R_{eye} - \sqrt{R_{eye}^2 - \left( \frac{d_p}{2} * \sin \phi \right)^2} \right) \right) * t \quad (\text{B-146})$$

$$F_{Rd,v} = 0.7 * f_u * 2 * A_{eff} \quad (\text{B-147})$$

Pin bending

$$M = F * \frac{t + 2 * t_2 + 4 * s}{8} \quad (\text{B-148})$$

$$W = \frac{\pi * d_p^3}{32} \quad (\text{B-149})$$

$$F_{Rd,pb} = \frac{8 * f_{yp} * W}{t + 2 * t_2 + 4 * s} \quad (\text{B-150})$$

Pin shear

$$A = \frac{\pi * d_p^2}{4} \quad (\text{B-151})$$

$$F_{Rd,pv} = \frac{2 * A * f_{yp}}{\sqrt{3}} \quad (\text{B-152})$$

## **AISC 360-10**

**Design restrictions**

$$a \geq 1.33 * b_e \quad (\text{B-153})$$

$$w \geq 2 * b_e + d_p \quad (\text{B-154})$$

$$d_h - d_p \leq 1 \quad (\text{B-155})$$

## Strength calculations

$$b_e = 2 * t + 16 \leq c \quad (\text{B-156})$$

Tension in the net section

$$F_{Rd,t} = 0.75 * f_u * 2 * t * b_e \quad (\text{B-157})$$

Bearing

$$F_{Rd,b} = 0.75 * 1.8 * f_y * d_p * t \quad (\text{B-158})$$

Shear

$$A_{sf} = 2 * t * \left( a + \frac{d_p}{2} \right) \quad (\text{B-159})$$

$$F_{Rd,v} = 0.75 * 0.6 * f_u * A_{sf} \quad (\text{B-160})$$

Gross section

$$F_{Rd,t} = 0.75 * f_y * t * \min(L_{gross}; 8 * t) \quad (\text{B-161})$$

## NEN 6786

In the NEN6786 some parameters have other symbols, this is stated in equations ( B-162 ) to ( B-165 ).

$$b = L_{gross} \quad (\text{B-162})$$

$$R = R_{eye} \quad (\text{B-163})$$

$$r = \frac{d_h}{2} \quad (\text{B-164})$$

$$r_z = \frac{R + r}{2} \quad (\text{B-165})$$

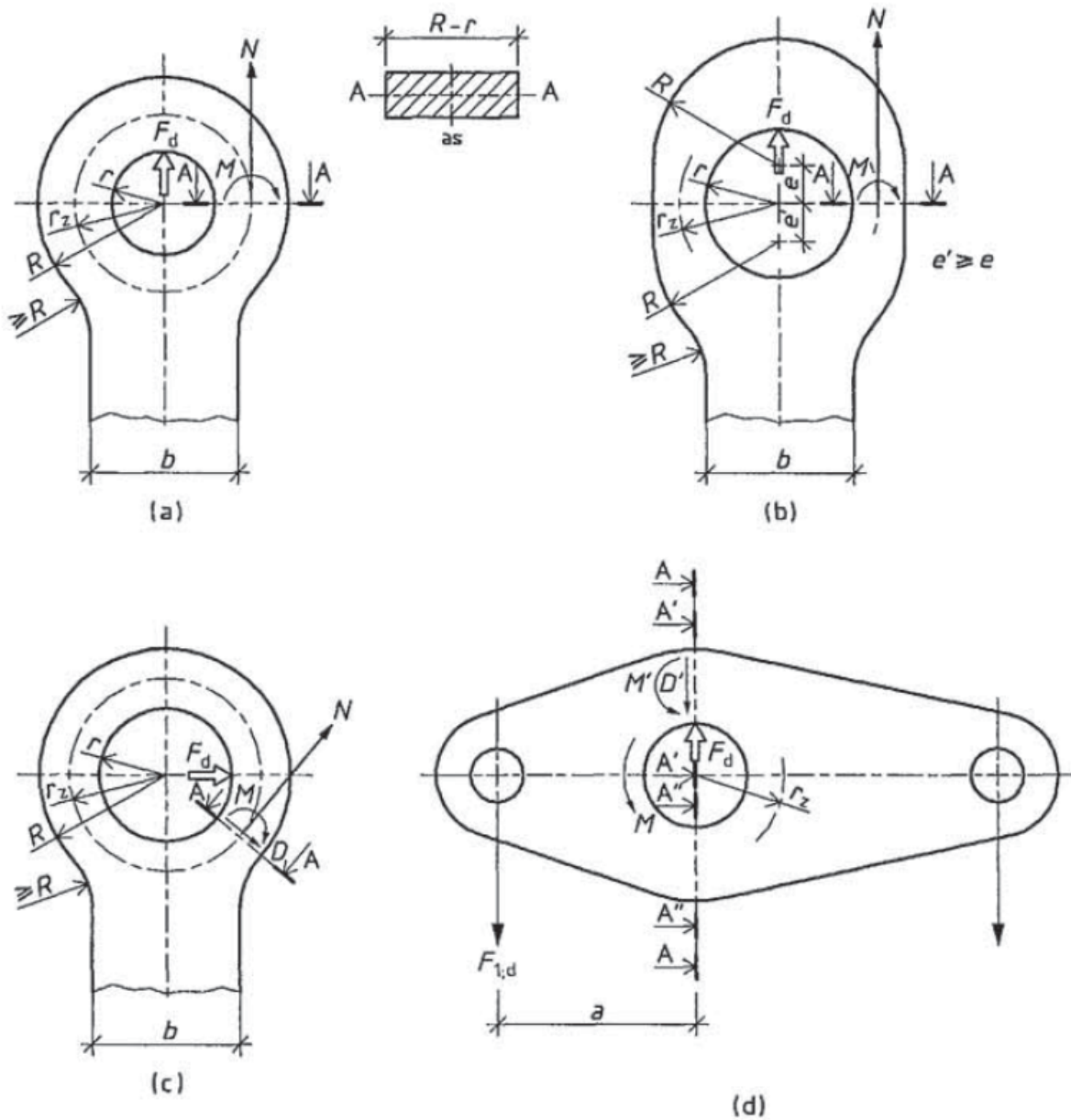


Figure B-10: Eyes according to NEN6786 (NEN6786 (2001), figure 23)

NEN6786 provides strength calculations for high and for small clearances between the pin and the hole. It is assumed that a small or high clearance is according to equations ( B-166 ) and ( B-167 ).

$$small = \frac{d_p}{d_h} \geq 0.98 \tag{ B-166 }$$

$$high = \frac{d_p}{d_h} < 0.98 \tag{ B-167 }$$

$$W = \frac{1}{6} * t * c^2 \tag{ B-168 }$$

k	$\frac{e}{R-r}$								
	0	0.05	0.10	0.30	0.60	0.90	1.20	1.50	
$\frac{R-r}{R+r}$	0.1	0.17	0.16	0.16	0.14	0.11	0.09	0.07	0.06
	0.2	0.17	0.16	0.16	0.13	0.10	0.08	0.06	0.04
	0.4	0.17	0.16	0.15	0.13	0.09	0.06	-	-
	0.5	0.17	0.16	0.15	0.13	0.09	-	-	-

Table B-1: Stress concentration factor k, according to NEN6786

### Small clearance

Load parallel to eye geometry, Section A-A of Figure B-10 (a and b)

$$\sigma_{Ed} = 0.5 * \frac{F}{c * t} + \frac{k * F * r_z}{W} \leq f_y \quad (\text{B-169})$$

$$F_{Rd,t} = \frac{f_y}{\frac{1}{2 * c * t} + \frac{k * r_z}{W}} \quad (\text{B-170})$$

Load perpendicular to eye geometry, Section A-A of Figure B-10 (c)

$$\sigma_{Ed} = \frac{0.55 * F}{c * t} + \frac{0.4 * F * r_z}{W} \leq f_y \quad (\text{B-171})$$

$$\tau = \frac{0.65 * F}{c * t} \quad (\text{B-172})$$

$$\sigma_{com} = \sqrt{\sigma_{Ed}^2 + 3 * \tau^2} = \sqrt{F^2 * \left( \left( \frac{0.55}{c * t} + \frac{0.4 * r_z}{W} \right)^2 + 3 * \left( \frac{0.65}{c * t} \right)^2 \right)} \leq f_y \quad (\text{B-173})$$

$$F_{Rd,t} = \sqrt{\frac{f_y^2}{\left( \frac{0.55}{c * t} + \frac{0.4 * r_z}{W} \right)^2 + 3 * \left( \frac{0.65}{c * t} \right)^2}} \quad (\text{B-174})$$

### High clearance

$$W_{top} = \frac{t * a^2}{6} \quad (\text{B-175})$$

Load parallel to eye geometry, Section A-A of Figure B-10 (a and b)

$$\sigma_{Ed} = 0.5 * \frac{F_{Ed}}{c * t} + \frac{0.17 * F * r_z}{W} \leq f_y \quad (\text{B-176})$$

$$F_{Rd,t} = \frac{f_y}{\frac{1}{2 * c * t} + \frac{0.17 * r_z}{W}} \quad (\text{B-177})$$

Fracture beyond the hole

$$\sigma_{Ed} = \frac{0.3 * F * r_z}{W_{top}} \quad (\text{B-178})$$

$$\tau = \frac{0.5 * F}{a * t} \quad (\text{B-179})$$

$$\sigma_{com} = \sqrt{\sigma_{Ed}^2 + 3 * \tau^2} = \sqrt{F^2 * \left( \left( \frac{0.3 * r_z}{W_{top}} \right)^2 + 3 * \left( \frac{0.5}{a * t} \right)^2 \right)} \leq f_y \quad (\text{B-180})$$

$$F_{Rd,t} = \sqrt{\frac{f_y^2}{\left( \frac{0.3 * r_z}{W_{top}} \right)^2 + 3 * \left( \frac{0.5}{a * t} \right)^2}} \quad (\text{B-181})$$

Load perpendicular to eye geometry, Section A-A of Figure B-10 (c)

$$\sigma_{Ed} = \frac{0.55 * F}{c * t} + \frac{0.4 * F * r_z}{W} \quad (\text{B-182})$$

$$\tau = \frac{0.65 * F}{c * t} \quad (\text{B-183})$$

$$\sigma_{com} = \sqrt{\sigma_{Ed}^2 + 3 * \tau^2} = \sqrt{F^2 * \left( \left( \frac{0.55}{c * t} + \frac{0.4 * r_z}{W} \right)^2 + 3 * \left( \frac{0.65}{c * t} \right)^2 \right)} \leq f_y \quad (\text{B-184})$$

$$F_{Rd,t} = \sqrt{\frac{f_y^2}{\left( \frac{0.55}{c * t} + \frac{0.4 * r_z}{W} \right)^2 + 3 * \left( \frac{0.65}{c * t} \right)^2}} \quad (\text{B-185})$$

## Stress Analysis Manual

In the Stress Analysis Manual some parameters have other symbols, this is stated in equations ( B-186 ) to ( B-188 ).

$$w = 2 * R_{eye} \quad (\text{B-186})$$

$$e = e + R_{eye} \quad (\text{B-187})$$

$$D = d_h \quad (\text{B-188})$$

$K_n$  follows from Figure B-11 and is dependent on ratios:

$$\frac{f_y}{f_u}, \quad \frac{f_u}{E * \varepsilon_u} \approx 0 \text{ for steel}, \quad D/w$$

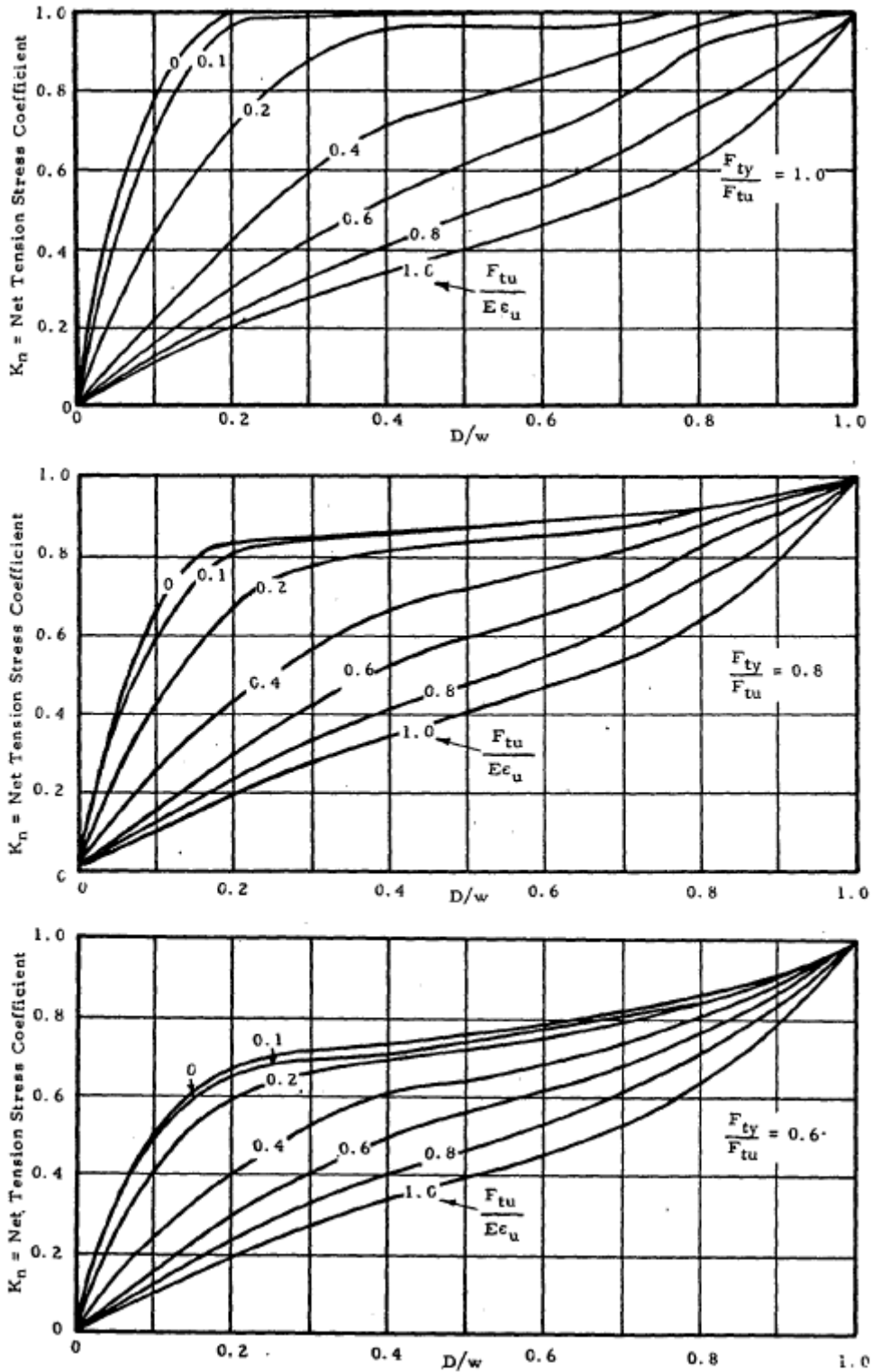


Figure B-11: Strength coefficient  $K_n$  (Stress Analysis Manual (1969), figure 9.4)

K follows from Figure B-12 and is dependent on ratio

$$e/D$$

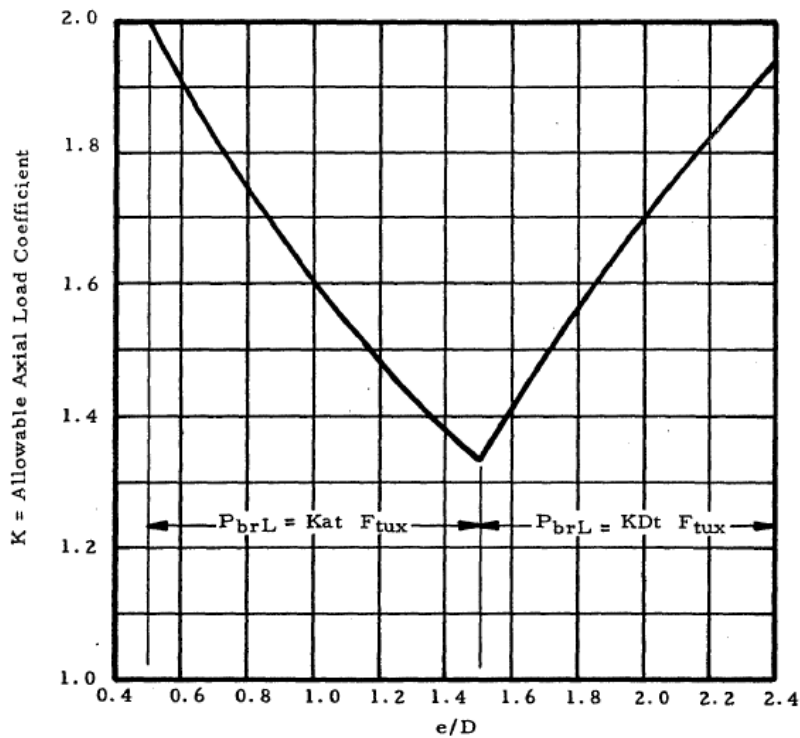


Figure B-12: Strength coefficient K (Stress Analysis Manual (1969), figure 9.2)

**Load parallel to the eye geometry**

Tension in the net section

$$F_{Rd,t} = K_n * f_u * (w - D) * t \tag{B-189}$$

Fracture beyond the hole/bearing strength

The Stress Analysis Manual provides a combined check for fracture beyond the hole and bearing.

$$\text{Bearing if } e/D > 1.5 \tag{B-190}$$

$$\text{Fracture beyond the hole if } e/D < 1.5 \tag{B-191}$$

Fracture beyond the hole

$$F_{Rd,t} = K * a * t * f_u \tag{B-192}$$

Bearing strength

$$F_{Rd,b} = K * D * t * f_u \tag{B-193}$$

**Load perpendicular to the eye geometry**

Strength of the eye for perpendicular loads

$h_{av}$  can be determined using Figure B-13 and equation ( B-194 ).

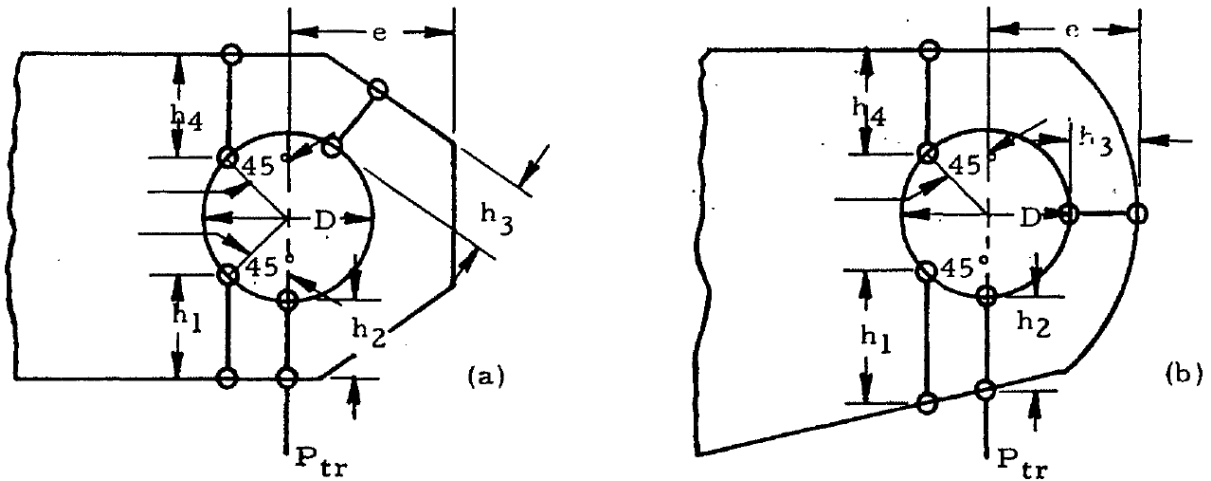


Figure B-13: Eye geometries in accordance with the Stress Analysis Manual (1969), figure 9.7)

$$h_{av} = \frac{6}{3/h_1 + 1/h_2 + 1/h_3 + 1/h_4} \tag{B-194}$$

$K_{tru}$  follows from Figure B-14.

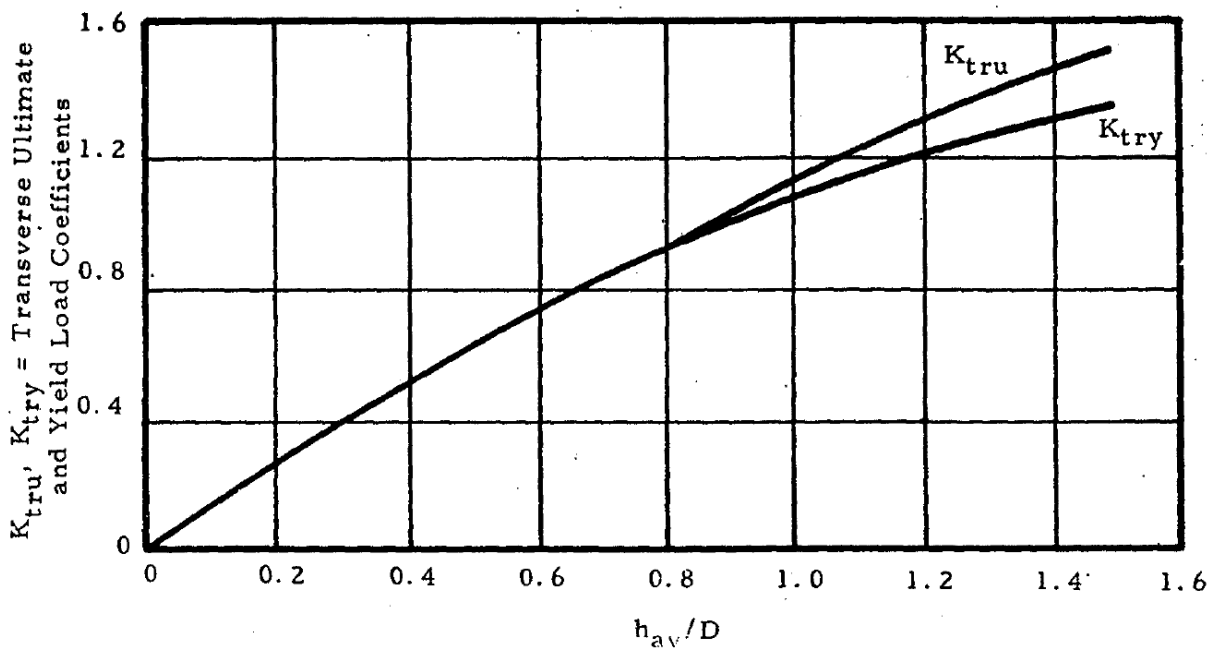


Figure B-14:  $K_{tru}$  (Stress Analysis Manual (1969), figure 9.8)

$$F_{Rd,t} = K_{tru} * f_u * D * t \tag{B-195}$$

Oblique loads ( $0^\circ < \alpha < 90^\circ$ )

$$F_{//} = F * \cos(\alpha) \tag{B-196}$$

$$F_{\perp} = F * \sin(\alpha) \tag{B-197}$$

$$\frac{F_{//}}{F_{Rd,t,parallel}} + \frac{F_{\perp}}{F_{Rd,t,perpendicular}} \leq 1 \tag{B-198}$$

$$F_{Rd,t} = \left( \frac{1}{\left( \frac{\cos(\alpha)}{K_n * f_u * (w - D)} \right)^{1.6} + \left( \frac{\sin(\alpha)}{K_{tru} * f_u * D * t} \right)^{1.6}} \right)^{1/1.6} \quad (\text{B-199})$$

Pin bending

$$M = F * \frac{t + 2 * t_2 + 4 * s}{8} \quad (\text{B-200})$$

$$W = \frac{\pi * d_p^3}{32} \quad (\text{B-201})$$

$$F_{Rd,pb} = \frac{8 * f_y * W}{t + 2 * t_2 + 4 * s} \quad (\text{B-202})$$

Pin shear

$$A = \frac{\pi * d_p^2}{4} \quad (\text{B-203})$$

$$F_{Rd,pv} = 2 * A * \frac{f_u}{\sqrt{3}} \quad (\text{B-204})$$

# C Comparative study

## C.1 Reference eyes

The input parameters used for the reference eyes are listed in Table C-1 to Table C-3.

Geometry				
$R_{eye}$	=	100	mm	radius eye
$e$	=	50	mm	eccentricity
$d_h$	=	82	mm	diameter pin hole
$d_p$	=	80	mm	diameter pin
$t$	=	25	mm	thickness eye
$L_{gross}$	=	200	mm	width eye bar
$\beta$	=	0	°	lug angle
$t_2$	=	20	mm	thickness side eyes
$s$	=	5	mm	clearance between eyes
Material eye				
$f_y$	=	690	N/mm <sup>2</sup>	yield stress
$f_u$	=	770	N/mm <sup>2</sup>	ultimate tensile stress
$E$	=	210000	N/mm <sup>2</sup>	Youngsmodulus
$\nu$	=	0.3	[ - ]	Poissons ratio
Load				
$F_d$	=	-	kN	load
$\alpha$	=	0	°	load angle
Material pin				
$f_{yp}$	=	690	N/mm <sup>2</sup>	yield stress
$f_{up}$	=	770	N/mm <sup>2</sup>	ultimate tensile stress
$E_p$	=	210000	N/mm <sup>2</sup>	Youngsmodulus
$\nu_p$	=	0.3	[ - ]	Poissons ratio

Table C-1: Input reference eye 1

Geometry				
$R_{eye}$	=	100	mm	radius eye
$e$	=	0	mm	eccentricity
$d_h$	=	82	mm	diameter pin hole
$d_p$	=	80	mm	diameter pin
$t$	=	40	mm	thickness eye
$L_{gross}$	=	200	mm	width eye bar
$\beta$	=	0	°	lug angle
$t_2$	=	20	mm	thickness side eyes
$s$	=	5	mm	clearance between eyes
Material eye				
$f_y$	=	690	N/mm <sup>2</sup>	yield stress
$f_u$	=	770	N/mm <sup>2</sup>	ultimate tensile stress
$E$	=	210000	N/mm <sup>2</sup>	Youngsmodulus
$\nu$	=	0.3	[ - ]	Poissons ratio
Load				
$F_d$	=	-	kN	load
$\alpha$	=	0	°	load angle
Material pin				
$f_{yp}$	=	690	N/mm <sup>2</sup>	yield stress
$f_{up}$	=	770	N/mm <sup>2</sup>	ultimate tensile stress
$E_p$	=	210000	N/mm <sup>2</sup>	Youngsmodulus
$\nu_p$	=	0.3	[ - ]	Poissons ratio

Table C-2: Input reference eye 2

Geometry				
$R_{eye}$	=	150	mm	radius eye
$e$	=	50	mm	eccentricity
$d_h$	=	82	mm	diameter pin hole
$d_p$	=	80	mm	diameter pin
$t$	=	40	mm	thickness eye
$L_{gross}$	=	300	mm	width eye bar
$\beta$	=	0	°	lug angle
$t_2$	=	20	mm	thickness side eyes
$s$	=	5	mm	clearance between eyes
Material eye				
$f_y$	=	690	N/mm <sup>2</sup>	yield stress
$f_u$	=	770	N/mm <sup>2</sup>	ultimate tensile stress
$E$	=	210000	N/mm <sup>2</sup>	Youngsmodulus
$\nu$	=	0.3	[ - ]	Poissons ratio
Load				
$F_d$	=	-	kN	load
$\alpha$	=	0	°	load angle
Material pin				
$f_{yp}$	=	690	N/mm <sup>2</sup>	yield stress
$f_{up}$	=	770	N/mm <sup>2</sup>	ultimate tensile stress
$E_p$	=	210000	N/mm <sup>2</sup>	Youngsmodulus
$\nu_p$	=	0.3	[ - ]	Poissons ratio

Table C-3: Input reference eye 3

For each reference eye, all possible capacities for all failure criteria are summarized in Table C-5 to Table C-7. In Table C-4 all failure criteria are listed and numbered.

Failure criteria	Failure criteria #
Tension in the net section	1
Fracture beyond the hole	2
Bearing	3
Shear	4
Lgross	5
Pin bending	6
Pin shear	7
Pin combined	8

**Table C-4: Failure criteria**

Note that failure criteria 6 to 8 mean failure in the pin, which is excluded from this research. These are only noted as reference.

Method	Failure criteria								Failure load [kN]
	1	2	3	4	5	6	7	8	
EN1993-1-8	1748	2999	3312			2220	4645	3277	1748
EN13001-3-1	1785		2453	3667		2775	3004		1785
ASME BTH-1	2869	4766	2760	5173		2775	4005		2760
AISC 360-10	2726		2981	4130	4140				2726
NEN6786	947	2073							947
Stress Analysis Manual	3152	4184	3994			2775	3004		2775
Peterson	1117								1117
Ekvall	3287								3287
Petersen	1748	2999				2274	3067		1748
Dietz	1050		219						219
Guo-Geruschkat	757								757
Duerr	2869	4766		5173					2869
Hertz			1059						1059
Schaper			1935						1935
Bleich	924	2188	1734						924
Reissner	788								788
Reidelbach	906								906
Poócza	1435	2524							1435

Table C-5: Capacities for all failure criteria of reference eye 1

Method	Failure criteria								Failure load [kN]
	1	2	3	4	5	6	7	8	
EN1993-1-8	1748	239	3312			2220	4645	3277	239
EN13001-3-1	1619		2453	2073		2775	3004		1619
ASME BTH-1	2869	3026	2760	3017		2775	4005		2760
AISC 360-10	2726		2981	2744	4140				2726
NEN6786	789	585							585
Stress Analysis Manual	3152	2667	2810			2775	3004		2667
Peterson	865								865
Ekvall	2575								2575
Petersen	1748	239				2274	3067		239
Dietz	955		219						219
Guo-Geruschkat	757								757
Duerr	2869	3026		3017					2869
Hertz			1059						1059
Schaper			1935						1935
Bleich	924	2188	1734						924
Reissner	788								788
Reidelbach	906								906
Poócza	737	1138							737

Table C-6: Capacities for all failure criteria of reference eye 2

Method	Failure criteria								Failure load [kN]
	1	2	3	4	5	6	7	8	
EN1993-1-8	4508	5759	3312			2220	4645	3277	2220
EN13001-3-1	2836		2453	5299		2775	3004		2453
ASME BTH-1	3899	6860	2760	7408		2775	4005		2760
AISC 360-10	4435		2981	5516	6210				2981
NEN6786	2159	3168							2159
Stress Analysis Manual	5742	6033	4952			2775	3004		2775
Peterson	1559								1559
Ekvall	4927								4927
Petersen	4508	5759				2274	3067		2274
Dietz	1312		219						219
Guo-Geruschkat	1399								1399
Duerr	3899	6860		7408					3899
Hertz			1059						1059
Schaper			1935						1935
Bleich	1730	5618	1734						1730
Reissner	1168								1168
Reidelbach	1463								1463
Poócza	2221	4462							2221

Table C-7: Capacities for all failure criteria of reference eye 3

To point out the first three failure criteria, these capacities are plotted in charts for the different methods (see below).

- Elastic methods, which provide “Elastic capacity”
  - Peterson

- Dietz
- Guo-Geruschkat
- Hertz
- Schaper
- Bleich
- Reissner
- Reidelbach
- Poócza
- Fully plastic methods, which provide “Ultimate capacity”
  - ASME BTH-1
  - AISC 360-10
  - Ekvall
  - Duerr
  - Stress Analysis Manual
- Partial plastic methods, which provide “Reduced ultimate capacity”
  - EN1993-1-8
  - EN13001-3-1
  - NEN6786
  - Petersen

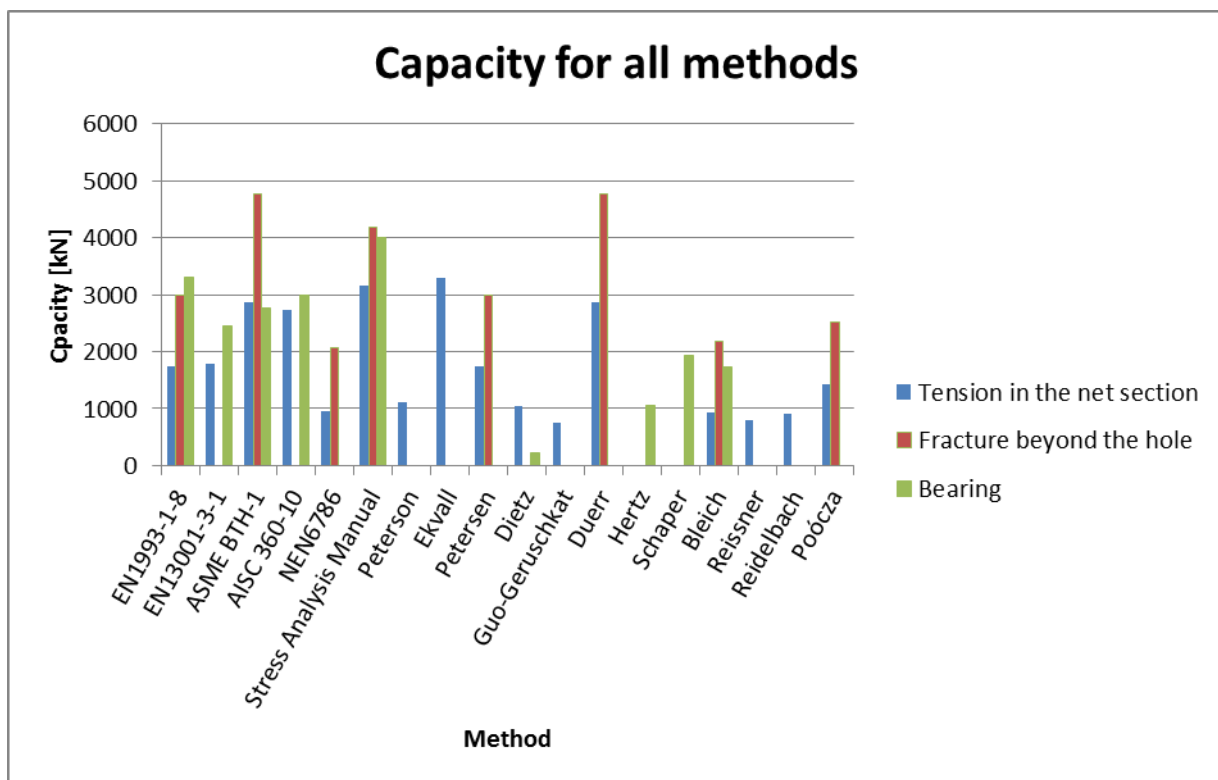


Chart C-1: Capacities reference eye 1

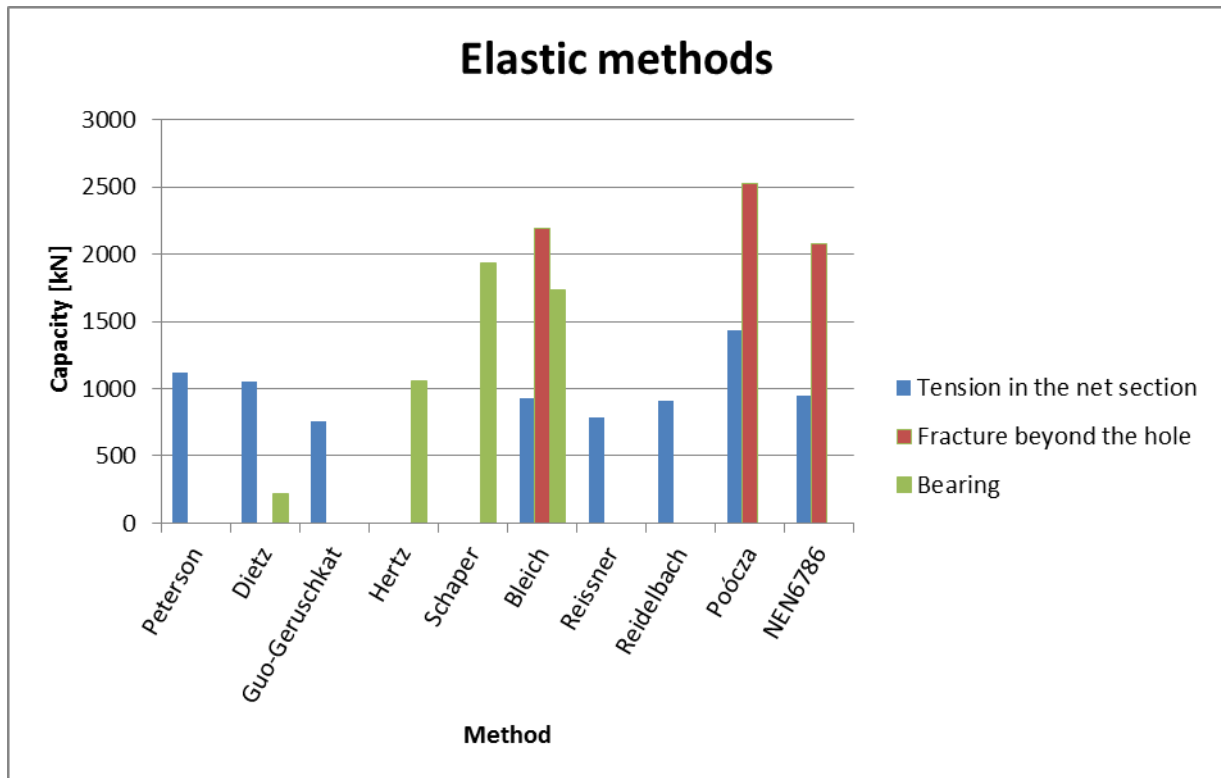


Chart C-2: Elastic capacities reference eye 1

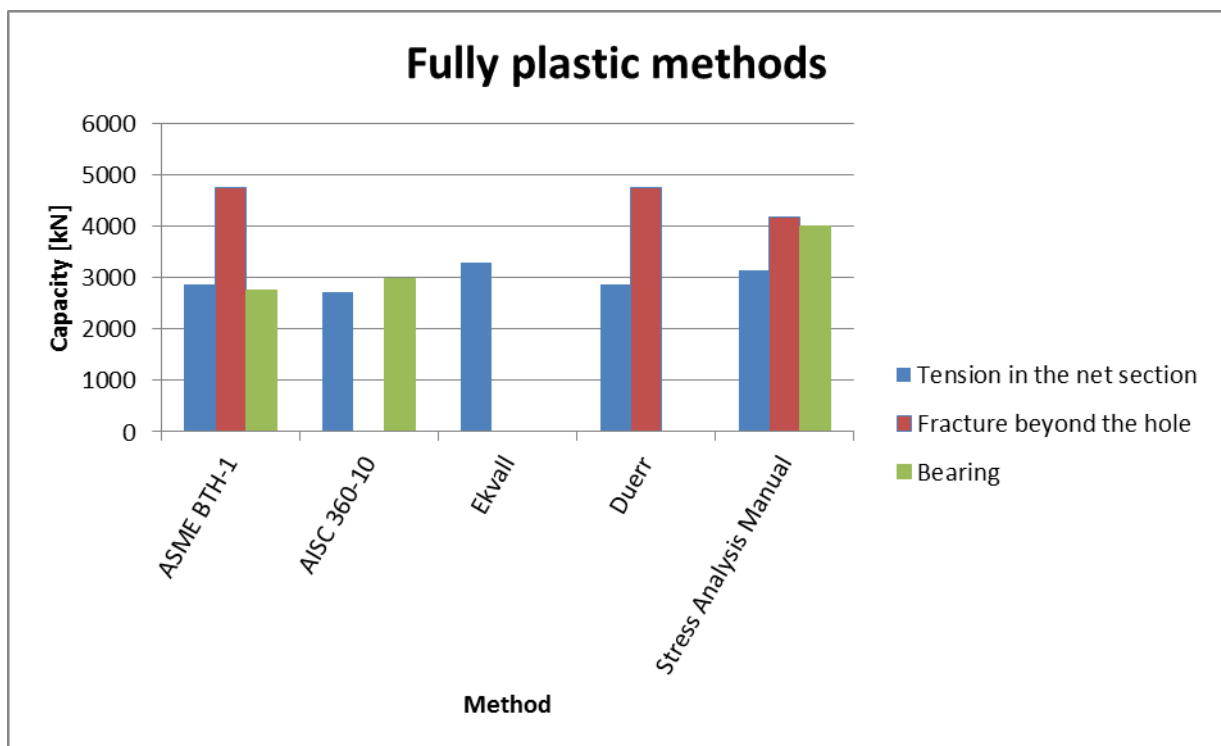


Chart C-3: Fully plastic capacities reference eye 1

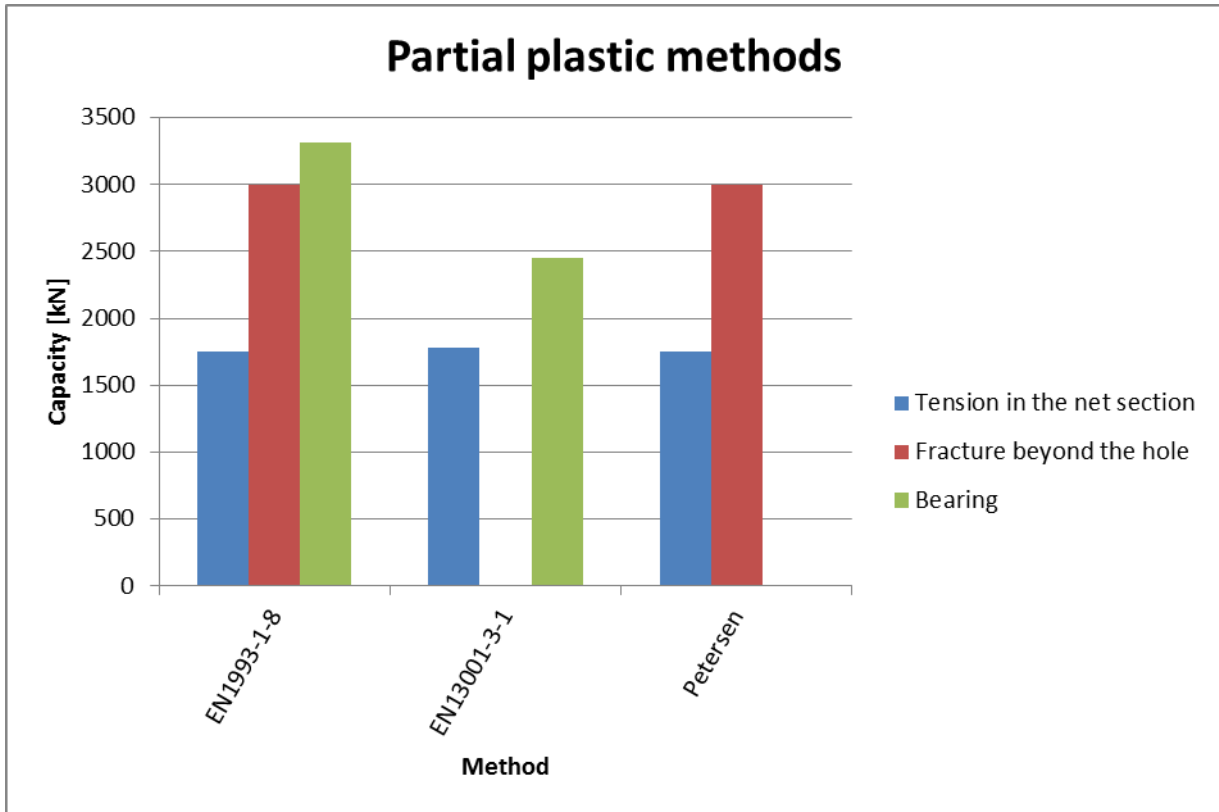


Chart C-4: Partial plastic capacities reference eye 1

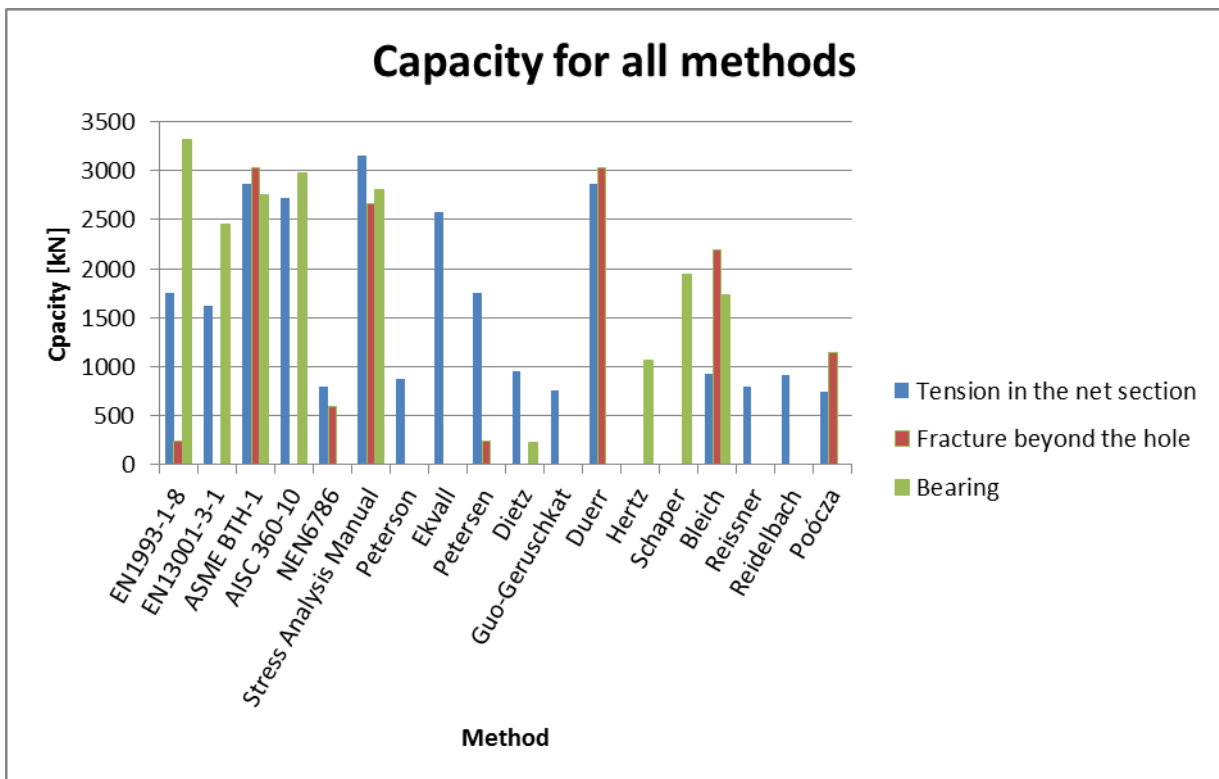


Chart C-5: Capacities reference eye 2

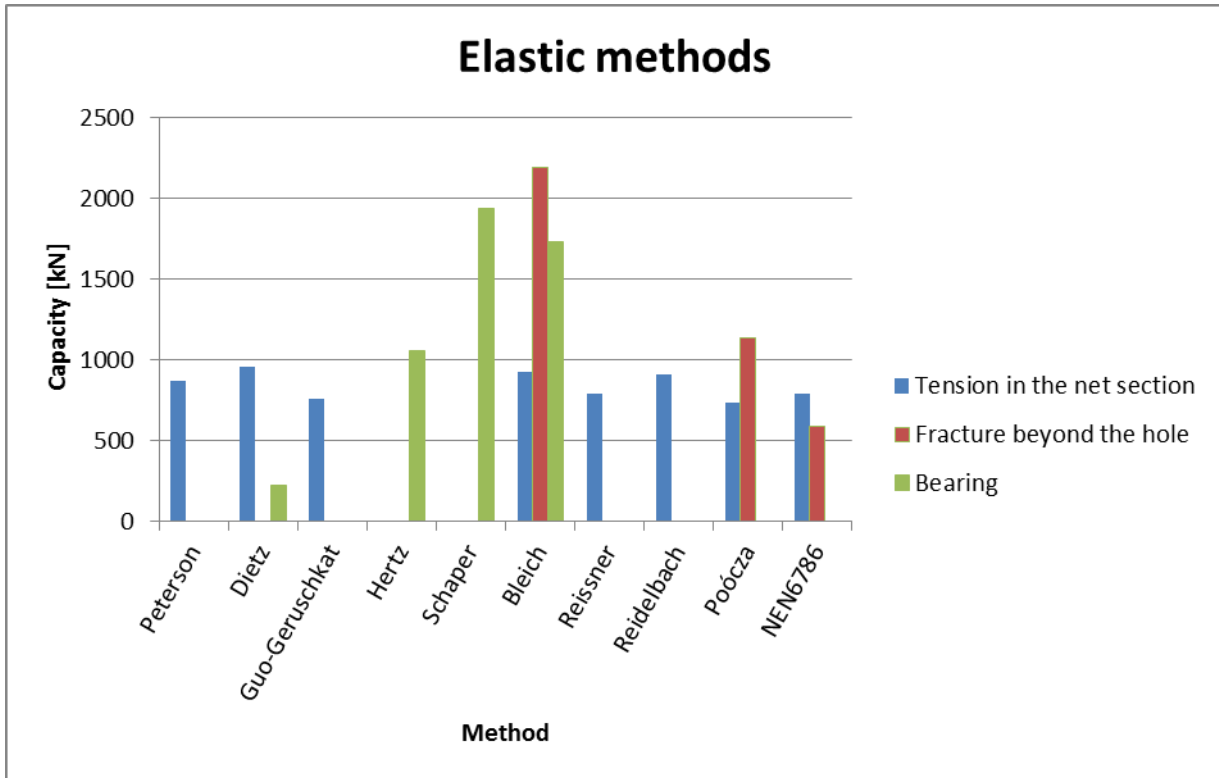


Chart C-6: Elastic capacities reference eye 2

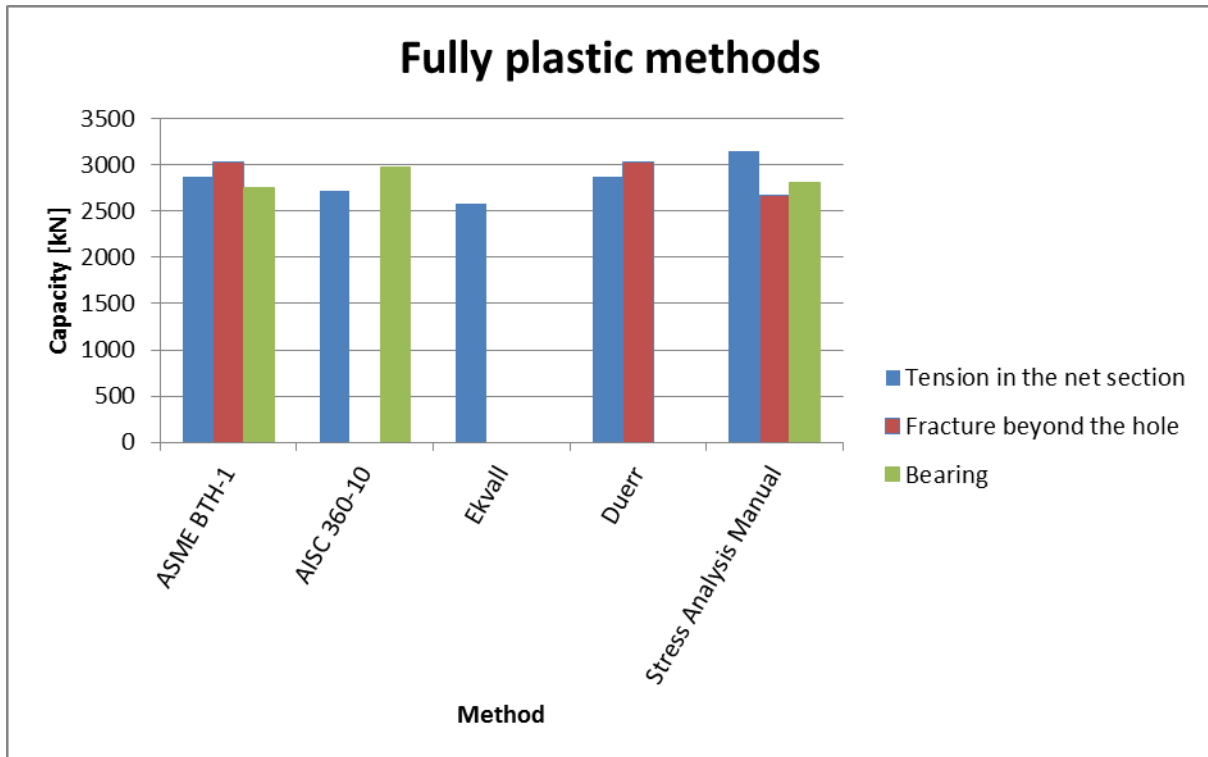


Chart C-7: Fully plastic capacities reference eye 2

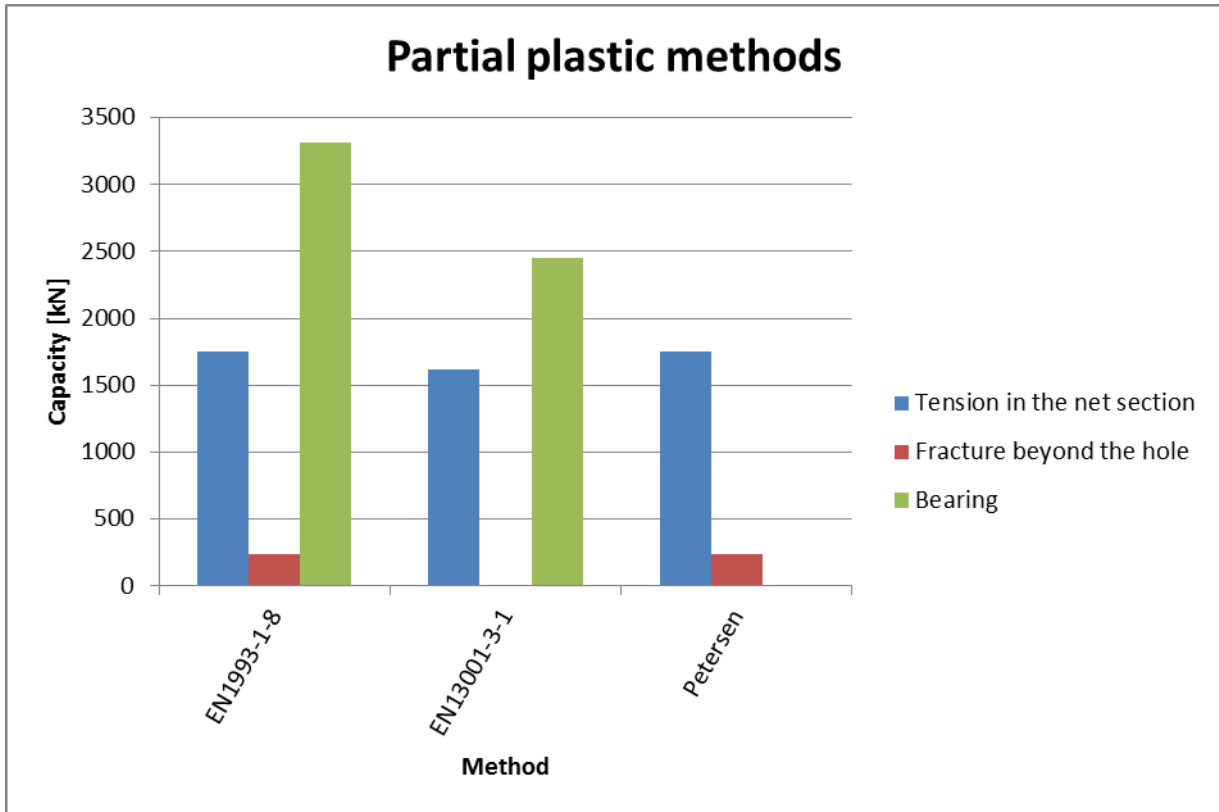


Chart C-8: Partial plastic capacities reference eye 2

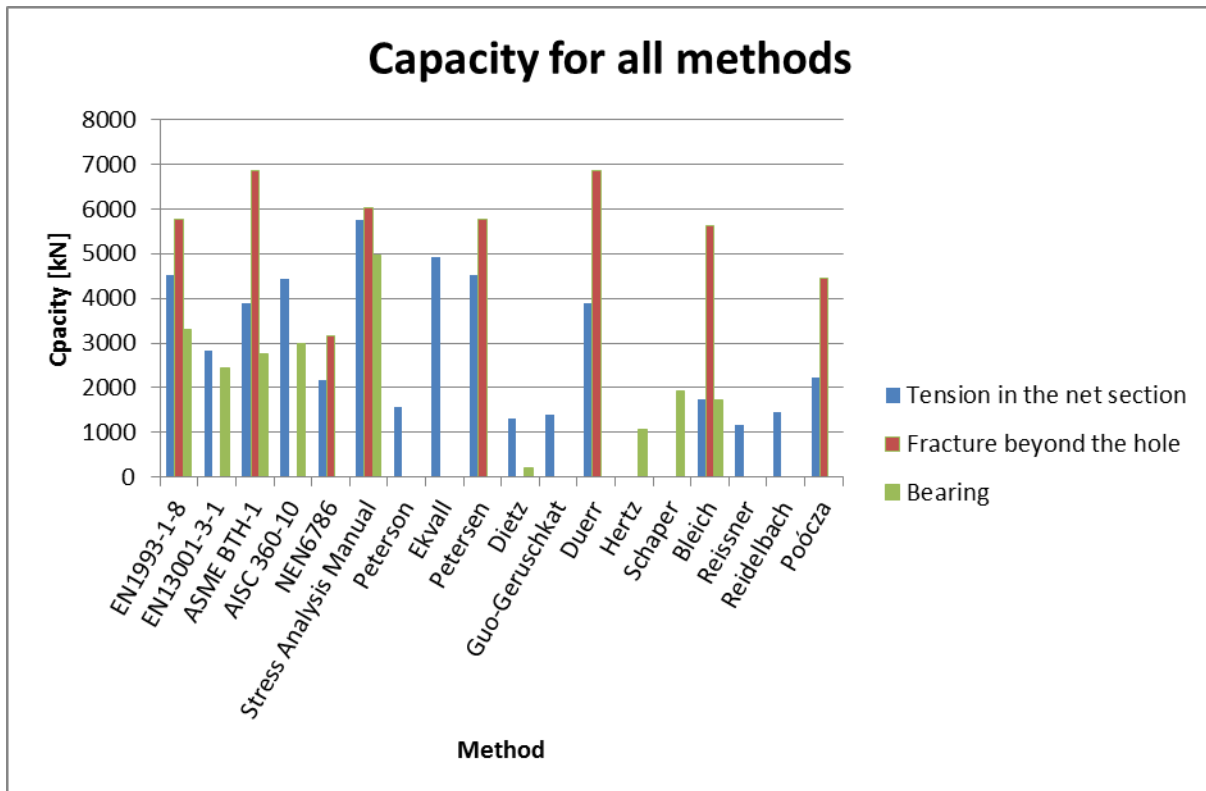


Chart C-9: Capacities reference eye 3

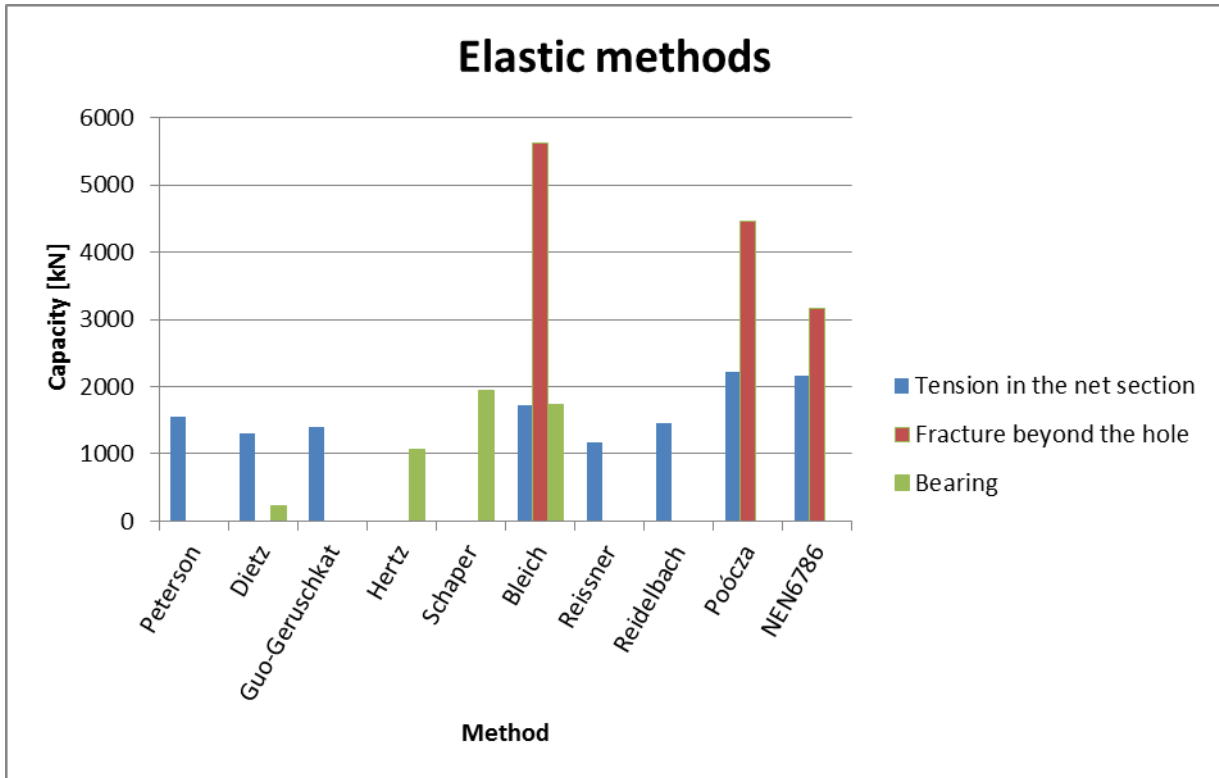


Chart C-10: Elastic capacities reference eye 3

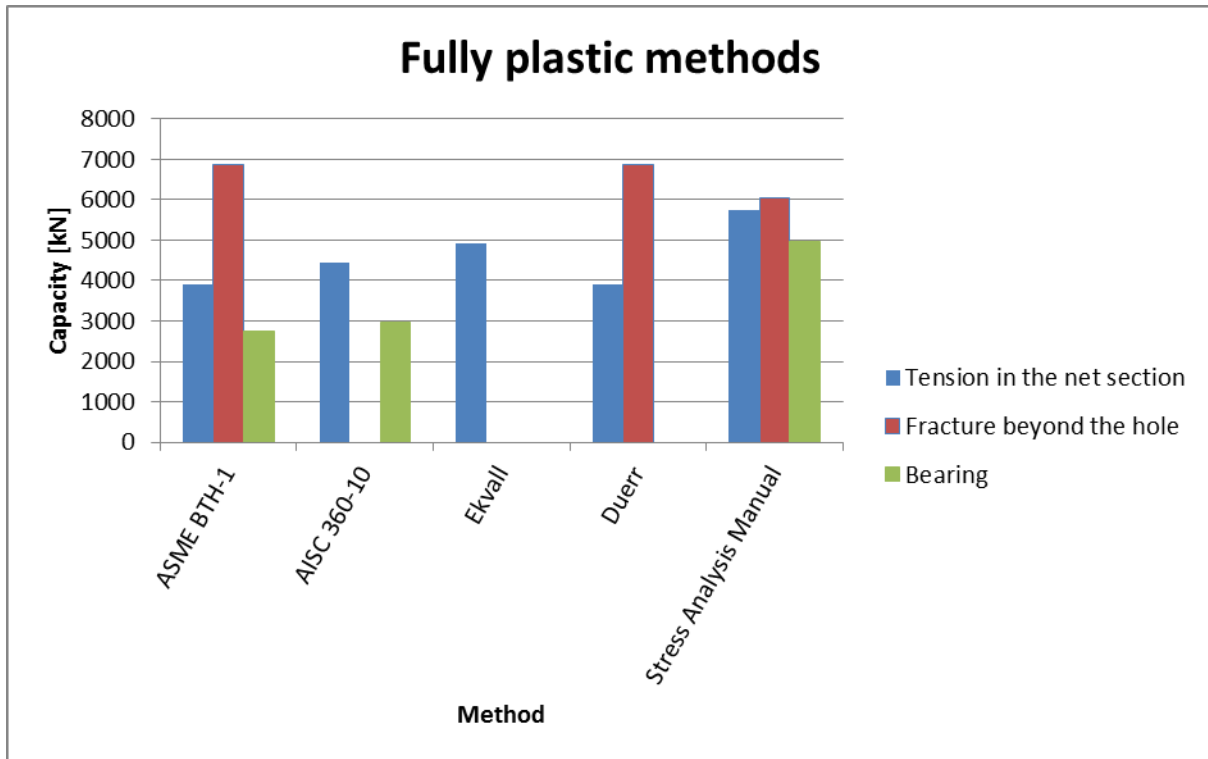
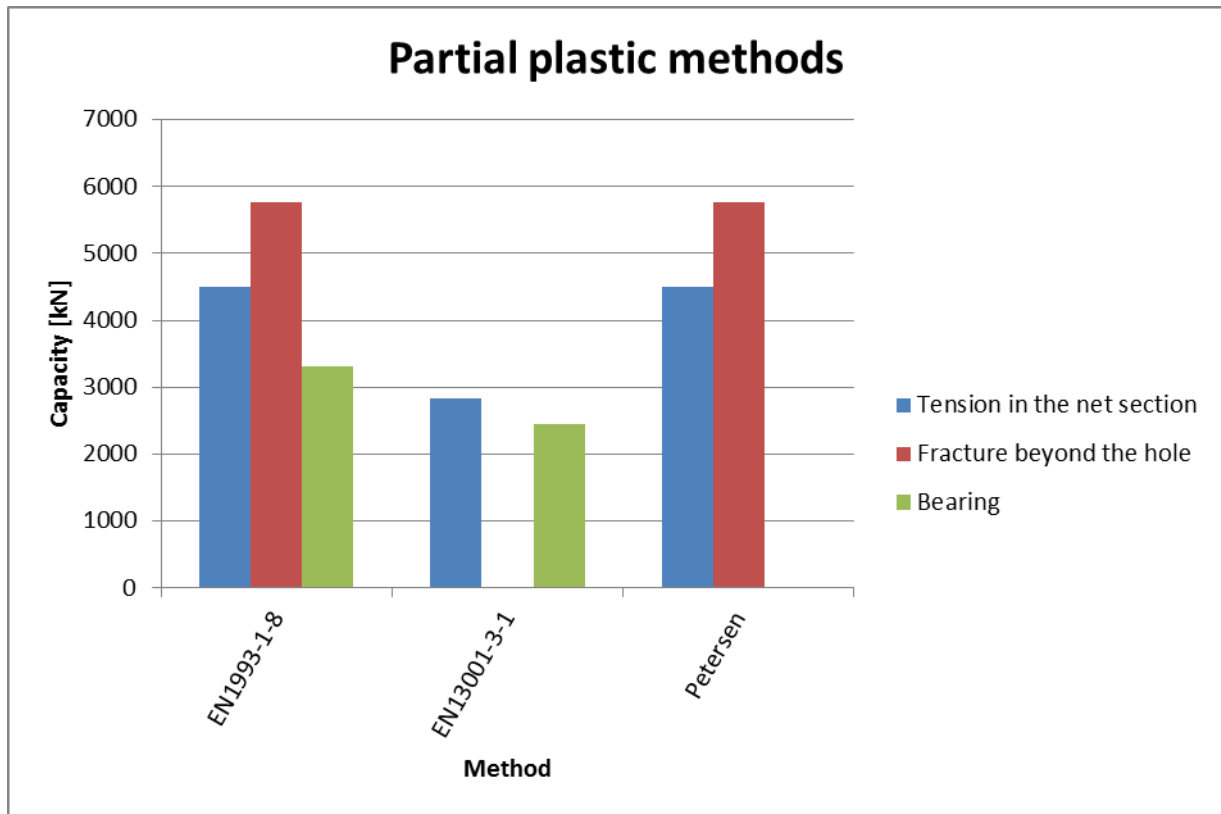


Chart C-11: Fully plastic capacities reference eye 3



**Chart C-12: Partial plastic capacities reference eye 3**

To point out the differences between all methods the averages, standard deviations and variances are listed in Table C-8 to Table C-16.

Average tension in the net section [kN]			
	Reference eye 1	Reference eye 2	Reference eye 3
<b>All capacities</b>	1757	1627	2985
<b>Elastic capacities</b>	991	840	1626
<b>Fully plastic capacities</b>	2980	2838	4580
<b>Partial plastic capacities</b>	1760	1705	3951

**Table C-8: Average tension in the net section**

Standard deviation tension in the net section [kN]			
	Reference eye 1	Reference eye 2	Reference eye 3
All capacities	892	885	1492
Elastic capacities	202	78	361
Fully plastic capacities	206	191	695
Partial plastic capacities	18	61	788

Table C-9: Standard deviation tension in the net section

Variance tension in the net section [-]			
	Reference eye 1	Reference eye 2	Reference eye 3
All capacities	51%	54%	50%
Elastic capacities	20%	9%	22%
Fully plastic capacities	7%	7%	15%
Partial plastic capacities	1%	4%	20%

Table C-10: Variance tension in the net section

Average fracture beyond the hole [kN]			
	Reference eye 1	Reference eye 2	Reference eye 3
All capacities	3312	1639	5565
Elastic capacities	2262	1304	4416
Fully plastic capacities	4572	2906	6584
Partial plastic capacities	2999	239	5759

Table C-11: Average fracture beyond the hole

Standard deviation fracture beyond the hole [kN]			
	Reference eye 1	Reference eye 2	Reference eye 3
All capacities	1037	1145	1152
Elastic capacities	191	665	1001
Fully plastic capacities	274	169	390
Partial plastic capacities	0	0	0

Table C-12: Standard deviation fracture beyond the hole

Variance fracture beyond the hole [-]			
	Reference eye 1	Reference eye 2	Reference eye 3
All capacities	31%	70%	21%
Elastic capacities	8%	51%	23%
Fully plastic capacities	6%	6%	6%
Partial plastic capacities	0%	0%	0%

Table C-13: Variance fracture beyond the hole

Average bearing [kN]			
	Reference eye 1	Reference eye 2	Reference eye 3
All capacities	2272	2140	2378
Elastic capacities	1237	1237	1237
Fully plastic capacities	3245	2850	3564
Partial plastic capacities	2883	2883	2883

Table C-14: Average bearing

Standard deviation bearing [kN]			
	Reference eye 1	Reference eye 2	Reference eye 3
All capacities	1101	947	1292
Elastic capacities	671	671	671
Fully plastic capacities	537	95	986
Partial plastic capacities	429	429	429

Table C-15: Standard deviation bearing

Variance bearing [-]			
	Reference eye 1	Reference eye 2	Reference eye 3
All capacities	48%	44%	54%
Elastic capacities	54%	54%	54%
Fully plastic capacities	17%	3%	28%
Partial plastic capacities	15%	15%	15%

Table C-16: Variance bearing

In Chart C-13 to Chart C-15 these scatters for each reference eye are plotted.

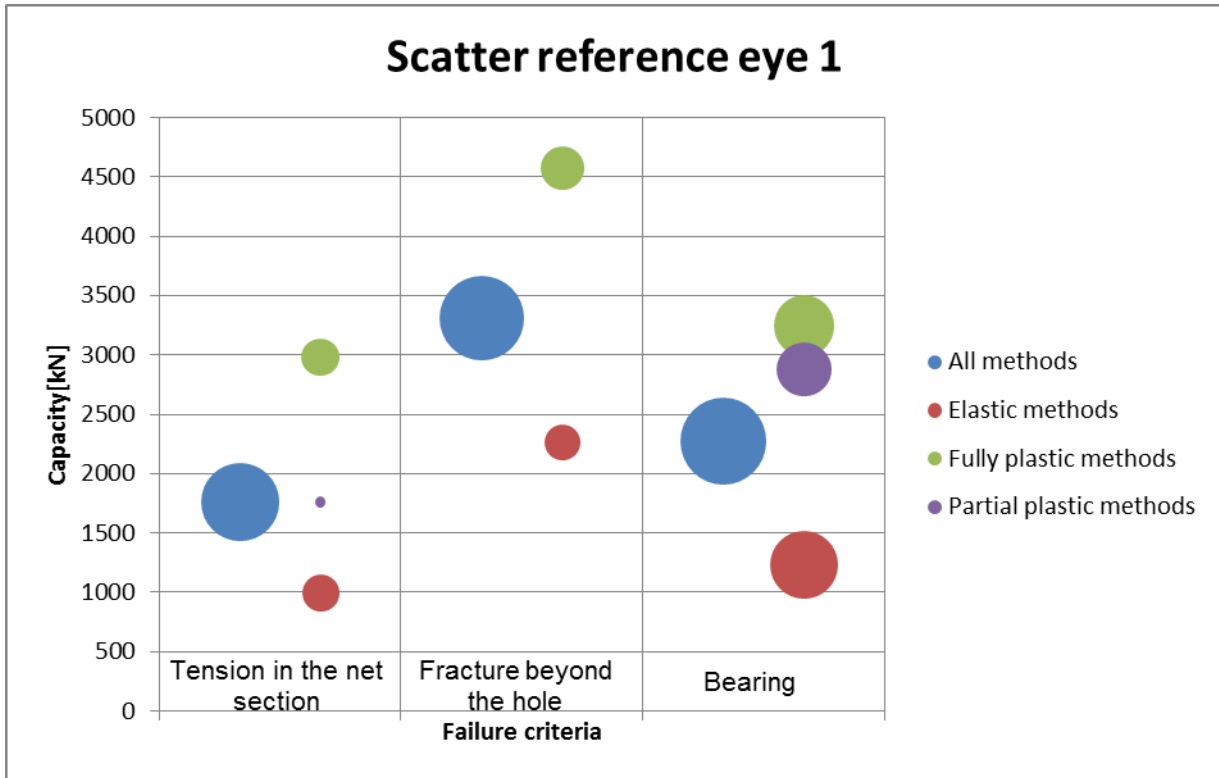


Chart C-13: Scatter reference eye 1

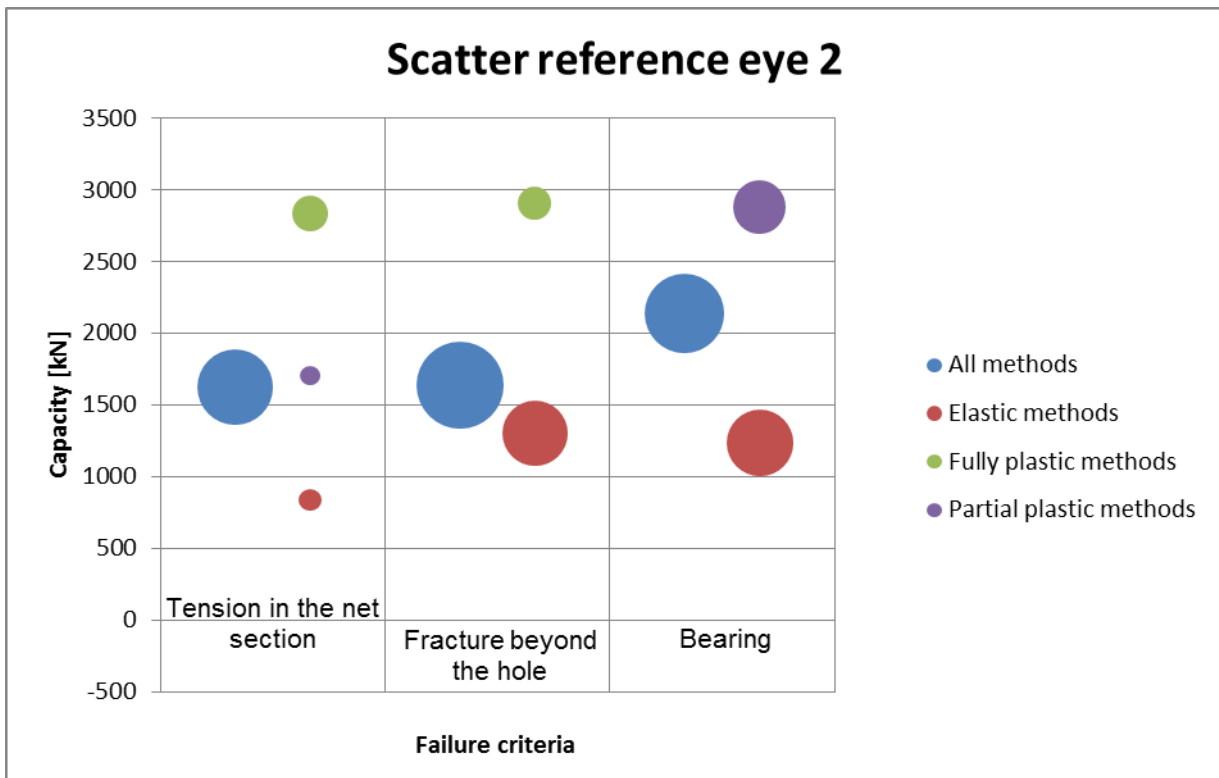


Chart C-14: Scatter reference eye 2

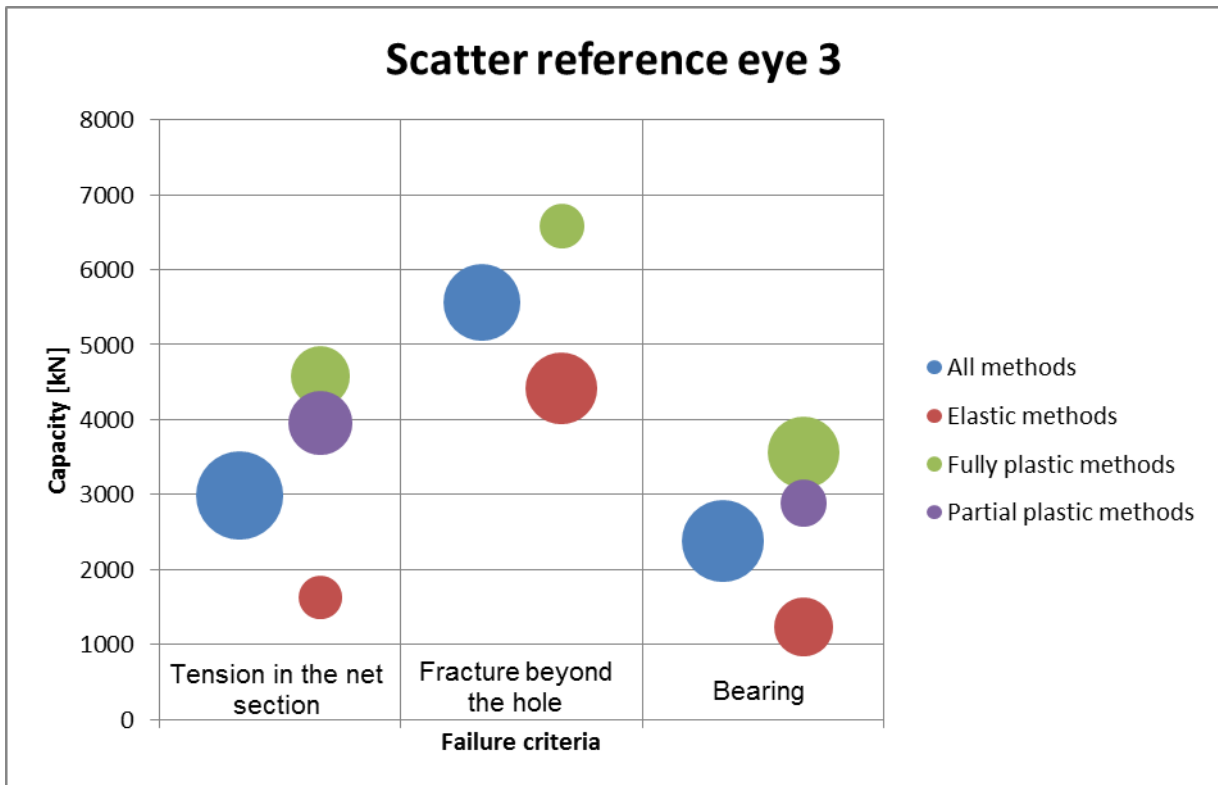


Chart C-15: Scatter reference eye 3

## C.2 Parameter influences

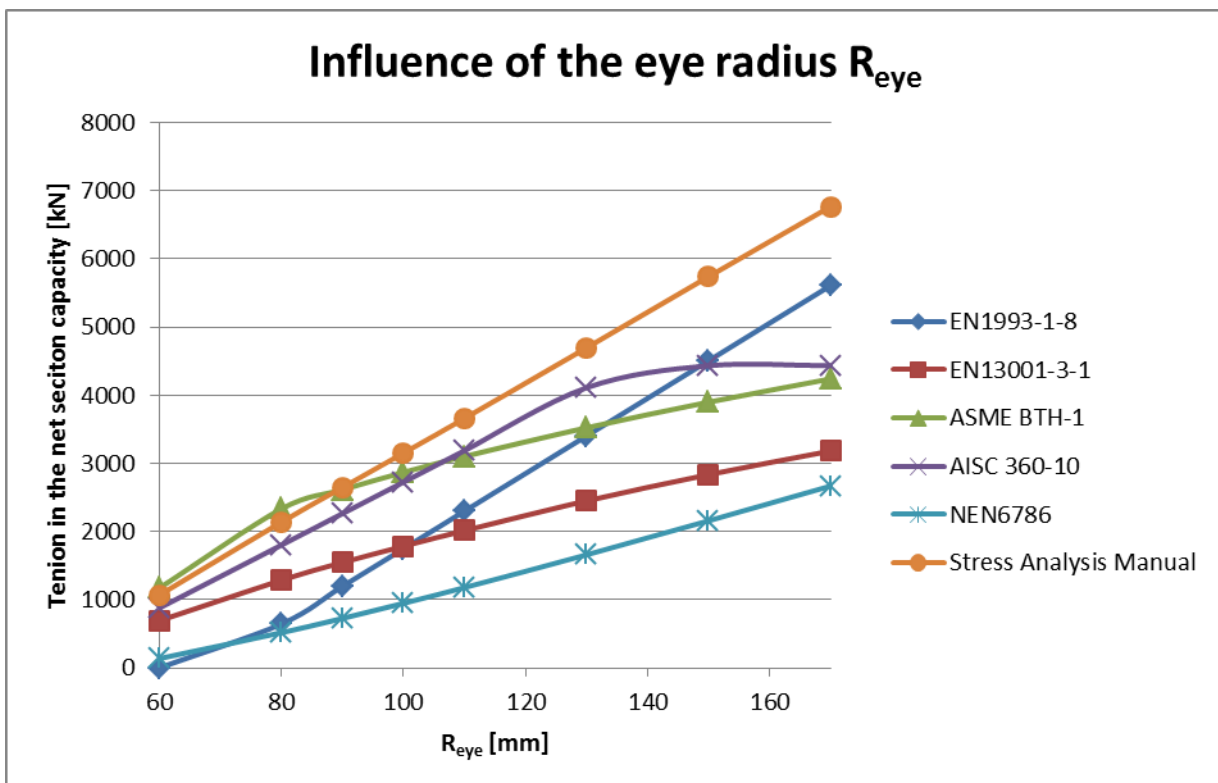


Chart C-16: Influence of the eye radius  $R_{eye}$

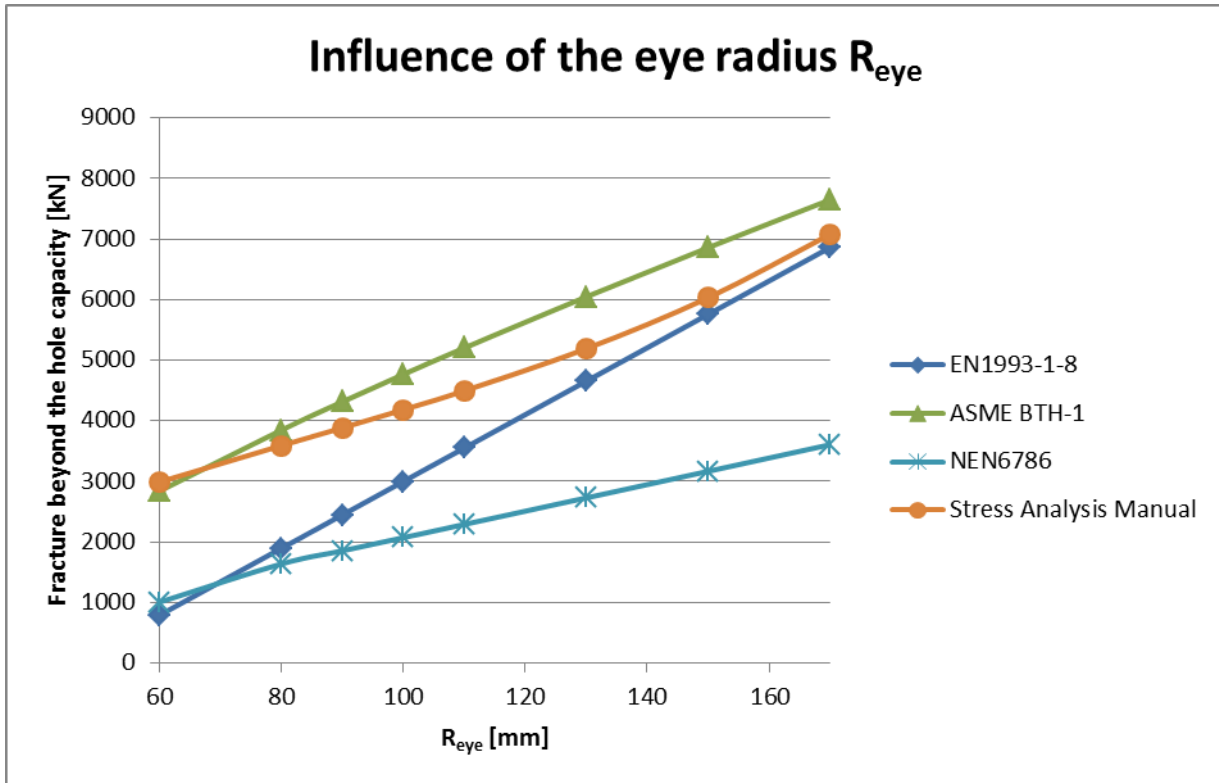


Chart C-17: Influence of the eye radius  $R_{eye}$

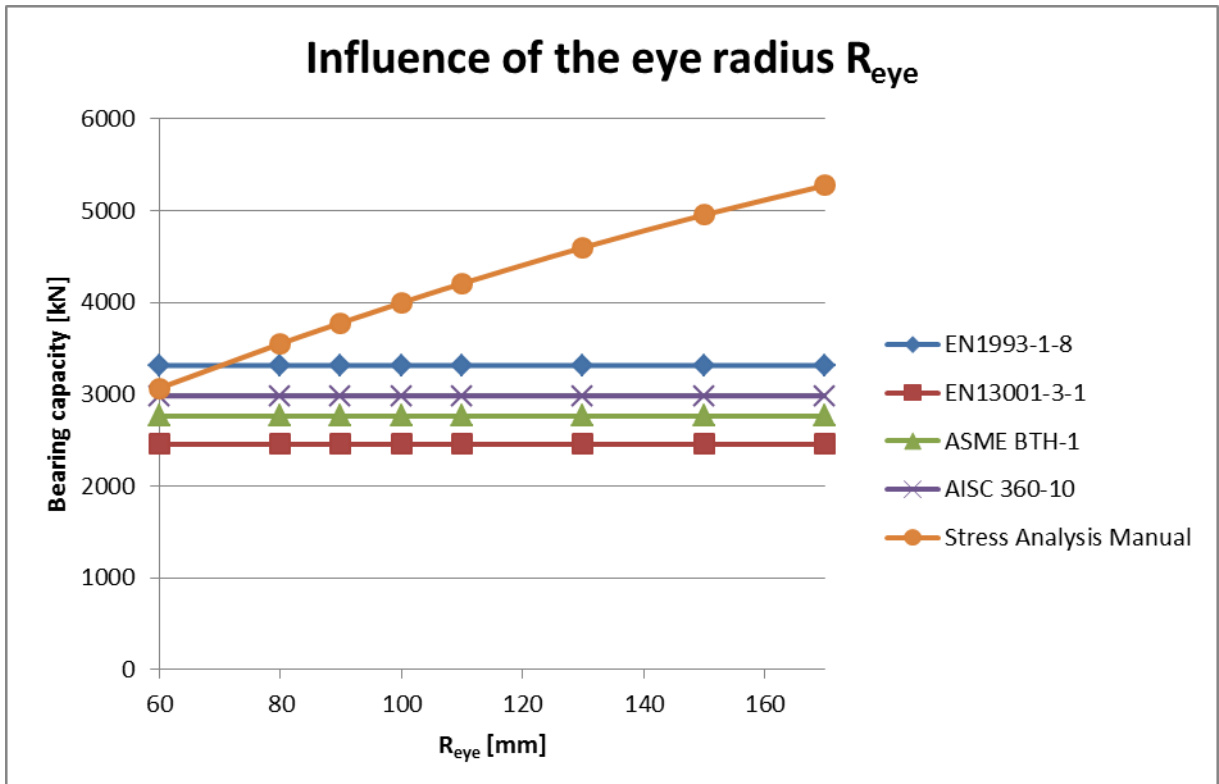


Chart C-18: Influence of the eye radius  $R_{eye}$

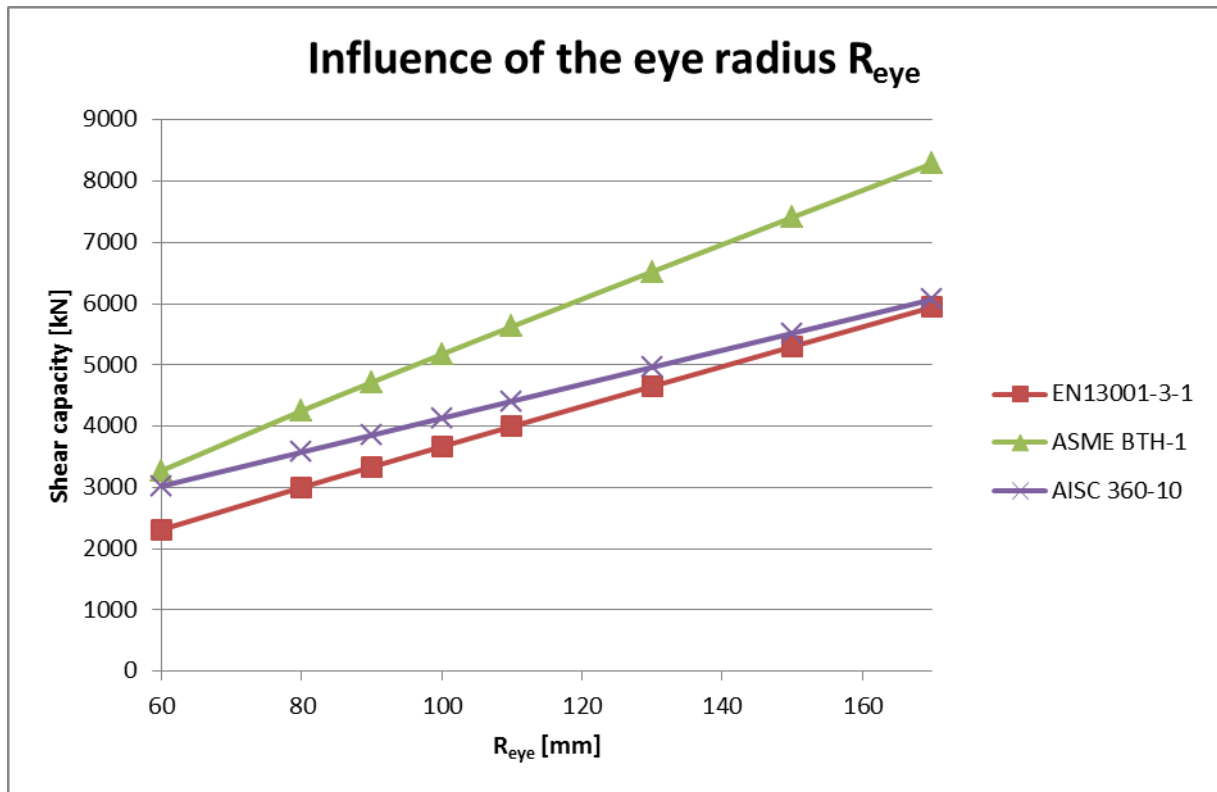


Chart C-19: Influence of the eye radius  $R_{eye}$

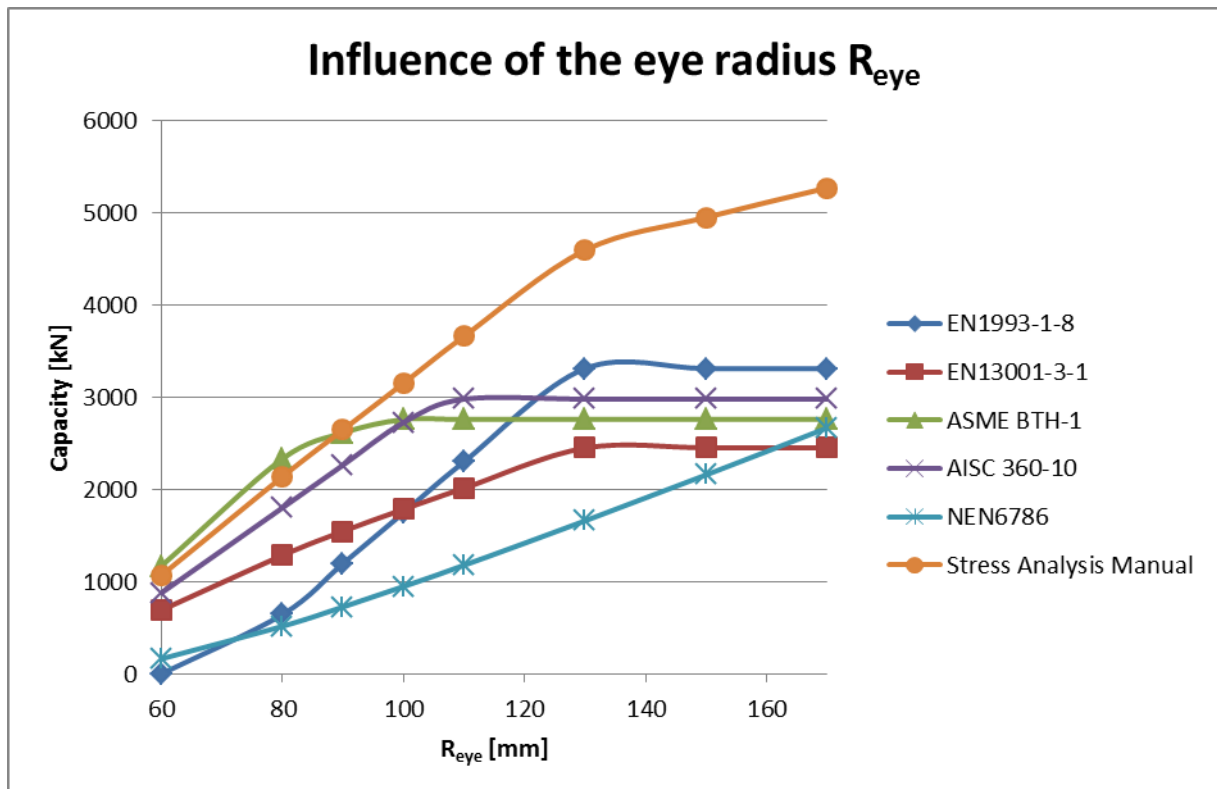


Chart C-20: Influence of the eye radius  $R_{eye}$

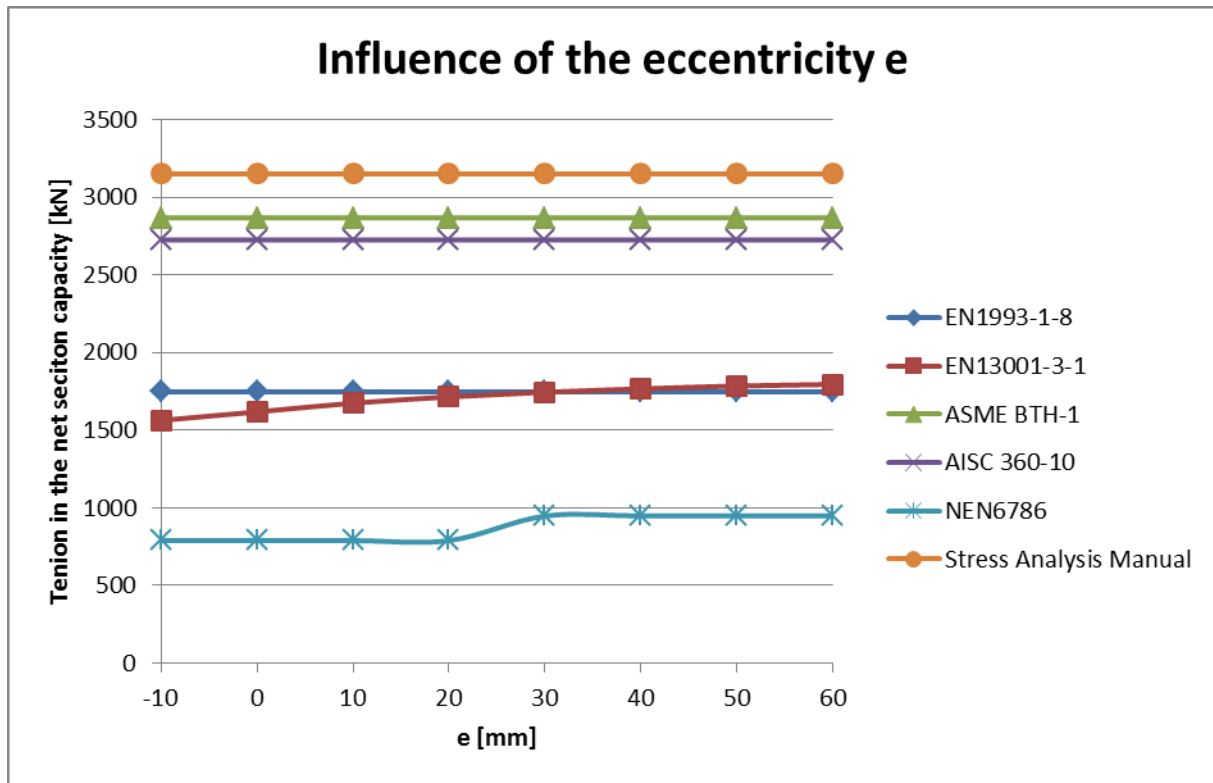


Chart C-21: Influence of the eccentricity  $e$

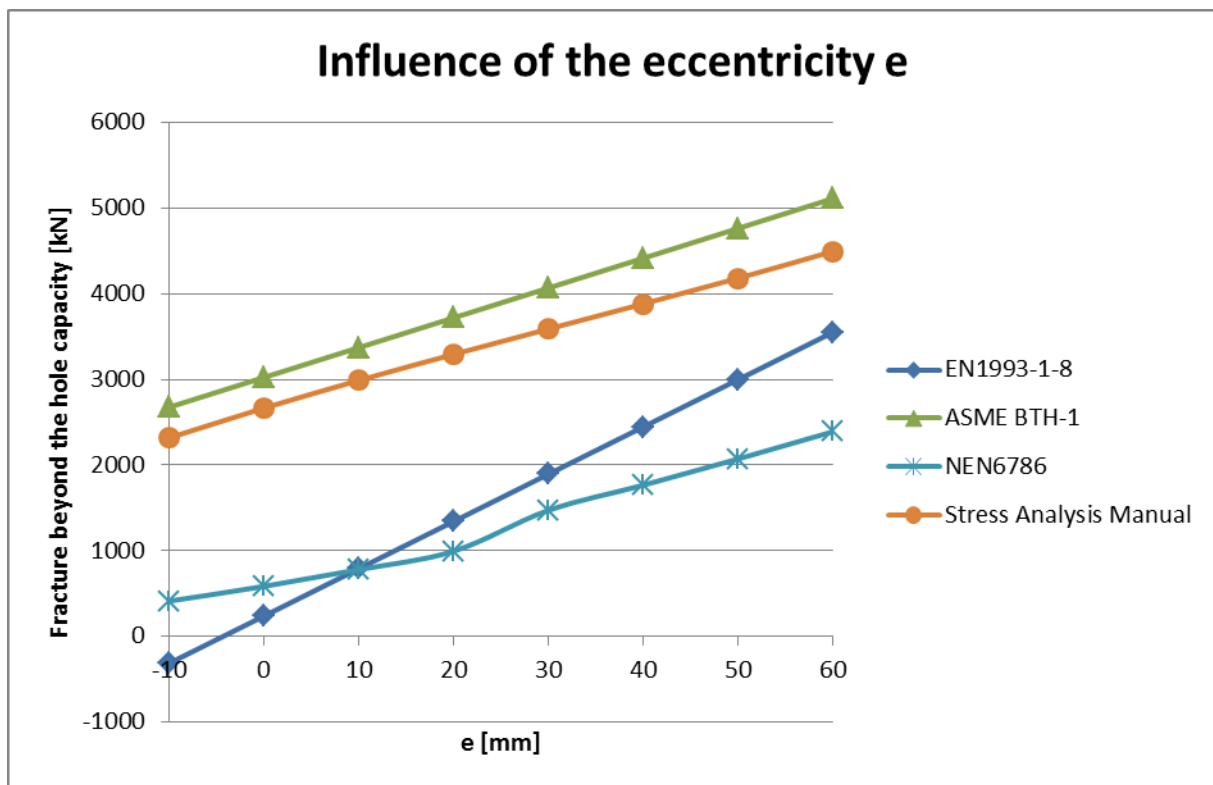


Chart C-22: Influence of the eccentricity  $e$

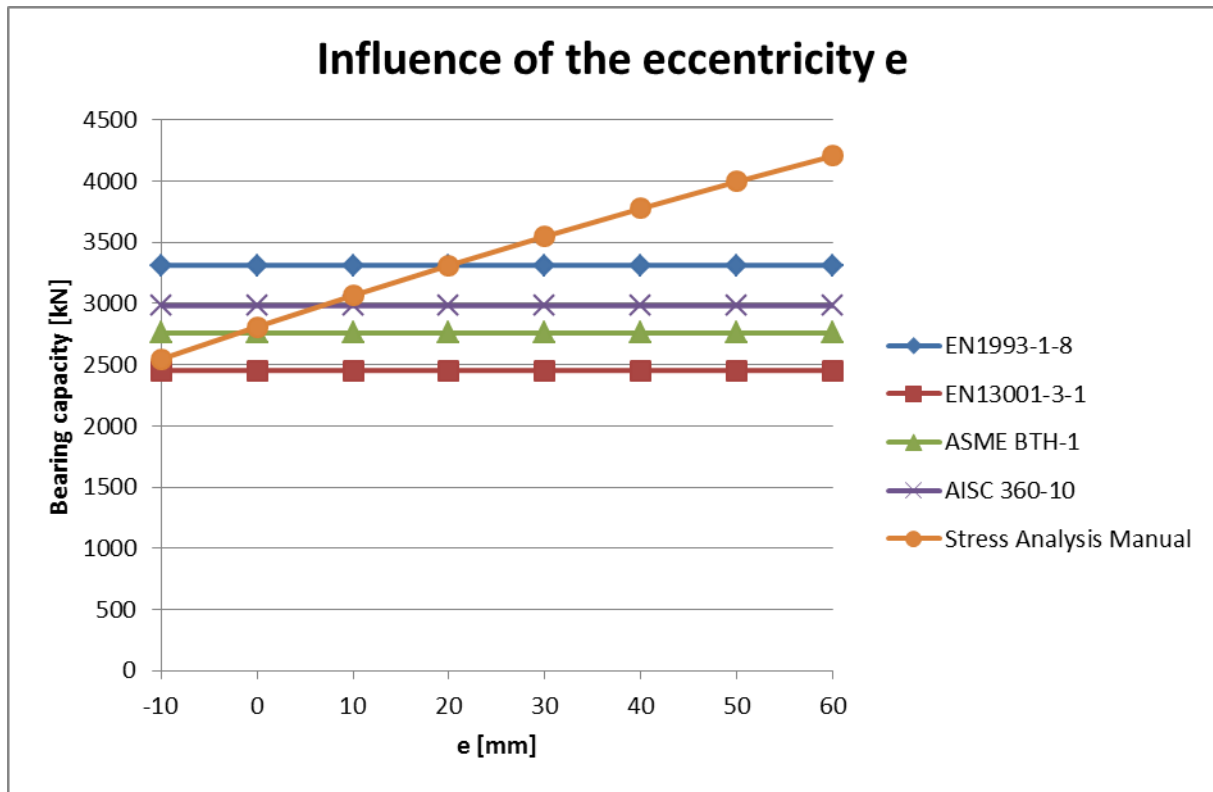


Chart C-23: Influence of the eccentricity e

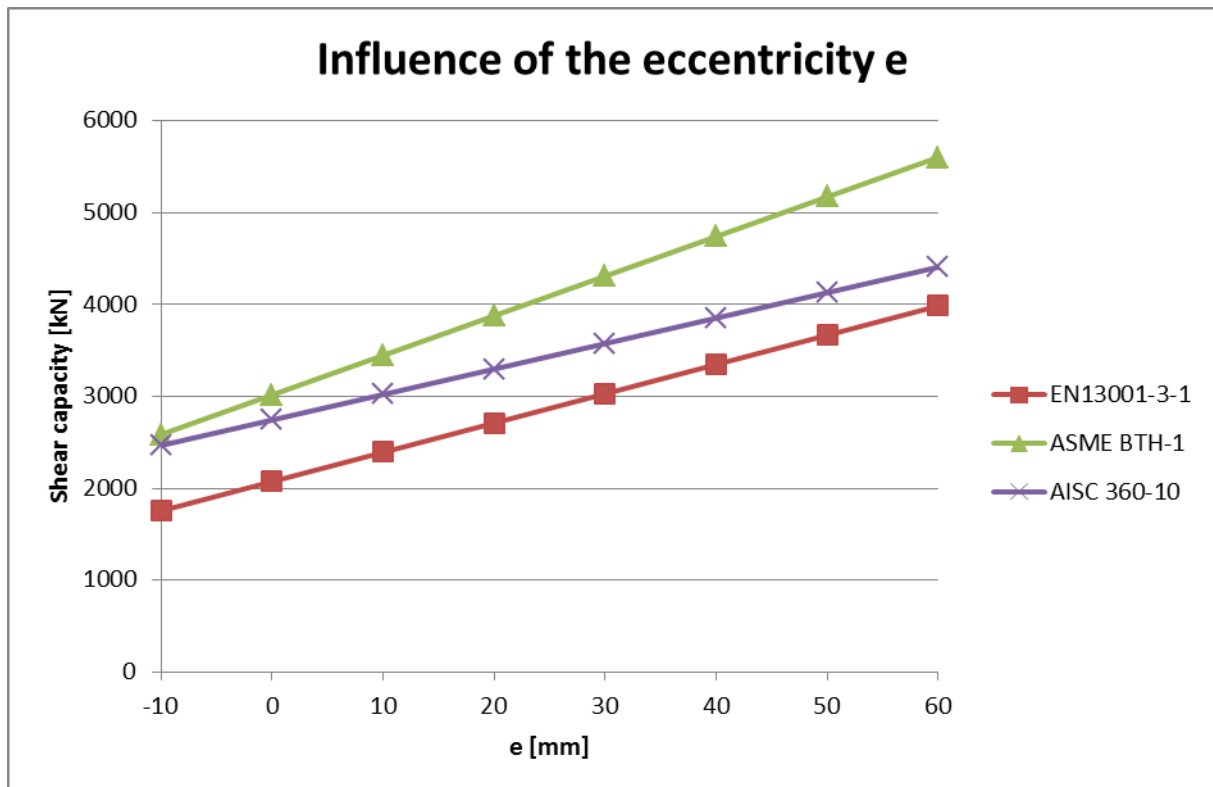


Chart C-24: Influence of the eccentricity e

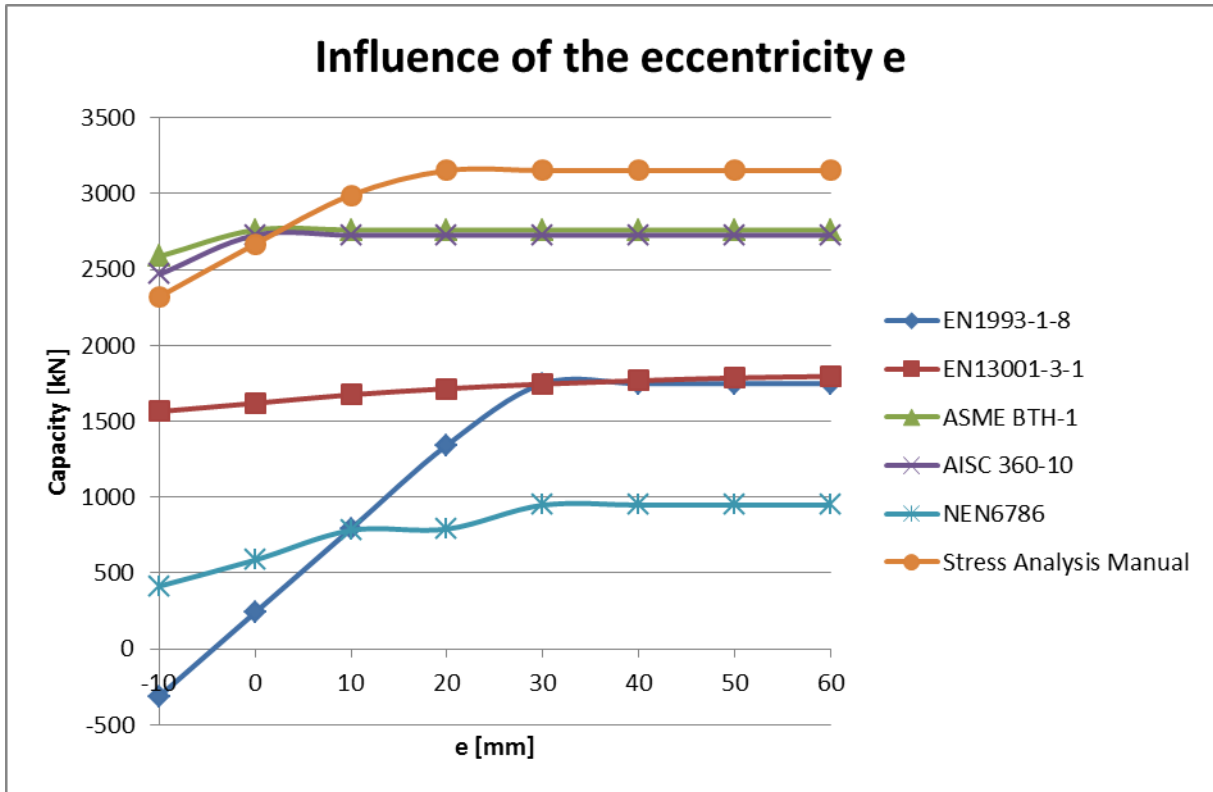


Chart C-25: Influence of the eccentricity  $e$

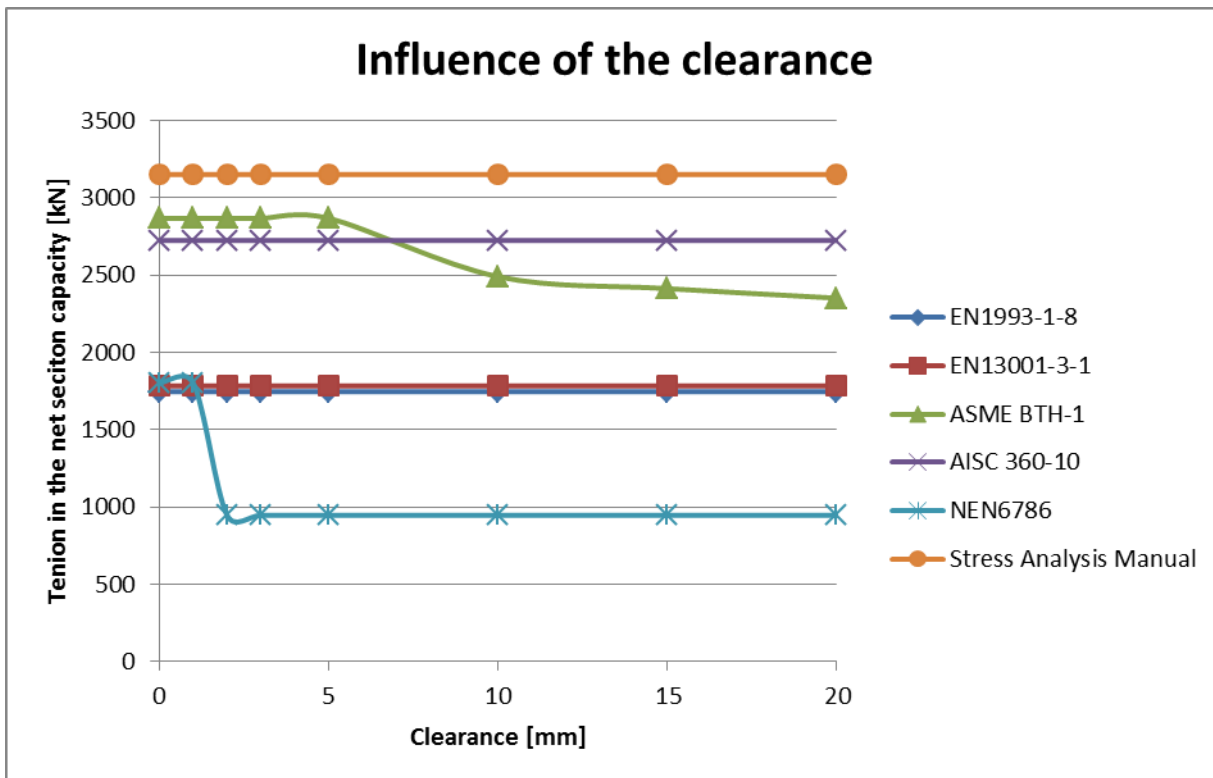


Chart C-26: Influence of the clearance

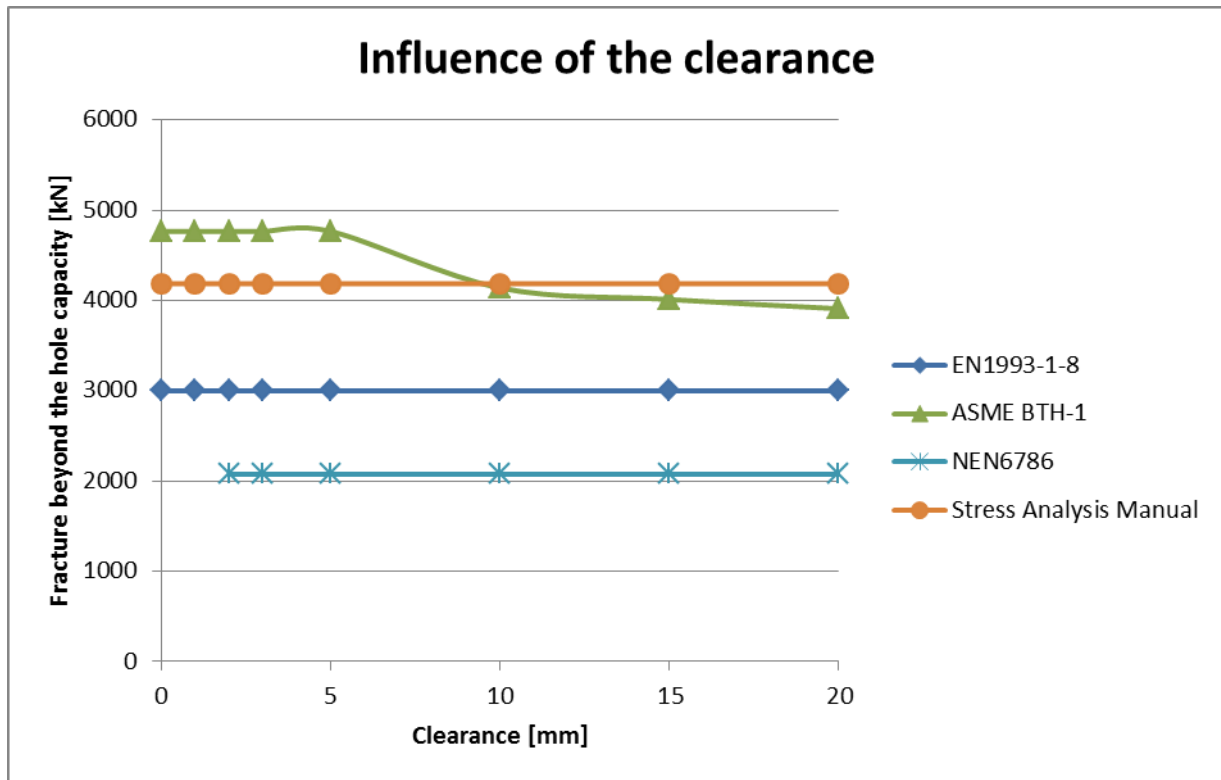


Chart C-27: Influence of the clearance

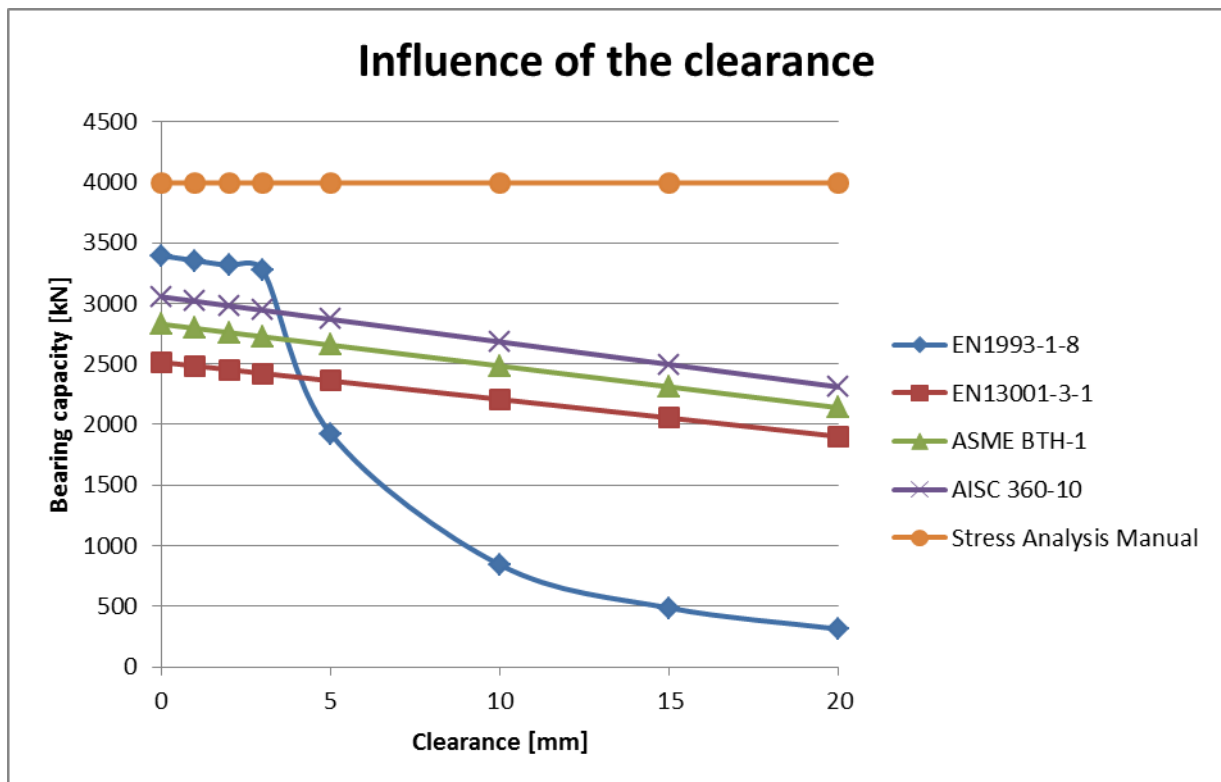


Chart C-28: Influence of the clearance

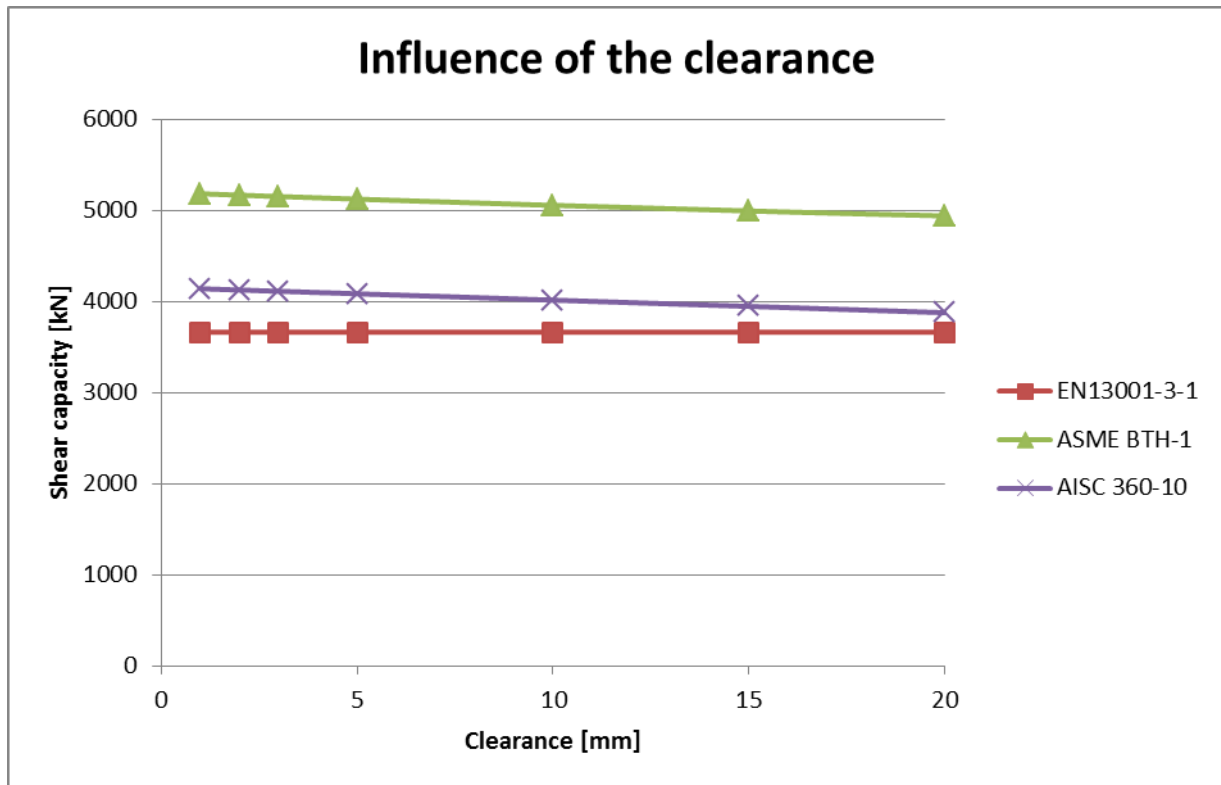


Chart C-29: Influence of the clearance

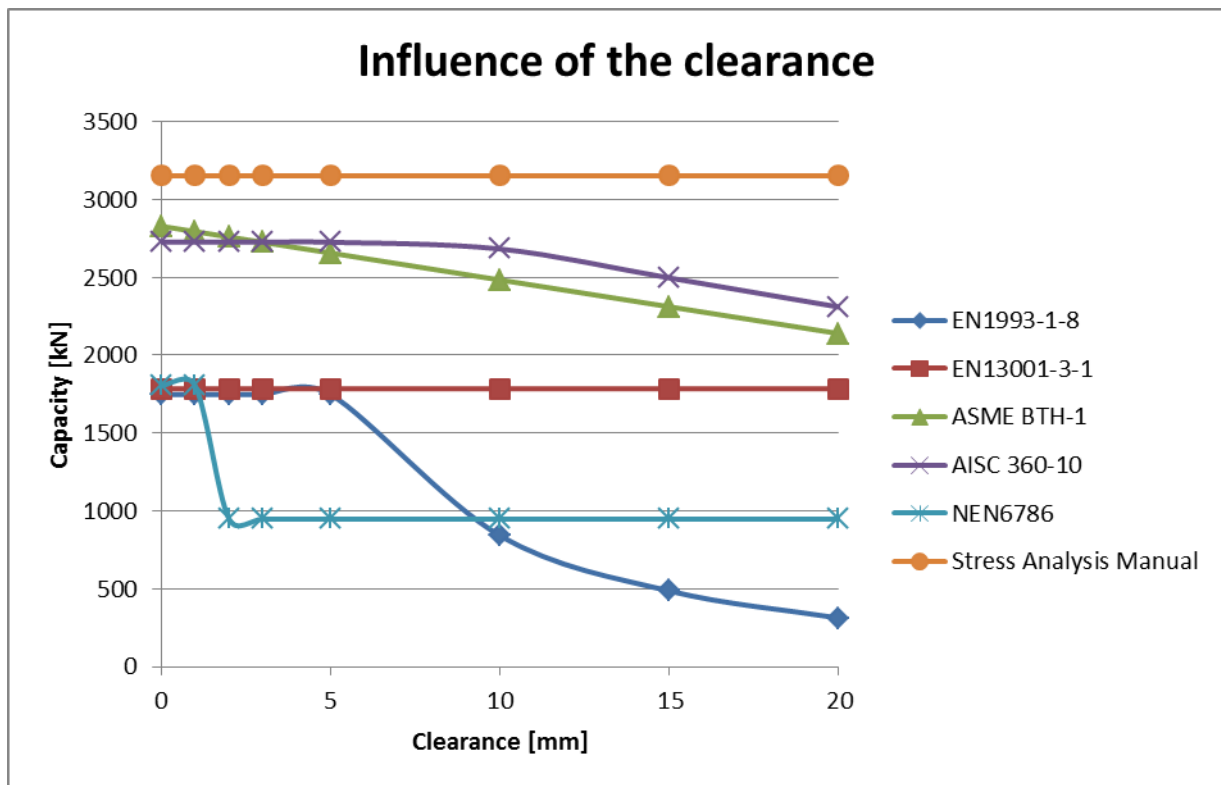


Chart C-30: Influence of the clearance

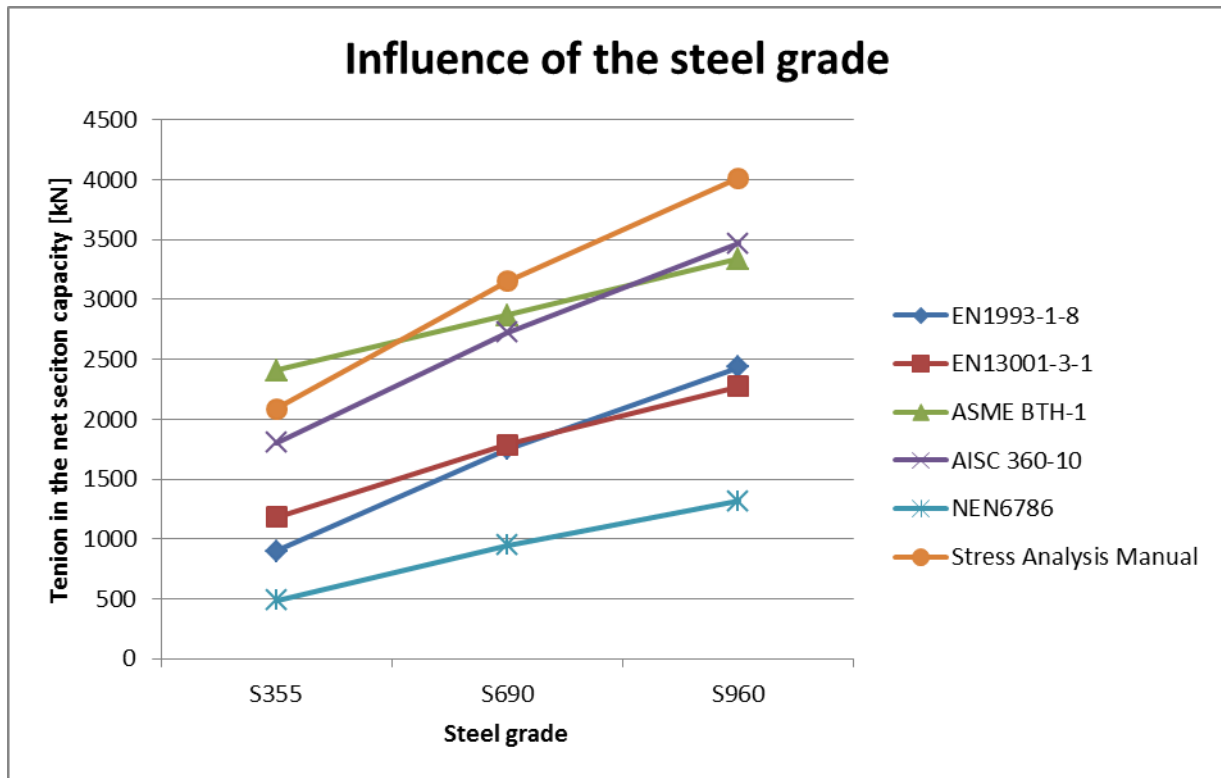


Chart C-31: Influence of the steel grade

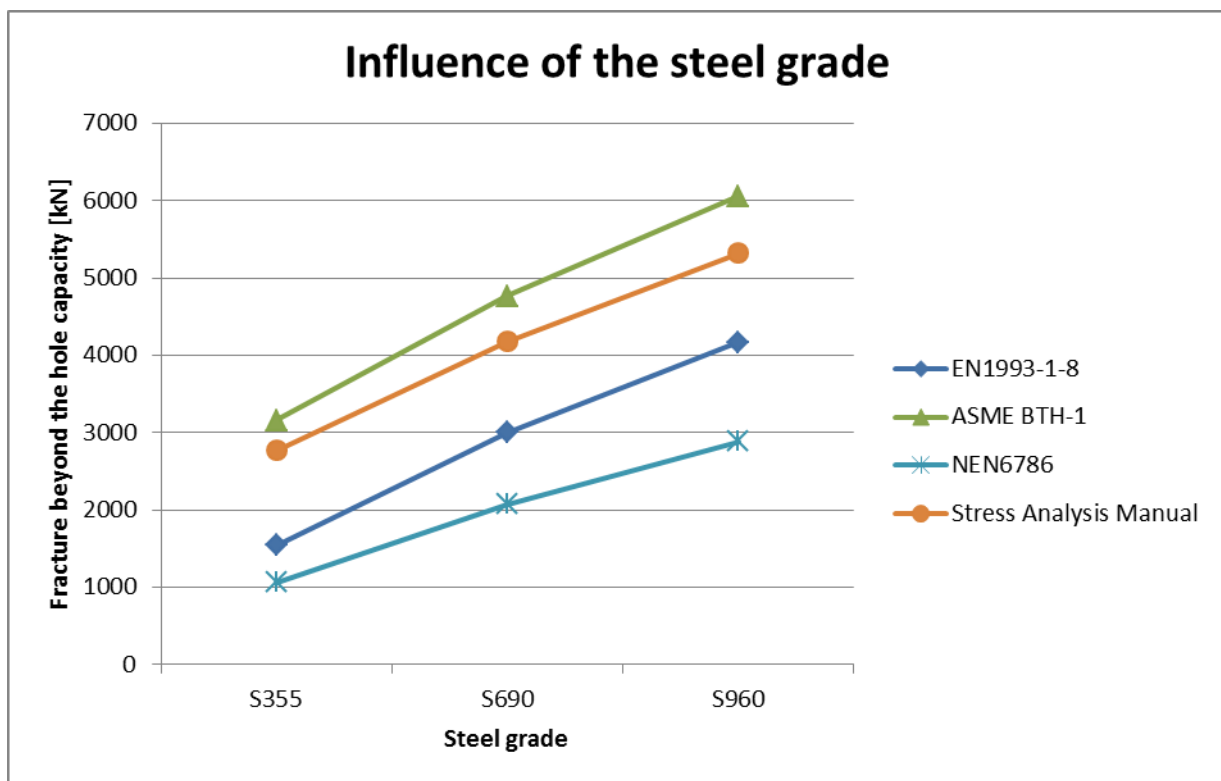


Chart C-32: Influence of the steel grade

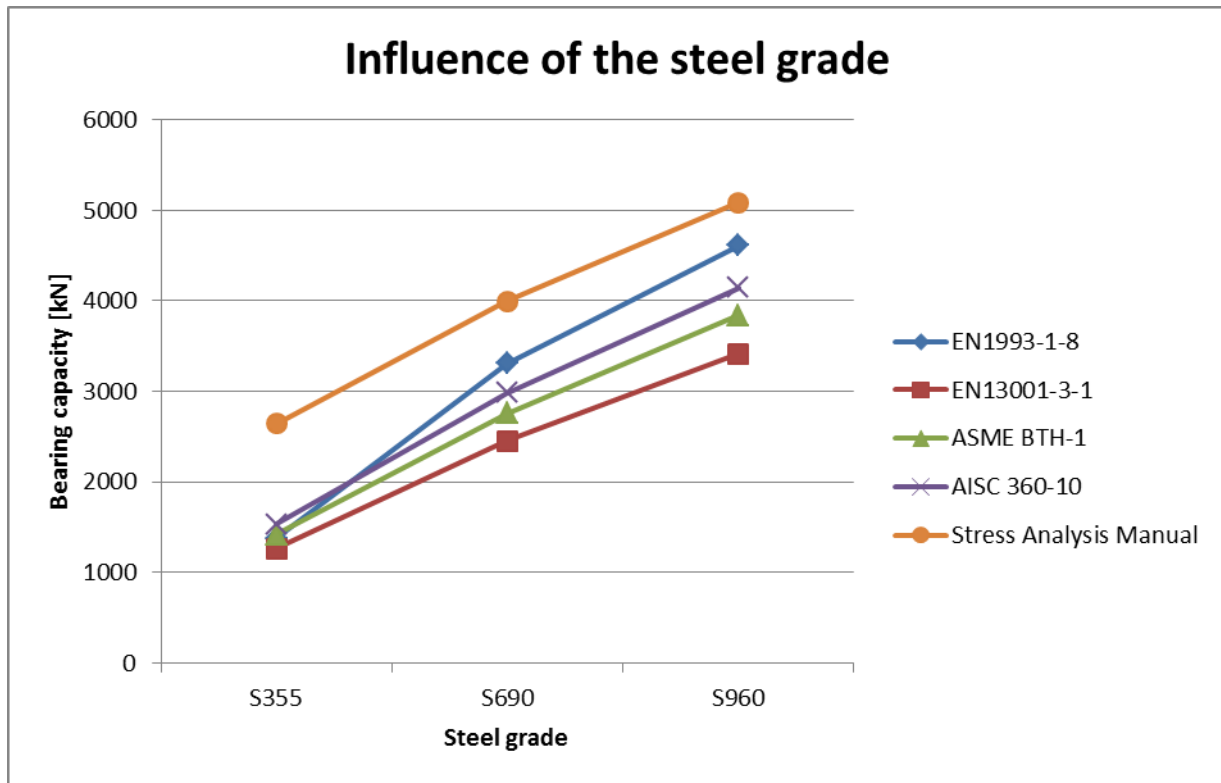


Chart C-33: Influence of the steel grade

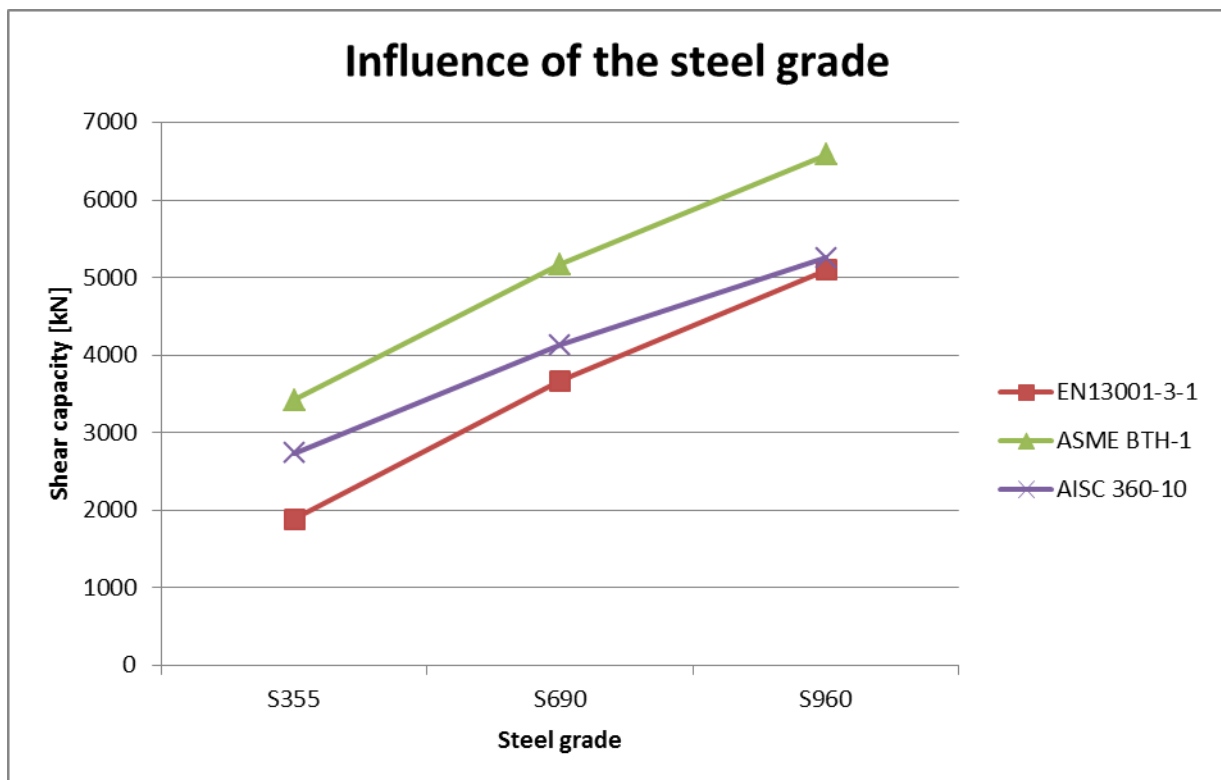


Chart C-34: Influence of the steel grade

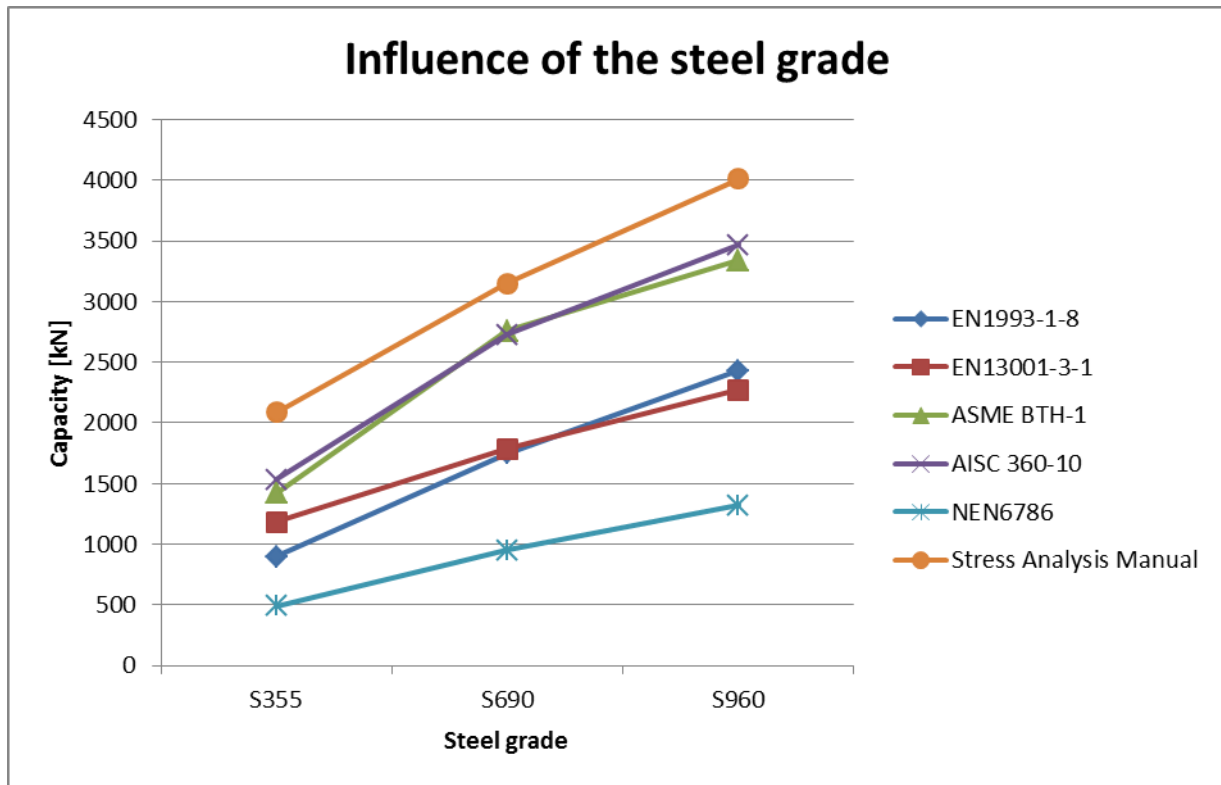


Chart C-35: Influence of the steel grade

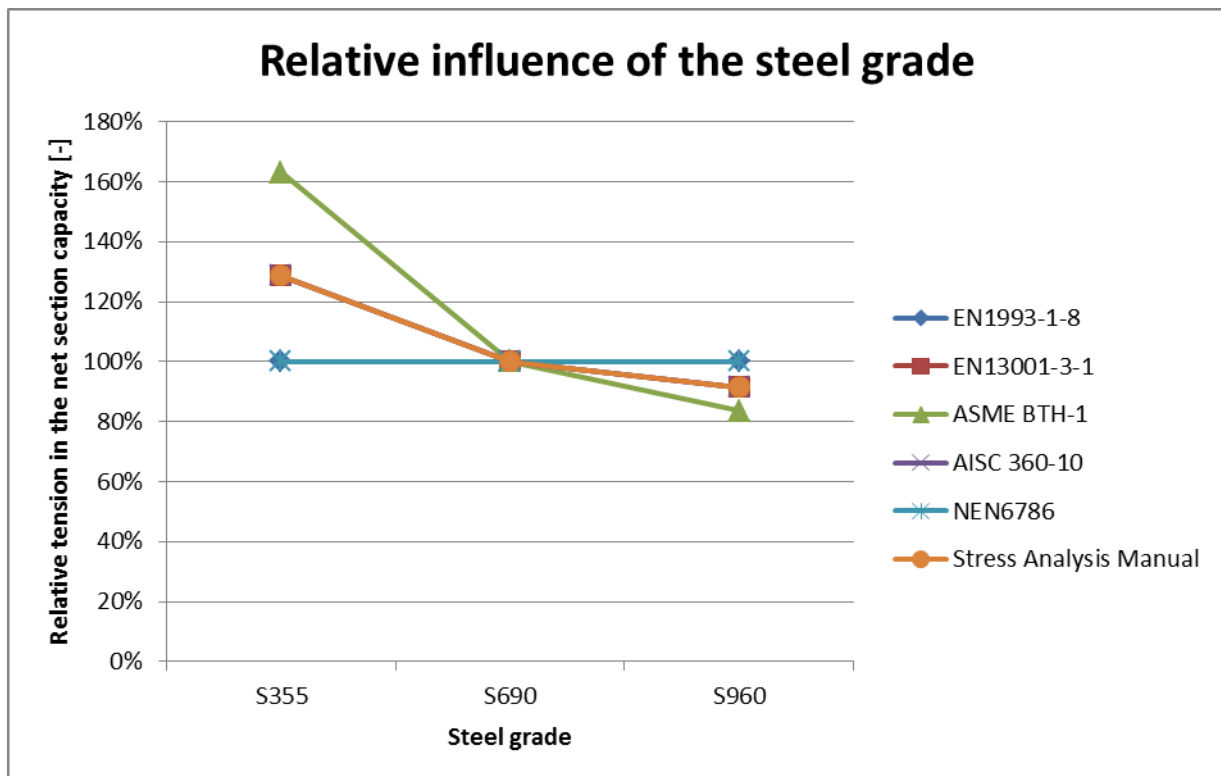


Chart C-36: Relative influence of the steel grade

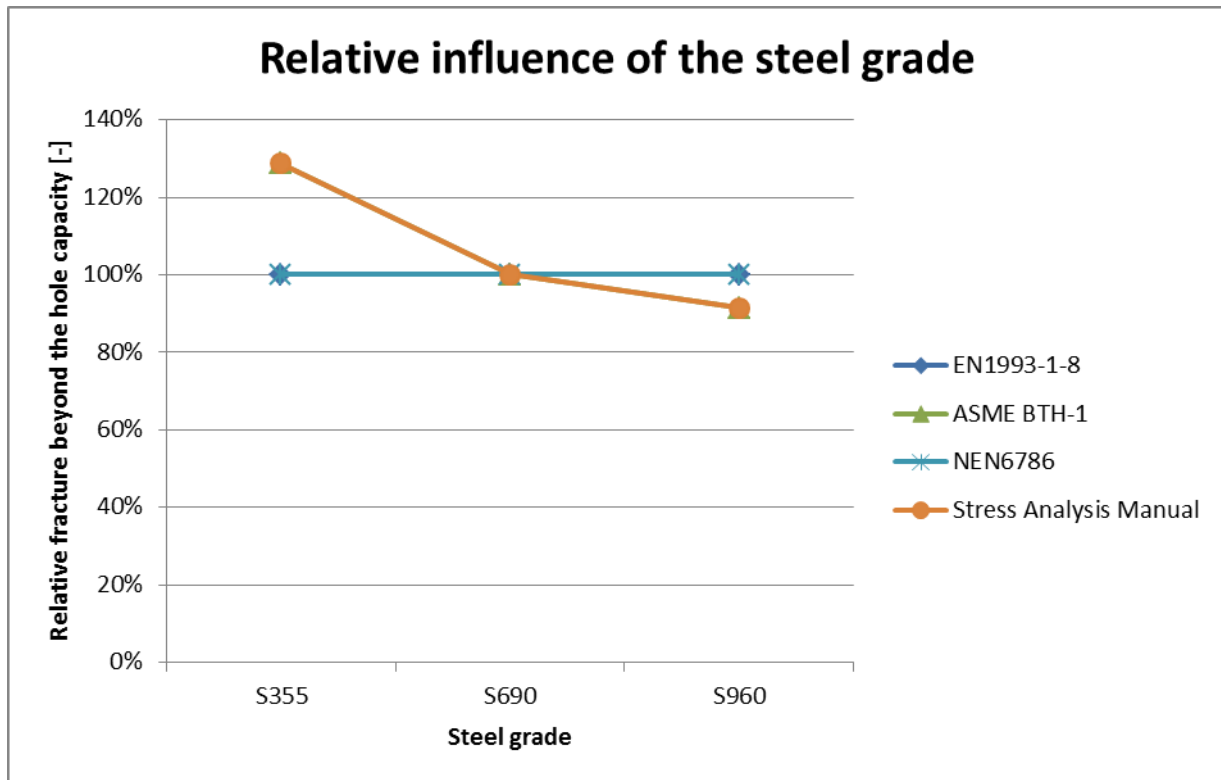


Chart C-37: Relative influence of the steel grade

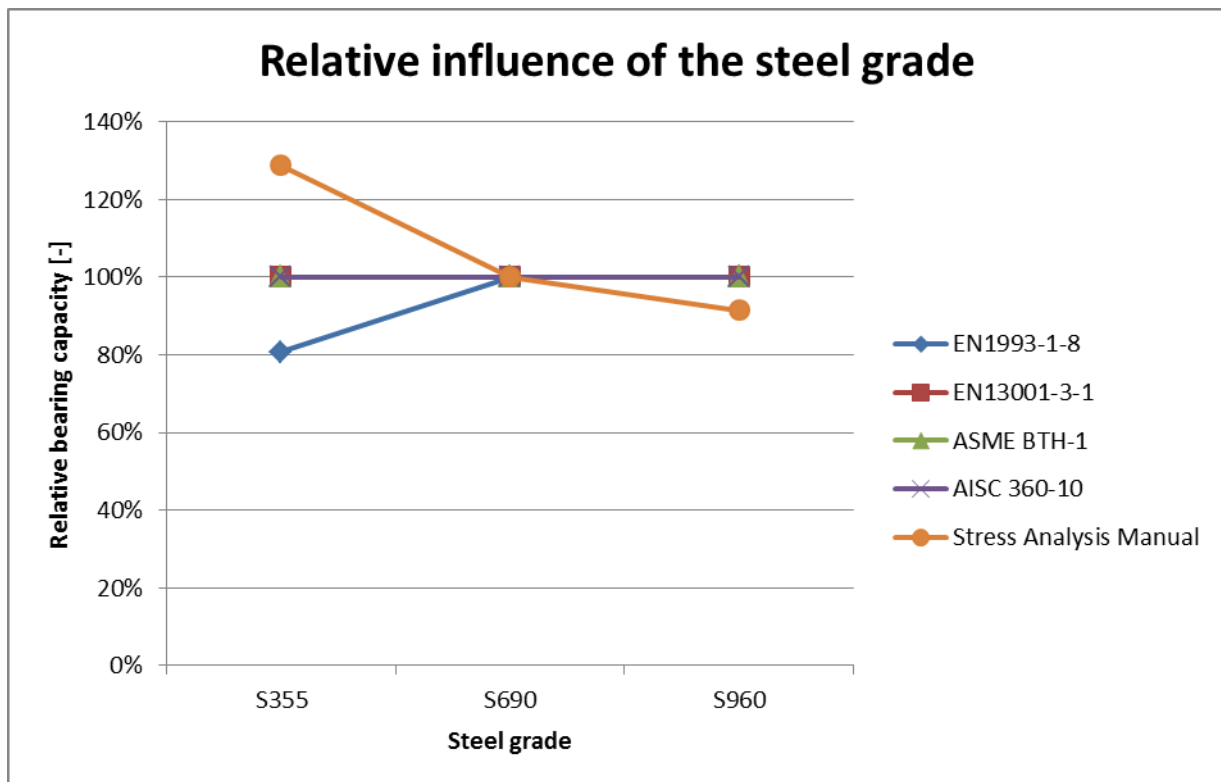


Chart C-38: Relative influence of the steel grade

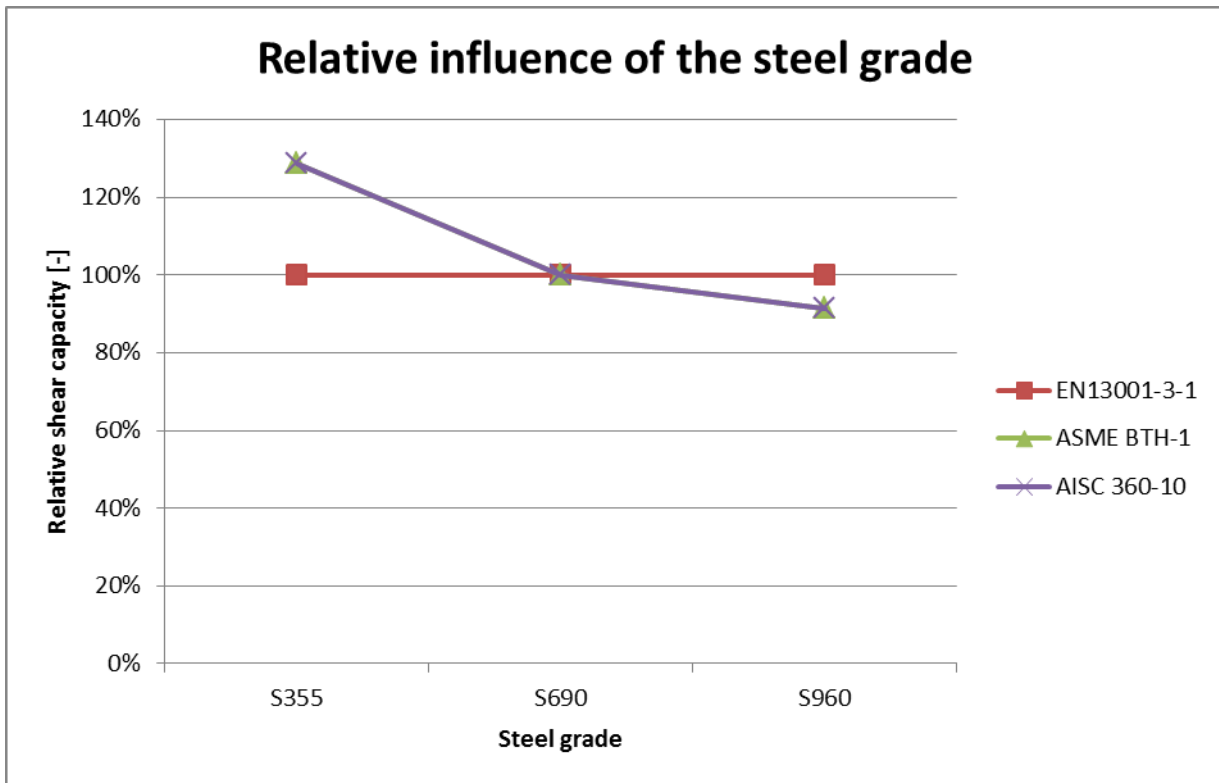


Chart C-39: Relative influence of the steel grade

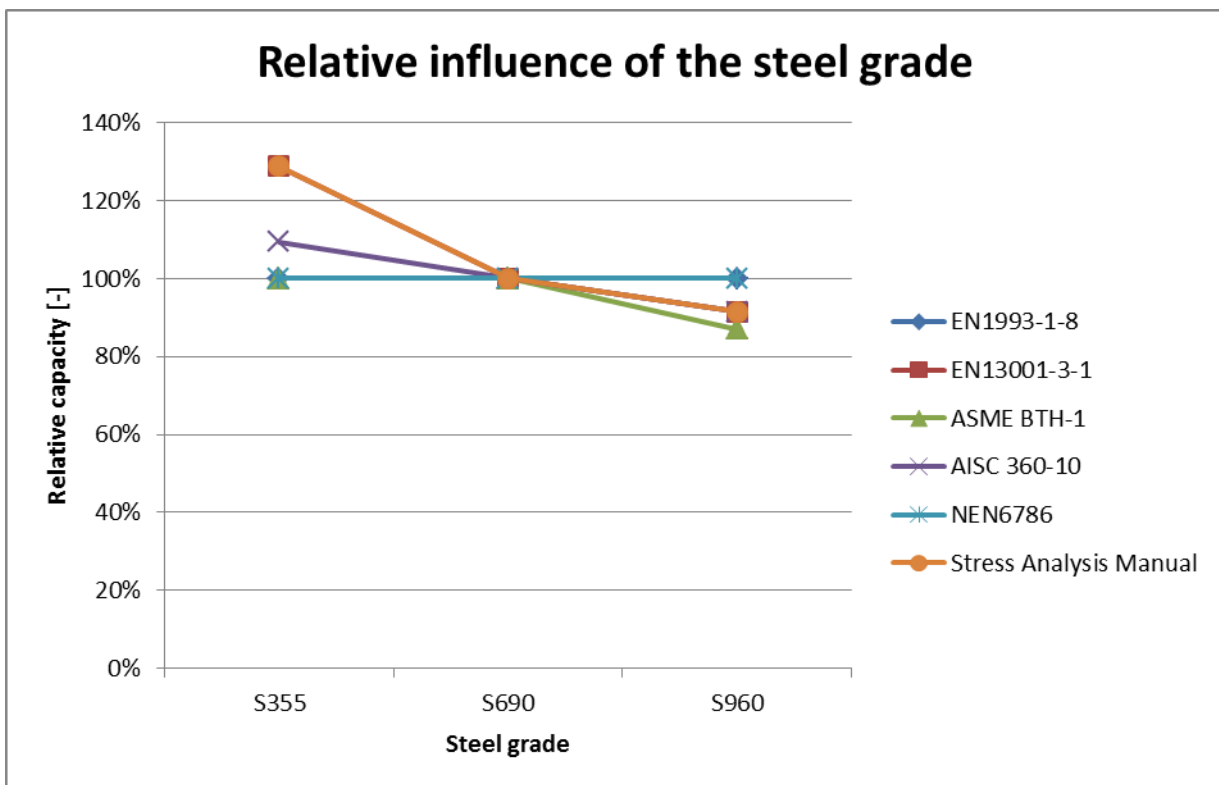


Chart C-40: Relative influence of the steel grade

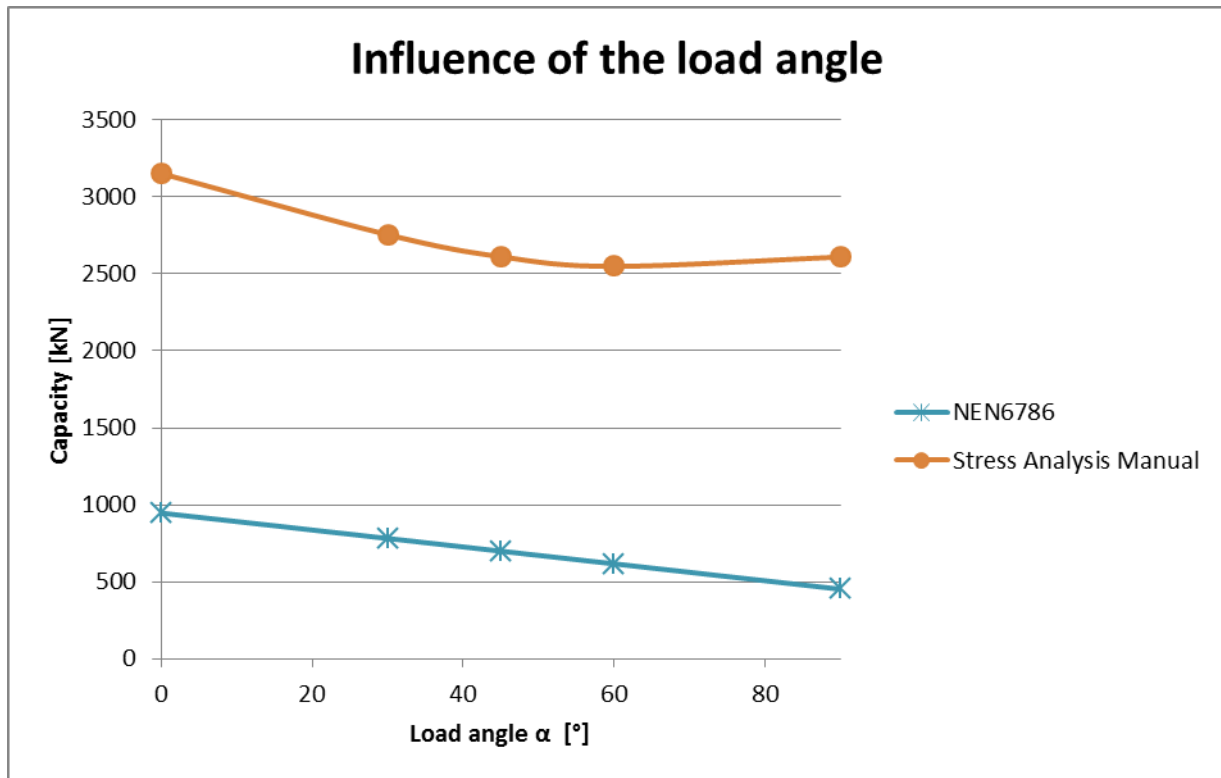


Chart C-41: Influence of the load angle

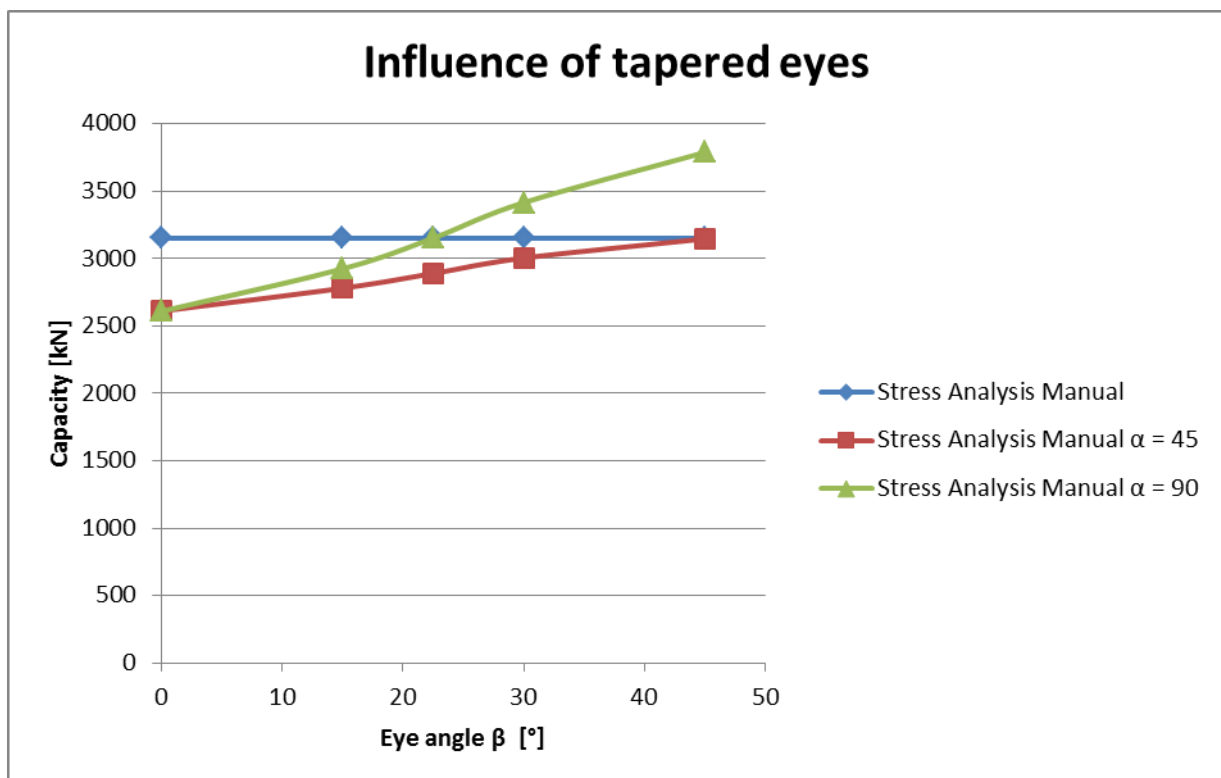


Chart C-42: Influence of tapered eyes

### C.3 Design factor influences

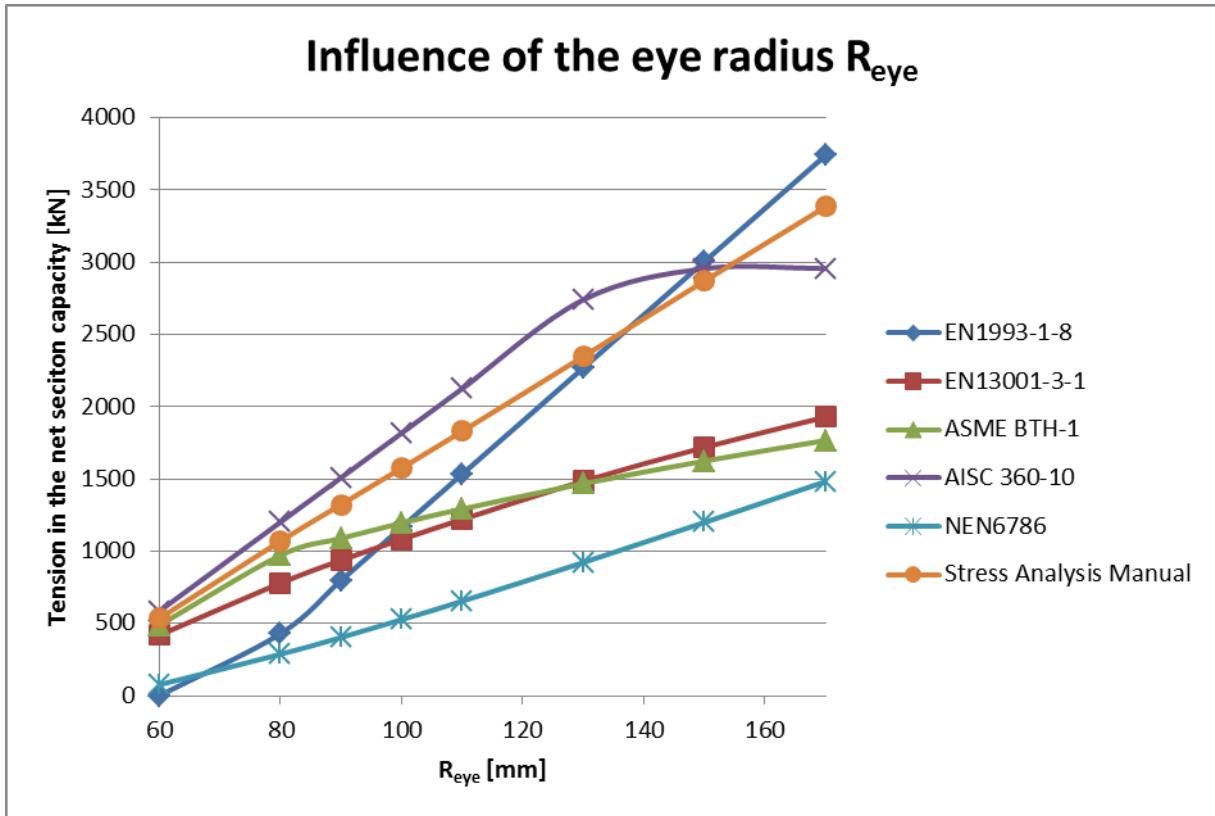


Chart C-43: Influence of the eye radius  $R_{eye}$

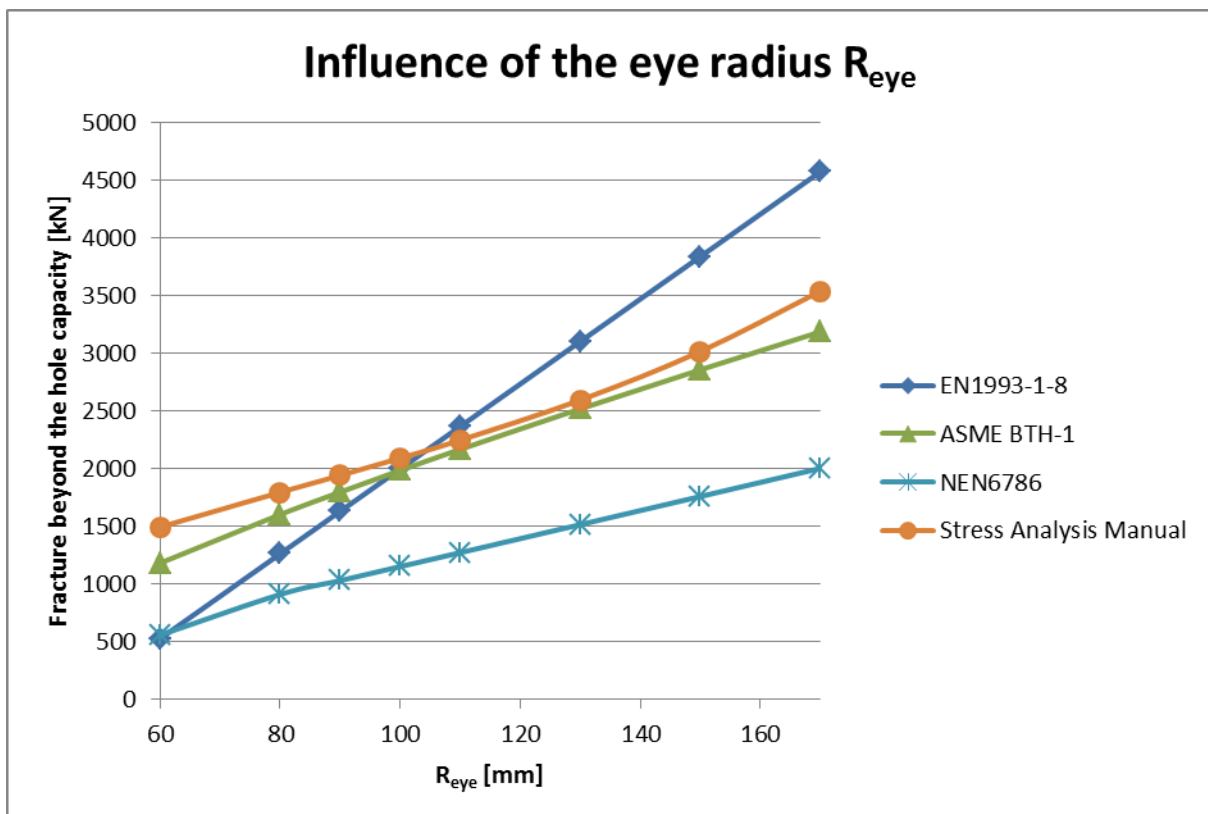


Chart C-44: Influence of the eye radius  $R_{eye}$

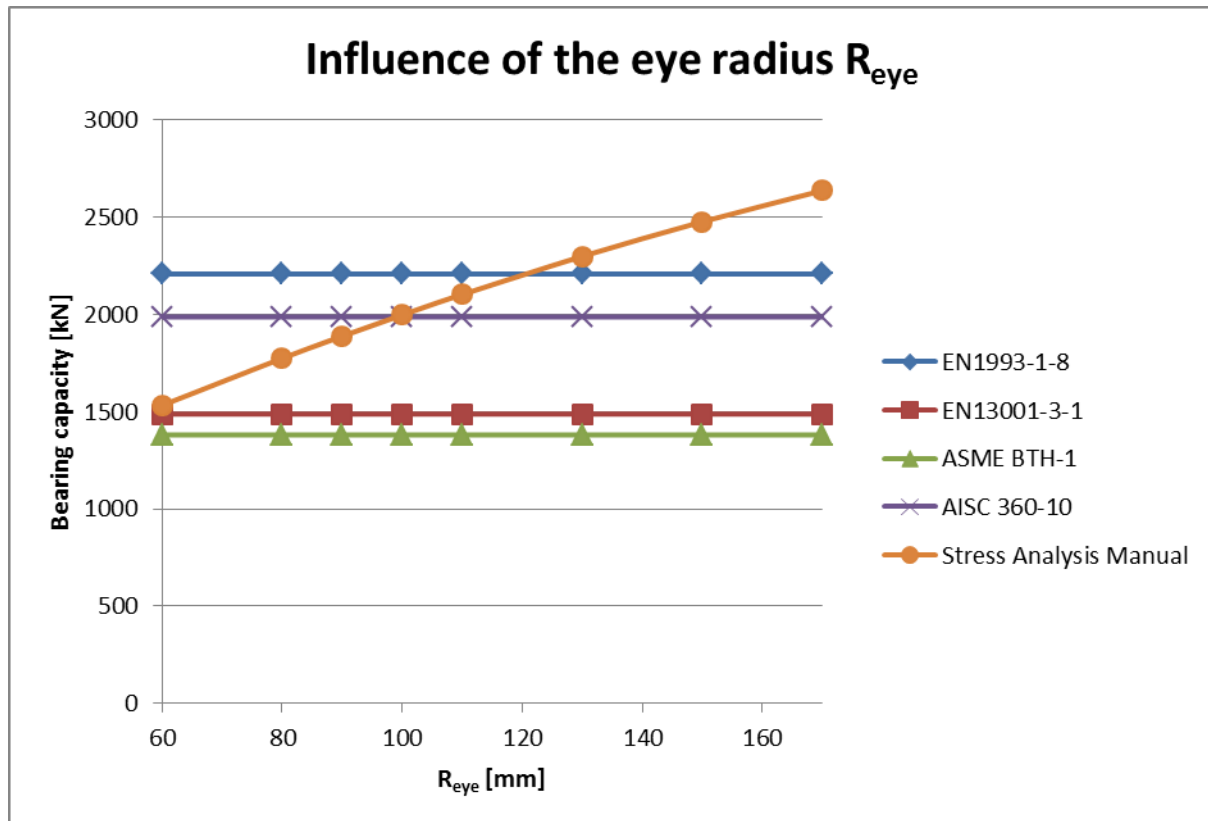


Chart C-45: Influence of the eye radius  $R_{eye}$

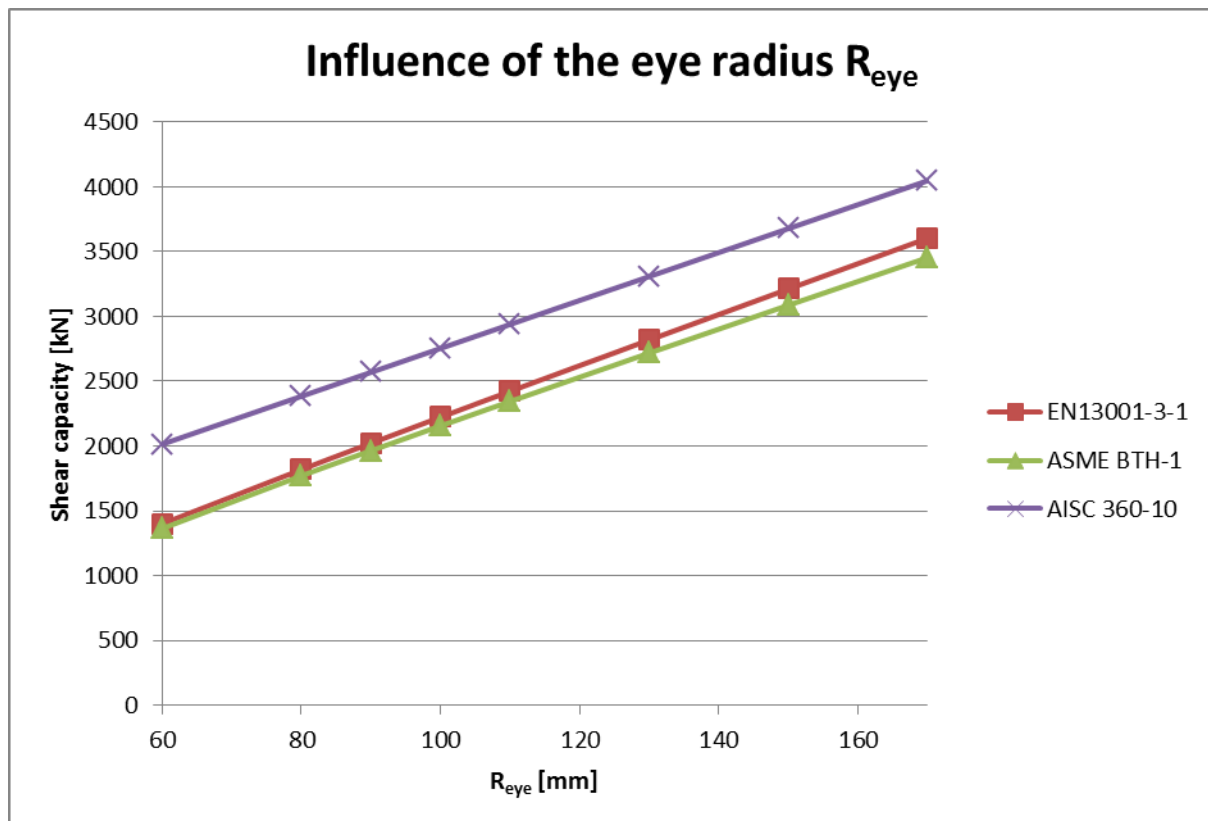


Chart C-46: Influence of the eye radius  $R_{eye}$

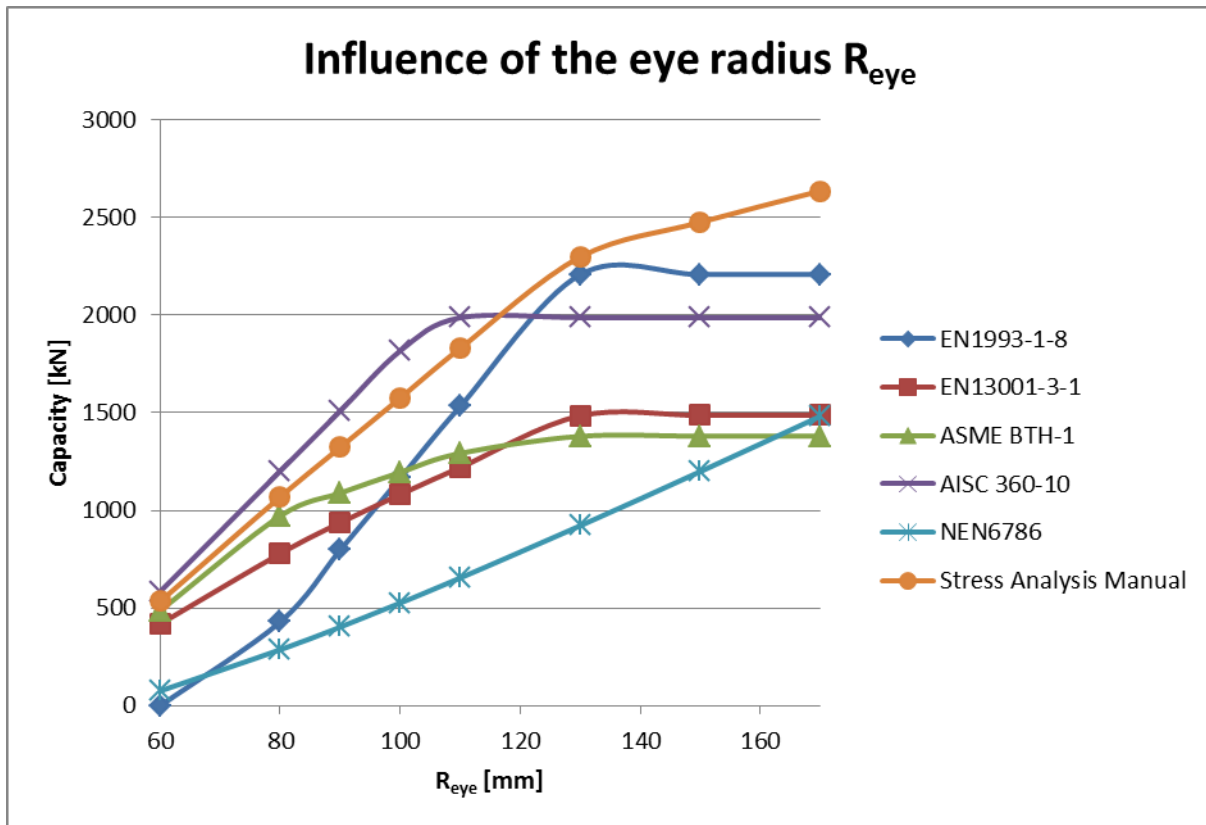


Chart C-47: Influence of the eye radius  $R_{eye}$

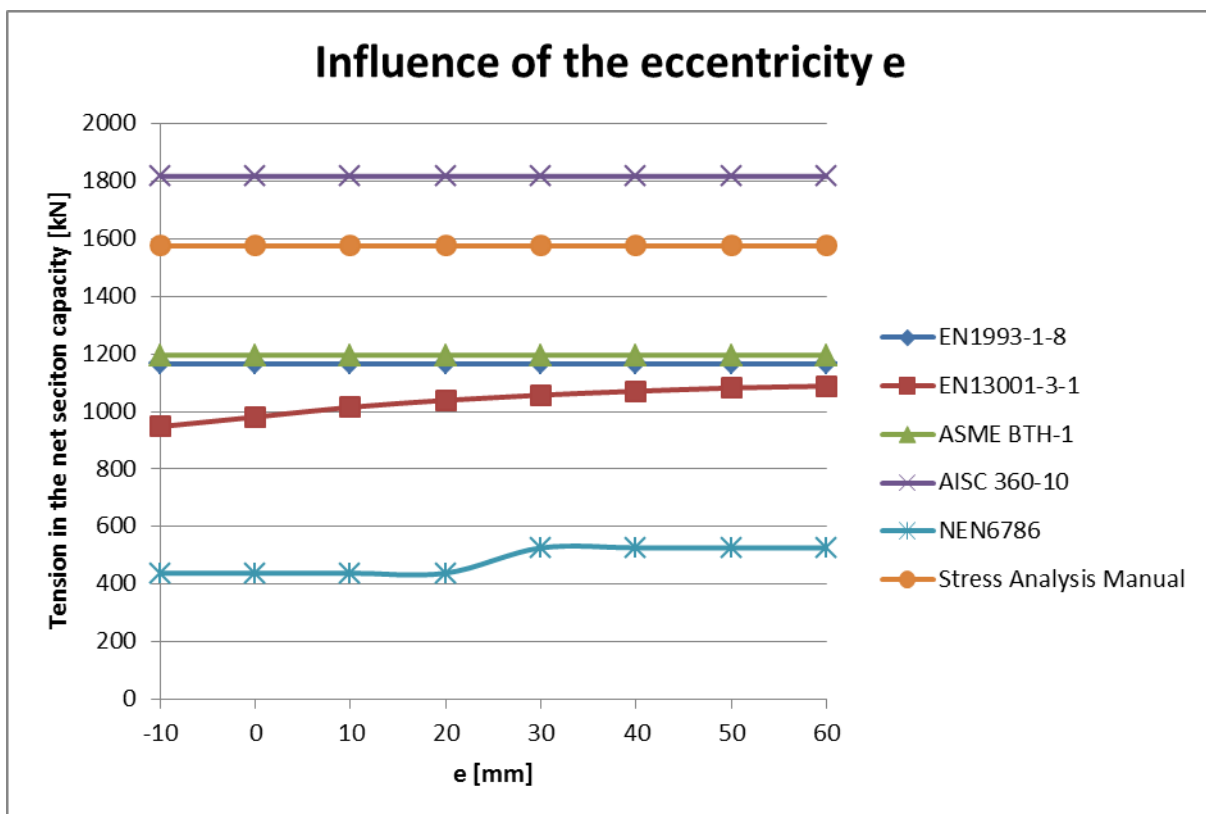


Chart C-48: Influence of the eccentricity  $e$

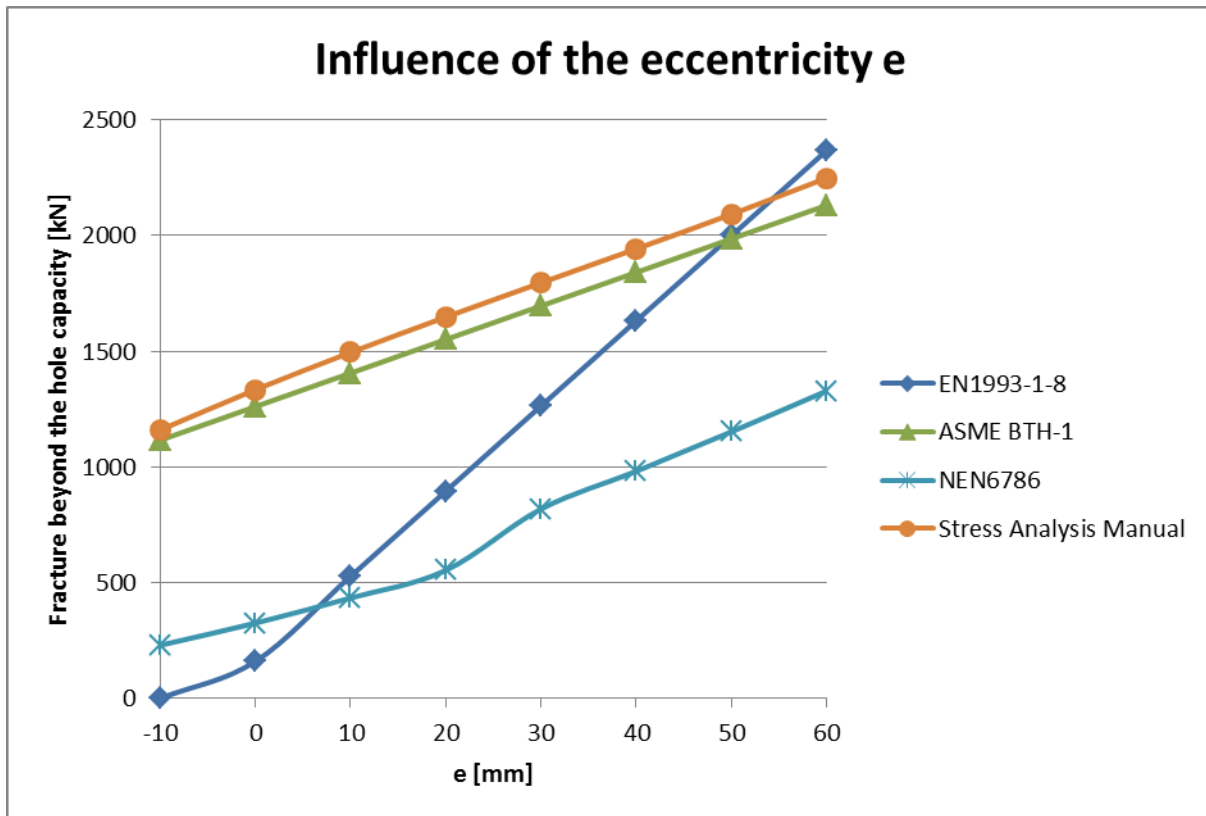


Chart C-49: Influence of the eccentricity e

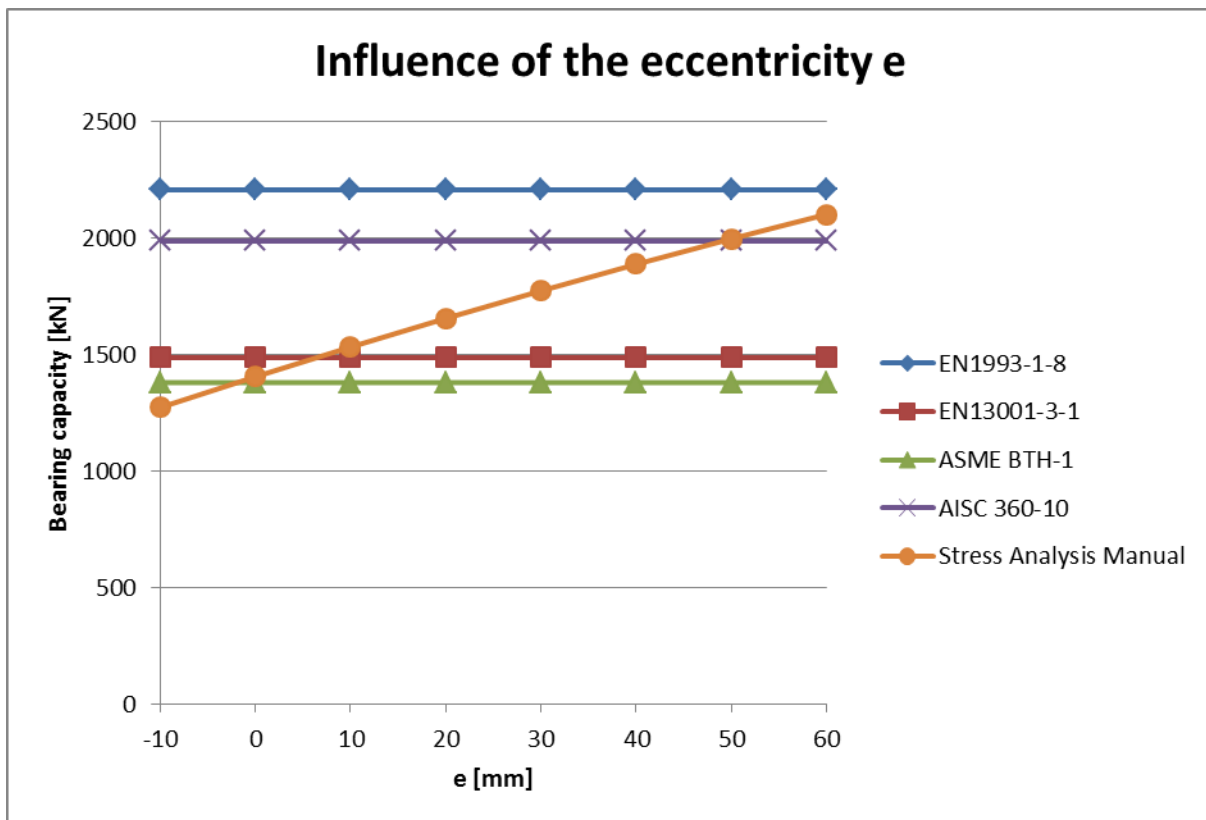


Chart C-50: Influence of the eccentricity e

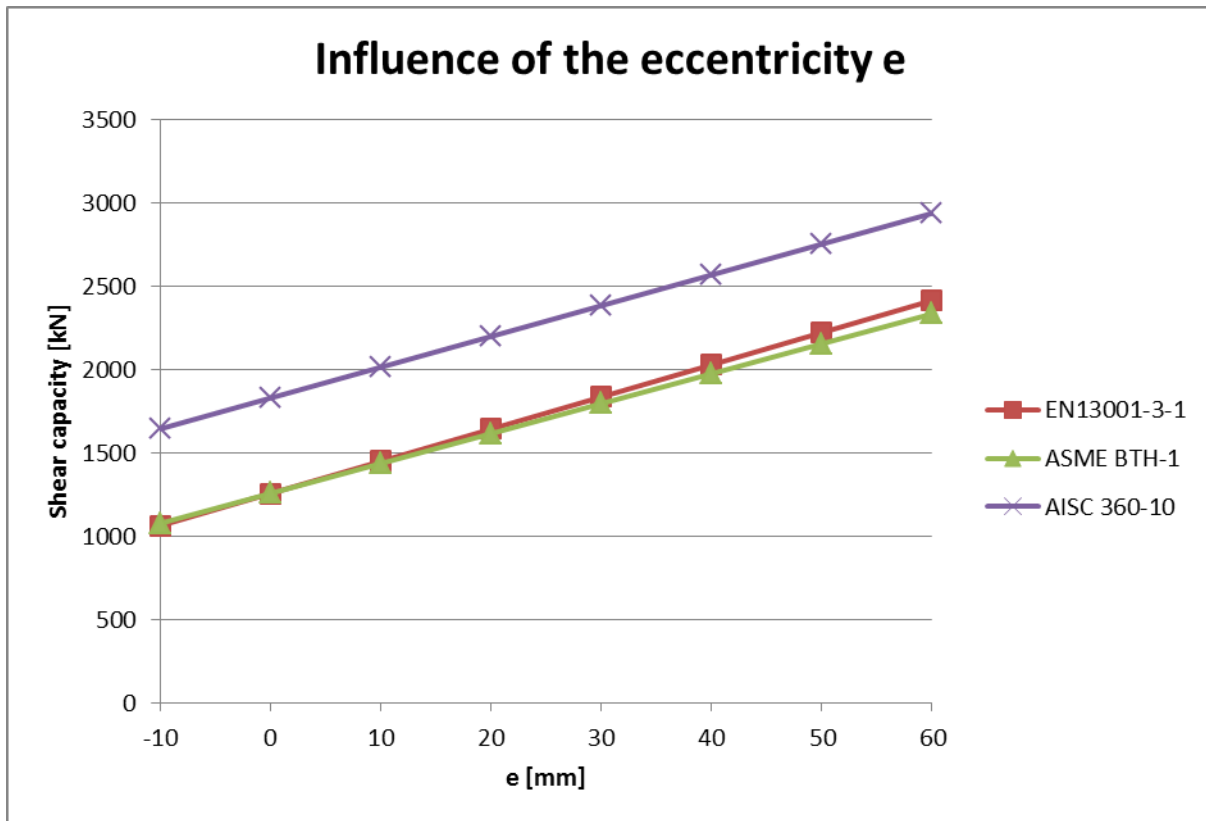


Chart C-51: Influence of the eccentricity  $e$

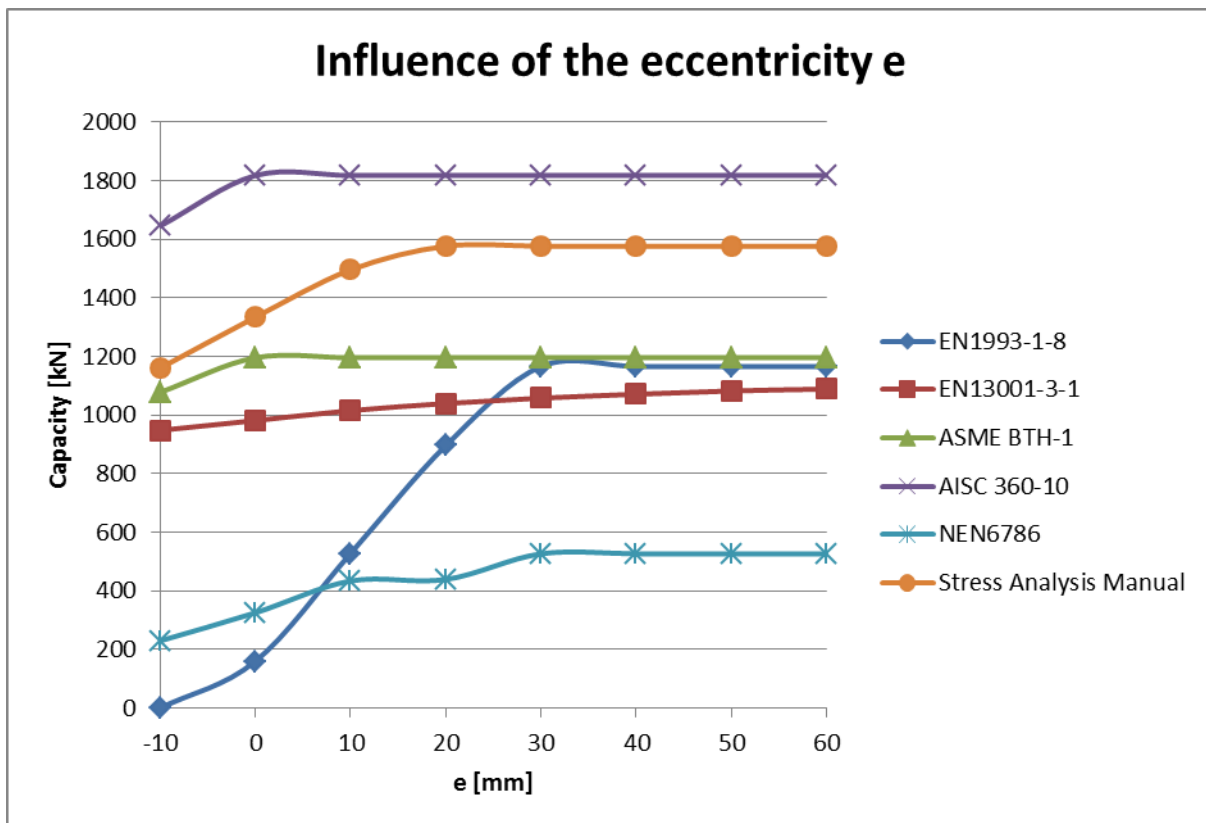


Chart C-52: Influence of the eccentricity  $e$

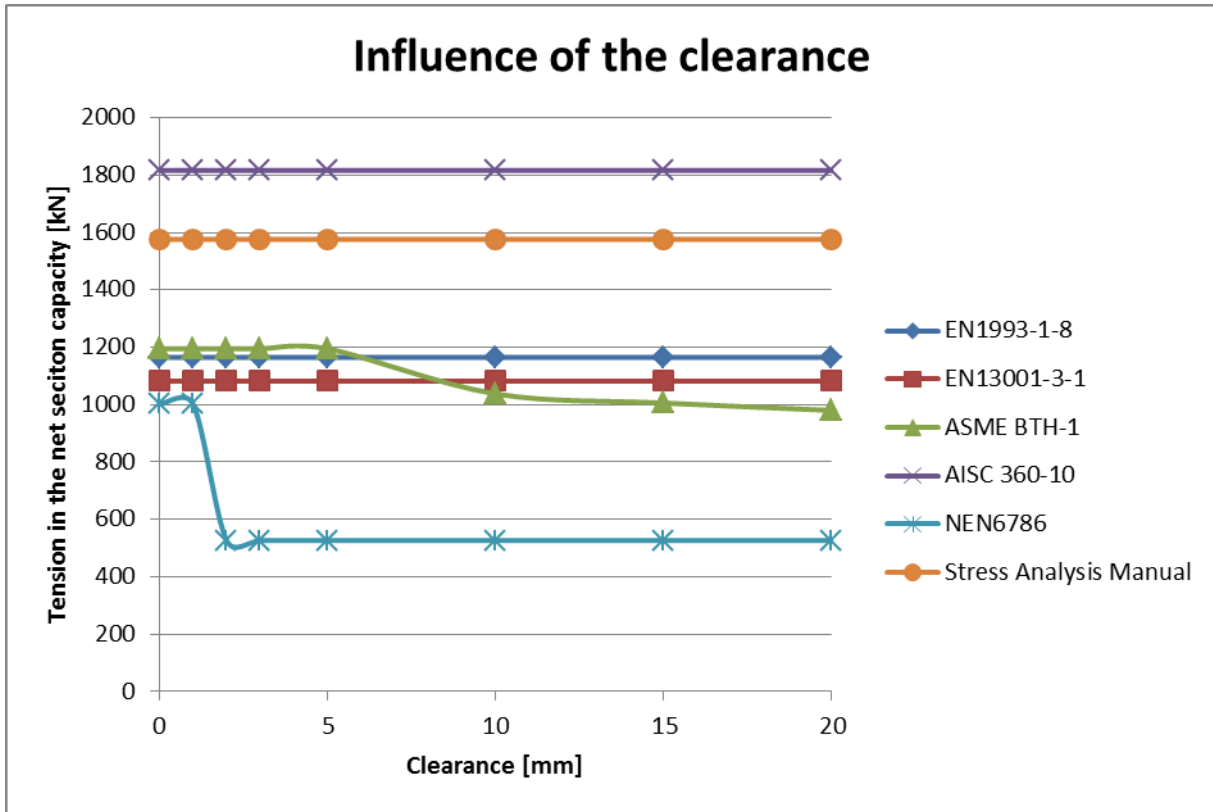


Chart C-53: Influence of the clearance

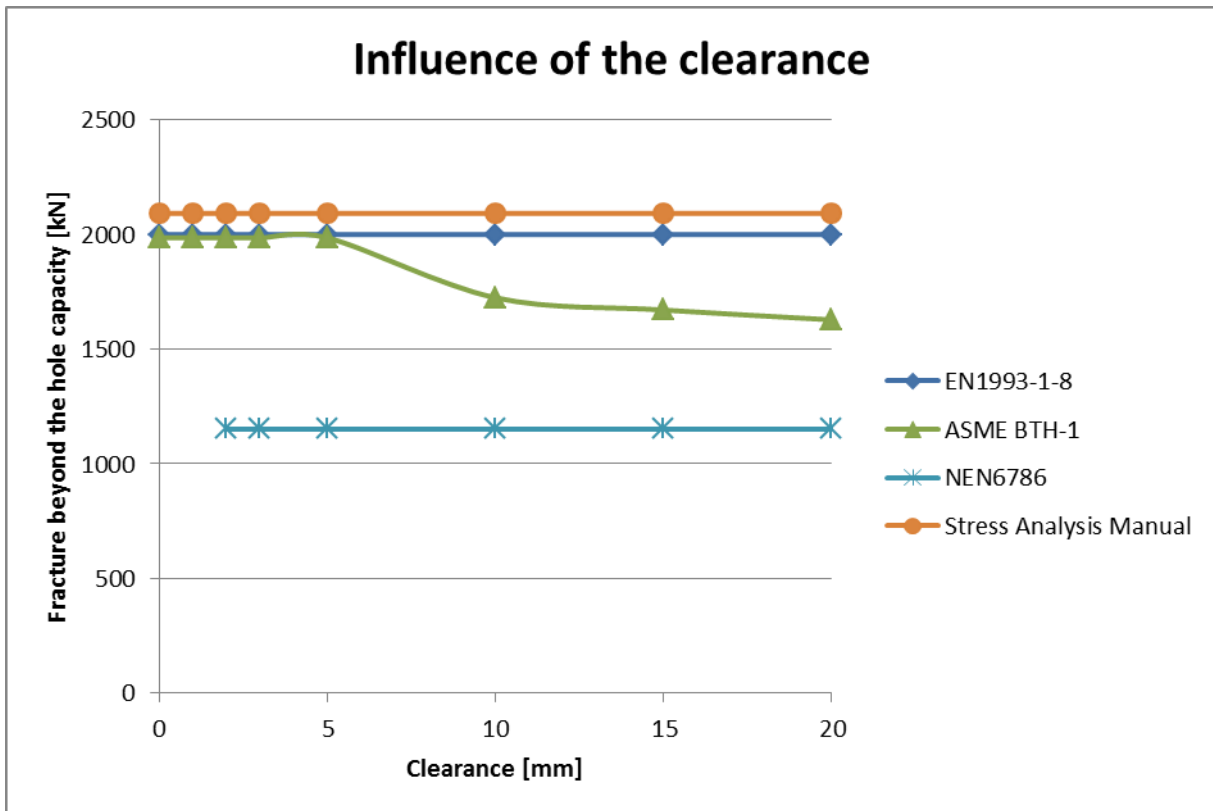


Chart C-54: Influence of the clearance

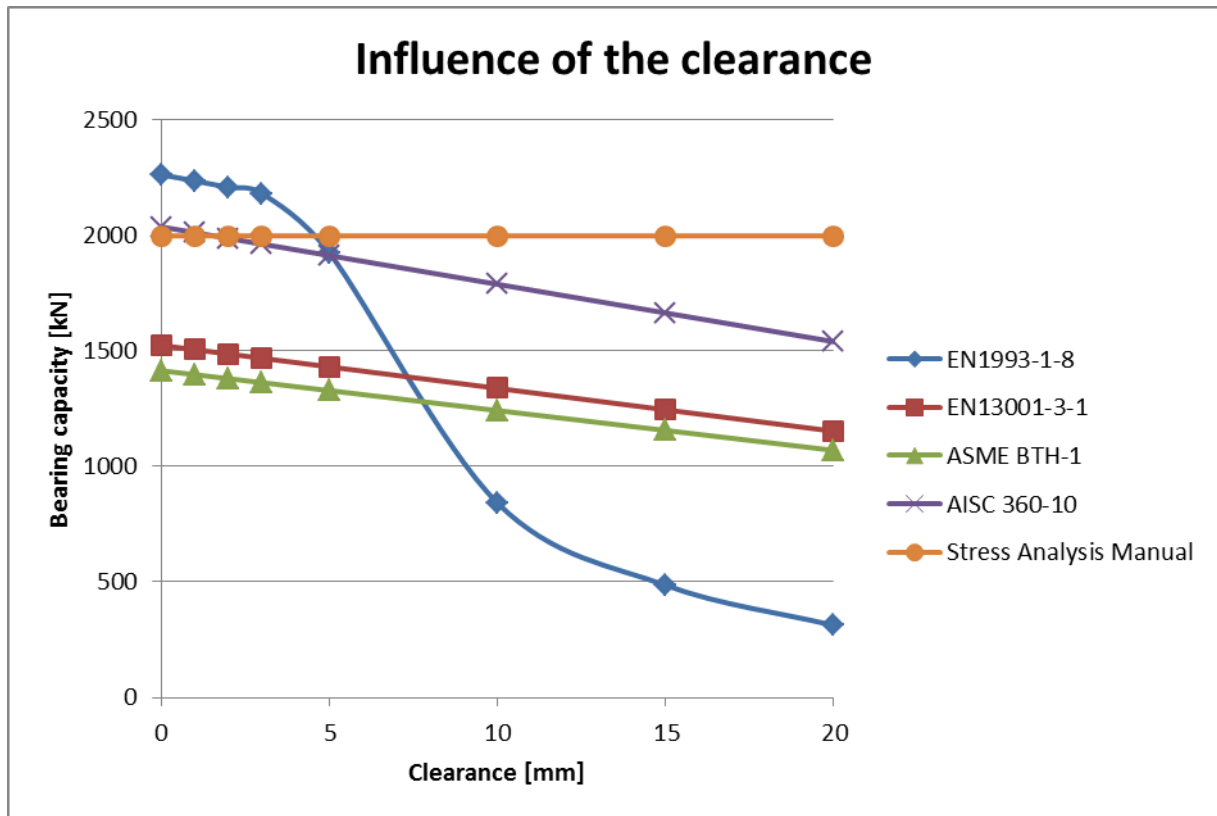


Chart C-55: Influence of the clearance

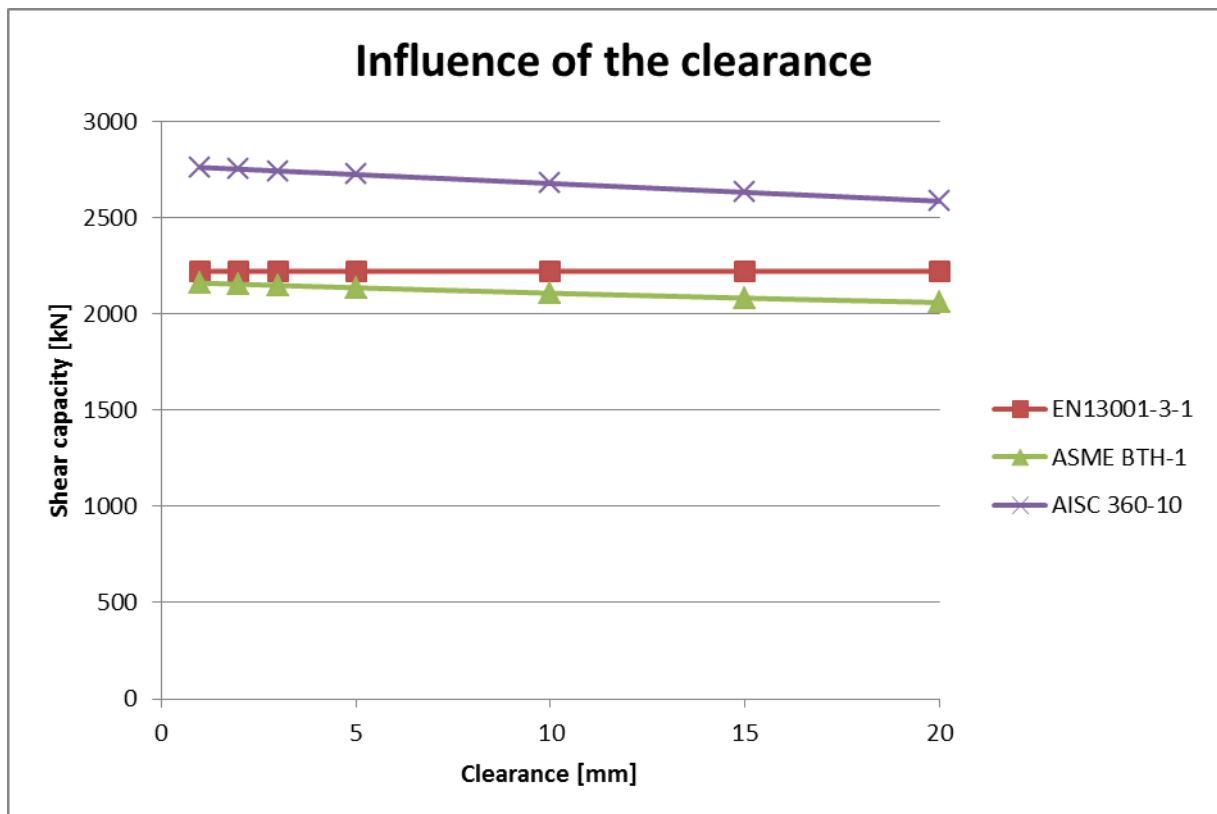


Chart C-56: Influence of the clearance

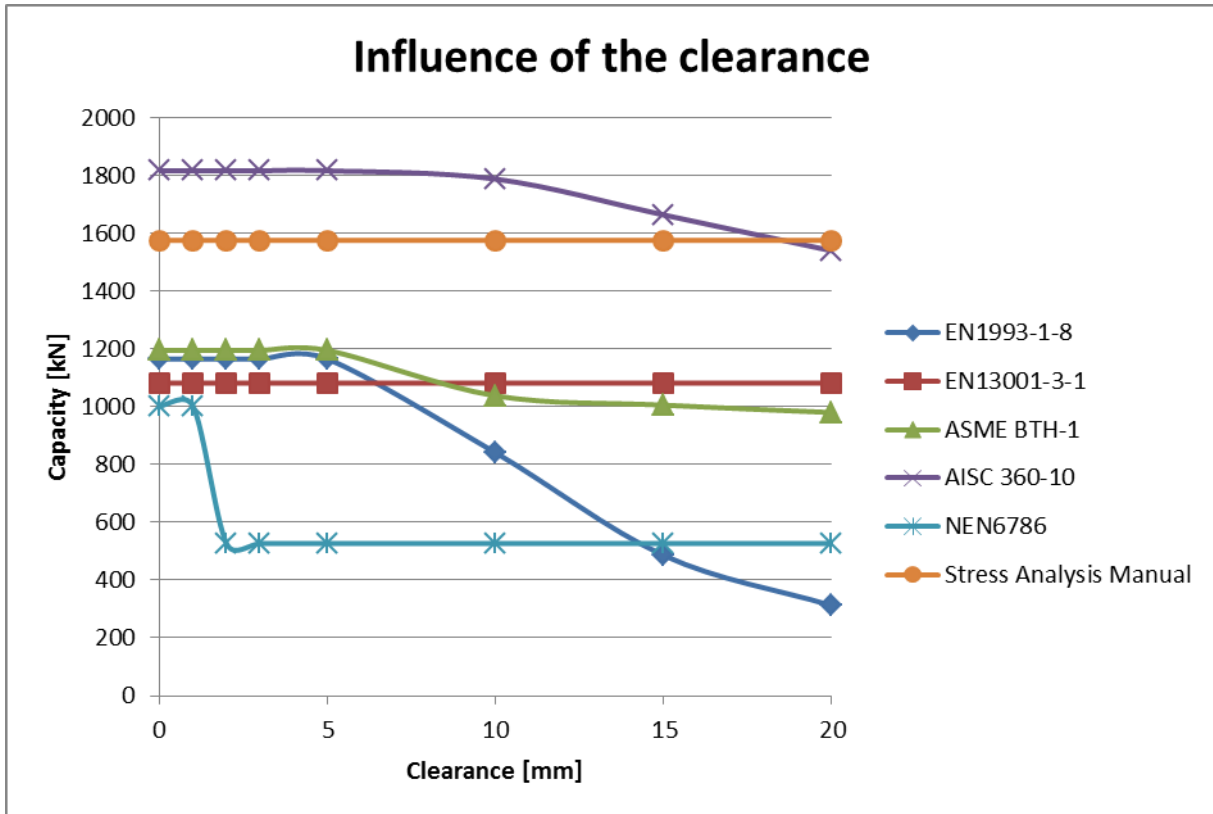


Chart C-57: Influence of the clearance

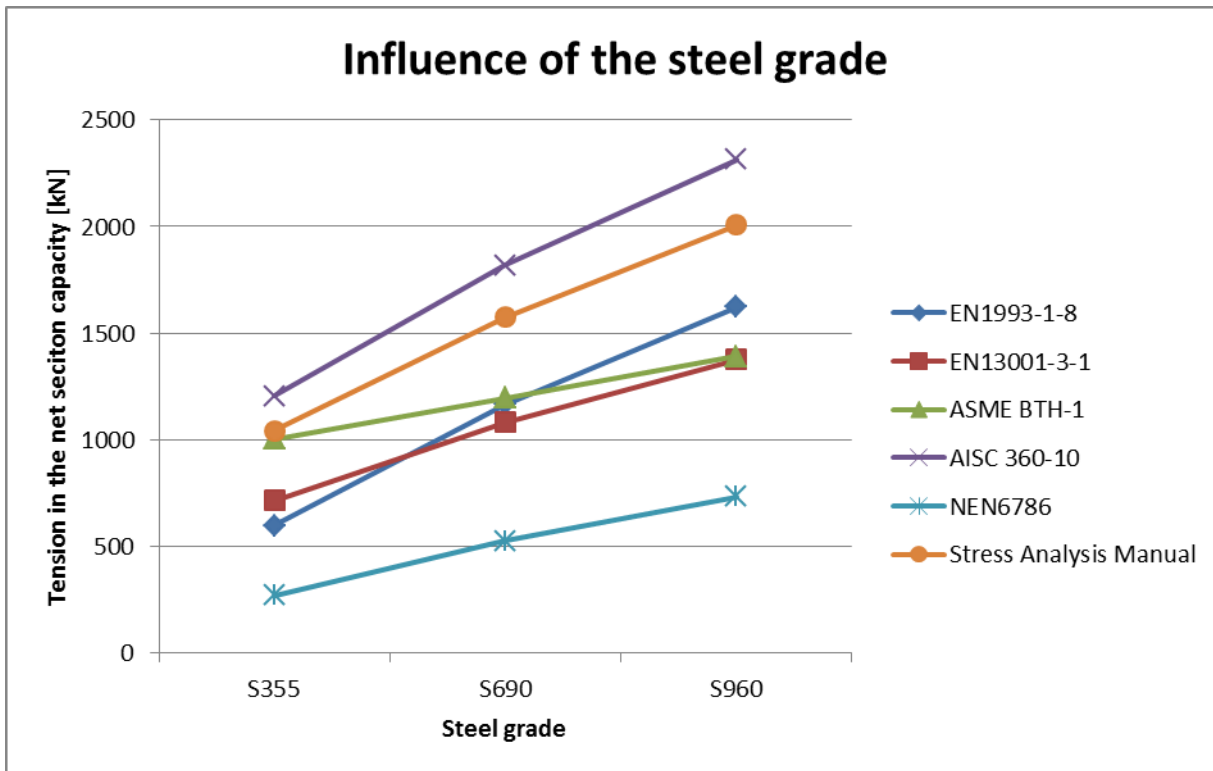


Chart C-58: Influence of the steel grade

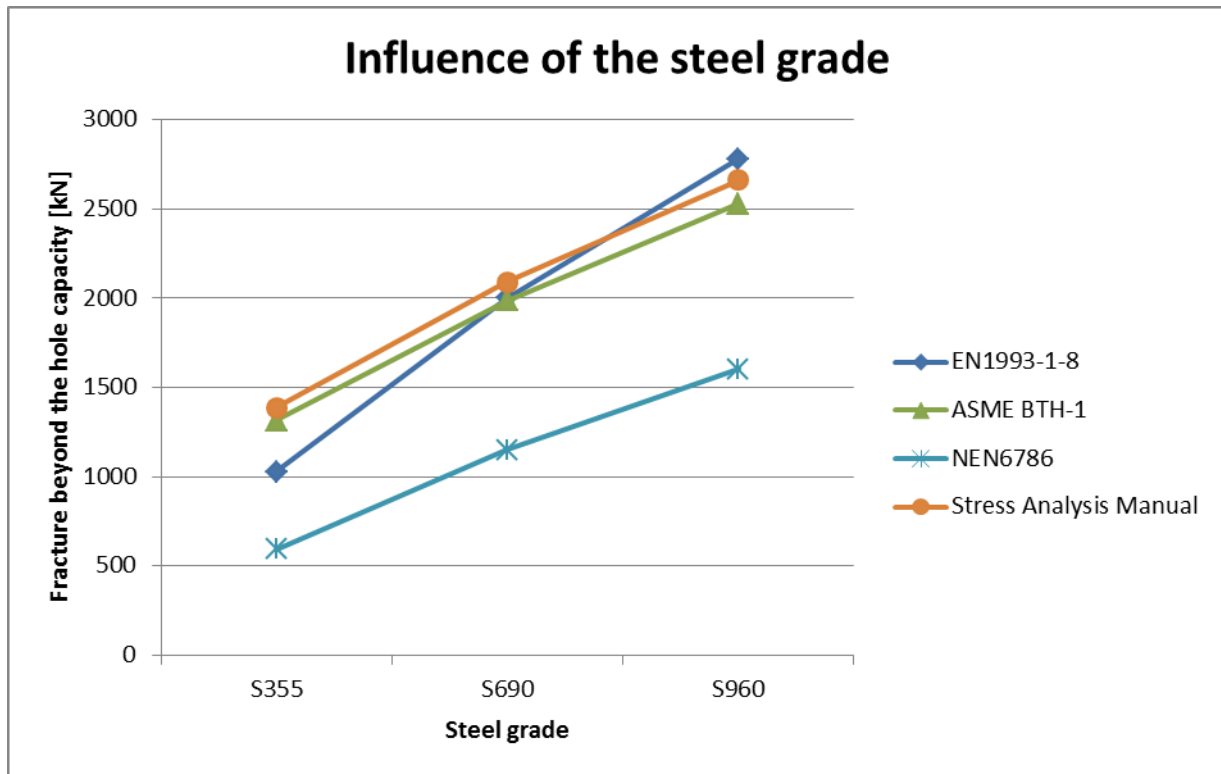


Chart C-59: Influence of the steel grade

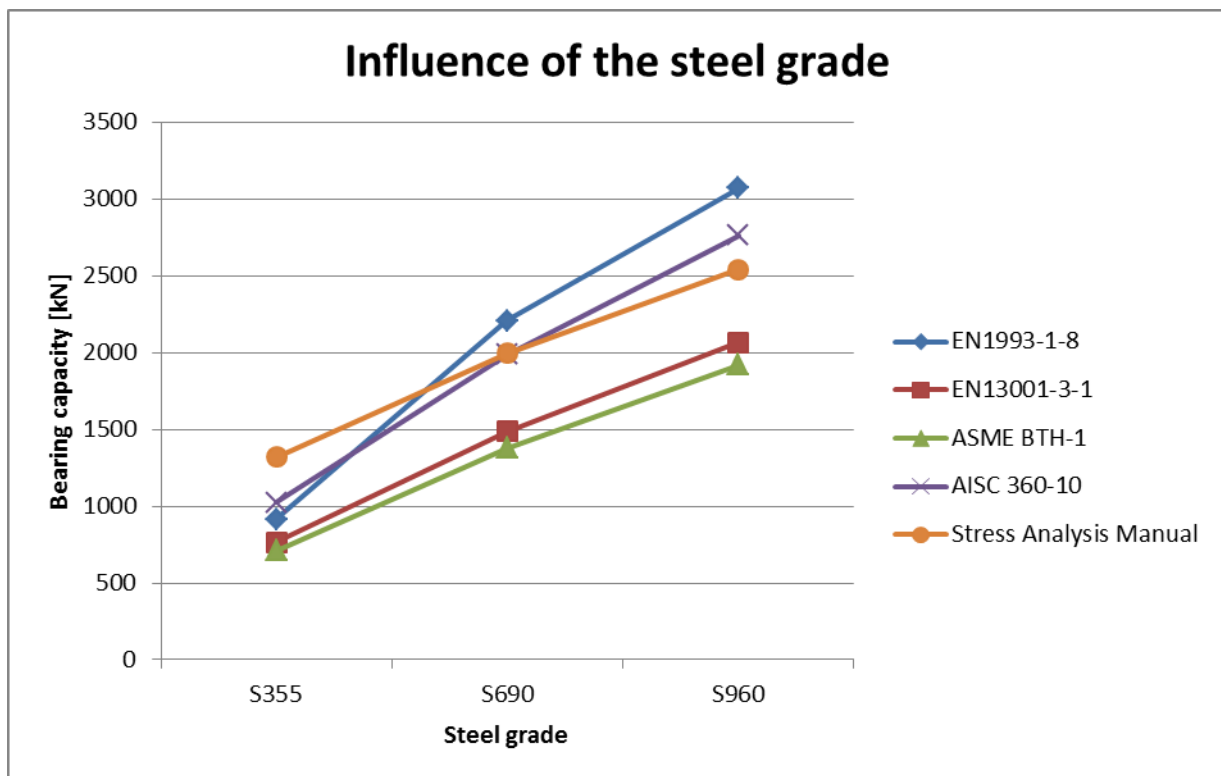


Chart C-60: Influence of the steel grade

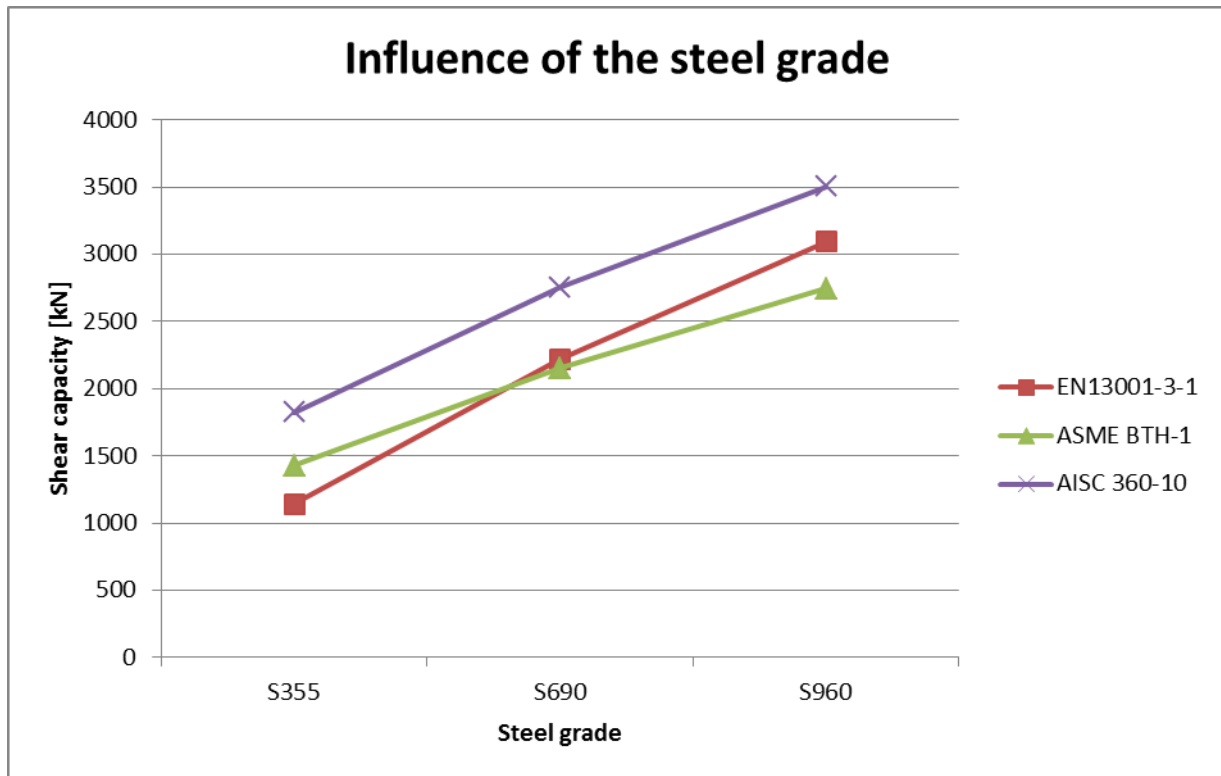


Chart C-61: Influence of the steel grade

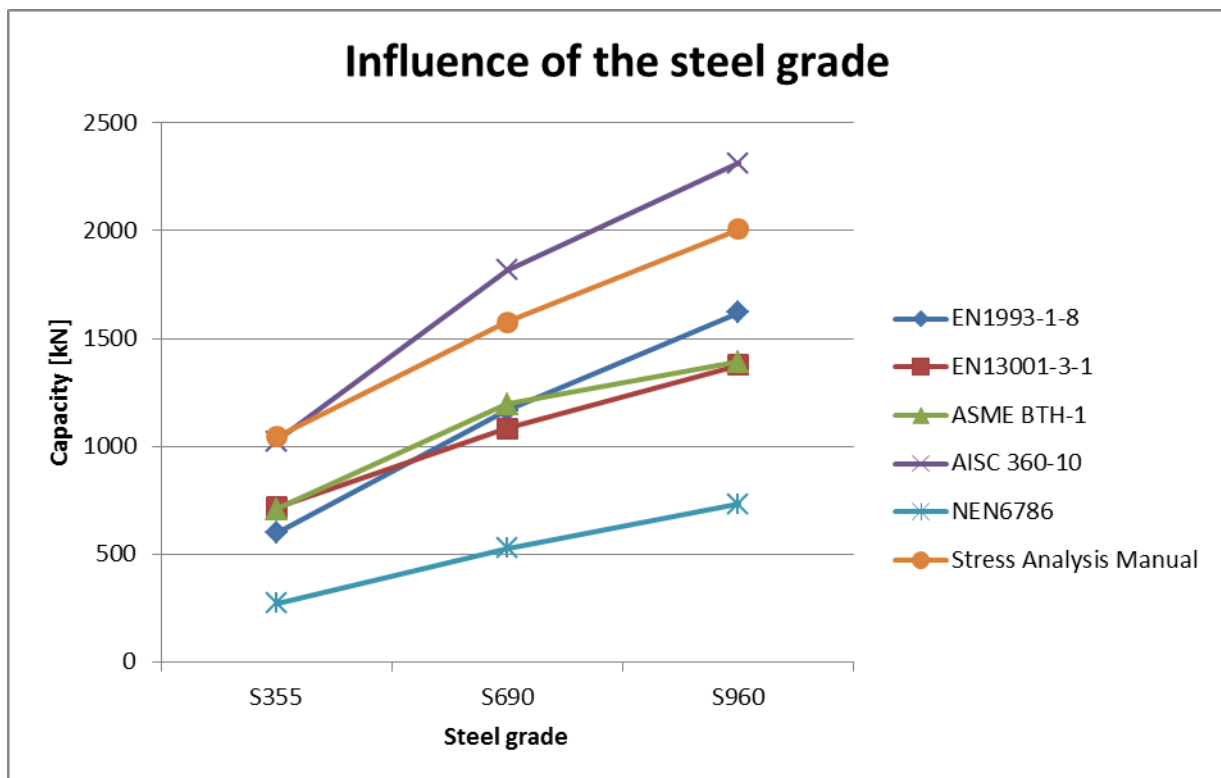


Chart C-62: Influence of the steel grade

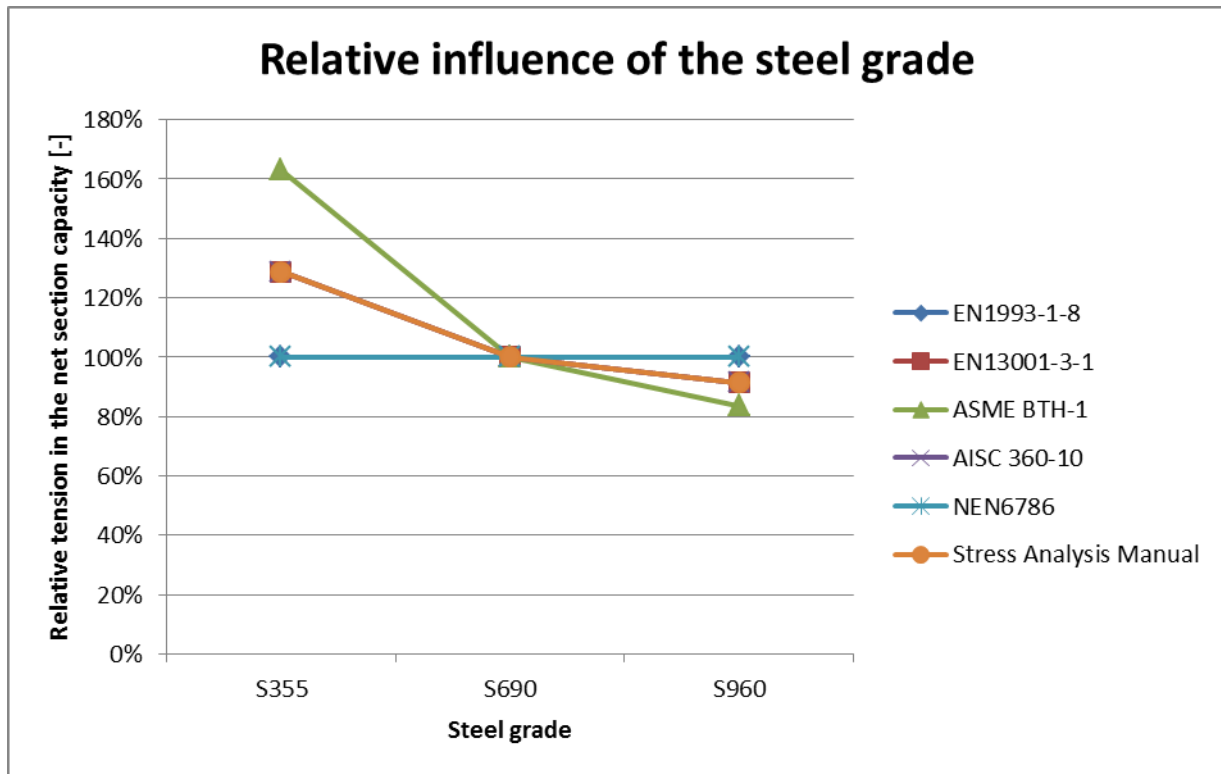


Chart C-63: Relative influence of the steel grade

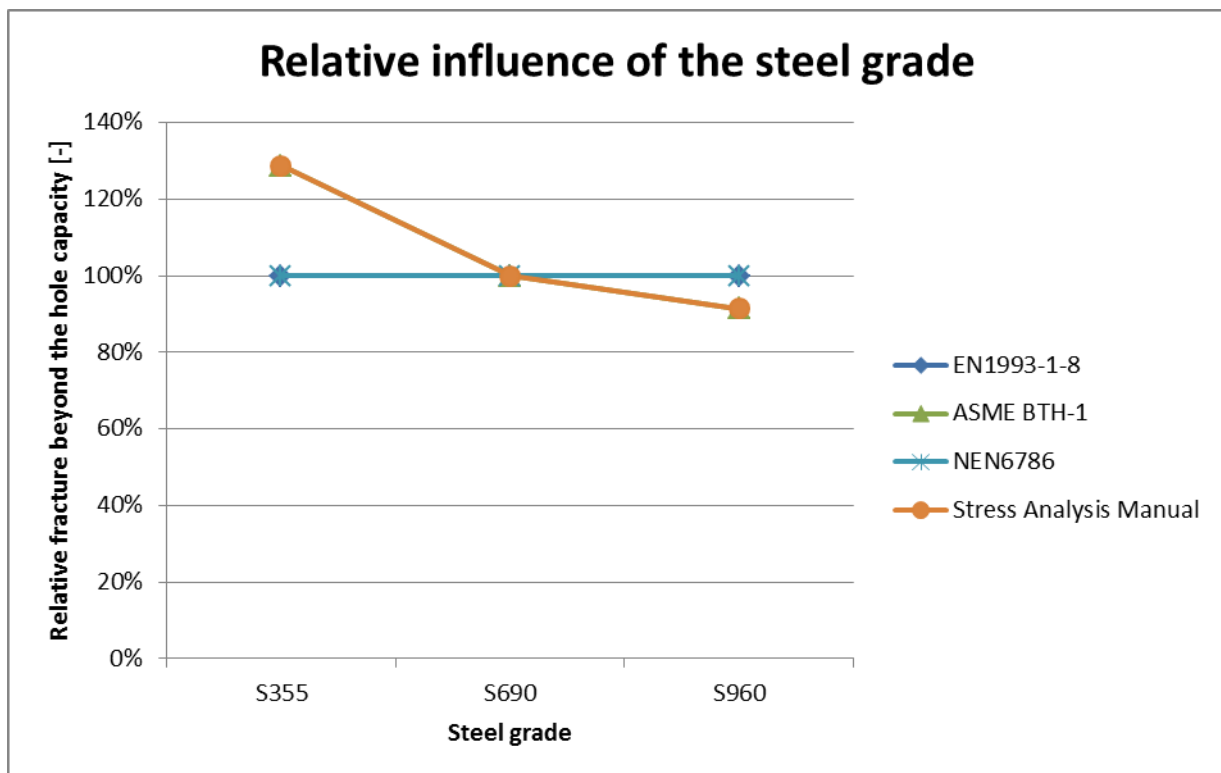


Chart C-64: Relative influence of the steel grade

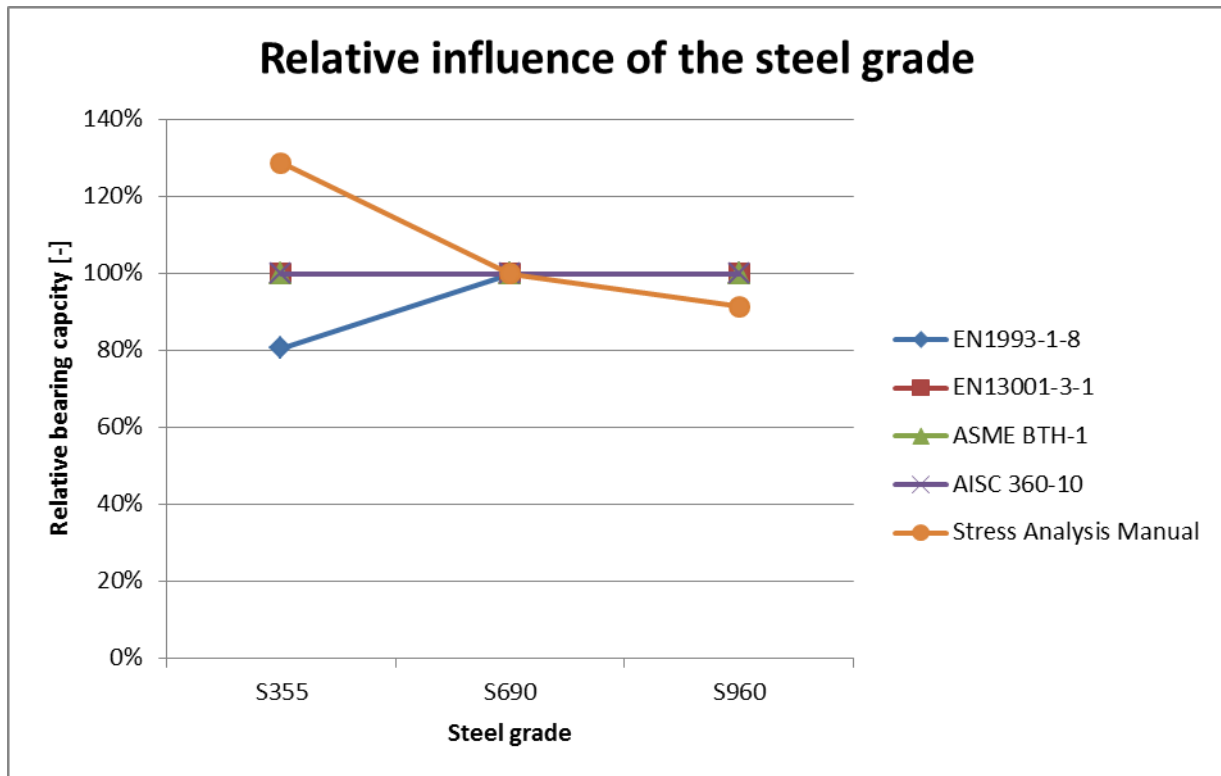


Chart C-65: Relative influence of the steel grade

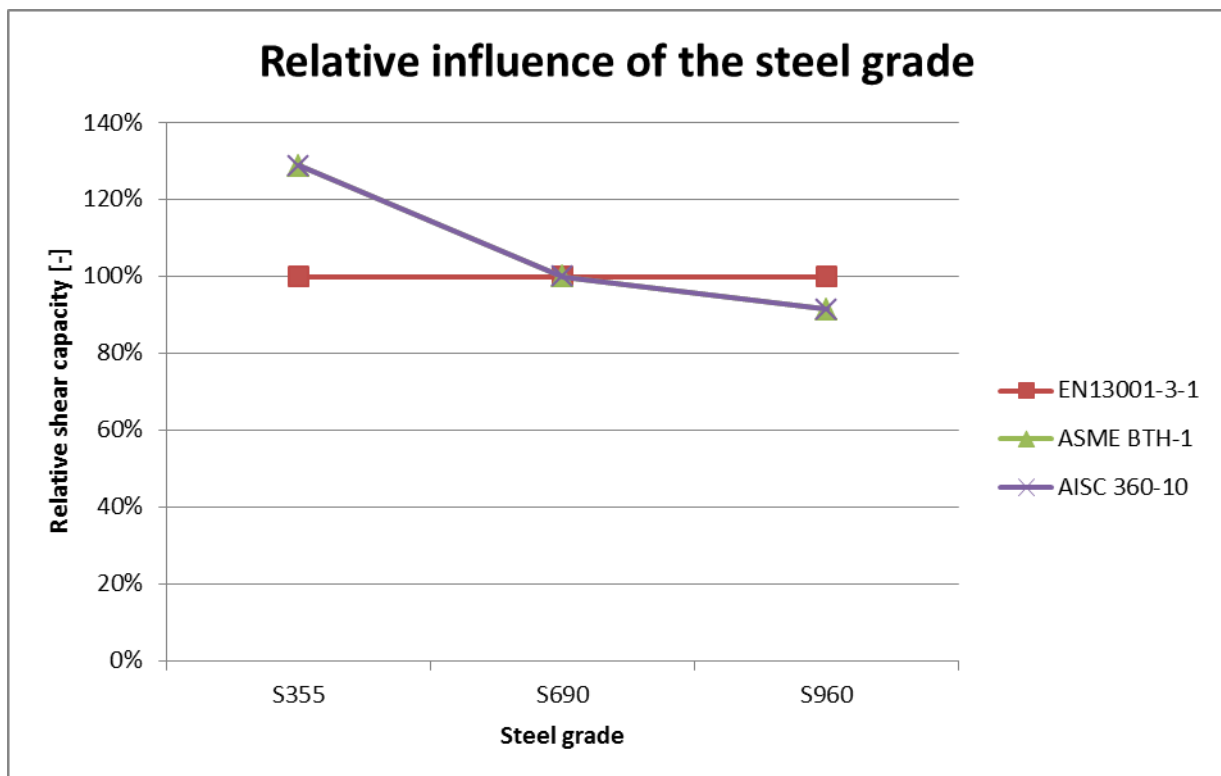


Chart C-66: Relative influence of the steel grade

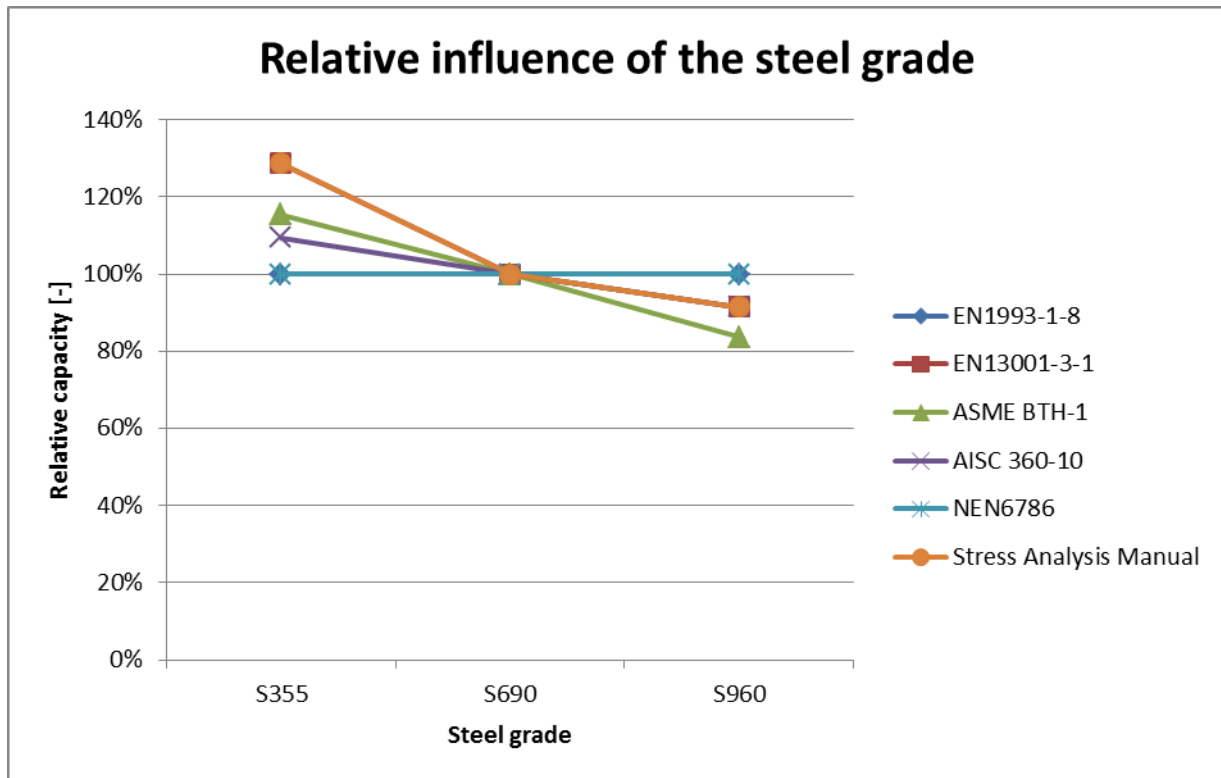


Chart C-67: Relative influence of the steel grade

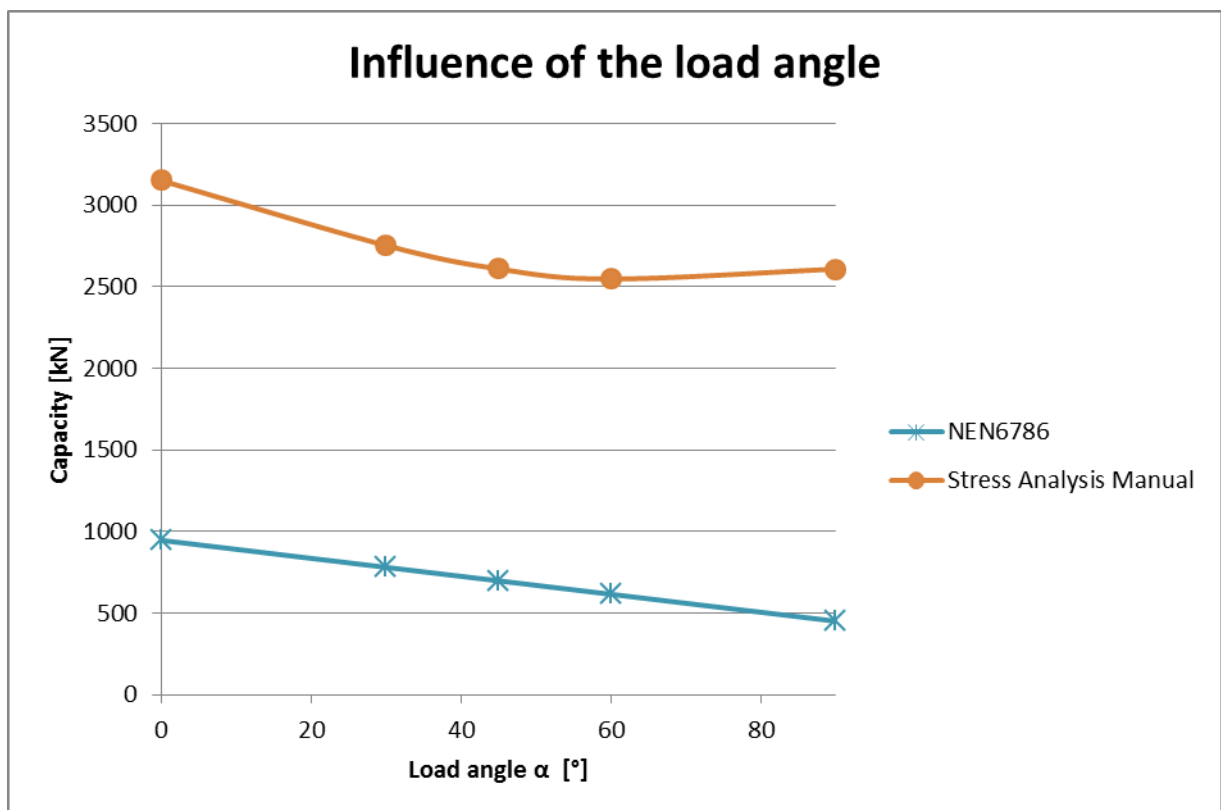


Chart C-68: Influence of the load angle

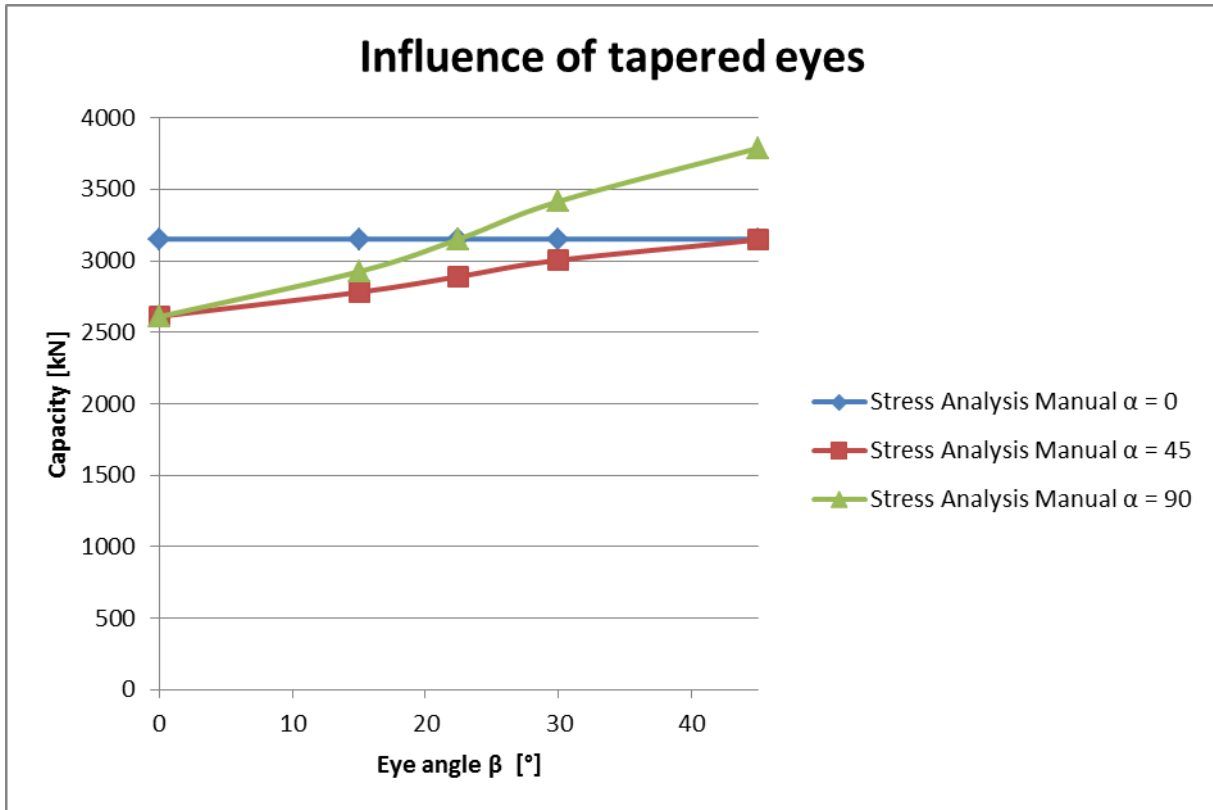


Chart C-69: Influence of tapered eyes

### C.3.1 Variance influences with NEN6786

The solid graphs in Chart C-70 to Chart C-73 are the variances without safety factors. The dashed graphs in Chart C-70 to Chart C-73 are the variances including the safety factors.

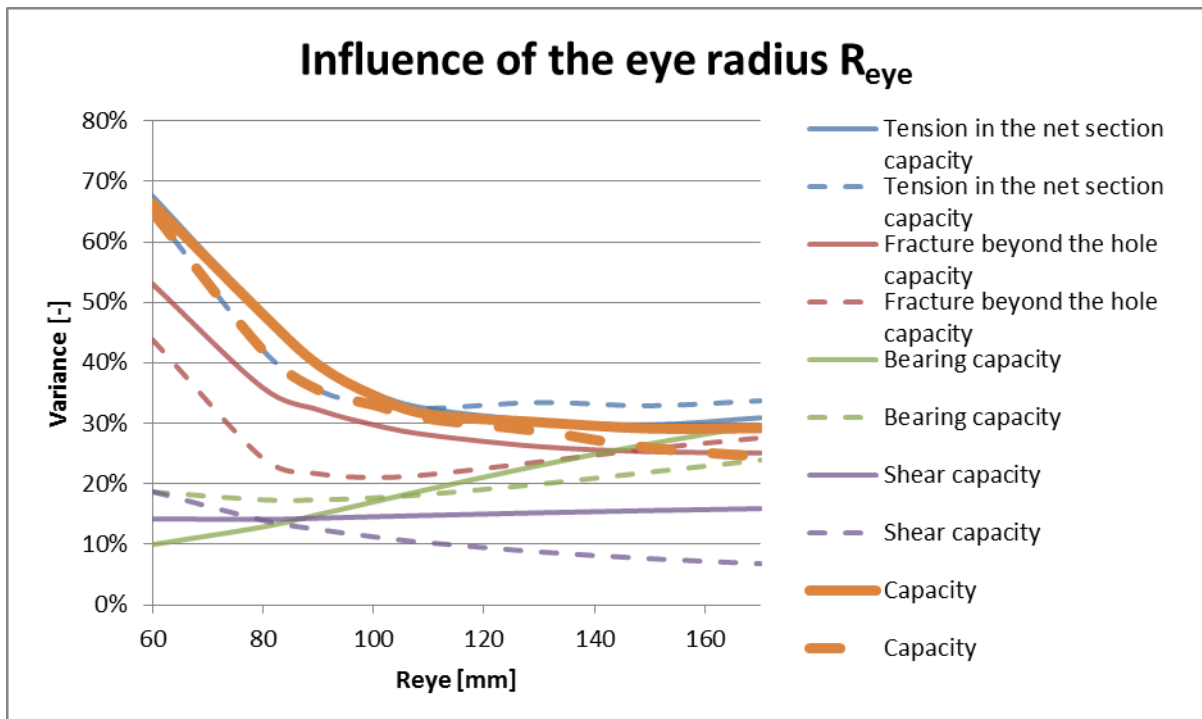


Chart C-70: Influence of the eye radius  $R_{eye}$

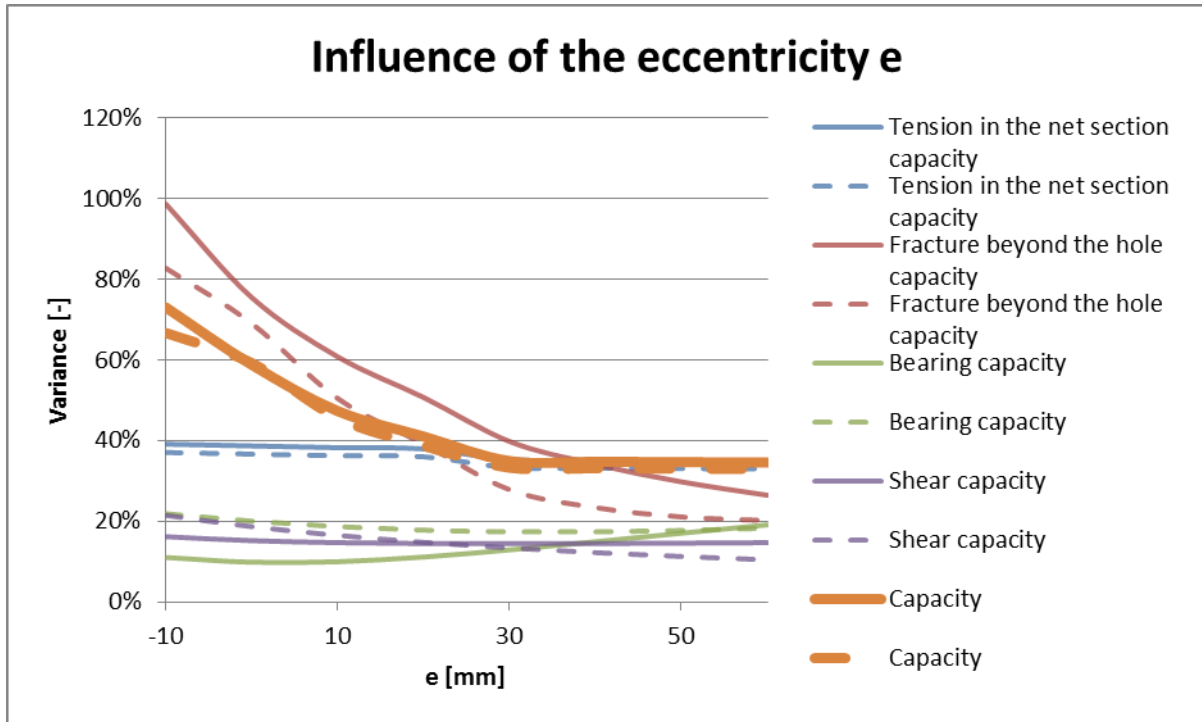


Chart C-71: Influence of the eccentricity  $e$

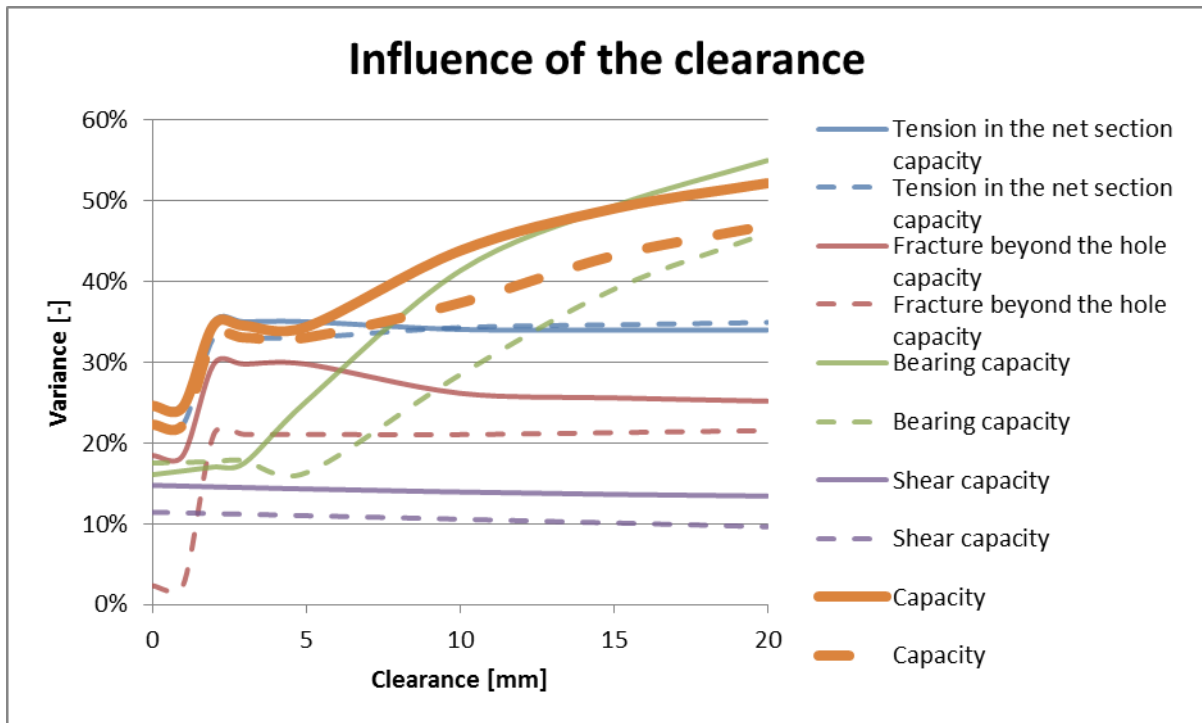


Chart C-72: Influence of the clearance

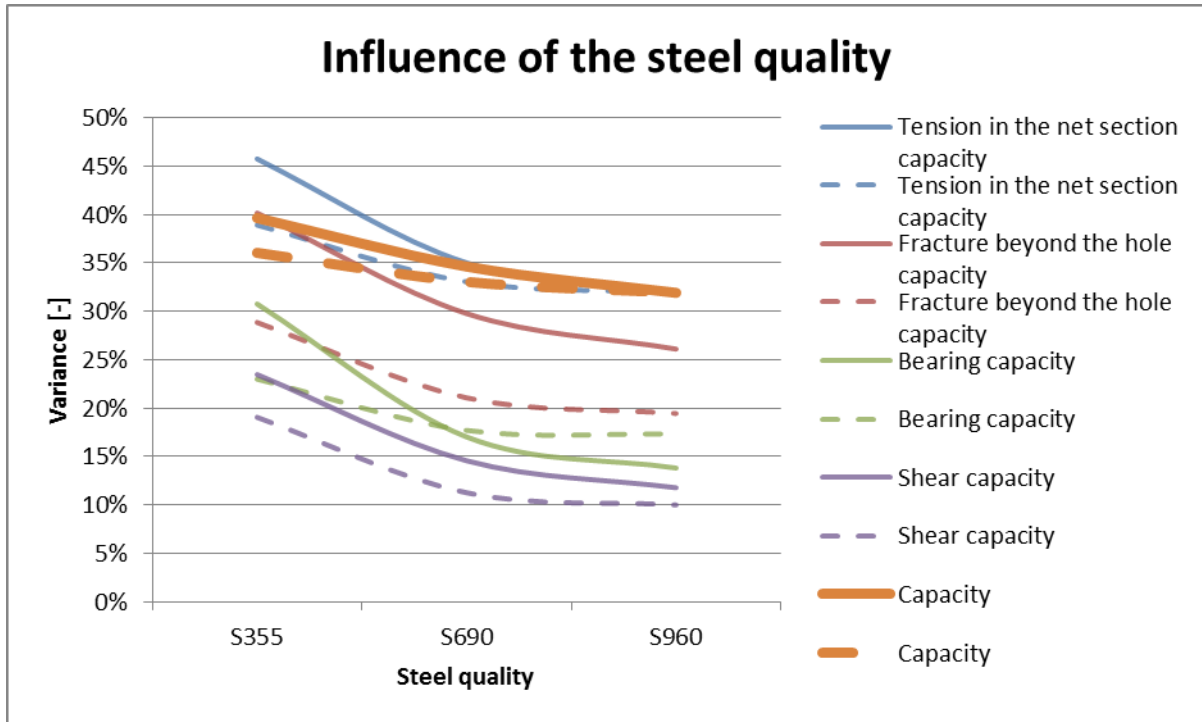


Chart C-73: Influence of the steel grade

### C.3.2 Variance influences without NEN6786

The solid graphs in Chart C-74 to Chart C-77 are the variances without safety factors. The dashed graphs in Chart C-74 to Chart C-77 are the variances including the safety factors.

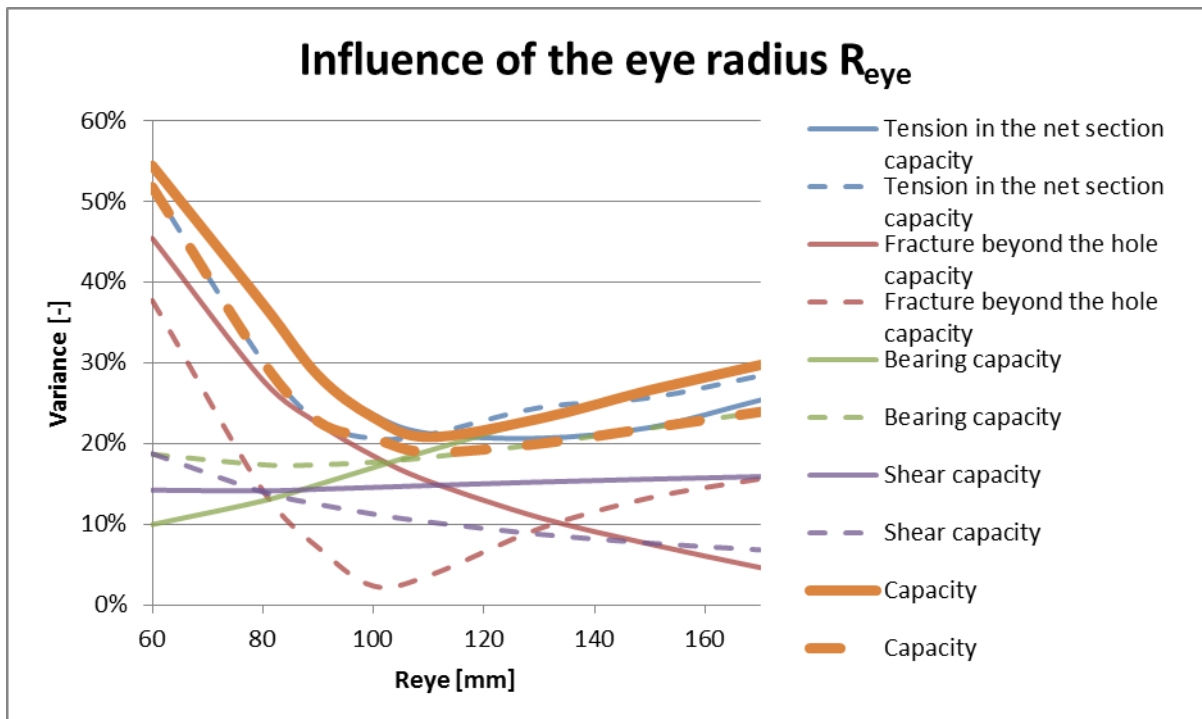


Chart C-74: Influence of the eye radius  $R_{eye}$

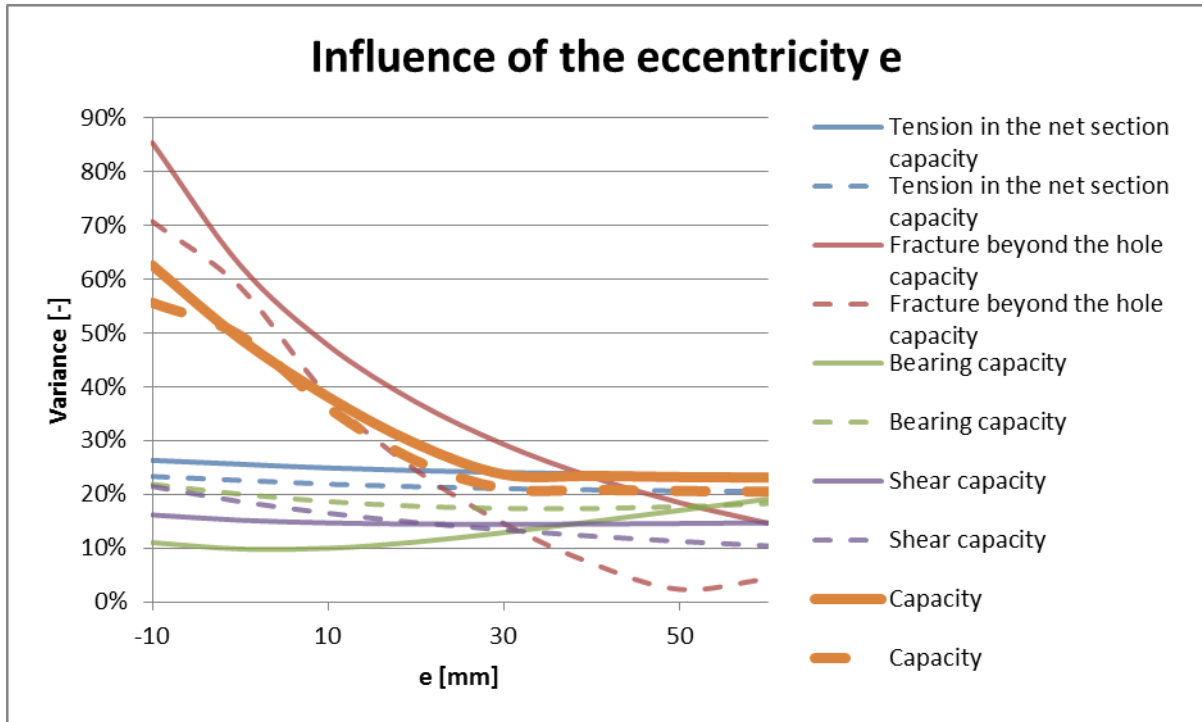


Chart C-75: Influence of the eccentricity  $e$

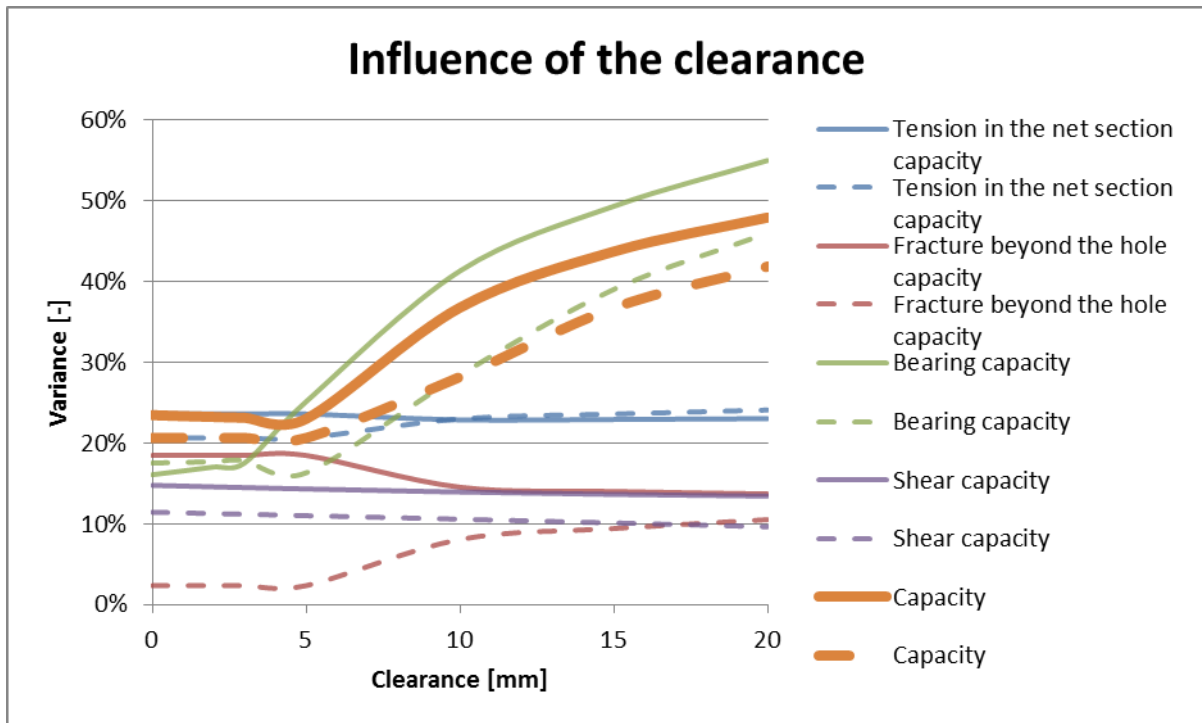


Chart C-76: Influence of the clearance

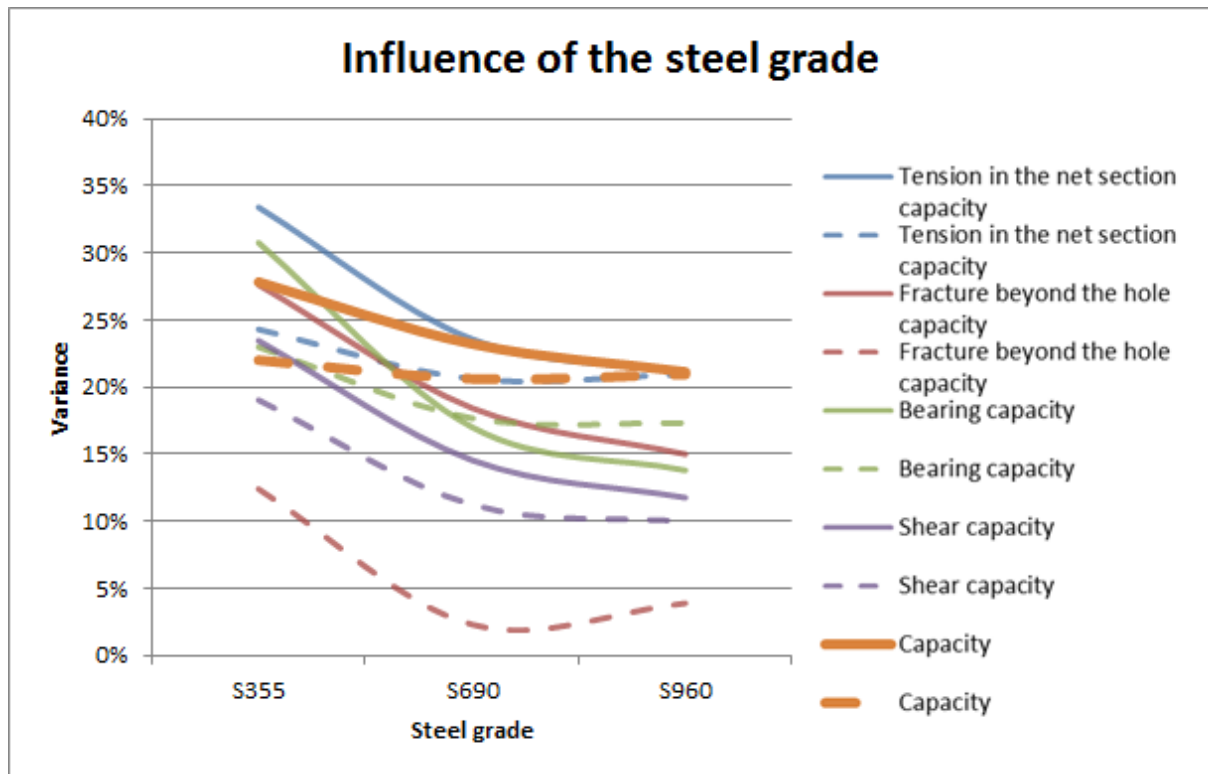


Chart C-77: Influence of the steel grade

## D FEM Modeling

The FEM models are done with the program ANSYS. The models are based on reference eye 1.

In Table D-1 and Table D-2 all analysis results of different element types<sup>16</sup> and different numerical integration options are listed. In these tables the 3<sup>rd</sup> column lists the numerical integration options, the 4<sup>th</sup> column lists the relative computation time compared with the reference (e.g. 171 means 171 times faster). The 5<sup>th</sup> column provides the difference in the VonMises stress, the 6<sup>th</sup> and 7<sup>th</sup> column provide the maximum and the summation of the stress differences. The VonMises stress ( $S_{eqv}$ ),  $S_{xx,min}$ ,  $S_{xx,max}$ ,  $S_{zz,min}$ ,  $S_{zz,max}$ ,  $S_{xz,min}$  and  $S_{xz,max}$  are compared and summed.

In Table D-3 and Table D-4 all analysis results of different element types and element sizes are listed. In these tables a column with a logarithmic relative computation time is added (e.g. 3 means  $10^3=1000$  times faster).

---

<sup>16</sup> PLANE182, PLANE183, SHELL181 and SHELL281 are 2D elements. SOLID185 and SOLID186 are 3d elements.

No bending reference							
Contact model	Element type	KEYOPT	Relative computing time	S <sub>EQV</sub> difference	Max stress difference	Sum stress difference	
Holespar	PLANE182	1,0	115	1%	11%	42%	
Holespar	PLANE182	1,3	104	0%	9%	35%	
Holespar	PLANE183	-	85	0%	3%	12%	<--
Holespar	SHELL181	3,0	78	9%	25%	96%	
Holespar	SHELL181	3,2	66	1%	26%	67%	
Holespar	SHELL281	-	28	1%	23%	59%	
Contact/target	PLANE182	1,0	58	0%	11%	40%	
Contact/target	PLANE182	1,1	91	8%	16%	78%	
Contact/target	PLANE182	1,2	57	2%	12%	47%	
Contact/target	PLANE182	1,3	59	2%	12%	47%	
Contact/target	PLANE183	-	51	2%	9%	20%	<--
Contact/target	SOLID185	2,0	4	0%	9%	34%	
Contact/target	SOLID185	2,1	6	9%	14%	64%	
Contact/target	SOLID185	2,2	3	0%	8%	29%	
Contact/target	SOLID185	2,3	4	0%	8%	29%	
Contact/target	SOLID186	2,0	1	0%	1%	1%	
Contact/target	SOLID186	2,1	1	0%	0%	0%	Reference

Table D-1: Result differences of different element types and different numerical integration options (bending of the pin is neglected)

Bending reference						
Contact/geometry model	Element type	KEYOPT	Relative computing time	$S_{EQV}$ difference	Max stress difference	Sum stress difference
Holespar	PLANE182	1,0	171	17%	47%	154%
Holespar	PLANE182	1,3	155	15%	52%	157%
Holespar	PLANE183	-	126	15%	50%	144%
Holespar	SHELL181	3,0	116	23%	63%	218%
Holespar	SHELL181	3,2	98	16%	64%	190%
Holespar	SHELL281	-	41	16%	62%	182%
Contact	PLANE182	1,0	92	16%	53%	173%
Contact	PLANE182	1,1	135	23%	57%	205%
Contact	PLANE182	1,2	85	14%	57%	174%
Contact	PLANE182	1,3	88	14%	57%	174%
Contact	PLANE183	-	75	14%	53%	154%
Contact, no bending	SOLID185	2,0	6	15%	50%	167%
Contact, no bending	SOLID185	2,1	10	23%	54%	194%
Contact, no bending	SOLID185	2,2	5	16%	54%	162%
Contact, no bending	SOLID185	2,3	5	16%	54%	162%
Contact, no bending	SOLID186	2,0	2	16%	51%	142%
Contact, no bending	SOLID186	2,1	1	16%	51%	142%
Contact, bending	SOLID185	2,0	5	1%	18%	67%
Contact, bending	SOLID185	2,1	8	16%	31%	133%
Contact, bending	SOLID185	2,2	4	3%	11%	41%
Contact, bending	SOLID185	2,3	4	3%	12%	43%
Contact, bending	SOLID186	2,0	1	1%	1%	4%
Contact, bending	SOLID186	2,1	1	0%	0%	0%

Table D-2: Result differences of different element types and different numerical integration options (bending of the pin is included)

No bending reference								
Relative scale	Element type	KEYOPT	Relative computing time	Logarithmic relative computing time	S <sub>EQV</sub> difference	Max stress difference	Sum stress difference	
1	PLANE182	1,0	1752	3.2	0%	11%	44%	
2	PLANE182	1,0	449	2.7	1%	7%	31%	
3	PLANE182	1,0	215	2.3	1%	7%	27%	
4	PLANE182	1,0	101	2.0	2%	7%	26%	
5	PLANE182	1,0	63	1.8	2%	7%	25%	
8	PLANE182	1,0	26	1.4	2%	7%	24%	
1	PLANE183	-	1440	3.2	1%	8%	24%	<--
2	PLANE183	-	379	2.6	2%	8%	23%	
4	PLANE183	-	96	2.0	3%	8%	24%	
0.5	SOLID185	2,0	933	3.0	1%	17%	69%	
1	SOLID185	2,0	116	2.1	0%	9%	35%	
2	SOLID185	2,0	11	1.0	0%	4%	19%	
0.25	SOLID186	2,1	1955	3.3	4%	6%	23%	
0.5	SOLID186	2,1	297	2.5	1%	3%	10%	<--
1	SOLID186	2,1	28	1.5	0%	3%	6%	
2	SOLID186	2,1	1	0.0	0%	0%	0%	Reference

Table D-3: Result differences of different element types and element sizes (bending of the pin is neglected)

Bending reference									
Relative scale	Geometry model	Element type	KEYOPT	Relative computing time	Logarithmic relative computing time	S <sub>EQV</sub> difference	Max stress difference	Sum stress difference	
1	No bending	PLANE182	1,0	2983	3.5	18%	56%	181%	
2	No bending	PLANE182	1,0	764	2.9	17%	56%	170%	
3	No bending	PLANE182	1,0	367	2.6	17%	56%	166%	
4	No bending	PLANE182	1,0	173	2.2	16%	56%	164%	
5	No bending	PLANE182	1,0	107	2.0	16%	56%	163%	
8	No bending	PLANE182	1,0	44	1.6	16%	56%	162%	
1	No bending	PLANE183	-	2452	3.4	17%	56%	163%	<--
2	No bending	PLANE183	-	644	2.8	16%	56%	161%	
4	No bending	PLANE183	-	164	2.2	15%	56%	160%	
0.5	No bending	SOLID185	2,0	1589	3.2	19%	53%	206%	
1	No bending	SOLID185	2,0	197	2.3	18%	54%	176%	
2	No bending	SOLID185	2,0	18	1.3	18%	54%	162%	
0.25	No bending	SOLID186	2,1	3329	3.5	21%	51%	160%	
0.5	No bending	SOLID186	2,1	506	2.7	19%	53%	154%	
1	No bending	SOLID186	2,1	48	1.7	18%	54%	150%	
2	No bending	SOLID186	2,1	2	0.2	18%	53%	148%	
0.25	Bending	SOLID185	2,0	6613	3.8	14%	50%	211%	
0.5	Bending	SOLID185	2,0	1231	3.1	8%	36%	135%	
1	Bending	SOLID185	2,0	175	2.2	4%	23%	81%	<--
2	Bending	SOLID185	2,0	12	1.1	0%	13%	40%	
0.25	Bending	SOLID186	2,0	3530	3.5	11%	24%	84%	
0.5	Bending	SOLID186	2,0	428	2.6	7%	17%	52%	
1	Bending	SOLID186	2,0	35	1.5	3%	8%	24%	
2	Bending	SOLID186	2,0	1	0.0	1%	3%	4%	
0.25	Bending	SOLID186	2,1	2682	3.4	11%	26%	85%	
0.5	Bending	SOLID186	2,1	359	2.6	7%	16%	54%	<--
1	Bending	SOLID186	2,1	33	1.5	3%	7%	23%	
2	Bending	SOLID186	2,1	1	0.0	0%	0%	0%	Reference

Table D-4: Result differences of different element types and element sizes (bending of the pin is included)

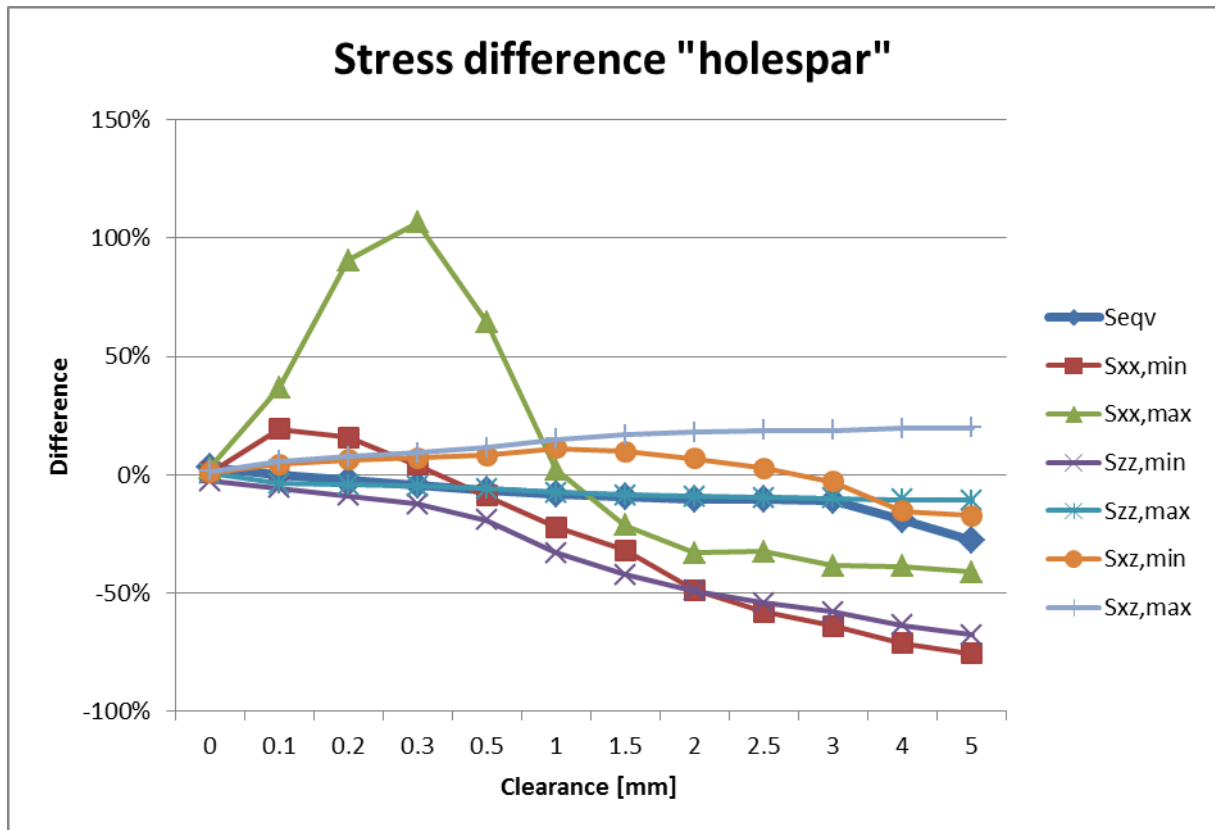


Chart D-1: Stress differences for different stress direction compared to a reference model with contact/target and SOLID186 elements (bending neglected).

	Stress orientation	Stress [N/mm <sup>2</sup> ]	Stress [N/mm <sup>2</sup> ]	Difference
		No bending	Bending	
max	VonMises	892	1084	-18%
min	xx	-297	-632	-53%
max	xx	270	291	-7%
min	zz	-532	-927	-43%
max	zz	931	930	0%
min	xz	-430	-586	-27%
max	xz	260	259	0%
	Computing time	13392	22800	-41%

Table D-5: Comparison if pin bending is neglected

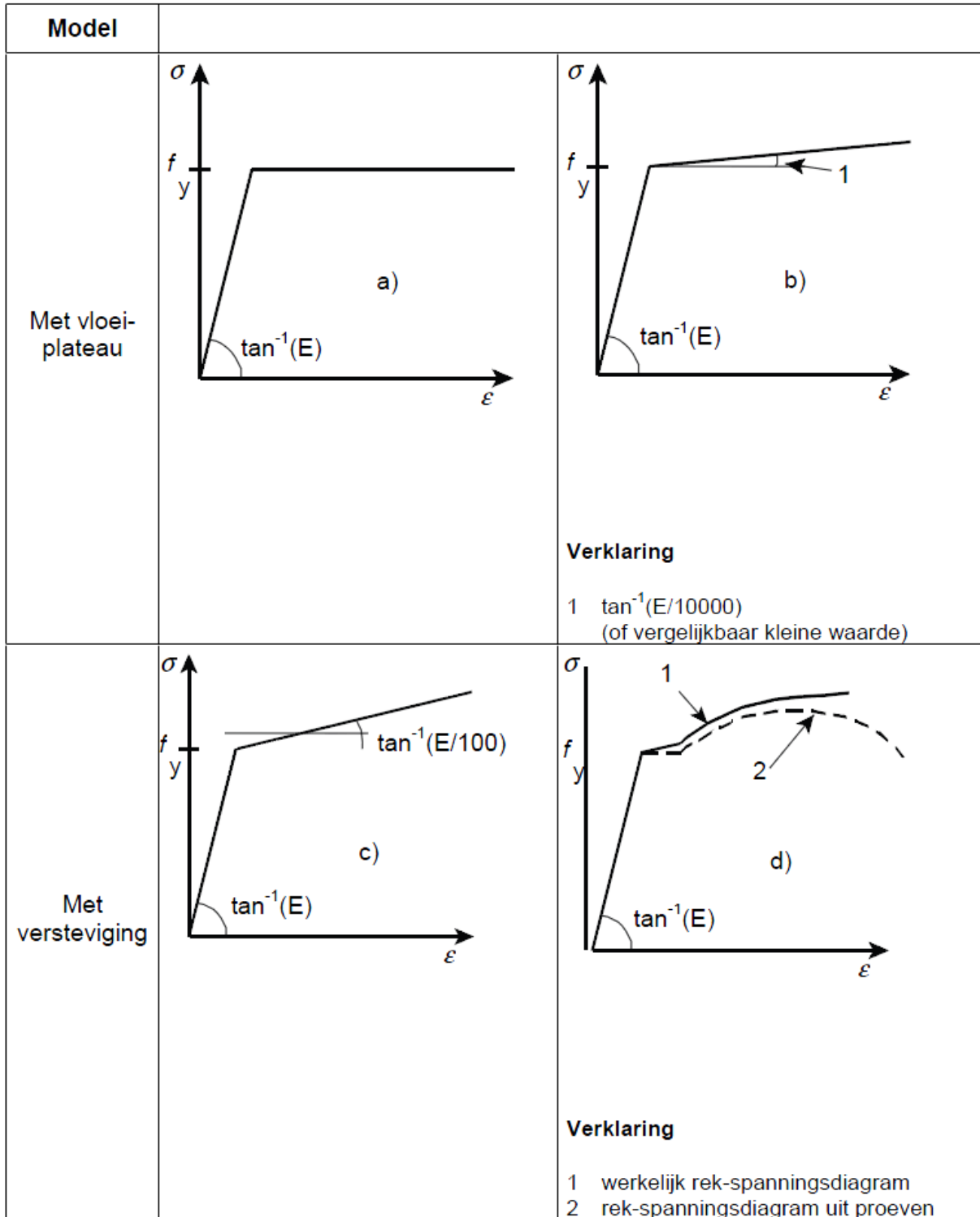


Figure D-1: Stress-Strain curves according to EN1993-1-5 [22]

# E FEM Analysis

## E.1 Analysis of the results based on the capacities of the standards

In this appendix most Ansys results are shown in charts for all failure criteria. The charts are briefly explained.

In the plastic strains which appear in the net section are plotted for different eye radii. The plastic strains are only plotted for eye radii in which tension in the net section is governing according to the standard. For example in the AISC 360-10, tension in the net section is only governing for an eye radius smaller or equal to 100mm. For a larger eye radius bearing becomes governing and therefore these plastic strains in the net section are not normative.

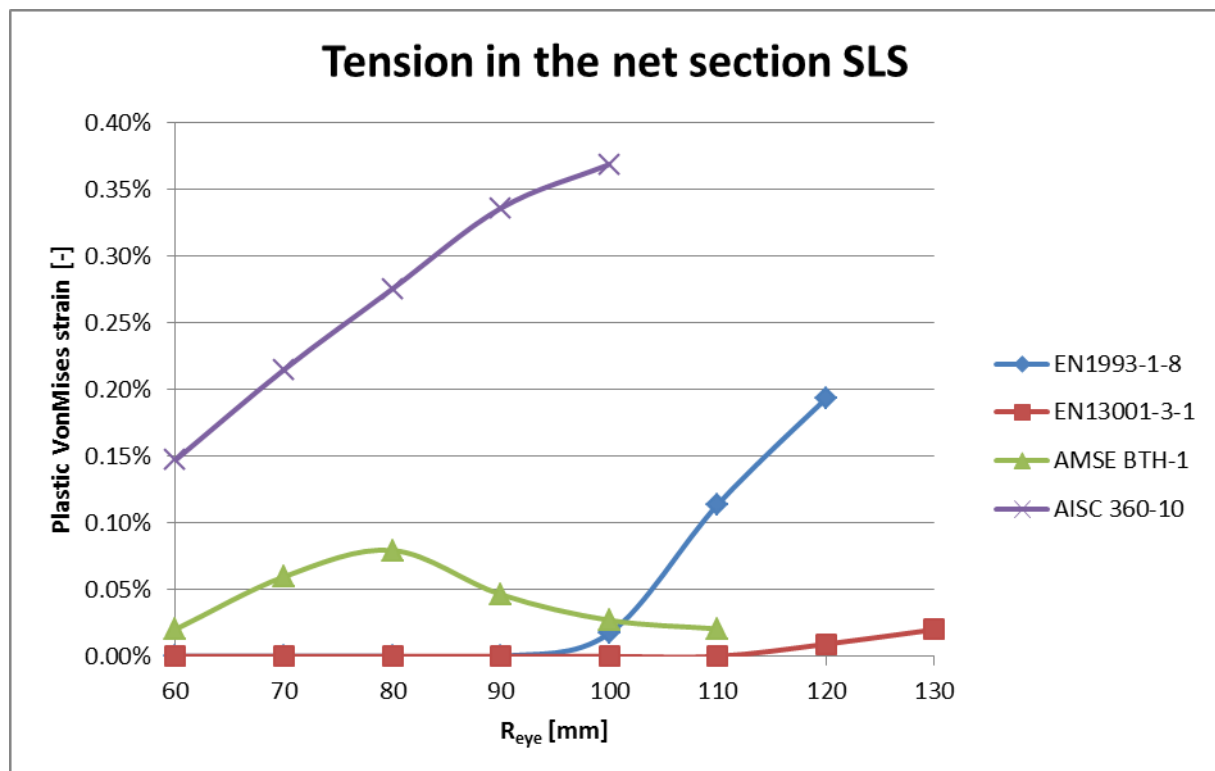


Chart E-1: Plastic strains in the net section for SLS capacities as input for various eye radii with an eccentricity of 50mm

From Chart E-1 can be concluded that the plastic strains are different not only for each standard, but for each eye radius too.

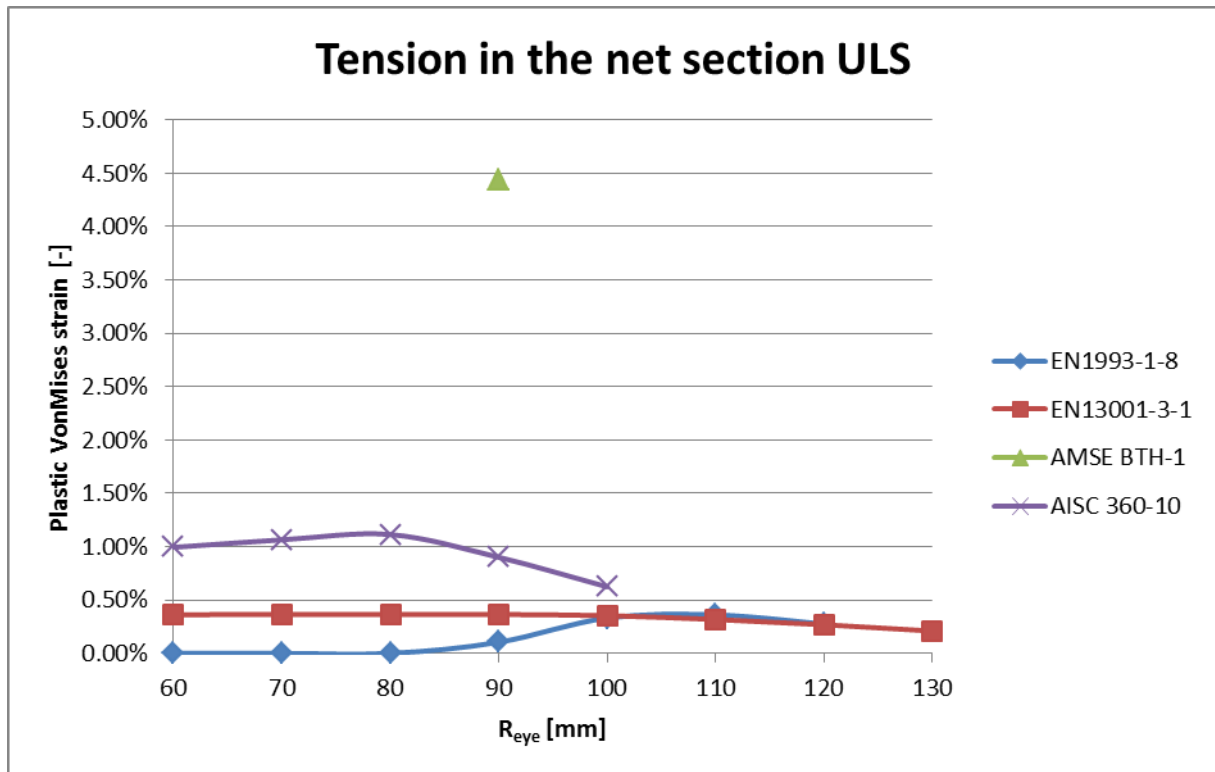


Chart E-2: Plastic strains in the net section for ULS capacities as input for various eye radii with an eccentricity of 50mm

For the ULS capacities as input the results are more similar for different eye radii (see Chart E-2). The ULS capacities based on the ASME BTH-1 standard are that high so the FEM model is not always capable to find a solution. This is due because these ULS capacities are based on real empirical results of failure of the connection.

In Chart E-3 the plastic strains which appear in the net section are plotted for different eye radii without an eccentricity. The plastic strains are only plotted for eye radii in which tension in the net section is governing according to the standard. ULS capacities according to the ASME BTH-1 or according to the AISC 360-10 standard are that high that a FEM analysis can't find equilibrium anymore, so therefore these results are not plotted.

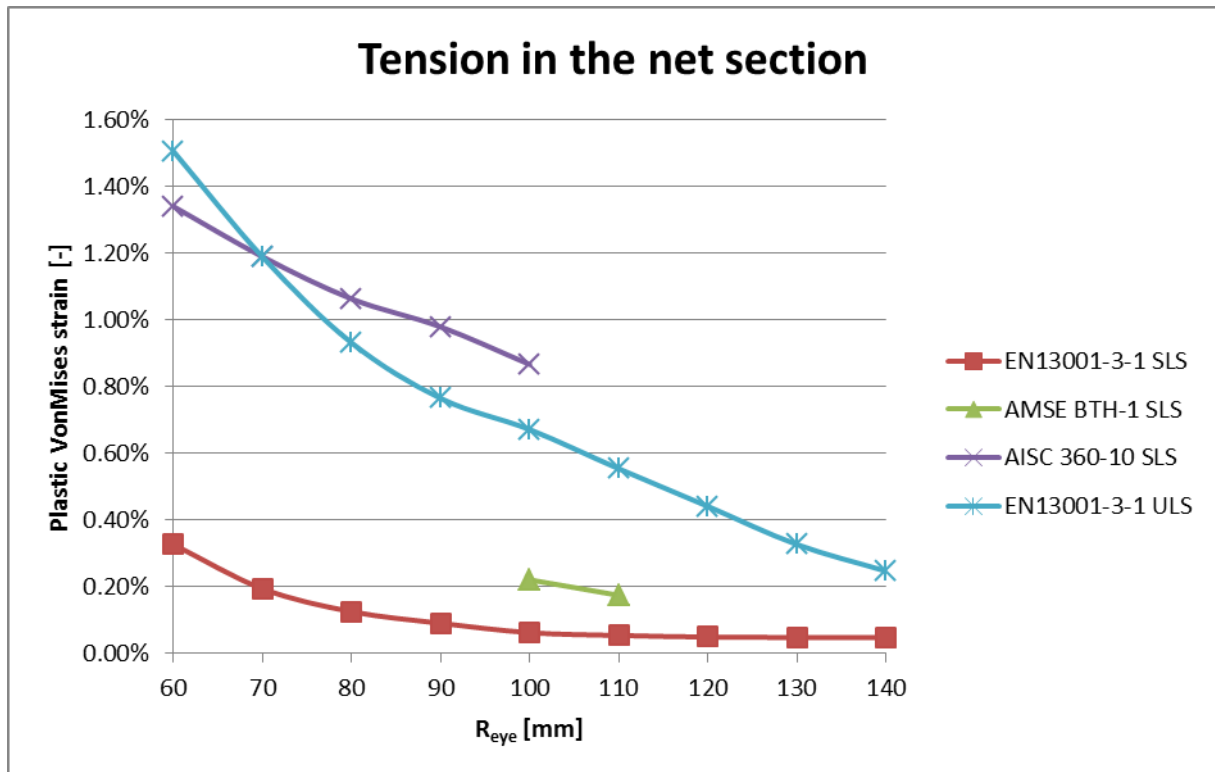


Chart E-3: Plastic strains in the net section for SLS and ULS capacities as input for various eye radii without an eccentricity

The eccentricity has an influence on the plastic strains in the net section although only the EN13001-3-1 standard includes this effect. Chart E-4 and Chart E-5 the plastic strains in the net section are plotted for SLS and ULS capacities as input, for an eye radius of 80mm and 100mm. From these charts can be concluded that for larger eccentricities the plastic strains in the net section will reduce. Even for the EN13001-3-1 standard which already includes the effect of the eccentricity.

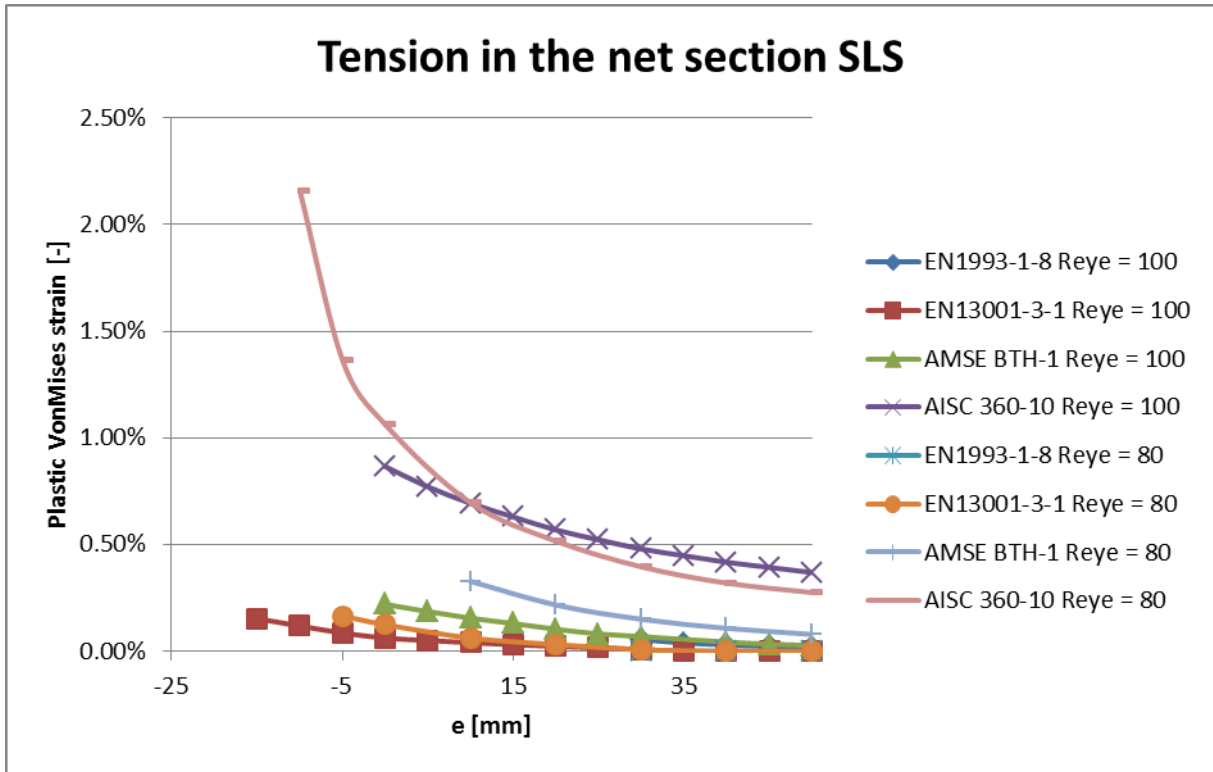


Chart E-4: Plastic strains in the net section for SLS capacities as input for various eccentricities

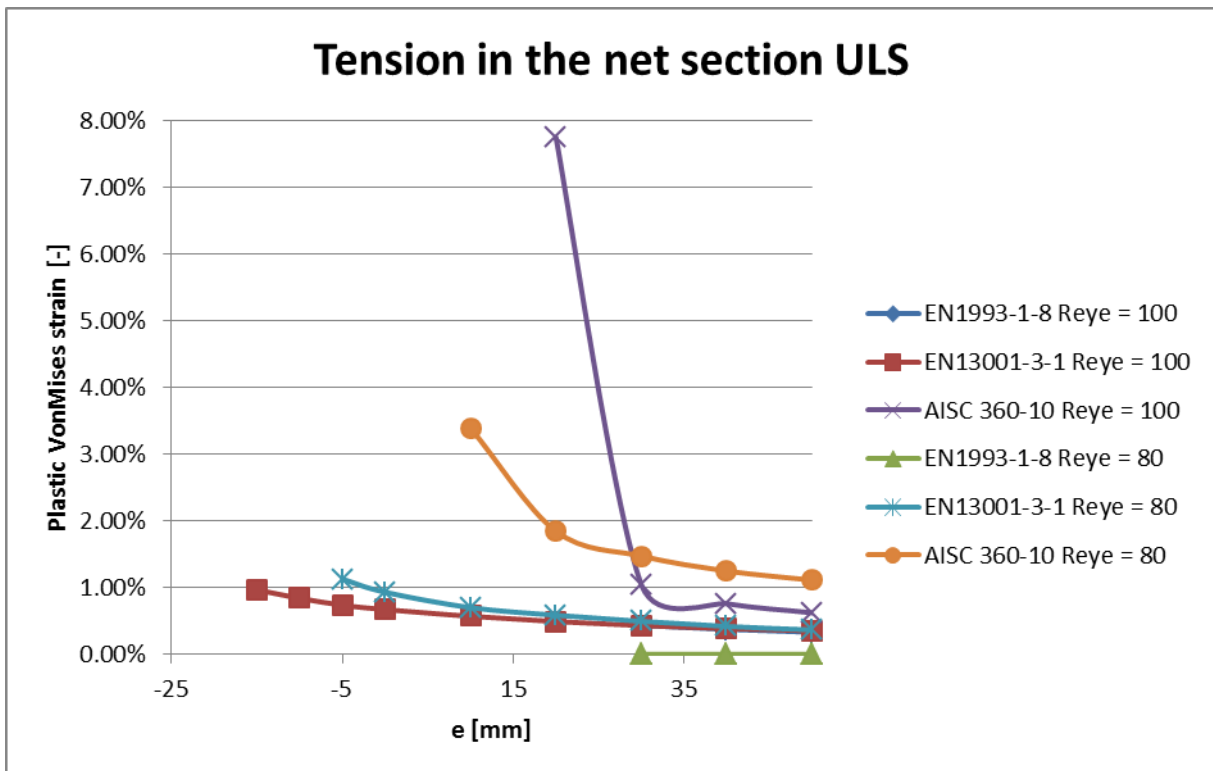


Chart E-5: Plastic strains in the net section for ULS capacities as input for various eccentricities

The eccentricity has an influence for the fracture beyond the hole strains/stresses. Each standard includes the effect of eccentricity for checking the fracture beyond the hole criteria or for the shear criteria. Since the shear strains/stresses are hardly notable by a FEM analysis, only the strains/stresses in the top of the eye are useful. In Chart E-6 to Chart E-9 all stresses (or plastic

strains if they occur) are plotted for different eccentricities, SLS and ULS capacities as input, and for an eye radius of 80mm and 100mm. From these charts can be concluded that all standards provide different stress/strains and the effect of different eccentricities is different for each standard. Only the EN1993-1-8 standard has a critical unity check for fracture beyond the hole and or shear for positive eccentricities. For the other standards this becomes critical only for negative eccentricities which are not used at Mammoet.

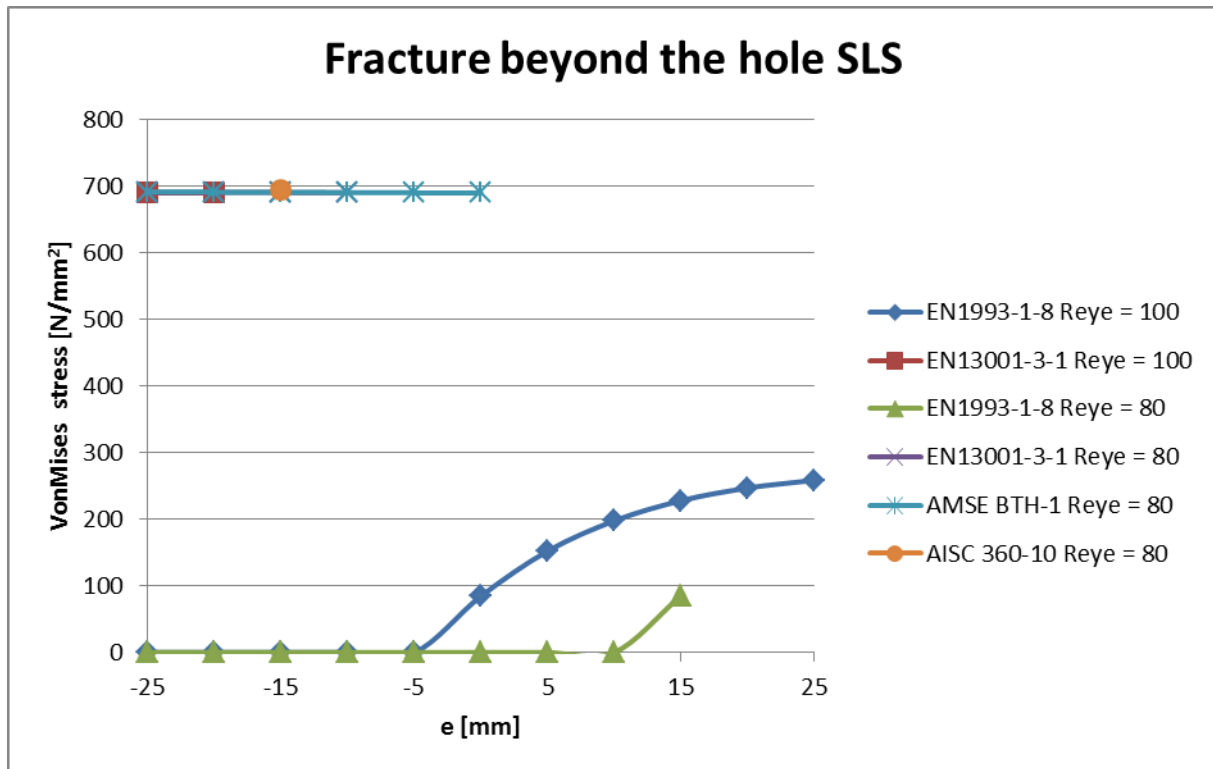


Chart E-6: VonMises stresses on top of the eye for SLS capacities as input for various eccentricities

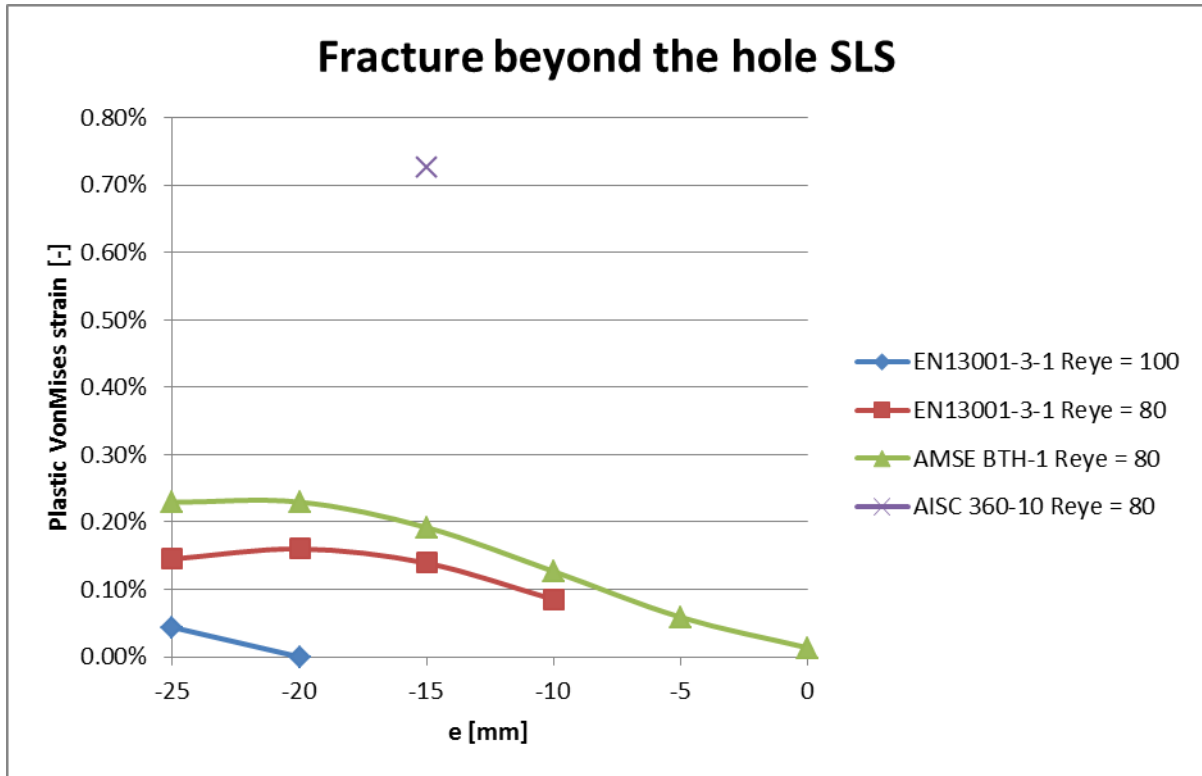


Chart E-7: Plastic strains on top of the eye for SLS capacities as input for various eccentricities

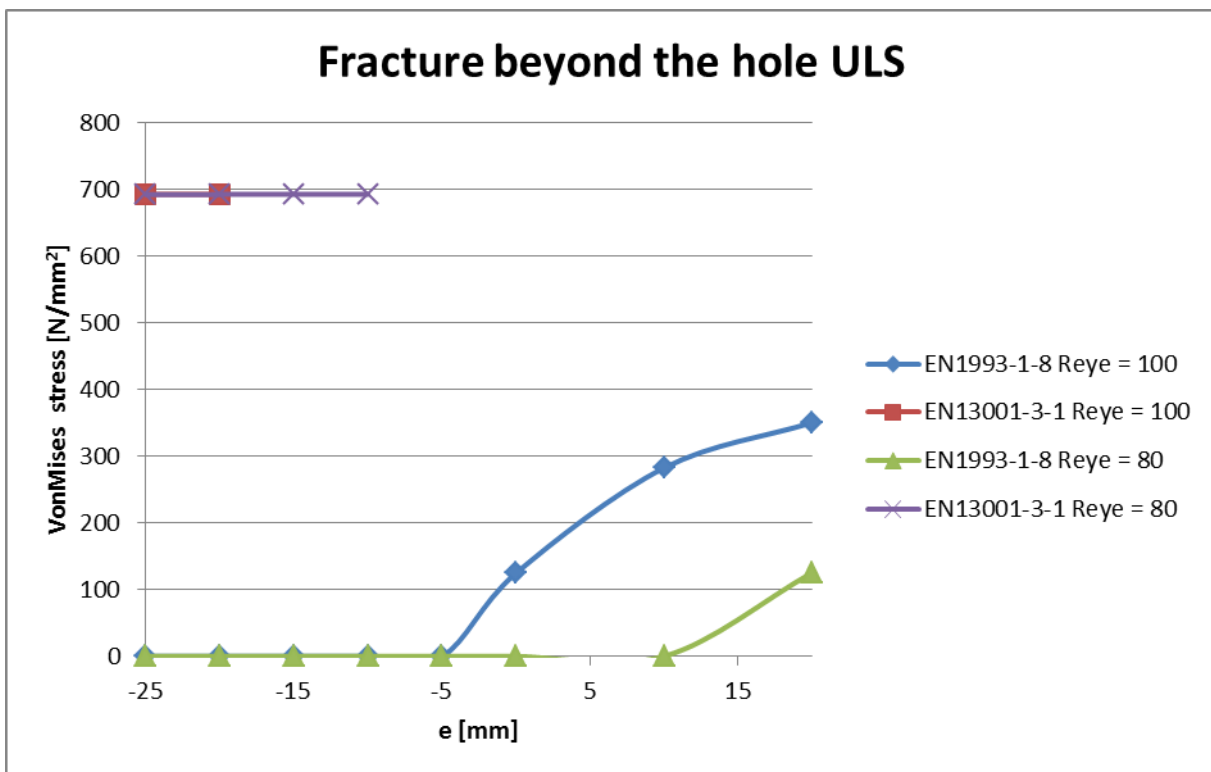


Chart E-8: VonMises stresses on top of the eye for ULS capacities as input for various eccentricities

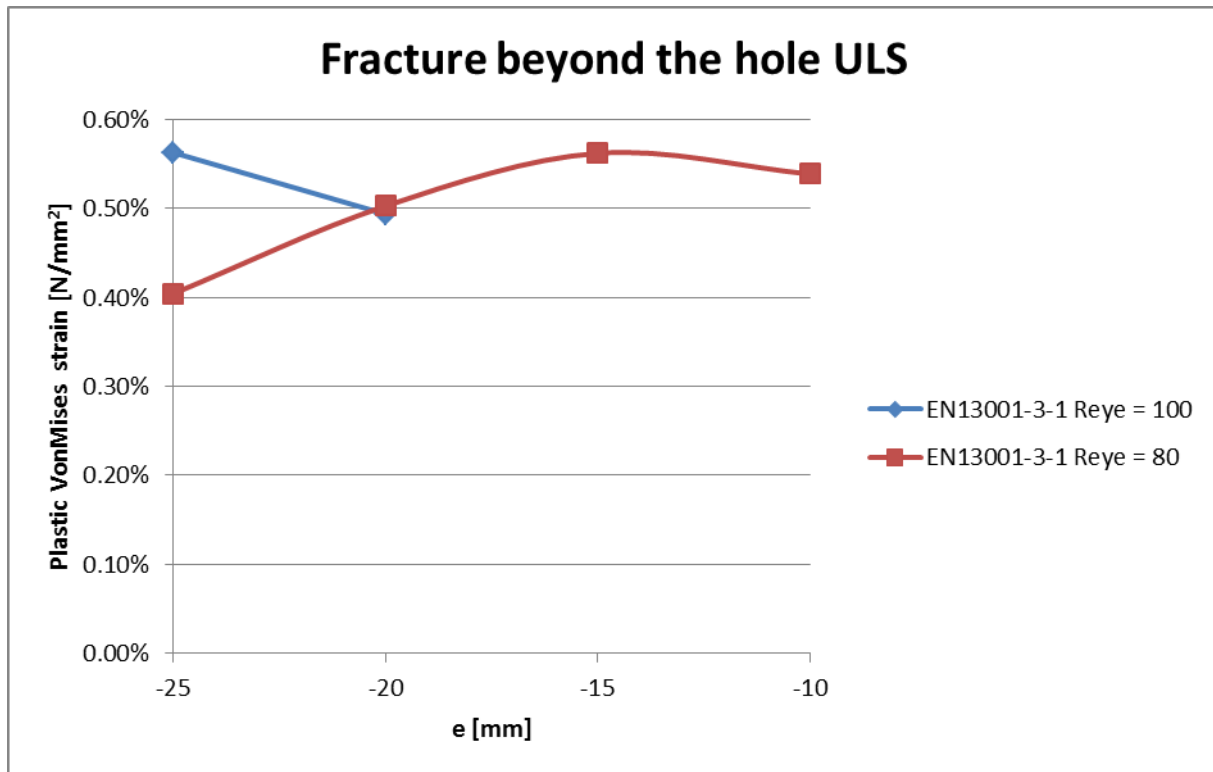


Chart E-9: Plastic strains on top of the eye for ULS capacities as input for various eccentricities

The influence of the clearance has most influence on the bearing stress/strain. For the chosen geometries in Figure 5-5 bearing is the governing criteria for all compared standards. In Chart E-10 and Chart E-11 the plastic bearing strains are plotted for different clearances. From these charts can be concluded that the plastic strains are increasing for an increasingly clearance. Even for SLS capacities there appear already quite large plastic strains (above 5%), although these strains are only present on a very small part of the connection (see Figure 5-6).

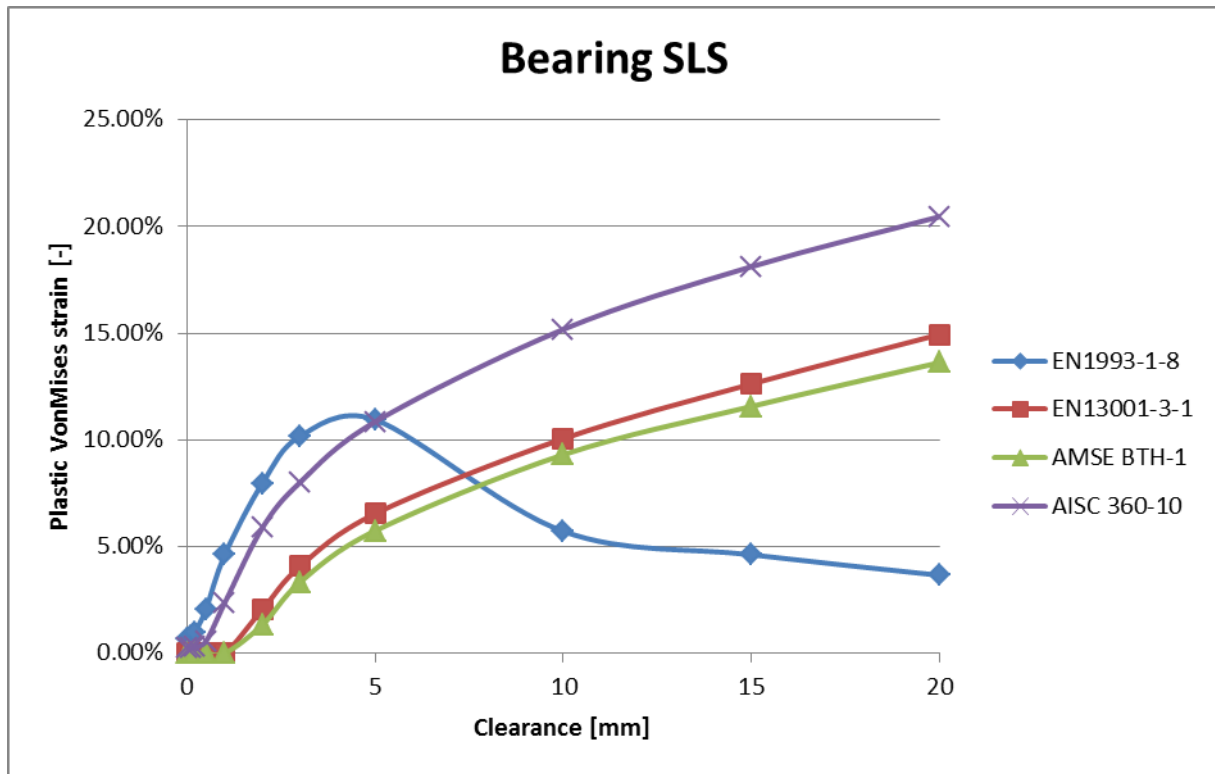


Chart E-10: Plastic bearing strains for SLS capacities as input for various clearances

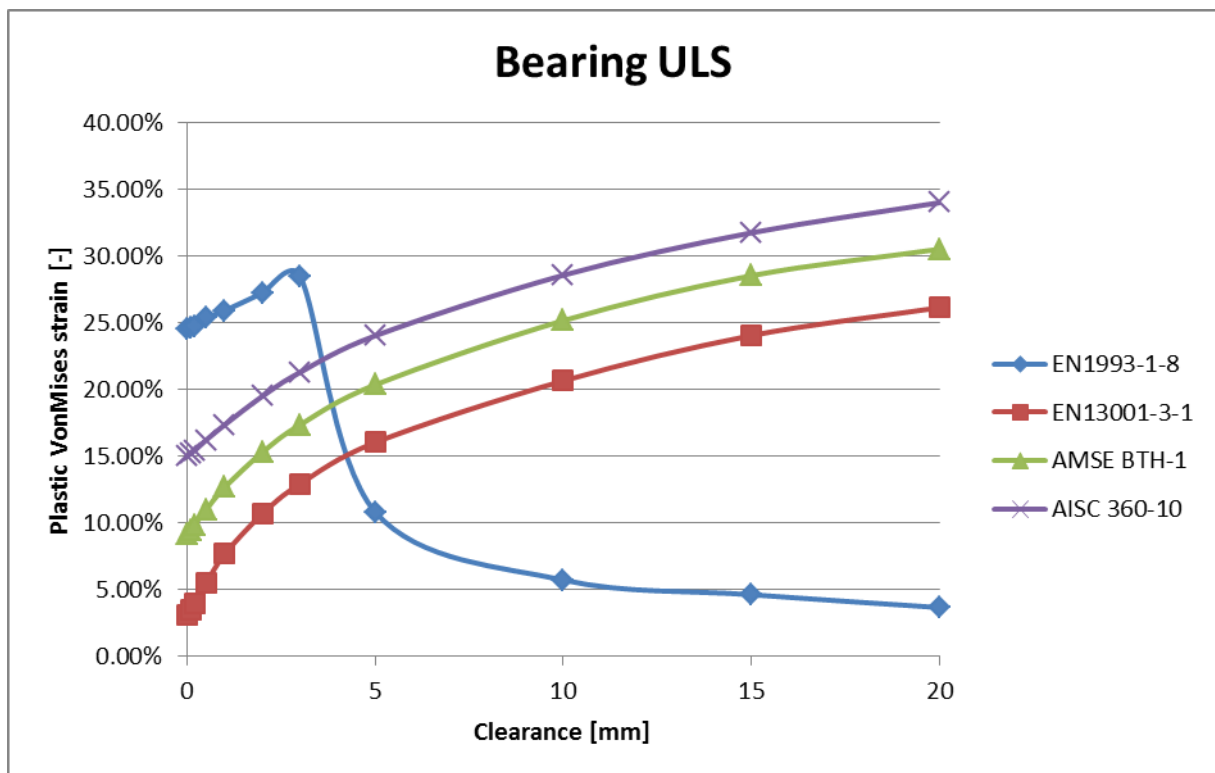


Chart E-11: Plastic bearing strains for ULS capacities as input for various clearances

## E.2 Analysis of the loads based on results

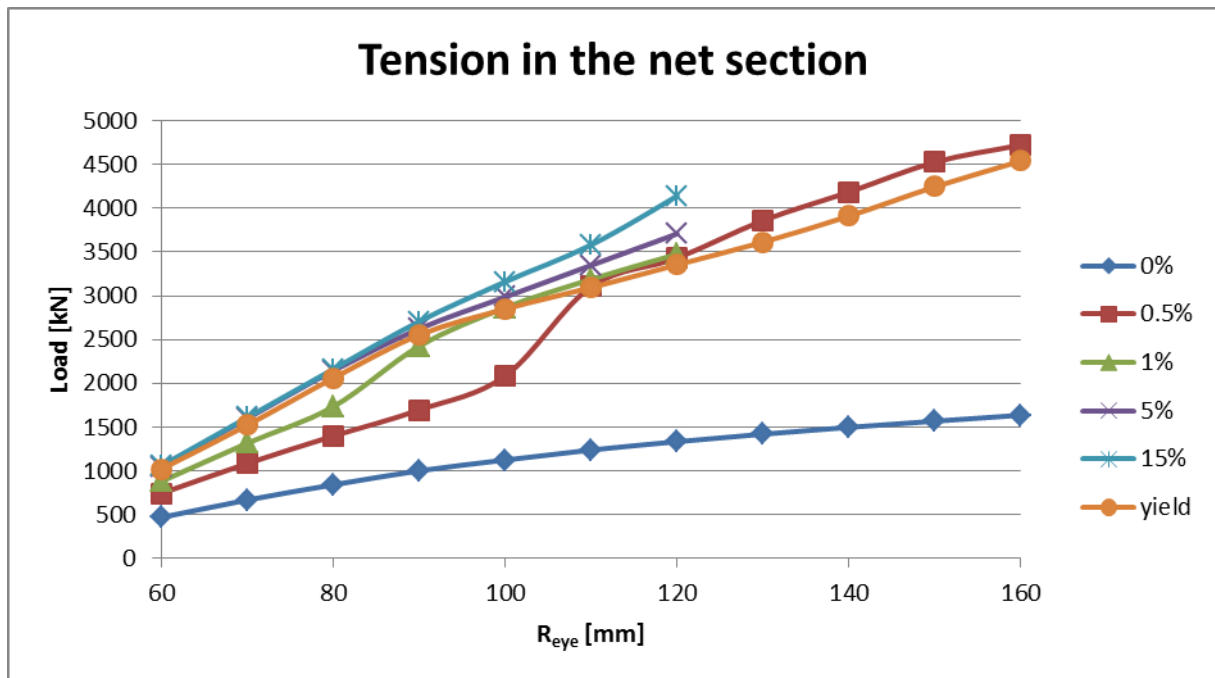


Chart E-12: Influence of  $R_{eye}$  with an eccentricity for tension in the net section

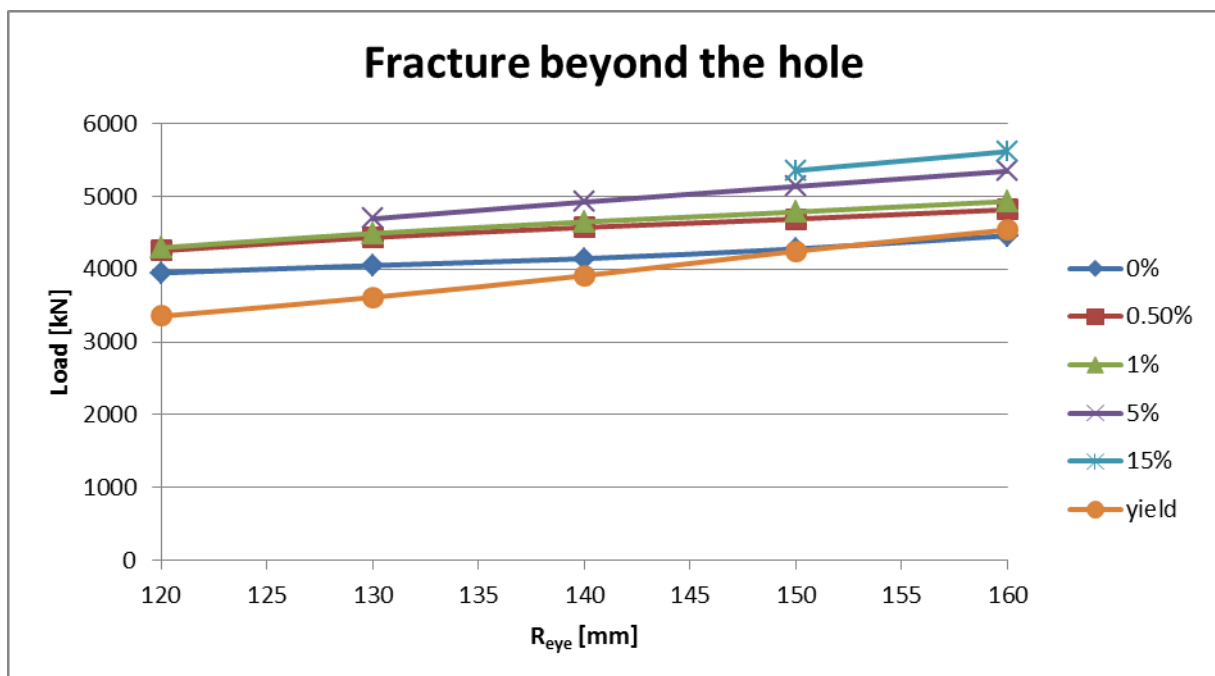


Chart E-13 : Influence of  $R_{eye}$  with an eccentricity for fracture beyond the hole

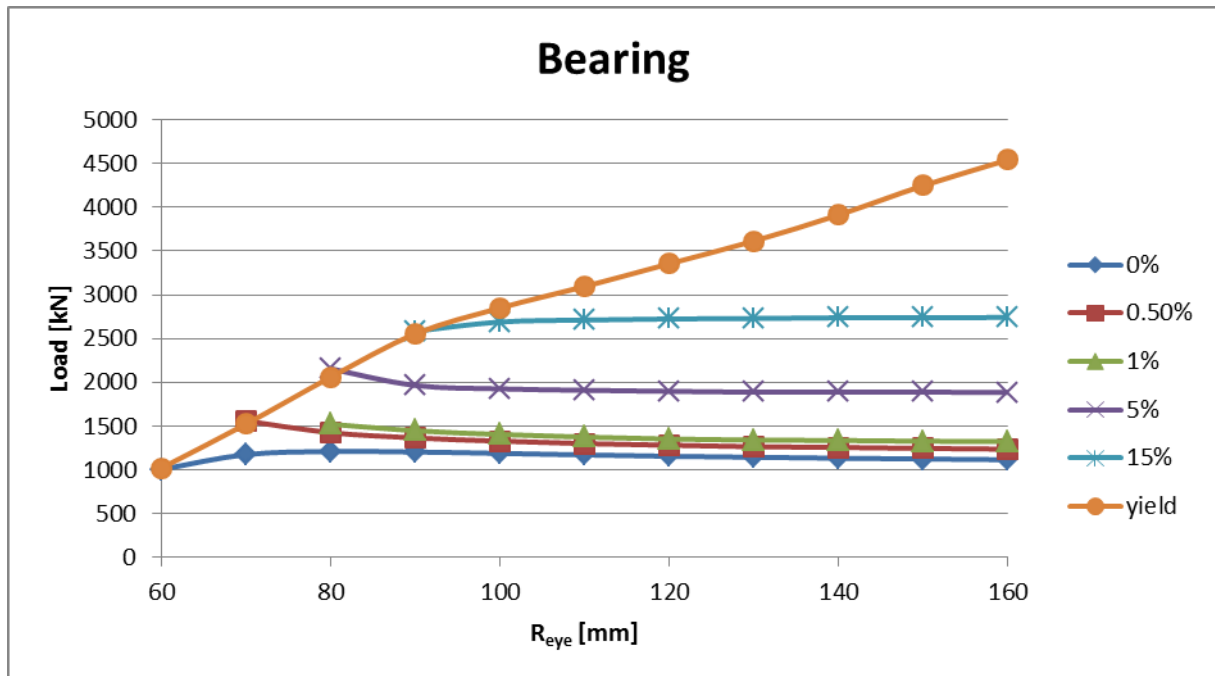


Chart E-14: Influence of  $R_{eye}$  with an eccentricity for bearing

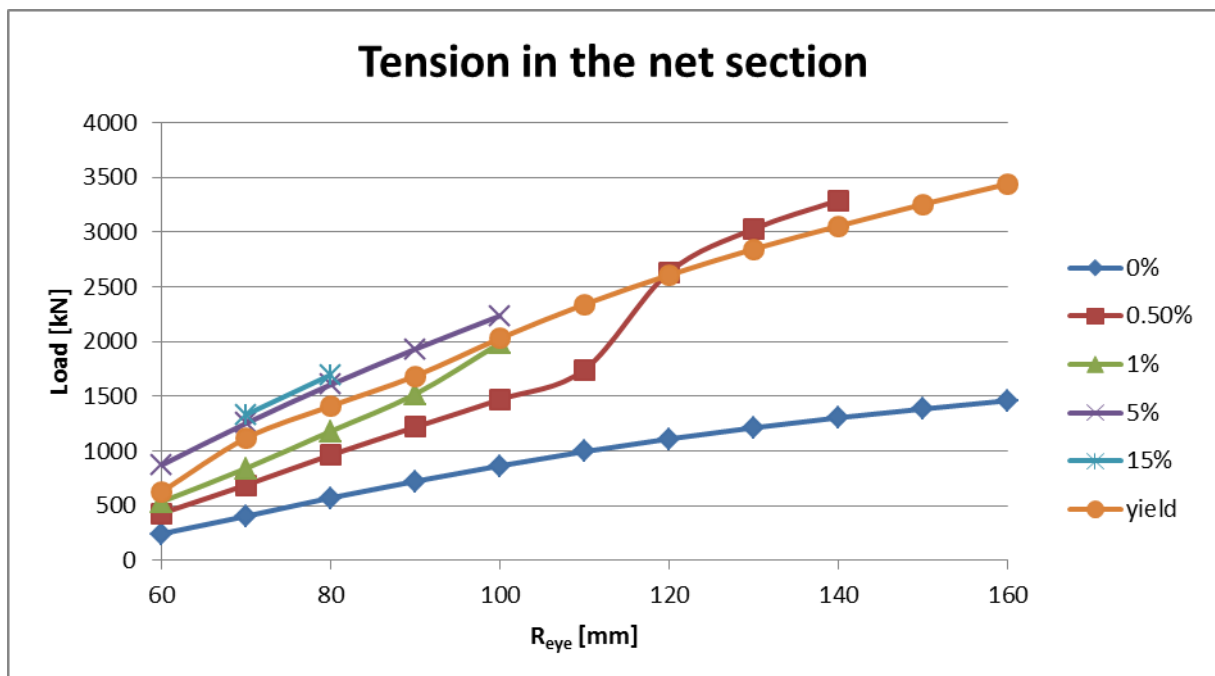


Chart E-15: Influence of  $R_{eye}$  without an eccentricity for tension in the net section

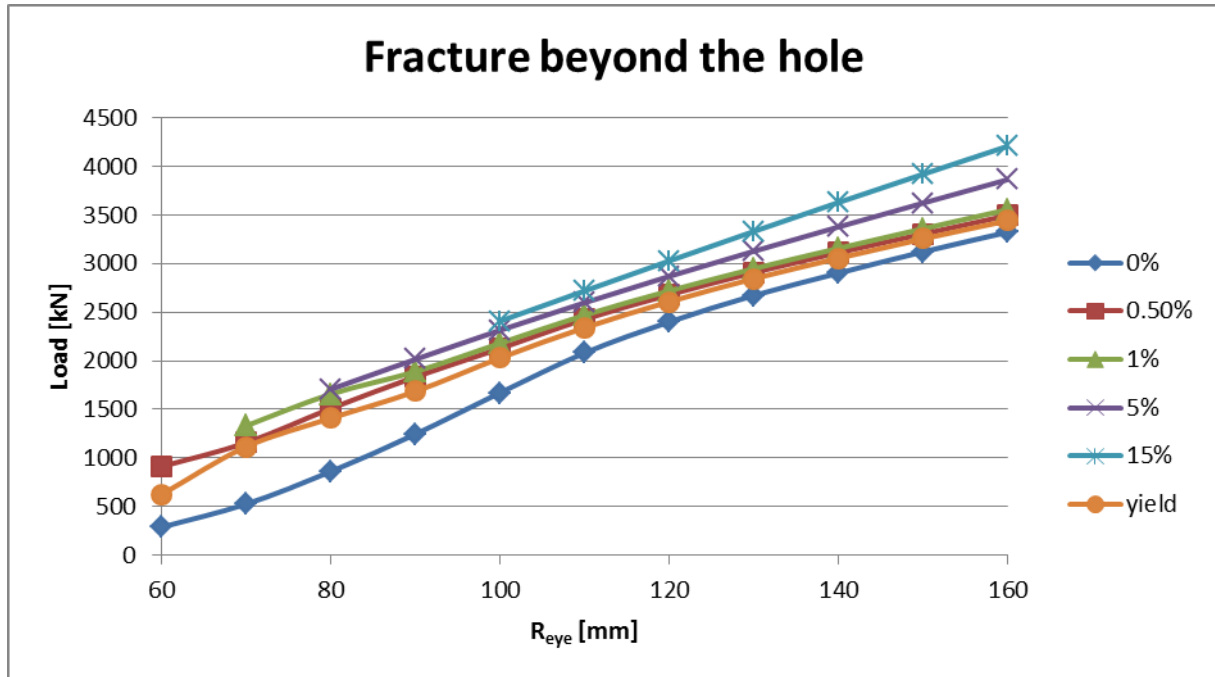


Chart E-16: Influence of  $R_{eye}$  without an eccentricity for fracture beyond the hole

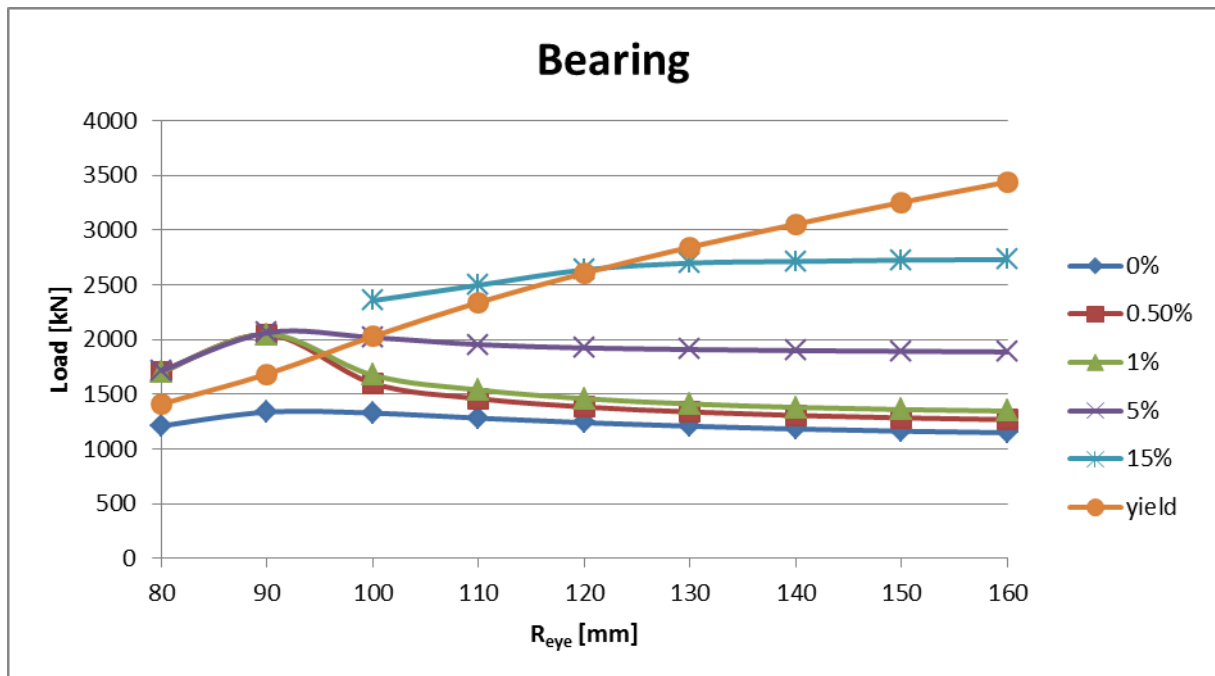


Chart E-17: Influence of  $R_{eye}$  for bearing

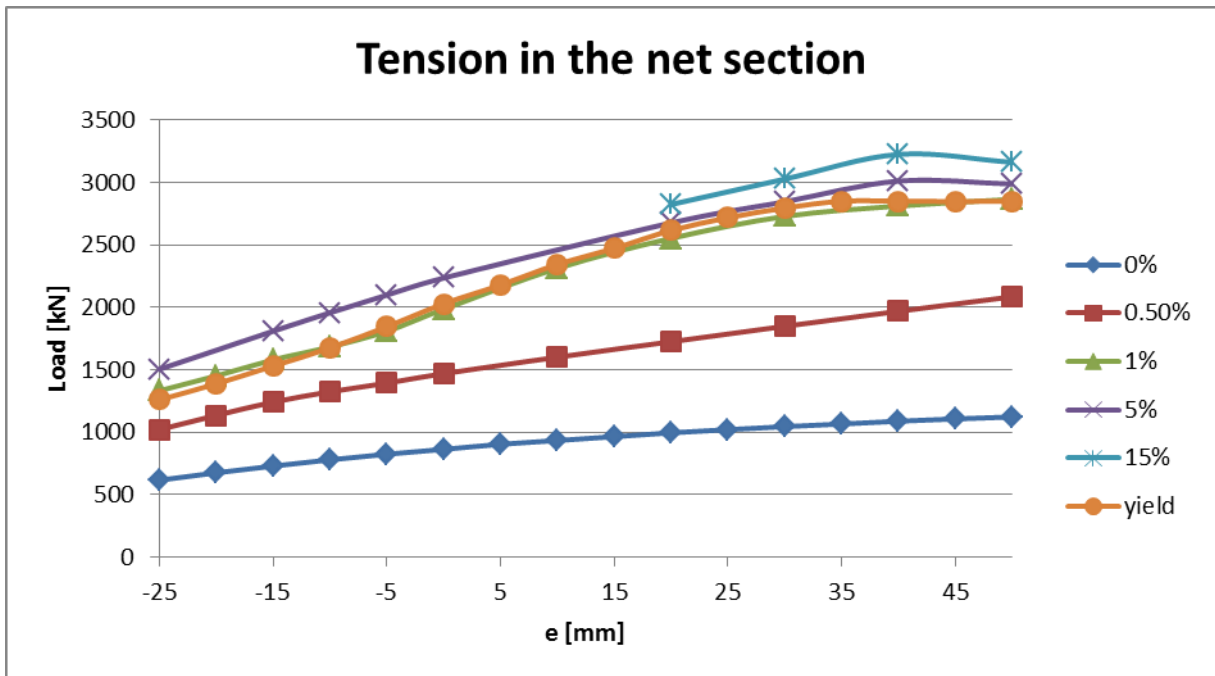


Chart E-18: Influence of the eccentricity with an eye radius of 100mm for tension in the net section

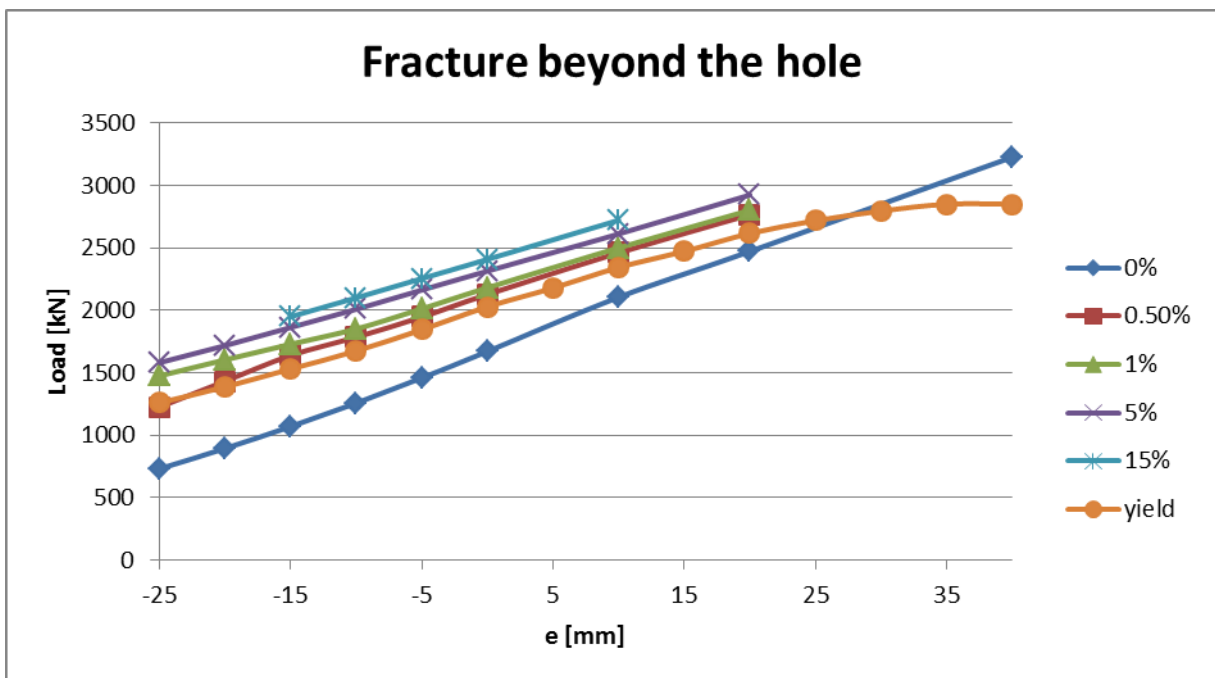


Chart E-19: Influence of the eccentricity with an eye radius of 100mm for fracture beyond the hole

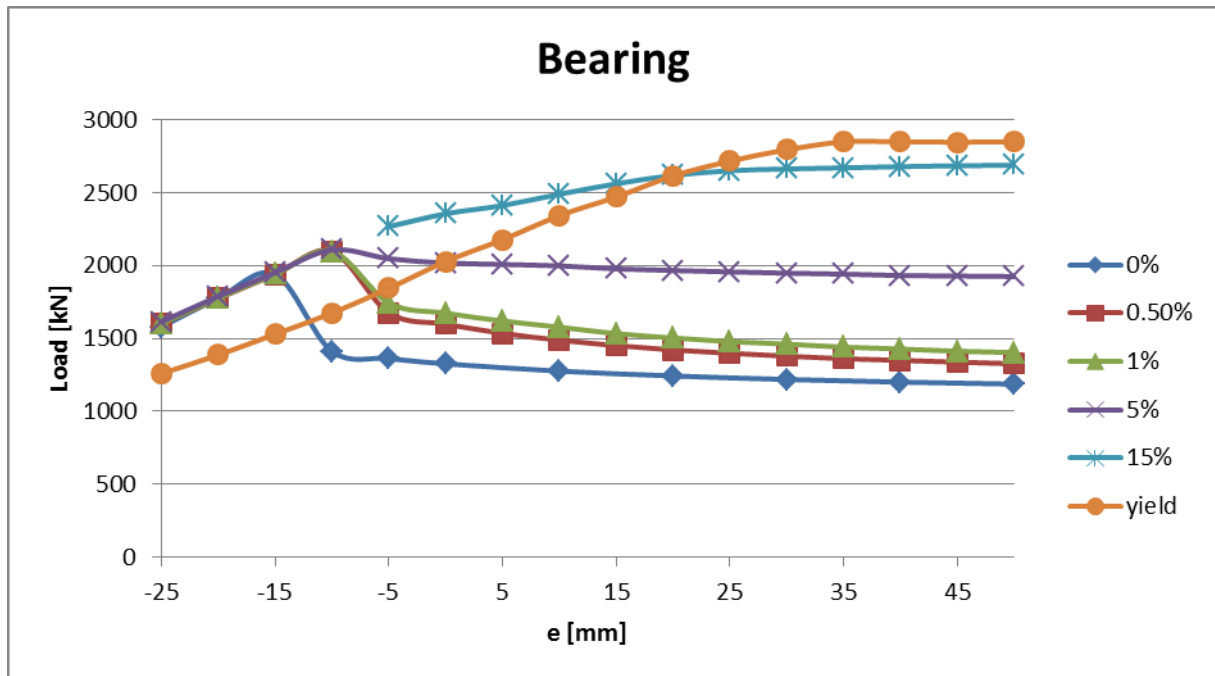


Chart E-20: Influence of the eccentricity with an eye radius of 100mm for bearing

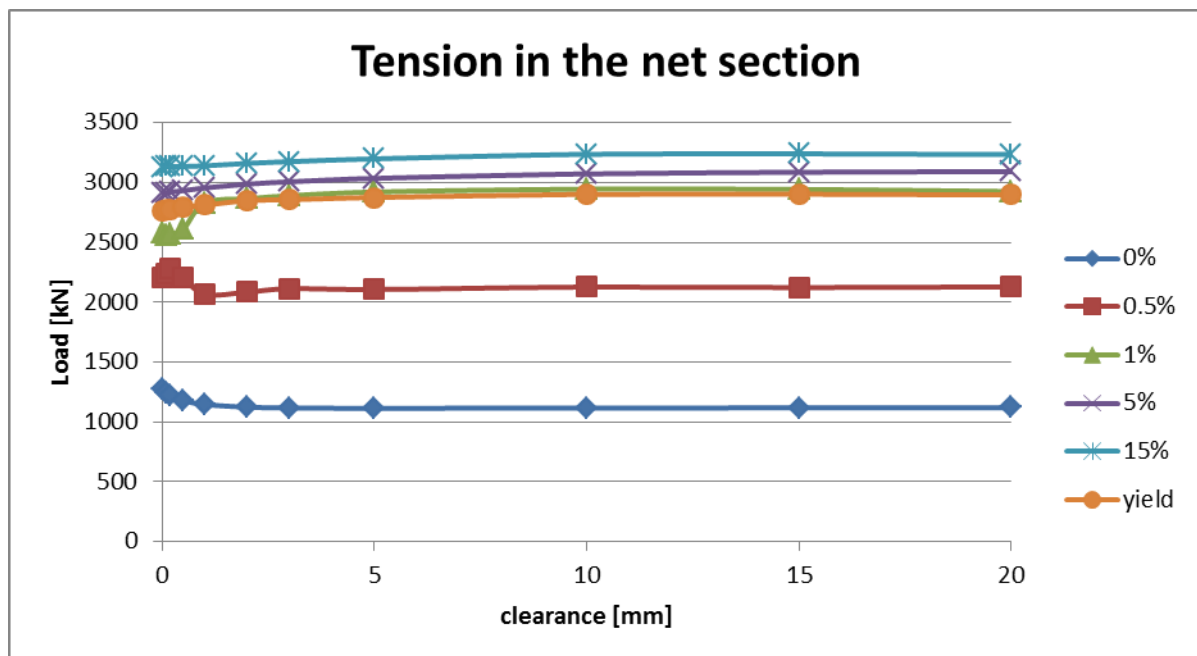


Chart E-21: Influence of the clearance for tension in the net section with an eccentricity of 50mm and an eye radius of 100mm

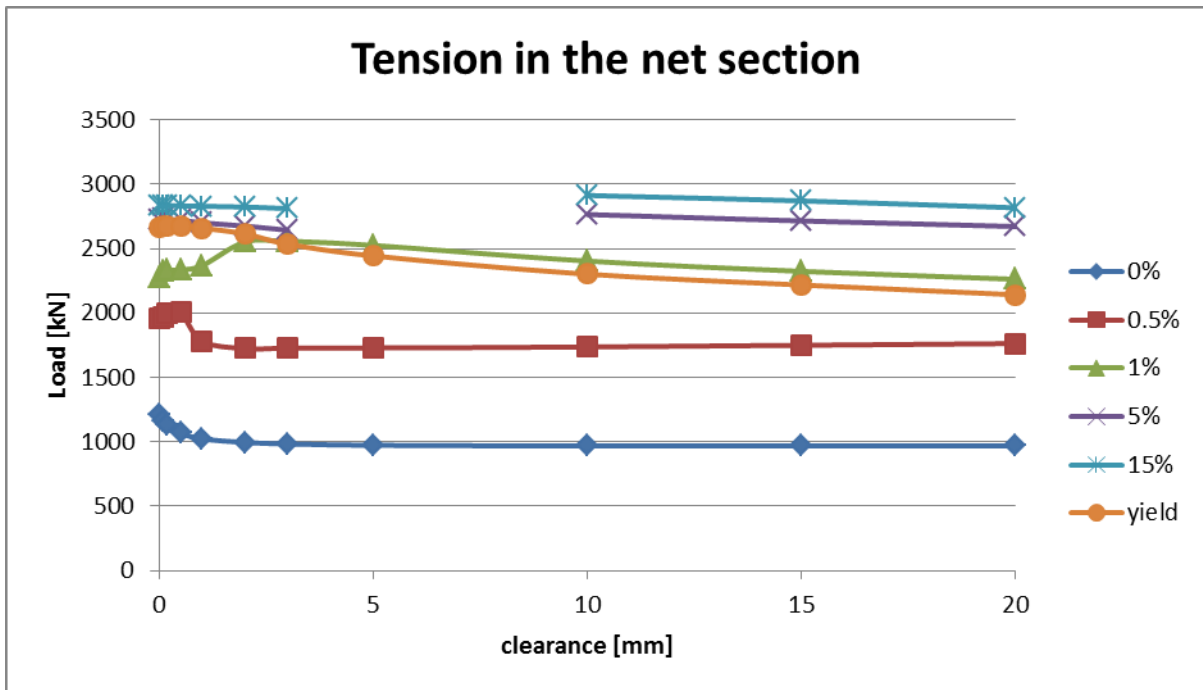


Chart E-22: Influence of the clearance for tension in the net section with an eccentricity of 20mm and an eye radius of 100mm

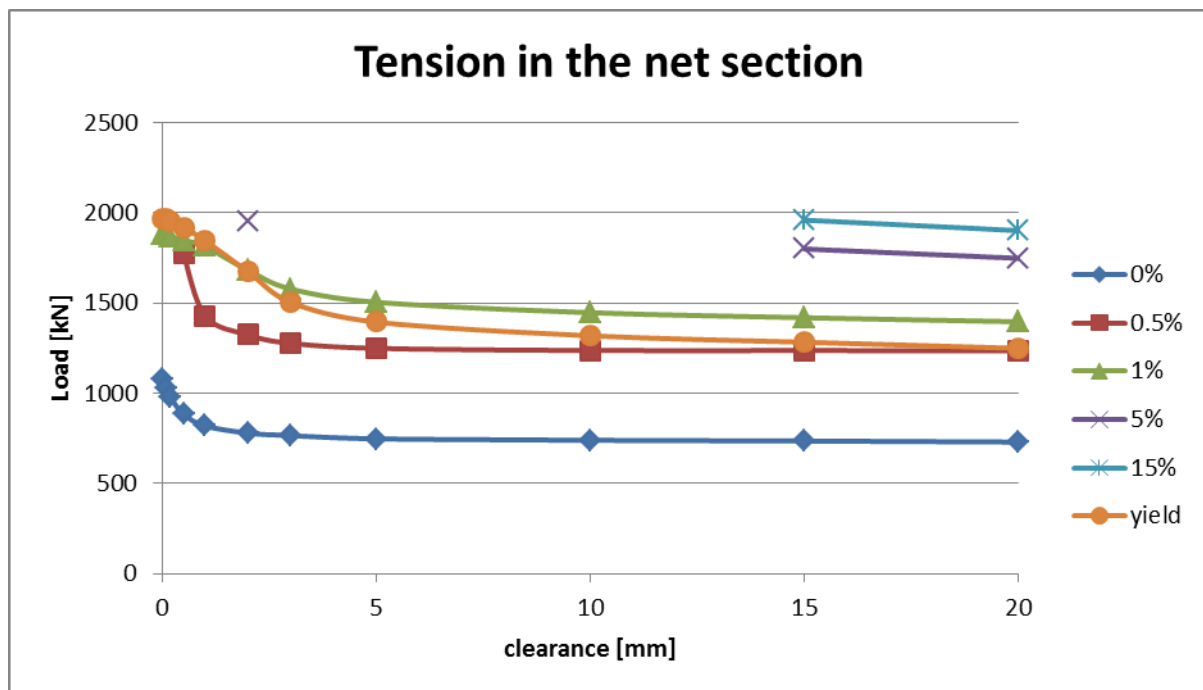


Chart E-23: Influence of the clearance for tension in the net section with an eccentricity of -10mm and an eye radius of 100mm

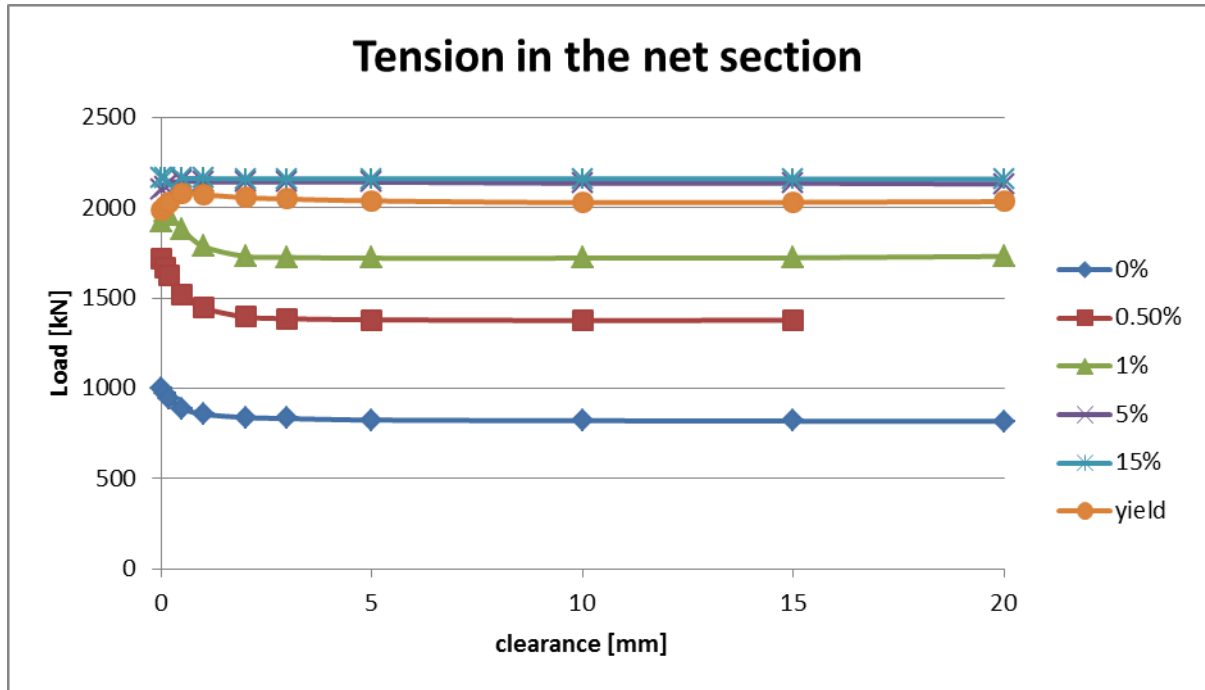


Chart E-24: Influence of the clearance for tension in the net section with an eccentricity of 50mm and an eye radius of 80mm

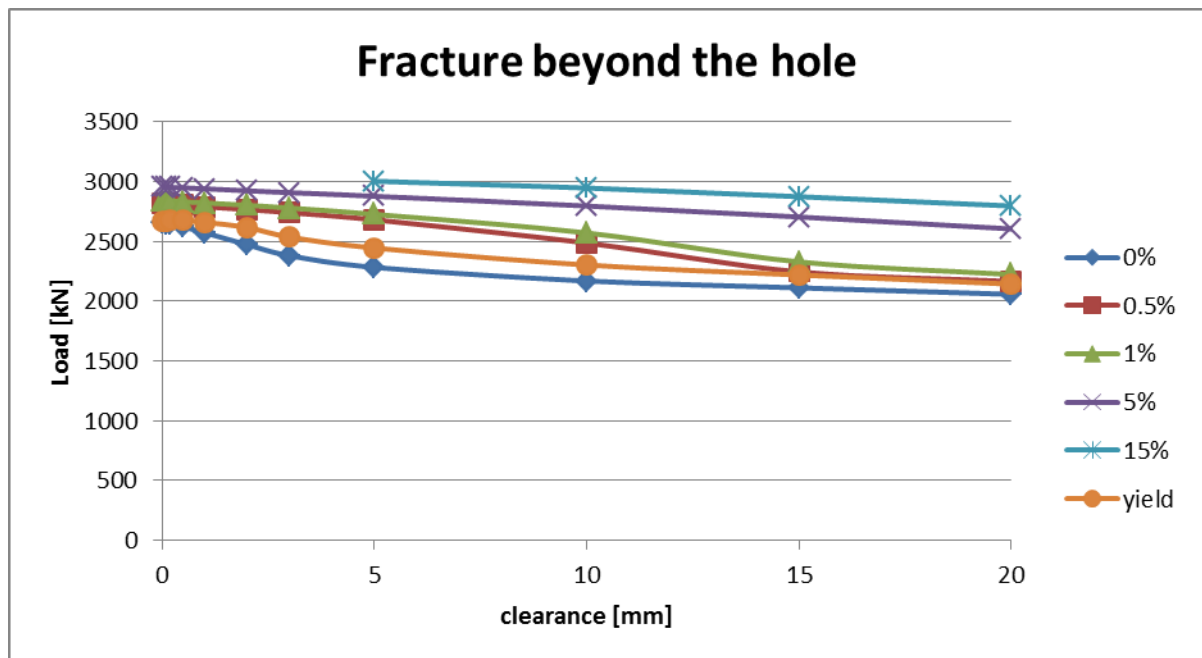


Chart E-25: Influence of the clearance for fracture beyond the hole with an eccentricity of 20mm and an eye radius of 100mm

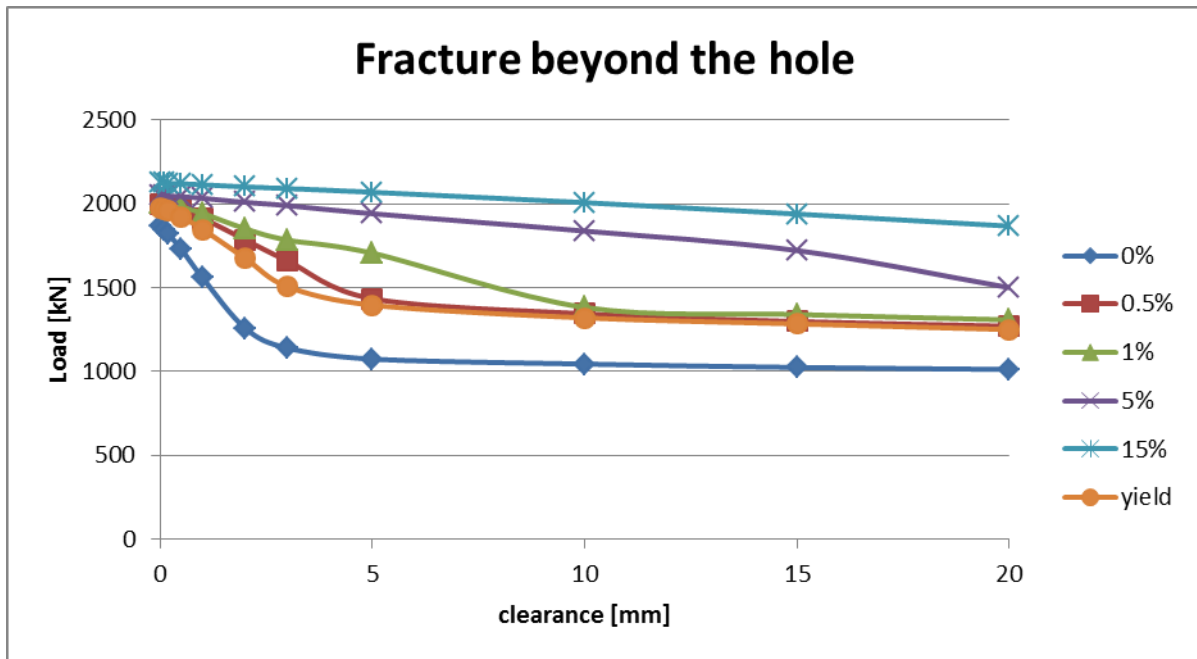


Chart E-26: Influence of the clearance for fracture beyond the hole with an eccentricity of -10mm and an eye radius of 100mm

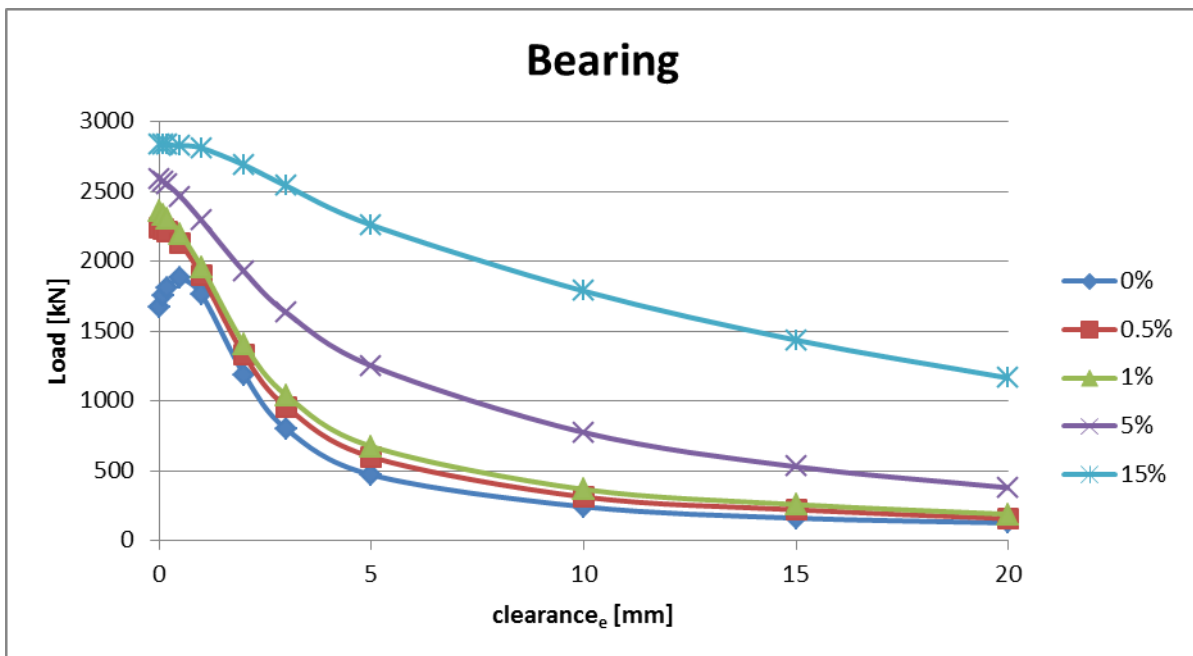


Chart E-27: Influence of the clearance for bearing with an eccentricity of 50mm and an eye radius of 100mm

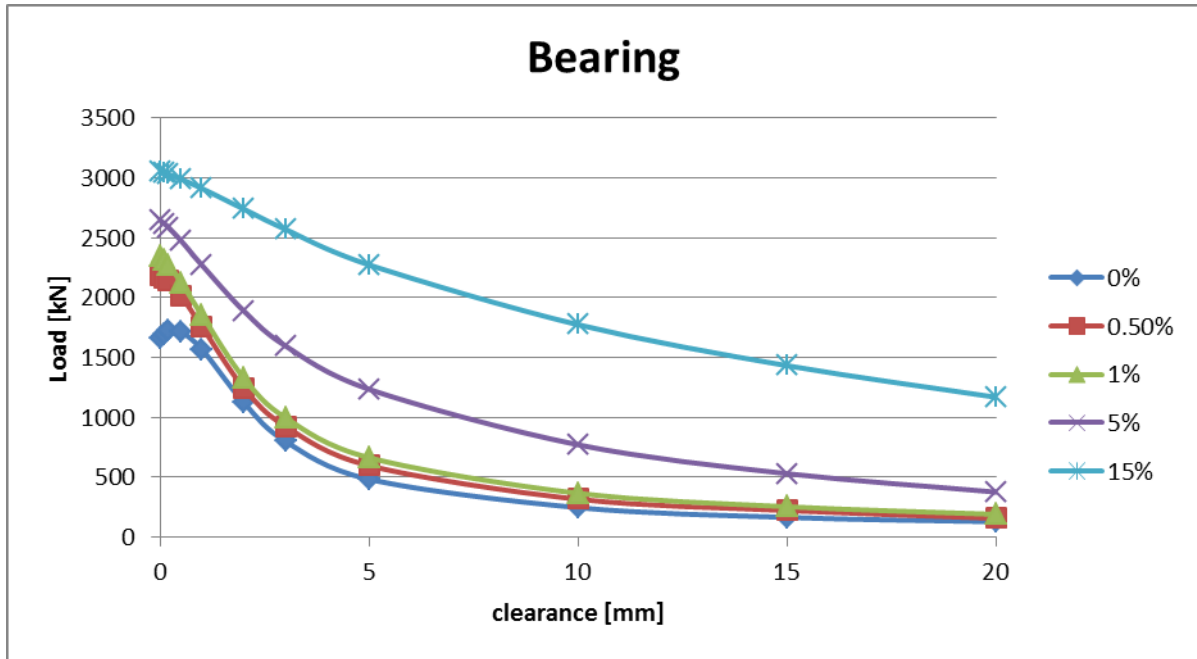


Chart E-28: Influence of the clearance for bearing with an eccentricity of 50mm and an eye radius of 150mm

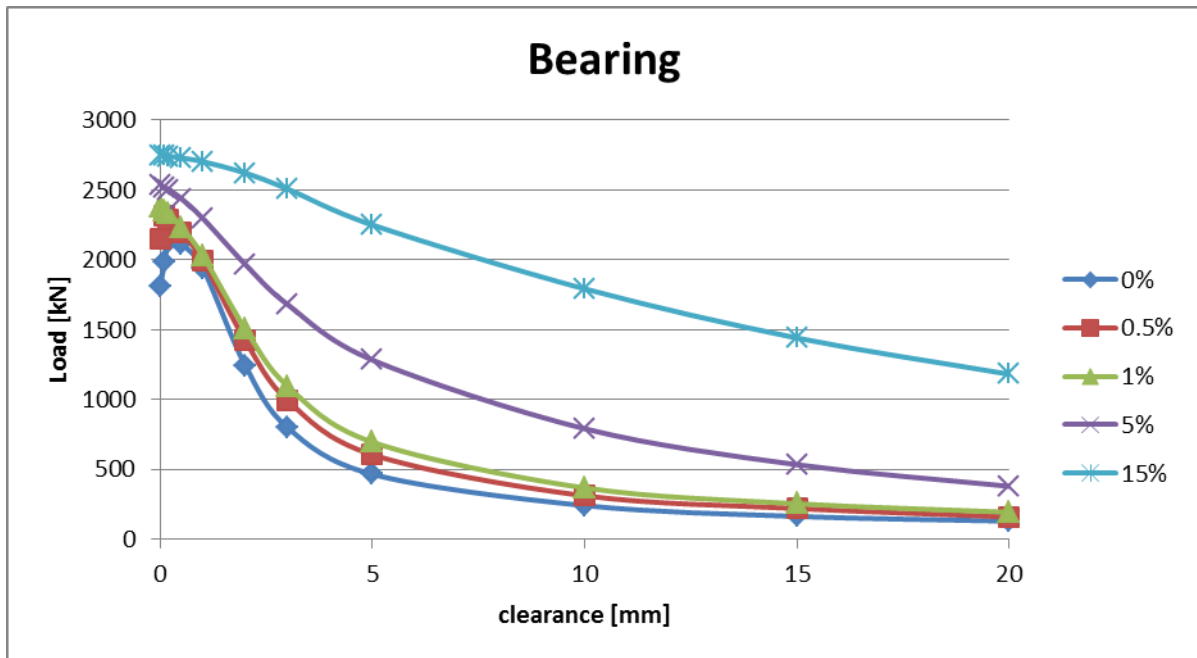


Chart E-29: Influence of the clearance for bearing with an eccentricity of 20mm and an eye radius of 100mm

### E.3 Analysis of cheek plates

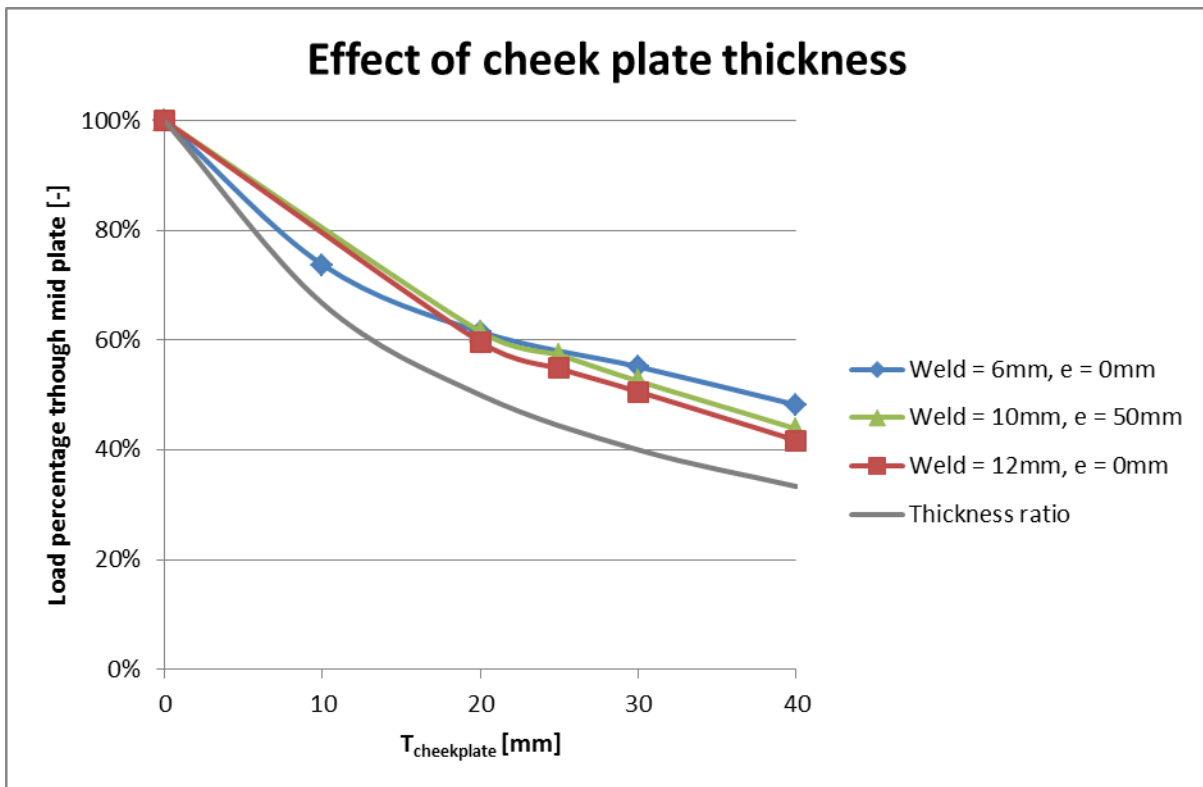


Chart E-30: Load percentage through mid plate, (Reye = 100mm, T = 40mm, dh = 82mm, dp = 80mm)

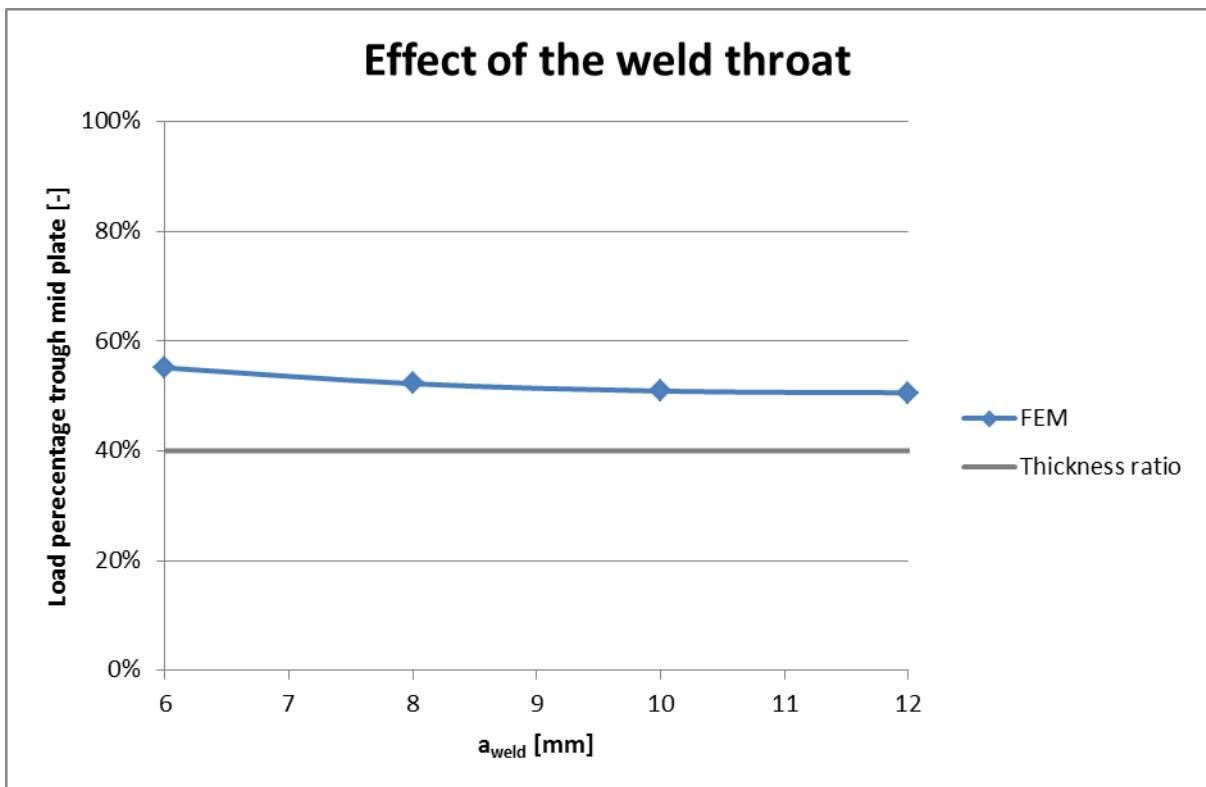


Chart E-31: Load percentage through mid plate, (Reye = 100mm, e = 0mm, T = 40mm, Rcheek = 80mm, Tcheek = 30mm, dh = 82mm, dp = 80)

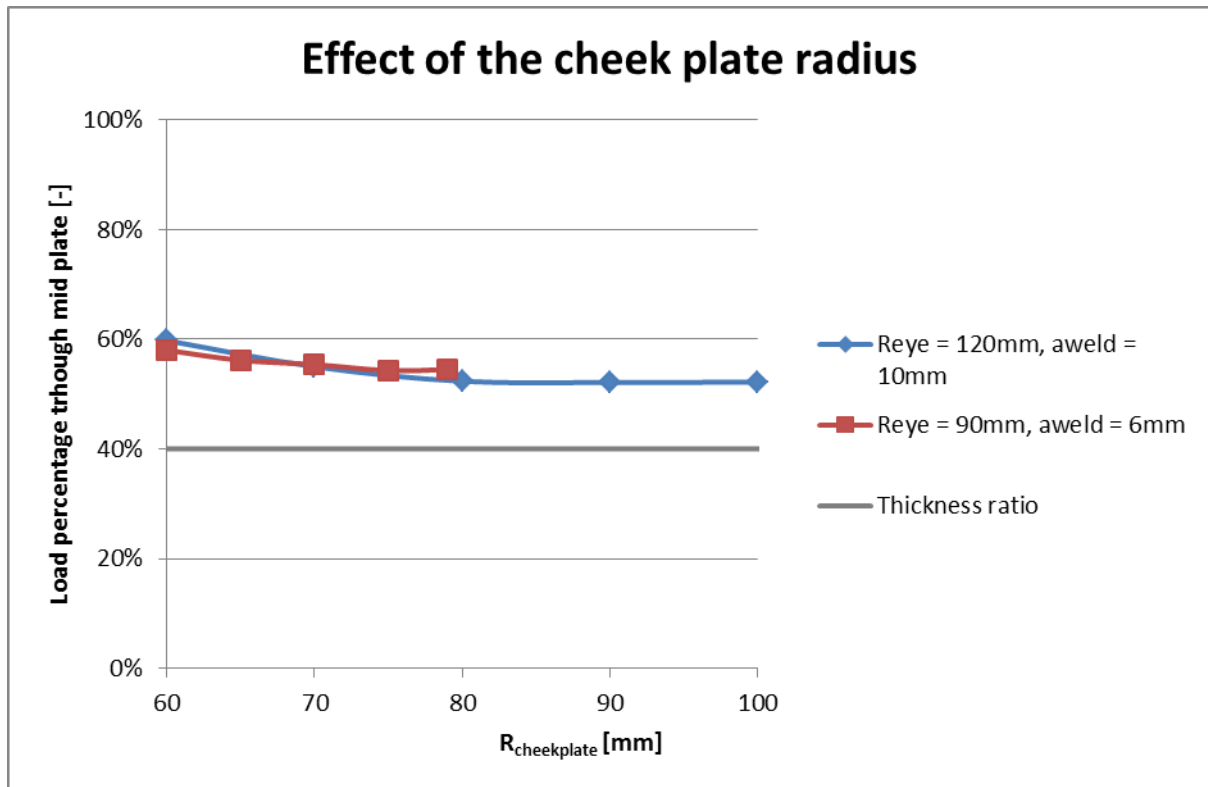


Chart E-32: Load percentage through mid plate, ( $e = 0\text{mm}$ ,  $T = 40\text{mm}$ ,  $T_{\text{cheek}} = 30\text{mm}$ ,  $dh = 82\text{mm}$ ,  $dp = 80\text{mm}$ )

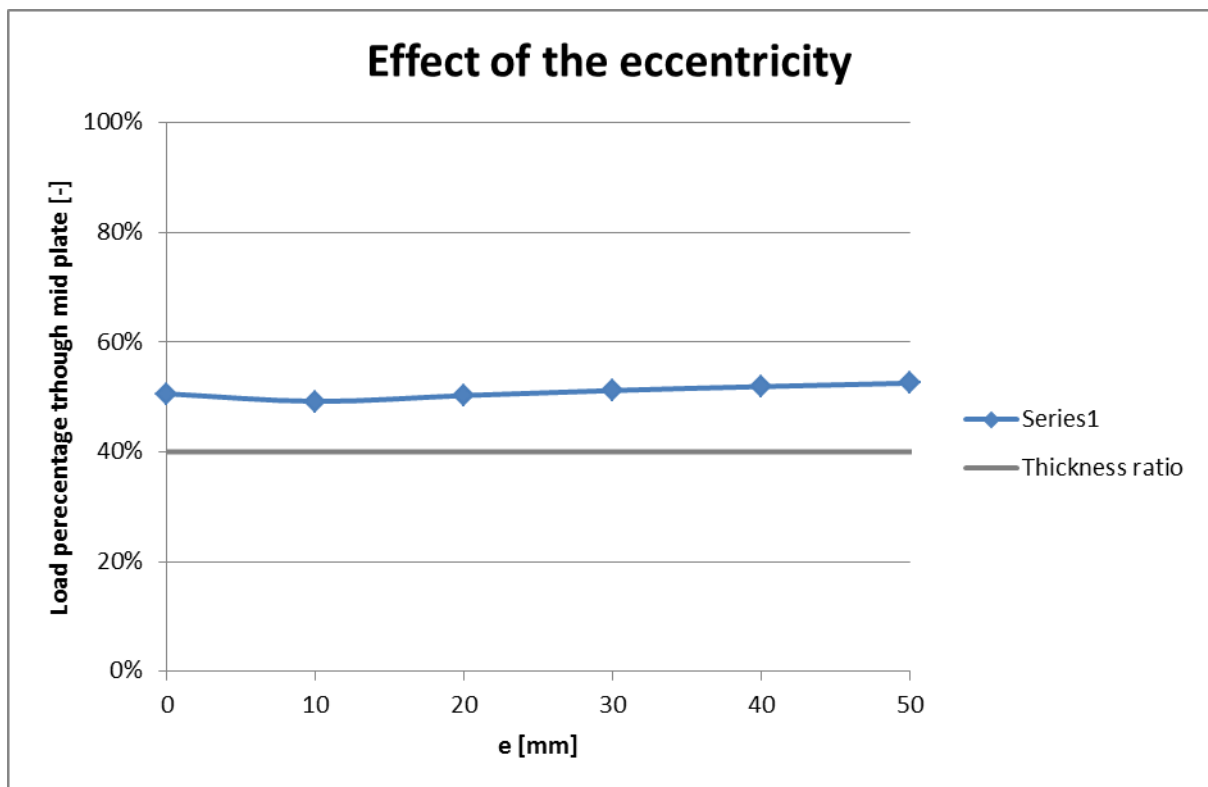


Chart E-33: Load percentage through mid plate, (Reye = 100mm,  $T = 40\text{mm}$ ,  $R_{\text{cheek}} = 80\text{mm}$ ,  $T_{\text{cheek}} = 30\text{mm}$ , aweld = 10mm,  $dh = 82\text{mm}$ ,  $dp = 80\text{mm}$ )

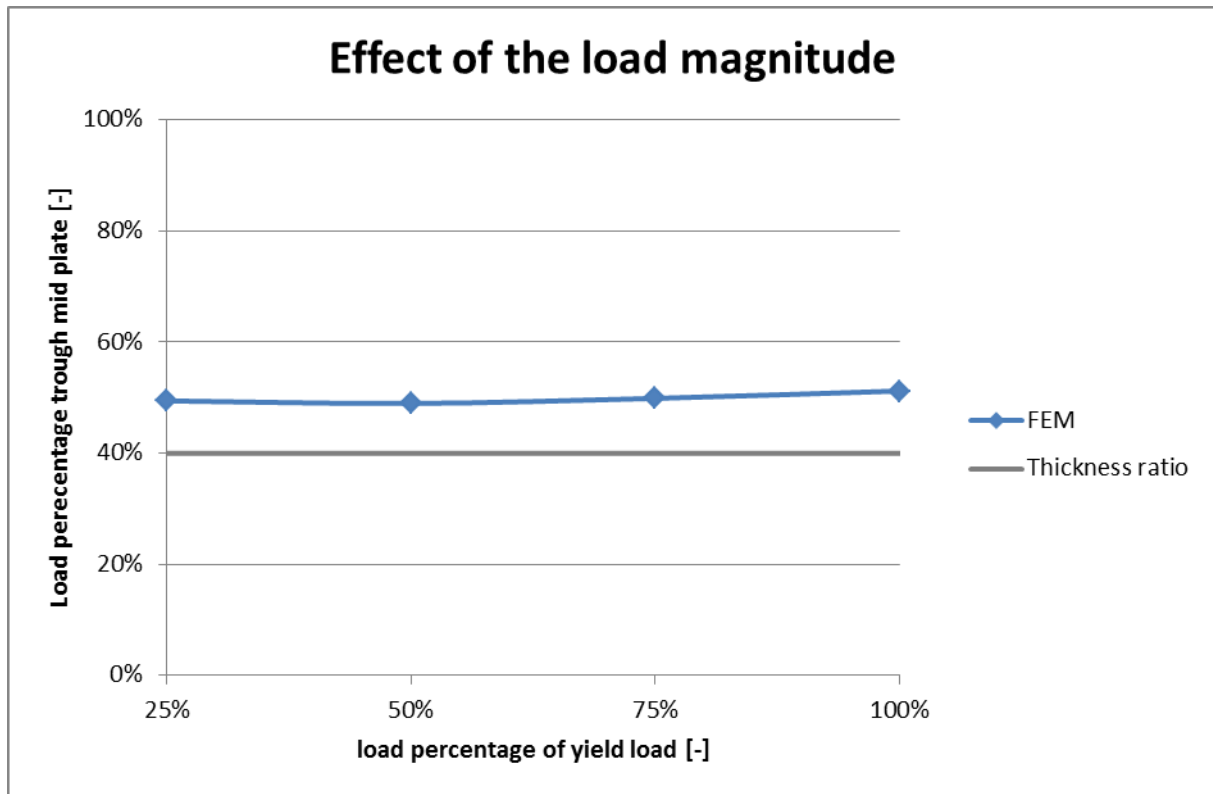


Chart E-34: Load percentage through mid plate, (Reye = 100mm, e = 30, T = 40mm, Rcheek = 80mm, Tcheek = 30mm, aweld = 10mm, dh = 82mm, dp = 80mm)

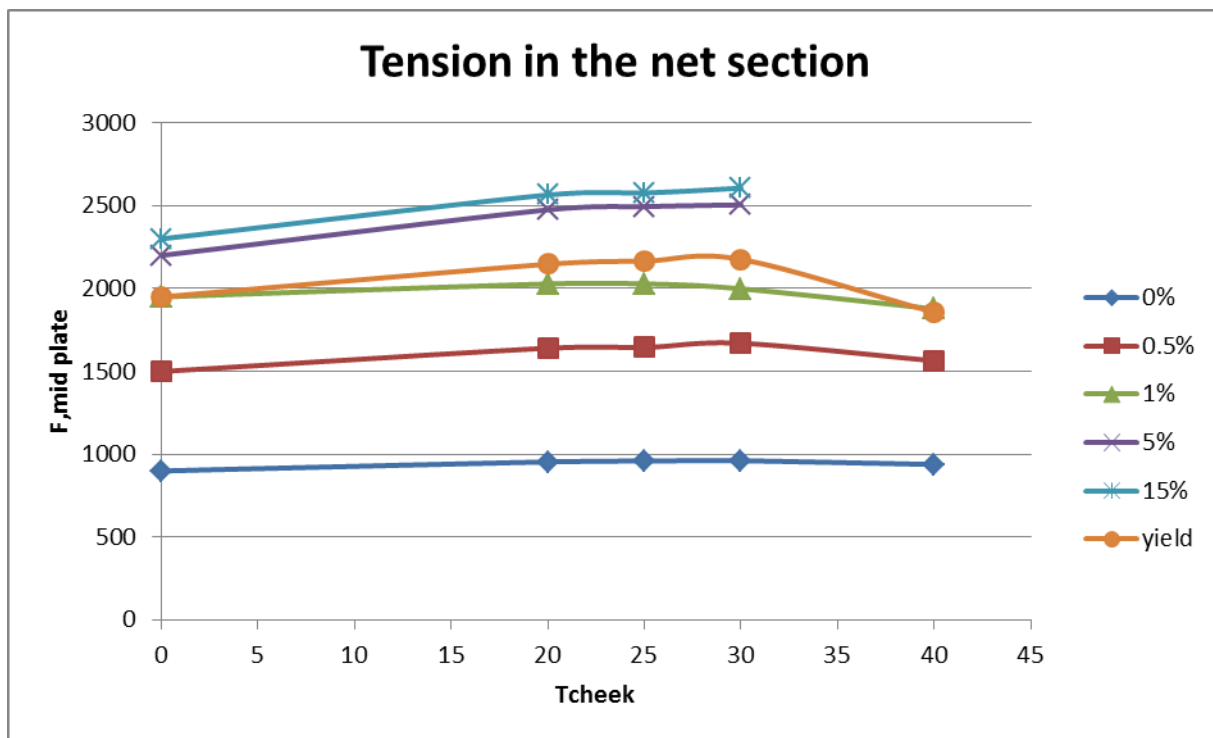


Chart E-35: Influence of the cheek plate thickness for tension in the net section in the mid plate (Reye = 100mm, e = 0, T = 40mm, Rcheek = 80mm, Tcheek = 30mm, aweld = 12mm, dh = 82mm, dp = 80mm)

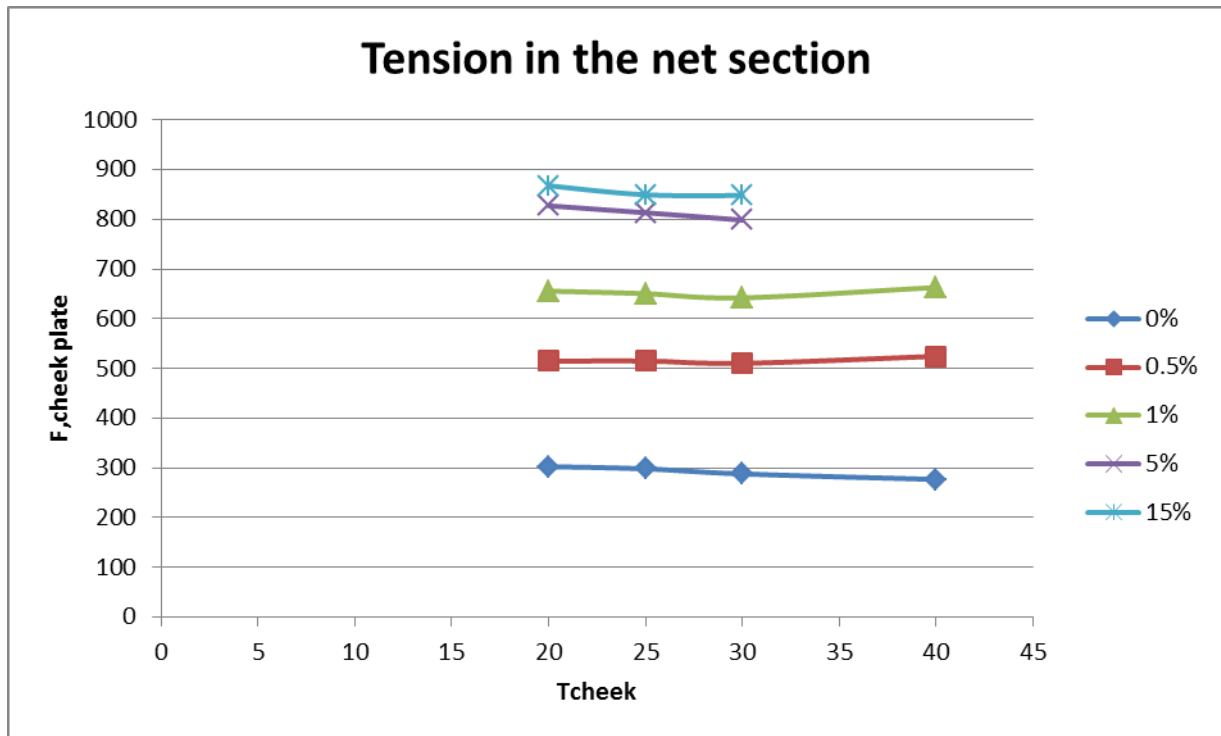


Chart E-36: Influence of the cheek plate thickness for tension in the net section in the cheek plate (Reye = 100mm, e = 0, T = 40mm, Rcheek = 80mm, Tcheek = 30mm, aweld = 12mm, dh = 82mm, dp = 80mm)

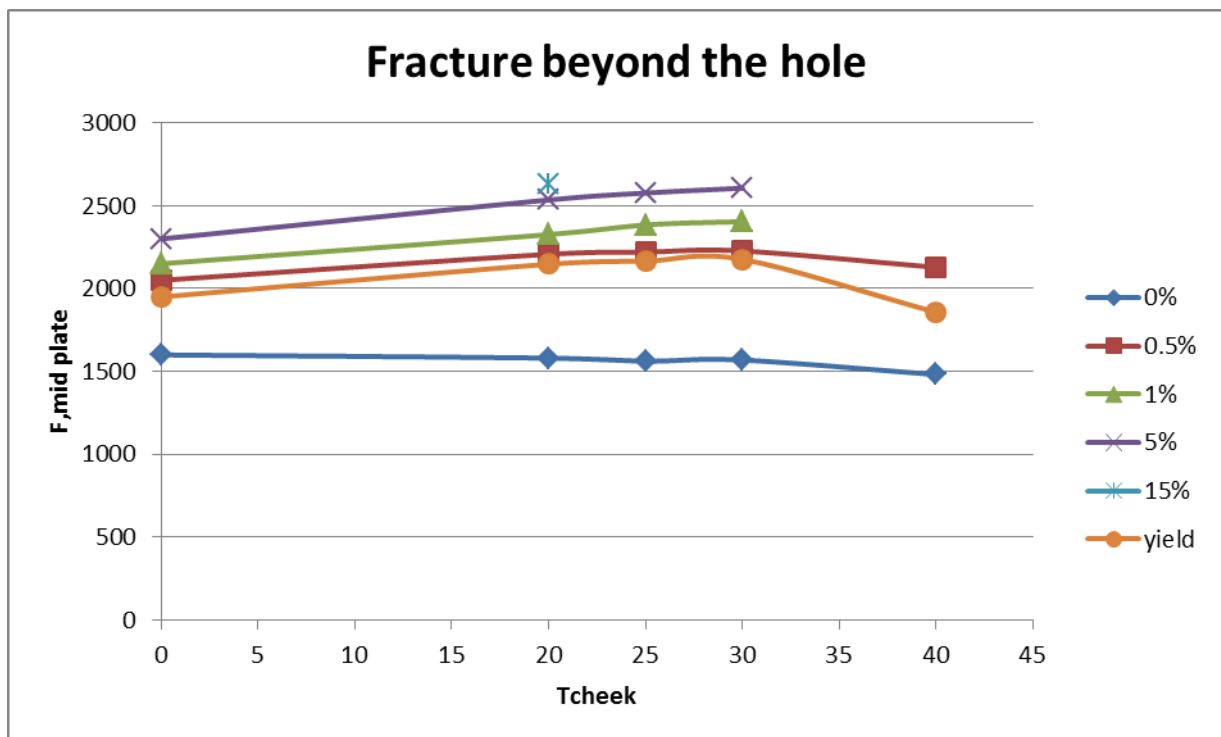


Chart E-37: Influence of the cheek plate thickness for fracture beyond the hole in the mid plate (Reye = 100mm, e = 0, T = 40mm, Rcheek = 80mm, Tcheek = 30mm, aweld = 12mm, dh = 82mm, dp = 80mm)

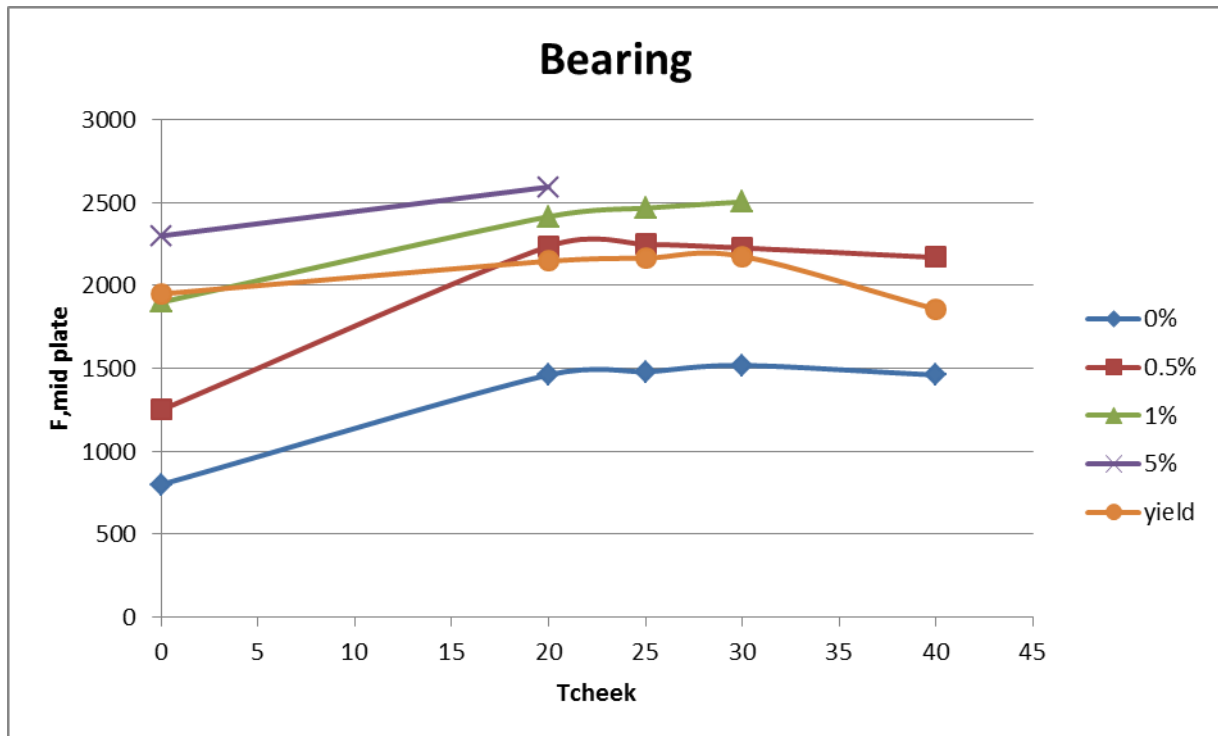


Chart E-38: Influence of the cheek plate thickness for bearing in the mid plate (Reye = 100mm, e = 0, T = 40mm, Rcheek = 80mm, Tcheek = 30mm, aweld = 12mm, dh = 82mm, dp = 80mm)

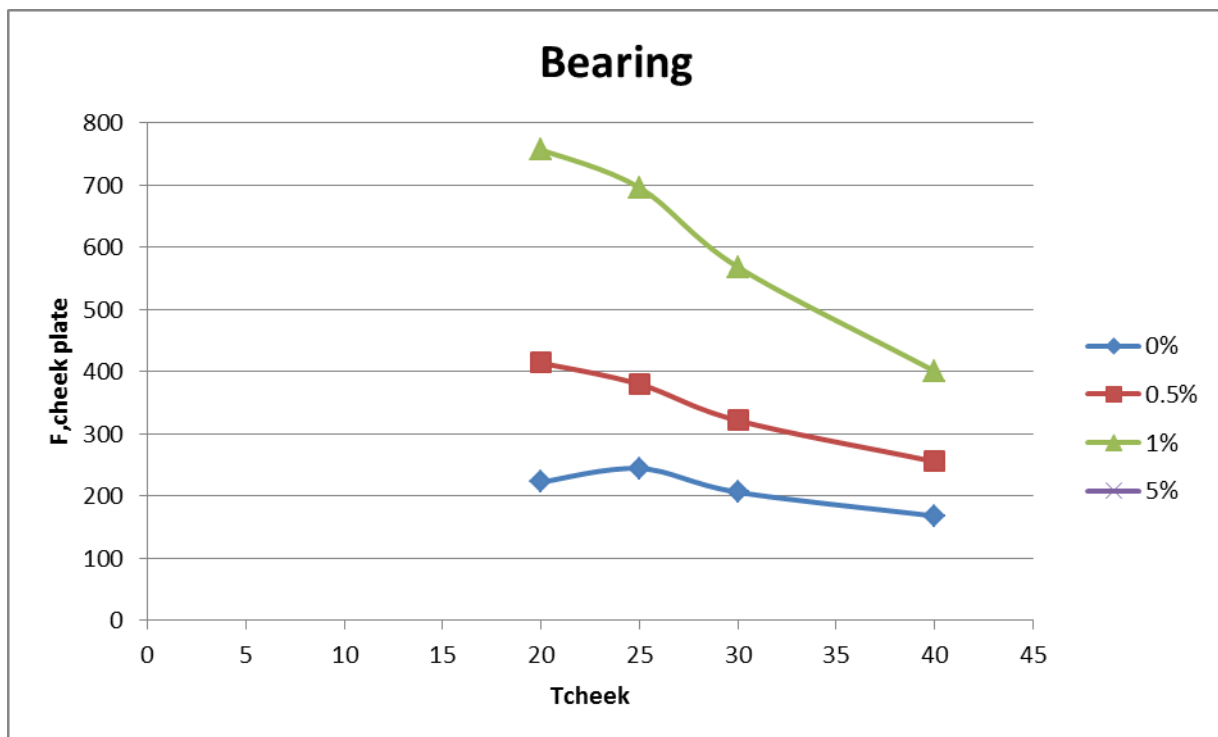


Chart E-39: Influence of the cheek plate thickness for bearing in the cheek plate (Reye = 100mm, e = 0, T = 40mm, Rcheek = 80mm, Tcheek = 30mm, aweld = 12mm, dh = 82mm, dp = 80mm)

# F FEM and Formula results

## F.1 Results

PINNED CONNECTIONS

Reye	0%				0.50%				1%				5%				15%				Section yield	
	1	2	3	4	1	2	3	4	1	2	3	4	1	2	3	4	1	2	3	4	Criteria	
60	467		1005		742				878				1050				1056				1019	1
70	666		1173		1084		1559		1316				1598				1610				1522	1
80	840		1209		1397		1425		1733		1521		2144		2156		2162				2058	1
90	1000		1203		1695		1364		2424		1447		2623		1964		2707		2583		2553	1
100	1123		1188		2084		1327		2865		1404		2987		1925		3160		2689		2849	1
110	1238		1170		3105		1299		3189		1373		3348		1909		3582		2712		3095	1
120	1333	3950	1155		3432	4255	1281		3476	4296	1351		3710		1897		4141		2724		3355	1
130	1419	4052	1144		3862	4437	1263			4492	1340			4694	1887				2730		3614	1
140	1497	4146	1132		4188	4575	1255			4650	1335			4924	1890				2738		3912	1
150	1567	4280	1123		4529	4691	1244			4787	1327			5138	1888		5357		2738		4248	1
160	1635	4462	1115		4725	4819	1236			4933	1322			5348	1885		5617		2742		4541	2/4

Table F-1: FEM results [kN] for various eye radii [mm], plastic strains [%] and failure criteria [#] (e = 50mm, t = 40mm, dh = 82mm, dp = 80mm)

Reye	0%				0.50%				1%				5%				15%				Section yield	
	1	2	3	4	1	2	3	4	1	2	3	4	1	2	3	4	1	2	3	4	Criteria	
60																						
70	666	2169			1084	3596								1919				2651			1522	1
80	849	2949			1368	3671								1926				2665			2058	1
90	1000	3357			1715	3796								1928				2677			2517	1
100	1128	3607			2084	3943								1925				2689			2849	1
110	1238	3793			3105	4099								1920				2700			3083	1
120	1335	3950			3506	4255								1913				2710			3355	1
130	1420	4093			3862	4407								1905				2719			3647	1
140	1497	4226			4180	4552								1897				2727			3947	1
150	1567	4349			4466	4690								1888				2735			4248	1
160	1630	4462			4725	4819								1880				2742			4541	2/4

Table F-2: Formula results [kN] for various eye radii [mm], plastic strains [%] and failure criteria [#] (e = 50mm, t = 40mm, dh = 82mm, dp = 80mm)

Reye	0%				0.50%				1%				5%				15%				Section yield	
	1	2	3	4	1	2	3	4	1	2	3	4	1	2	3	4	1	2	3	4	Criteria	
60																						
70	1.00				1.00																1.00	1
80	1.01				0.98									0.89							1.00	1
90	1.00				1.01									0.98				1.04			0.99	1
100	1.00				1.00									1.00				1.00			1.00	1
110	1.00				1.00									1.01				1.00			1.00	1
120	1.00	1.00			1.02	1.00								1.01				0.99			1.00	1
130	1.00	1.01			1.00	0.99								1.01				1.00			1.01	1
140	1.00	1.02			1.00	1.00								1.00				1.00			1.01	1
150	1.00	1.02			0.99	1.00								1.00				1.00			1.00	1
160	1.00	1.00			1.00	1.00								1.00				1.00			1.00	2/4

Table F-3: Formula/FEM ratios [-] for various eye radii [mm], plastic strains [%] and failure criteria [#] (e = 50mm, t = 40mm, dh = 82mm, dp = 80mm)

Reye	0%				0.50%				1%				5%				15%				Section yield		
	1	2	3	4	1	2	3	4	1	2	3	4	1	2	3	4	1	2	3	4	Criteria		
60	242	288			428	912			534				870								624	1	
70	402	526		960	688	1157		1120	840	1331		1150	1251				1331				1115	2/4	
80	570	860	1209	1178	962	1509	1699	1405	1178	1657	1703	1453	1605	1707	1714	1615	1695				1409	2/4	
90	722	1245	1337	1375	1217	1835	2046	1675	1519	1889	2048	1741	1930	2014	2062	1928				2018	1685	2/4	
100	864	1671	1327	1523	1469	2126	1599	1877	1985	2180	1674	2027	2234	2314	2019	2216			2408	2356	2313	2029	2/4
110	994	2081	1281		1743	2428	1459			2470	1539			2598	1955	2468			2720	2498	2582	2340	2/4
120	1110	2400	1240		2634	2680	1383			2720	1459			2870	1923				3027	2638		2608	2/4
130	1212	2672	1208		3029	2908	1338			2948	1411			3127	1909				3331	2700		2846	2/4
140	1304	2902	1182		3291	3114	1306			3157	1380			3377	1899				3629	2714		3056	2/4
150	1384	3122	1162			3305	1284			3359	1360			3623	1893				3920	2726		3255	2/4
160	1460	3324	1148			3495	1268			3555	1346			3865	1887				4208	2732		3441	2/4

Table F-4: FEM results [kN] for various eye radii [mm], plastic strains [%] and failure criteria [#] (e = 0mm, t = 40mm, dh = 82mm, dp = 80mm)

Reye	0%				0.50%				1%				5%				15%				Section yield		
	1	2	3	4	1	2	3	4	1	2	3	4	1	2	3	4	1	2	3	4	Criteria		
60																							
70	402	526			688	1157									2050				2584			1115	2/4
80	576	860			931	1509									2050				2611			1409	2/4
90	731	1278			1217	1835									2050				2635			1707	2/4
100	870	1698			1521	2135									2019				2654			2000	2/4
110	994	2081			1828	2410									1987				2672			2280	2/4
120	1106	2415			2505	2663									1959				2687			2546	2/4
130	1208	2698			2920	2895									1935				2700			2798	2/4
140	1300	2932			3291	3108									1913				2712			3034	2/4
150	1384	3122			3624	3305									1893				2722			3255	2/4
160	1461	3273			3925	3487									1880				2732			3462	2/4

Table F-5: Formula results [kN] for various eye radii [mm], plastic strains [%] and failure criteria [#] (e = 0mm, t = 40mm, dh = 82mm, dp = 80mm)

Reye	0%				0.50%				1%				5%				15%				Section yield		
	1	2	3	4	1	2	3	4	1	2	3	4	1	2	3	4	1	2	3	4	Criteria		
60																							
70	1.00	1.00			1.00	1.00																1.00	2/4
80	1.01	1.00			0.97	1.00									1.20							1.00	2/4
90	1.01	1.03			1.00	1.00									0.99							1.01	2/4
100	1.01	1.02			1.04	1.00									1.00							0.99	2/4
110	1.00	1.00			1.05	0.99									1.02							0.97	2/4
120	1.00	1.01			0.95	0.99									1.02							0.98	2/4
130	1.00	1.01			0.96	1.00									1.01							0.98	2/4
140	1.00	1.01			1.00	1.00									1.01							0.99	2/4
150	1.00	1.00				1.00									1.00							1.00	2/4
160	1.00	0.98				1.00									1.00							1.01	2/4

Table F-6: Formula/FEM ratios [-] for various eye radii [mm], plastic strains [%] and failure criteria [#] (e = 0mm, t = 40mm, dh = 82mm, dp = 80mm)

PINNED CONNECTIONS

e	0%				0.50%				1%				5%				15%				Section yield		
	1	2	3	4	1	2	3	4	1	2	3	4	1	2	3	4	1	2	3	4	Criteria		
-25	617	732	1580	1036	1021	1226	1601	1225	1332	1476	1603	1299	1504	1580	1615	1479				1580	1260	2/4	
-20	676	895	1776	1150	1136	1433	1776	1365	1452	1603	1779	1425		1717	1790	1631				1732	1387	2/4	
-15	730	1070	1941	1263	1242	1639	1941	1515	1580	1729	1943	1589	1809	1863	1953	1784			1949	1884	1530	2/4	
-10	780	1257	1413	1365	1324	1785	2098	1647	1683	1851	2098	1735	1957	2009	2108	1931			2100	2031	1675	2/4	
-5	825	1459	1363	1451	1394	1947	1677	1773	1809	2013	1745	1883	2098	2162	2048	2074			2254	2268	2173	1845	2/4
0	864	1671	1327	1523	1469	2126	1599	1877	1985	2180	1674	2027	2234	2314	2019	2216			2408	2356	2313	2029	2/4
5	904						1536				1621				2009					2413		2178	2/4
10	934	2104	1277		1601	2460	1489		2312	2500	1578			2612	1999	2474			2721	2490		2343	2/4
15	966						1452				1534				1979					2562		2472	2/4
20	996	2472	1243		1725	2765	1422		2552	2801	1504		2675	2923	1967				2823	2620		2616	2/4
25	1022						1399				1479				1958					2652		2717	2/4
30	1046		1219		1849		1379		2727		1462		2845		1948				3027	2663		2795	2/4
35	1066						1362				1442				1942					2671		2849	1
40	1089	3226	1202		1969		1350		2811		1428		3011		1932				3224	2679		2849	1
45	1107						1338				1413				1929					2685		2847	1
50	1123		1188		2084		1327		2865		1404		2987		1925				3160	2689		2849	1

Table F-7: FEM results [kN] for various eccentricities [mm], plastic strains [%] and failure criteria [#] (Reye = 100mm, t = 40mm, dh = 82mm, dp = 80mm)

e	0%				0.50%				1%				5%				15%				Section yield		
	1	2	3	4	1	2	3	4	1	2	3	4	1	2	3	4	1	2	3	4	Criteria		
-25																							
-20																							
-15																							
-10																							
-5																							
0	870	1698			1521	2135									2019					2654		2000	2/4
5	903	1862			1563	2289									2006					2659		2182	2/4
10	935	2043			1613	2460									1993					2664		2343	2/4
15	965	2234			1667	2641									1982					2668		2487	2/4
20	993	2431			1725	2827									1972					2672		2616	2/4
25	1019	2631			1784	3017									1963					2675		2732	2/4
30	1043	2831			1845	3206									1954					2678		2838	2/4
35	1066	3030			1905	3395									1946					2681		2849	1
40	1088	3226			1966	3581									1938					2684		2849	1
45	1109	3419			2025	3764									1931					2687		2849	1
50	1128	3607			2084	3943									1925					2689		2849	1

Table F-8: Formula results [kN] for various eccentricities [mm], plastic strains [%] and failure criteria [#] (Reye = 100mm, t = 40mm, dh = 82mm, dp = 80mm)

e	0%				0.50%				1%				5%				15%				Section yield	
	1	2	3	4	1	2	3	4	1	2	3	4	1	2	3	4	1	2	3	4	Criteria	
-25																						
-20																						
-15																						
-10																						
-5																						
0	1.01	1.02			1.04	1.00								1.00				1.13		0.99	2/4	
5	1.00													1.00				1.10		1.00	2/4	
10	1.00	0.97			1.01	1.00								1.00				1.07		1.00	2/4	
15	1.00													1.00				1.04		1.01	2/4	
20	1.00	0.98			1.00	1.02								1.00				1.02		1.00	2/4	
25	1.00													1.00				1.01		1.01	2/4	
30	1.00				1.00									1.00				1.01		1.02	2/4	
35	1.00													1.00				1.00		1.00	1	
40	1.00	1.00			1.00									1.00				1.00		1.00	1	
45	1.00													1.00				1.00		1.00	1	
50	1.00				1.00									1.00				1.00		1.00	1	

Table F-9: Formula/FEM ratios [-] for various eccentricities [mm], plastic strains [%] and failure criteria [#] (Reye = 100mm, t = 40mm, dh = 82mm, dp = 80mm)

PINNED CONNECTIONS

e	0%				0.50%				1%				5%				15%				Section yield		
	1	2	3	4	1	2	3	4	1	2	3	4	1	2	3	4	1	2	3	4	Criteria		
-25	272	242	714	508	502	680	716	634	648		718	684			734				776		596	2/4	
-20	340	318	956	658	582	768	958	786	774		960	838			976	982			1008		782	2/4	
-15	404	424	1171	802	692	894	1171	946	868	1183	1173	998			1189	1153				1203	976	2/4	
-10	464	550	1361	934	782	1038	1361		972	1369	1361	1159			1311	1377	1311			1377	1127	2/4	
-5	522	704	1535	1058	880	1257	1535	1257	1079	1513	1537	1309			1459	1551	1463	1541			1273	2/4	
0	570	860	1209	1178	962	1509	1699	1405	1178	1657	1703	1453			1605	1707	1714	1615	1695		1409	2/4	
5																							
10	646	1221	1209	1405	1079	1902	1998	1697	1345	1934	2000	1737			1880	2009	2011		1970		1675	2/4	
15																							
20	710	1643	1215	1611	1189		1824	1966	1479		2096	2008			2038			2084	2136		1934	2/4	
25																							
30	764	2098	1219	1759	1275		1609	2142	1589		1761				2100				2160		1978	1	
35																							
40	808		1217		1352		1486		1675		1613				2140				2162		2024	1	
45																							
50	840		1209		1397		1425		1733		1521				2144		2156		2162		2058	1	

Table F-10: FEM results [kN] for various eccentricities [mm], plastic strains [%] and failure criteria [#] (Reye = 80mm, t = 40mm, dh = 82mm, dp = 80mm)

e	0%				0.50%				1%				5%				15%				Section yield		
	1	2	3	4	1	2	3	4	1	2	3	4	1	2	3	4	1	2	3	4	Criteria		
-25																							
-20																							
-15																							
-10																							
-5																							
0	576	860			931	1509									2050				2611		1409	2/4	
5	614	1027			1014	1694									2050				2620		1572	2/4	
10	648	1221			1083	1902									2049				2627		1711	2/4	
15	680	1432			1140	2124									2028				2633		1830	2/4	
20	710	1652			1189	2352									2009				2639		1934	2/4	
25	738	1875			1231	2582									1992				2644		2025	2/4	
30	763	2098			1266	2810									1977				2649		1978	1	
35	787	2318			1297	3034									1962				2653		2001	1	
40	809	2534			1324	3253									1949				2657		2021	1	
45	830	2745			1347	3465									1937				2661		2040	1	
50	849	2949			1368	3671									1926				2665		2058	1	

Table F-11: Formula results [kN] for various eccentricities [mm], plastic strains [%] and failure criteria [#] (Reye = 80mm, t = 40mm, dh = 82mm, dp = 80mm)

e	0%				0.50%				1%				5%				15%				Section yield	
	1	2	3	4	1	2	3	4	1	2	3	4	1	2	3	4	1	2	3	4	Criteria	
-25																						
-20																						
-15																						
-10																						
-5																						
0	1.01	1.00			0.97	1.00									1.20						1.00	2/4
5																						2/4
10	1.00	1.00			1.00	1.00									1.02						1.02	2/4
15																						2/4
20	1.00	1.01			1.00																1.00	2/4
25																						2/4
30	1.00	1.00			0.99																1.00	2/4
35																						1
40	1.00				0.98																1.00	1
45																						1
50	1.01				0.98										0.89						1.00	1

Table F-12: Formula/FEM ratios [-] for various eccentricities [mm], plastic strains [%] and failure criteria [#] (Reye = 80mm, t = 40mm, dh = 82mm, dp = 80mm)

PINNED CONNECTIONS

dp	0%				0.50%				1%				5%				15%				Section yield			
	1	2	3	4	1	2	3	4	1	2	3	4	1	2	3	4	1	2	3	4	Criteria			
82	1082	1863	2115			1995	2115	1645	1883	2005	2118			2048	2128	2017			2126		2058	1971	2/4	
81.9	1028	1843	2114			1991	2116	1637	1881	2001	2116			2048	2126	2015			2124		2056	1965	2/4	
81.8	976	1817	2114			1987	2114	1627	1871	1997	2116			2046	2125	2013			2122		2056	1957	2/4	
81.5	884	1727	2110		1773	1963	2110	1637	1849	1981	2112			2042	2122	2005			2118		2052	1921	2/4	
81	820	1557	2106		1429	1913	2106	1691	1815	1943	2108			2033	2117	1985			2113		2046	1847	2/4	
80	780	1257	1413	1365	1324	1785	2098	1647	1683	1851	2098	1735	1957	2009	2108	1931			2100		2031	1675	2/4	
79	766	1140	790	1231	1277	1659	1156	1567	1579	1783	1365	1649		1989	2094	1873			2090		2013	1505	2/4	
77	748	1074	444		1249	1433	624	1391	1505	1705	762	1477		1941	1409	1781			2068	2090	1975	1395	2/4	
72	740	1044	240		1237	1343	314		1447	1381	374			1837	816	1613			2007	1713	1871	1319	2/4	
67	736	1024	166		1237	1297	218		1419	1339	252			1801	1721	542			1961	1939	1425	1777	1283	2/4
62	730	1012	130		1235	1269	156		1397	1307	192			1749	1499	382			1903	1867	1219	1681	1249	2/4

Table F-13: FEM results [kN] for various pin diameters [mm], plastic strains [%] and failure criteria [#] (Reye = 100mm, e = -10mm, t = 40mm, dh = 82mm)

dp	0%				0.50%				1%				5%				15%				Section yield			
	1	2	3	4	1	2	3	4	1	2	3	4	1	2	3	4	1	2	3	4	Criteria			
82																								
81.9																								
81.8																								
81.5																								
81																								
80																								
79																								
77																								
72																								
67																								
62																								

Table F-14: Formula results [kN] for pin diameters [mm], plastic strains [%] and failure criteria [#] (Reye = 100mm, e = -10mm, t = 40mm, dh = 82mm)

dp	0%				0.50%				1%				5%				15%				Section yield			
	1	2	3	4	1	2	3	4	1	2	3	4	1	2	3	4	1	2	3	4	Criteria			
82																								
81.9																								
81.8																								
81.5																								
81																								
80																								
79																								
77																								
72																								
67																								
62																								

Table F-15: Formula/FEM ratios [-] for various pin diameters [mm], plastic strains [%] and failure criteria [#] (Reye = 100mm, e = -10mm, t = 40mm, dh = 82mm)

dp	0%				0.50%				1%				5%				15%				Section yield	
	1	2	3	4	1	2	3	4	1	2	3	4	1	2	3	4	1	2	3	4	Criteria	
82	1215	2655	1807		1955	2813	2150		2280	2843	2378		2729	2954	2534		2839		2743		2669	1
81.9	1162	2650	1979		1973	2811	2312		2328	2841	2354		2731	2953	2518		2839		2741		2671	1
81.8	1128	2642	2122		1999	2809	2288		2334	2839	2328		2727	2951	2500		2837		2739		2675	1
81.5	1068	2620	2110		2009	2801	2196		2336	2831	2232		2721	2947	2436		2831		2727		2679	1
81	1024	2572	1941		1781	2789	1993		2368	2821	2029		2701	2939	2296		2829		2701		2659	2/4
80	996	2472	1243		1725	2765	1422		2552	2801	1504		2675	2923	1967		2823		2620		2616	2/4
79	984	2380	798		1727	2739	993		2557	2778	1095		2644	2907	1679		2811		2506		2536	2/4
77	974	2282	464		1729	2679	604		2526	2725	694			2877	1281			3002	2248		2444	2/4
72	968	2168	240		1737	2486	310		2404	2570	366		2765	2795	790		2913	2945	1791		2302	2/4
67	970	2110	162		1750	2244	219		2324	2328	253		2715	2703	533		2871	2873	1439		2218	2/4
62	968	2056	128		1763	2164	158		2262	2222	192		2671	2604	378		2817	2795	1180		2142	2/4

**Table F-16: FEM results [kN] for various pin diameters [mm], plastic strains [%] and failure criteria [#] (Reye = 100mm, e = 20mm, t = 40mm, dh = 82mm)**

dp	0%				0.50%				1%				5%				15%				Section yield	
	1	2	3	4	1	2	3	4	1	2	3	4	1	2	3	4	1	2	3	4	Criteria	
82	1155	2683			1992	3011								2725					3028		2771	2/4
81.9	1135	2683			1959	3011								2678					3008		2771	2/4
81.8	1117	2683			1929	3011								2633					2989		2771	2/4
81.5	1074	2664			1859	2999								2503					2932		2761	2/4
81	1030	2569			1787	2936								2305					2841		2708	2/4
80	993	2431			1725	2827								1972					2672		2616	2/4
79	981	2341			1707	2738								1706					2519		2539	2/4
77	977	2245			1699	2605								1318					2252		2423	2/4
72	977	2182			1699	2434								809					1757		2267	2/4
67	977	2175			1699	2370								560					1409		2205	2/4
62	977	2174			1699	2347								385					1140		2181	2/4

**Table F-17: Formula results [kN] for pin diameters [mm], plastic strains [%] and failure criteria [#] (Reye = 100mm, e = 20mm, t = 40mm, dh = 82mm)**

dp	0%				0.50%				1%				5%				15%				Section yield	
	1	2	3	4	1	2	3	4	1	2	3	4	1	2	3	4	1	2	3	4	Criteria	
82	0.95	1.01			1.02	1.07								1.08					1.10		1.04	2/4
81.9	0.98	1.01			0.99	1.07								1.06					1.10		1.04	2/4
81.8	0.99	1.02			0.97	1.07								1.05					1.09		1.04	2/4
81.5	1.01	1.02			0.93	1.07								1.03					1.08		1.03	2/4
81	1.01	1.00			1.00	1.05								1.00					1.05		1.02	2/4
80	1.00	0.98			1.00	1.02								1.00					1.02		1.00	2/4
79	1.00	0.98			0.99	1.00								1.02					1.01		1.00	2/4
77	1.00	0.98			0.98	0.97								1.03					1.00		0.99	2/4
72	1.01	1.01			0.98	0.98								1.02					0.98		0.98	2/4
67	1.01	1.03			0.97	1.06								1.05					0.98		0.99	2/4
62	1.01	1.06			0.96	1.08								1.02					0.97		1.02	2/4

**Table F-18: Formula/FEM ratios [-] for various pin diameters [mm], plastic strains [%] and failure criteria [#] (Reye = 100mm, e = 20mm, t = 40mm, dh = 82mm)**

PINNED CONNECTIONS

dp	0%				0.50%				1%				5%				15%				Section yield	
	1	2	3	4	1	2	3	4	1	2	3	4	1	2	3	4	1	2	3	4	Criteria	
82	1277		1675		2202		2244	2196	2584		2358		2909		2592		3128		2835		2759	1
81.9	1241		1753		2240		2232	2214	2562		2334		2915		2572		3132		2833		2769	1
81.8	1219		1811		2284		2212		2566		2306		2921		2548		3134		2833		2777	1
81.5	1178		1879		2204		2126		2612		2194		2933		2464		3134		2829		2793	1
81	1146		1759		2064		1897		2831		1957		2955		2290		3140		2811		2811	1
80	1123		1188		2084		1327		2865		1404		2987		1925		3160		2689		2849	1
79	1116		796		2113		956		2890		1038		3007		1631		3175		2539		2857	1
77	1114		470		2106		598		2921		674		3035		1251		3198		2260		2875	1
72	1116		242		2126		312		2945		366		3073		774		3236		1787		2901	1
67	1118		160		2122		220		2943		258		3087		528		3240		1435		2903	1
62	1120		126		2128		156		2925		188		3093		378		3234		1164		2897	1

Table F-19: FEM results [kN] for various pin diameters [mm], plastic strains [%] and failure criteria [#] (Reye = 100mm, e = 50mm, t = 40mm, dh = 82mm)

dp	0%				0.50%				1%				5%				15%				Section yield	
	1	2	3	4	1	2	3	4	1	2	3	4	1	2	3	4	1	2	3	4	Criteria	
82	1272	3607			2255	4063									2660				3048		2849	1
81.9	1254	3607			2234	4063									2614				3028		2849	1
81.8	1238	3607			2215	4063									2570				3008		2849	1
81.5	1200	3607			2170	4055									2443				2951		2849	1
81	1161	3607			2123	4014									2250				2859		2849	1
80	1128	3607			2084	3943									1925				2689		2849	1
79	1118	3607			2072	3885									1665				2535		2849	1
77	1114	3607			2068	3798									1287				2267		2849	1
72	1114	3607			2067	3686									790				1768		2849	1
67	1114	3607			2067	3644									546				1419		2849	1
62	1114	3607			2067	3629									376				1147		2849	1

Table F-20: Formula results [kN] for pin diameters [mm], plastic strains [%] and failure criteria [#] (Reye = 100mm, e = 50mm, t = 40mm, dh = 82mm)

dp	0%				0.50%				1%				5%				15%				Section yield	
	1	2	3	4	1	2	3	4	1	2	3	4	1	2	3	4	1	2	3	4	Criteria	
82	1.00				1.02										1.03				1.07		1.03	1
81.9	1.01				1.00										1.02				1.07		1.03	1
81.8	1.02				0.97										1.01				1.06		1.03	1
81.5	1.02				0.98										0.99				1.04		1.02	1
81	1.01				1.03										0.98				1.02		1.01	1
80	1.00				1.00										1.00				1.00		1.00	1
79	1.00				0.98										1.02				1.00		1.00	1
77	1.00				0.98										1.03				1.00		0.99	1
72	1.00				0.97										1.02				0.99		0.98	1
67	1.00				0.97										1.04				0.99		0.98	1
62	0.99				0.97										0.99				0.99		0.98	1

Table F-21: Formula/FEM ratios [-] for various pin diameters [mm], plastic strains [%] and failure criteria [#] (Reye = 100mm, e = 50mm, t = 40mm, dh = 82mm)

dp	Bearing				
	0%	0.50%	1%	5%	15%
82	1658	2189	2343	2644	3052
81.9	1695	2165	2309	2616	3040
81.8	1719	2139	2271	2584	3030
81.5	1713	2015	2125	2473	2988
81	1565	1754	1850	2269	2910
80	1123	1244	1327	1888	2738
79	798	924	996	1595	2568
77	483	597	663	1234	2273
72	246	316	366	771	1773
67	164	222	254	530	1432
62	128	156	190	376	1168

Table F-22: FEM results [kN] for various pin diameters [mm] and plastic strains [%] (Reye = 150mm, e = 50mm, t = 40mm, dh = 82mm)

dp	Bearing				
	0%	0.50%	1%	5%	15%
82				2609	3100
81.9				2564	3079
81.8				2521	3060
81.5				2396	3001
81				2207	2908
80				1888	2735
79				1633	2578
77				1262	2306
72				775	1799
67				536	1443
62				369	1167

Table F-23: Formula results [kN] for pin diameters [mm] and plastic strains [%] (Reye = 150mm, e = 50mm, t = 40mm, dh = 82mm)

dp	Bearing				
	0%	0.50%	1%	5%	15%
82				0.99	1.02
81.9				0.98	1.01
81.8				0.98	1.01
81.5				0.97	1.00
81				0.97	1.00
80				1.00	1.00
79				1.02	1.00
77				1.02	1.01
72				1.01	1.01
67				1.01	1.01
62				0.98	1.00

Table F-24: Formula/FEM ratios [-] for various pin diameters [mm] and plastic strains [%] (Reye = 150mm, e = 50mm, t = 40mm, dh = 82mm)

PINNED CONNECTIONS

dp	0%				0.50%				1%				5%				15%				Section yield	
	1	2	3	4	1	2	3	4	1	2	3	4	1	2	3	4	1	2	3	4	Criteria	
82	1004		1647		1719				1924				2100				2165				1988	1
81.9	970		1765		1667				1980				2120				2165				2012	1
81.8	942		1868		1630				1958				2138								2034	1
81.5	890		2034		1519				1882				2150				2164				2084	1
81	858		1968		1447		2094		1789				2146				2164				2074	1
80	840		1209		1397		1425		1733		1521		2144		2156		2162				2058	1
79	834		772		1387		988		1727		1109		2144		1729		2162				2050	1
77	826		454		1381		596		1723		698		2144		1299		2162				2040	1
72	822		236		1377		308		1723		364		2138		794		2162		1824		2030	1
67	820		160		1379		218		1725		252		2138		534		2162		1457		2032	1
62	818		126				156		1733		186		2134		380		2160		1185		2036	1

Table F-25: FEM results [kN] for various pin diameters [mm], plastic strains [%] and failure criteria [#] (Reye = 80mm, e = 50mm, t = 40mm, dh = 82mm)

dp	0%				0.50%				1%				5%				15%				Section yield	
	1	2	3	4	1	2	3	4	1	2	3	4	1	2	3	4	1	2	3	4	Criteria	
82	965	2949			1667	3744								2662				3020			2058	1
81.9	951	2949			1629	3744								2616				3000			2058	1
81.8	938	2949			1596	3744								2572				2981			2058	1
81.5	908	2949			1518	3739								2445				2924			2058	1
81	876	2949			1437	3714								2252				2833			2058	1
80	849	2949			1368	3671								1926				2665			2058	1
79	841	2949			1347	3636								1666				2512			2058	1
77	838	2949			1339	3583								1288				2246			2058	1
72	838	2949			1338	3515								791				1752			2058	1
67	838	2949			1338	3490								547				1406			2058	1
62	838	2949			1338	3480								376				1137			2058	1

Table F-26: Formula results [kN] for pin diameters [mm], plastic strains [%] and failure criteria [#] (Reye = 80mm, e = 50mm, t = 40mm, dh = 82mm)

dp	0%				0.50%				1%				5%				15%				Section yield	
	1	2	3	4	1	2	3	4	1	2	3	4	1	2	3	4	1	2	3	4	Criteria	
82	0.96				0.97																1.04	1
81.9	0.98				0.98																1.02	1
81.8	1.00				0.98																1.01	1
81.5	1.02				1.00																0.99	1
81	1.02				0.99																0.99	1
80	1.01				0.98										0.89						1.00	1
79	1.01				0.97										0.96						1.00	1
77	1.02				0.97										0.99						1.01	1
72	1.02				0.97										1.00				0.96		1.01	1
67	1.02				0.97										1.02				0.96		1.01	1
62	1.02														0.99				0.96		1.01	1

Table F-27: Formula/FEM ratios [-] for various pin diameters [mm], plastic strains [%] and failure criteria [#] (Reye = 80mm, e = 50mm, t = 40mm, dh = 82mm)

dp	0%				0.50%				1%				5%				15%				Section yield	
	1	2	3	4	1	2	3	4	1	2	3	4	1	2	3	4	1	2	3	4	Criteria	
164	2431	5311	3610		3917	5626	4672		4560	5686	4756		5459	5909	5067		5678		5487		5339	1
163.8	2323	5299	3949		3949	5622	4600		4656	5682	4700		5463	5906	5035		5678		5483		5347	1
163.6	2255	5285	4243		4015	5616	4574		4662	5676	4654		5453	5904	4998		5676		5477		5353	1
163	2135	5237	4219		4019	5604	4391		4666	5664	4462		5441	5896	4870		5664		5457		5357	1
162	2047	5143	3881		3562	5578	3985		4732	5642	4057		5403	5878	4588		5658		5403		5323	2/4
160	1985	4948	2487		3450	5530	2847		5103	5602	3010		5351	5846	3935		5642		5239		5207	2/4
158	1967	4760	1596		3454	5479	1985		5113	5556	2189		5287	5814	3358		5622		5012		5071	2/4
154	1947	4564	928		3458	5359	1208		5051	5451	1388			5754	2563			6005	4496		4888	2/4
144	1935	4337	480		3474	4972	620		4808	5139	732		5531	5590	1580		5826	5890	3582		4604	2/4
134	1939	4221	324		3500	4488	438		4648	4656	507		5431	5407	1065		5742	5746	2879		4436	2/4
124	1935	4113	256		3526	4329	316		4524	4444	384		5343	5207	760		5634	5590	2351		4285	2/4

**Table F-28: FEM results [kN] for various pin diameters [mm], plastic strains [%] and failure criteria [#] (Reye = 200mm, e = 40mm, t = 40mm, dh = 164mm)**

dp	0%				0.50%				1%				5%				15%				Section yield	
	1	2	3	4	1	2	3	4	1	2	3	4	1	2	3	4	1	2	3	4	Criteria	
164	2310	5367			3984	6021									5449				6056		5543	2/4
163.8	2270	5367			3917	6021									5357				6017		5543	2/4
163.6	2234	5367			3858	6021									5266				5978		5543	2/4
163	2149	5328			3718	5997									5006				5864		5523	2/4
162	2060	5138			3573	5871									4611				5682		5417	2/4
160	1985	4862			3450	5654									3944				5343		5232	2/4
158	1963	4682			3413	5477									3411				5037		5079	2/4
154	1954	4489			3399	5211									2636				4505		4846	2/4
144	1953	4364			3397	4868									1619				3514		4534	2/4
134	1953	4350			3397	4741									1120				2819		4411	2/4
124	1953	4348			3397	4694									770				2280		4362	2/4

**Table F-29: Formula results [kN] for pin diameters [mm], plastic strains [%] and failure criteria [#] (Reye = 200mm, e = 40mm, t = 40mm, dh = 164mm)**

dp	0%				0.50%				1%				5%				15%				Section yield	
	1	2	3	4	1	2	3	4	1	2	3	4	1	2	3	4	1	2	3	4	Criteria	
164	0.95	1.01			1.02	1.07									1.08				1.10		1.04	2/4
163.8	0.98	1.01			0.99	1.07									1.06				1.10		1.04	2/4
163.6	0.99	1.02			0.96	1.07									1.05				1.09		1.04	2/4
163	1.01	1.02			0.93	1.07									1.03				1.07		1.03	2/4
162	1.01	1.00			1.00	1.05									1.00				1.05		1.02	2/4
160	1.00	0.98			1.00	1.02									1.00				1.02		1.00	2/4
158	1.00	0.98			0.99	1.00									1.02				1.01		1.00	2/4
154	1.00	0.98			0.98	0.97									1.03				1.00		0.99	2/4
144	1.01	1.01			0.98	0.98									1.02				0.98		0.98	2/4
134	1.01	1.03			0.97	1.06									1.05				0.98		0.99	2/4
124	1.01	1.06			0.96	1.08									1.01				0.97		1.02	2/4

**Table F-30: Formula/FEM ratios [-] for various pin diameters [mm], plastic strains [%] and failure criteria [#] (Reye = 200mm, e = 40mm, t = 40mm, dh = 164mm)**

PINNED CONNECTIONS

tcheek	0%							0.5%							1%						
	1	2	3	5	1 cheek	3 cheek	weld	1	2	3	5	1 cheek	3 cheek	weld	1	2	3	5	1 cheek	3 cheek	weld
0	900	1600	800					1500	2050	1250				1950	2150	1900					
10	1250	2100	1750	2550	1200	1150	2000	2100	2800	2800		2000	2250	2900	2600	3000	3000		2500	2950	3050
20	1500	2600	2250	2550	1450		2150	2600	3550	3500		2450	2200	3400	3200	3800	3900		3100		3850
30	1800	3050	2700	2600	1700	1350	2100	3050	4250	4100	4400	3050	2150	3100	3650	4600	4800	4800	3800		3600
40	2100	3500	3200	2700	1850	1150	2050	3400	4900	4950	4550	3450	1800	3000	4000			4800	4450	3150	3450
tcheek	5%							15%							Section yield		F ratio mid plate				
	1	2	3	5	1 cheek	3 cheek	weld	1	2	3	5	1 cheek	3 cheek	weld	Criteria	25%	25%	50%	75%	100%	
0	2200	2300	2300					2300						1950	2/4	100%	100%	100%	100%		
10	3100	3250	3250		3100	3285	3250	3250				3250		2700	2/4	72%	72%	72%	74%		
20	3950	4100			3900		4100	4100	4208			4100	4207.5	3400	2/4	61%	60%	60%	62%		
30	4750	4950			4700		4700	4950				4950	5000	4150	2/4	53%	52%	51%	55%		
40	5150			5273			4600						5050	4300	5	47%	45%	44%	48%		

Table F-31: FEM results [kN for various cheek plate thicknesses [mm], plastic strains [%] and failure criteria [#] (Reye = 100mm, e = 0mm, t = 40mm, dh = 82mm, dp = 80mm, Rcheek = 80mm, weld = 6mm)

tcheek	0%							0.5%							1%						
	1	2	3	5	1 cheek	3 cheek	weld	1	2	3	5	1 cheek	3 cheek	weld	1	2	3	5	1 cheek	3 cheek	weld
0	870	1698						1521	2135												
10	1256	2451			937			2196	3082			1515									
20	1376	2687			1564			2407	3379									2529			
30	1595	3114			1899			2790	3916			3071									
40	1922	3752			2104			3361	4718			3401									
tcheek	5%							15%							Section yield		F ratio mid plate				
	1	2	3	5	1 cheek	3 cheek	weld	1	2	3	5	1 cheek	3 cheek	weld	Criteria	25%	25%	50%	75%	100%	
0			2019							2654				2000	2/4					100%	
10			2915			3334				3832			4248	2887	2/4					69%	
20			3195			5568				4201			7093	3165	2/4					63%	
30			3704			6760				4869			8612	3668	2/4					55%	
40			4462			7488				5867			9538	4420	2/4					45%	

Table F-32: Formula results [kN] for various cheek plate thicknesses [mm], plastic strains [%] and failure criteria [#] (Reye = 100mm, e = 0mm, t = 40mm, dh = 82mm, dp = 80mm, Rcheek = 80mm, weld = 6mm)

tcheek	0%							0.5%							1%						
	1	2	3	5	1 cheek	3 cheek	weld	1	2	3	5	1 cheek	3 cheek	weld	1	2	3	5	1 cheek	3 cheek	weld
0	0.97	1.06						1.01	1.04												
10	1.00	1.17			0.78			1.05	1.10			0.76									
20	0.92	1.03			1.08			0.93	0.95			1.03									
30	0.89	1.02			1.12			0.91	0.92			1.01									
40	0.92	1.07			1.14			0.99	0.96			0.99									
tcheek	5%							15%							Section yield		F ratio mid plate				
	1	2	3	5	1 cheek	3 cheek	weld	1	2	3	5	1 cheek	3 cheek	weld	Criteria	25%	25%	50%	75%	100%	
0			0.88											1.03	2/4					1.00	
10			0.90			1.02								1.07	2/4					0.94	
20														0.93	2/4					1.03	
30														0.88	2/4					0.99	
40														1.03	2/4					0.94	

Table F-33: Formula/FEM ratios [-] for various cheek plate thicknesses [mm], plastic strains [%] and failure criteria [#] (Reye = 100mm, e = 0mm, t = 40mm, dh = 82mm, dp = 80mm, Rcheek = 80mm, weld = 6mm)

tcheek	0%							0.5%							1%						
	1	2	3	5	1 cheek	3 cheek	weld	1	2	3	5	1 cheek	3 cheek	weld	1	2	3	5	1 cheek	3 cheek	weld
0	900	1600	800					1500	2050	1250					1950	2150	1900				
20	1600	2650	2450	2900	1500	1100	2600	2750	3700	3750		2550	2050	3750	3400	3900	4050		3250	3750	3950
25	1750	2850	2700	2950	1650	1350	2750	3000	4050	4100	4600	2850	2100	4100	3700	4350	4500		3600	3850	4350
30	1900	3100	3000	3000	1750	1250	2950	3300	4400	4400	4700	3100	1950	4450	3950	4750	4950		3900	3450	4800
40	2250	3550	3500	3100	1900	1150	3000	3750	5100	5200	4950	3600	1750	5150	4500				4550	2750	
tcheek	5%							15%							Section yield		F ratio mid plate				
	1	2	3	5	1 cheek	3 cheek	weld	1	2	3	5	1 cheek	3 cheek	weld	Criteria	25%	25%	50%	75%	100%	
0	2200	2300	2300					2300							1950	2/4	100%	100%	100%	100%	
20	4150	4250	4350		4100		4250	4300	4405			4300		4405	3600	2/4	57%	57%	57%	60%	
25	4550	4700			4500		4700	4700				4700			3950	2/4	53%	52%	52%	55%	
30	4950	5150			4850		5150	5150				5150			4300	2/4	48%	48%	48%	51%	
40															4450	5	41%	40%	40%	42%	

**Table F-34: FEM results [kN for various cheek plate thicknesses [mm], plastic strains [%] and failure criteria [#] (Reye = 100mm, e = 0mm, t = 40mm, dh = 82mm, dp = 80mm, Rcheek = 80mm, weld = 12mm)**

tcheek	0%							0.5%							1%						
	1	2	3	5	1 cheek	3 cheek	weld	1	2	3	5	1 cheek	3 cheek	weld	1	2	3	5	1 cheek	3 cheek	weld
0	870	1698						1521	2135												
20	1474	2877			1405			2577	3618			2271									
25	1563	3052			1623			2734	3838			2623									
30	1681	3282			1790			2940	4127			2893									
40	2015	3934			2026			3524	4947			3276									
tcheek	5%							15%							Section yield		F ratio mid plate				
	1	2	3	5	1 cheek	3 cheek	weld	1	2	3	5	1 cheek	3 cheek	weld	Criteria	25%	25%	50%	75%	100%	
0			2019							2654					2000	2/4				100%	
20			3422			5001				4499			6370		3389	2/4				59%	
25			3629			5775				4772			7357		3595	2/4				56%	
30			3903			6370				5131			8115		3866	2/4				52%	
40			4679			7213				6151			9188		4634	2/4				43%	

**Table F-35: Formula results [kN] for various cheek plate thicknesses [mm], plastic strains [%] and failure criteria [#] (Reye = 100mm, e = 0mm, t = 40mm, dh = 82mm, dp = 80mm, Rcheek = 80mm, weld = 12mm)**

tcheek	0%							0.5%							1%						
	1	2	3	5	1 cheek	3 cheek	weld	1	2	3	5	1 cheek	3 cheek	weld	1	2	3	5	1 cheek	3 cheek	weld
0	0.97	1.06						1.01	1.04												
20	0.92	1.09			0.94			0.94	0.98			0.89									
25	0.89	1.07			0.98			0.91	0.95			0.92									
30	0.88	1.06			1.02			0.89	0.94			0.93									
40	0.90	1.11			1.07			0.94	0.97			0.91									
tcheek	5%							15%							Section yield		F ratio mid plate				
	1	2	3	5	1 cheek	3 cheek	weld	1	2	3	5	1 cheek	3 cheek	weld	Criteria	25%	25%	50%	75%	100%	
0			0.88												1.03	2/4				1.00	
20			0.79												0.94	2/4				0.99	
25															0.91	2/4				1.01	
30															0.90	2/4				1.02	
40															1.04	2/4				1.03	

**Table F-36: Formula/FEM ratios [-] for various cheek plate thicknesses [mm], plastic strains [%] and failure criteria [#] (Reye = 100mm, e = 0mm, t = 40mm, dh = 82mm, dp = 80mm, Rcheek = 80mm, weld = 12mm)**

PINNED CONNECTIONS

weld	0%							0.5%							1%						
	1	2	3	5	1 cheek	3 cheek	weld	1	2	3	5	1 cheek	3 cheek	weld	1	2	3	5	1 cheek	3 cheek	weld
6	1800	3050	2700	2600	1700	1350	2100	3050	4250	4100	4400	3050	2150	3100	3650	4600	4800	4800	3800		3600
8	1850	3100	2800	2800	1700	1300	2500	3150	4300	4250	4550	3050	2050	4000	3800	4650	4850		3800		4650
10	1900	3100	2900	2900	1700	1350	2900	3200	4350	4350	4650	3050	2100	4450	3900	4700	4850		3850		4750
12	1900	3100	3000	3000	1750	1250	2950	3300	4400	4400	4700	3100	1950	4450	3950	4750	4950		3900	3450	4800
weld	5%							15%							Section yield		F ratio mid plate				
	1	2	3	5	1 cheek	3 cheek	weld	1	2	3	5	1 cheek	3 cheek	weld	Criteria	25%	50%	75%	100%		
6	4750	4950			4700		4700	4950				4950		5000	4150	2/4	53%	52%	51%	55%	
8	4850	5000			4750		5050	5050				5000			4150	2/4	51%	50%	49%	52%	
10	4900	5100			4800		5100	5100				5050		5205	4200	2/4	49%	49%	49%	51%	
12	4950	5150			4850		5150	5150				5150			4300	2/4	48%	48%	48%	51%	

**Table F-37: FEM results [kN for various weld throats [mm], plastic strains [%] and failure criteria [#] (Reye = 100mm, e = 0mm, t = 40mm, dh = 82mm, dp = 80mm, Rcheek = 80mm, Tcheek = 30mm)**

weld	0%							0.5%							1%						
	1	2	3	5	1 cheek	3 cheek	weld	1	2	3	5	1 cheek	3 cheek	weld	1	2	3	5	1 cheek	3 cheek	weld
6	1595	3114			1899			2790	3916			3071									
8	1623	3168			1861			2838	3984			3009									
10	1651	3224			1825			2888	4054			2950									
12	1681	3282			1790			2940	4127			2893									
weld	5%							15%							Section yield		F ratio mid plate				
	1	2	3	5	1 cheek	3 cheek	weld	1	2	3	5	1 cheek	3 cheek	weld	Criteria	25%	50%	75%	100%		
6			3704			6760				4869			8612		3668	2/4				55%	
8			3768			6625				4954			8439		3732	2/4				54%	
10			3834			6495				5041			8274		3798	2/4				53%	
12			3903			6370				5131			8115		3866	2/4				52%	

**Table F-38: Formula results [kN] for various weld throats [mm], plastic strains [%] and failure criteria [#] (Reye = 100mm, e = 0mm, t = 40mm, dh = 82mm, dp = 80mm, Rcheek = 80mm, Tcheek = 30mm)**

weld	0%							0.5%							1%						
	1	2	3	5	1 cheek	3 cheek	weld	1	2	3	5	1 cheek	3 cheek	weld	1	2	3	5	1 cheek	3 cheek	weld
6	0.89	1.02			1.12			0.91	0.92			1.01									
8	0.88	1.02			1.09			0.90	0.93			0.99									
10	0.87	1.04			1.07			0.90	0.93			0.97									
12	0.88	1.06			1.02			0.89	0.94			0.93									
weld	5%							15%							Section yield		F ratio mid plate				
	1	2	3	5	1 cheek	3 cheek	weld	1	2	3	5	1 cheek	3 cheek	weld	Criteria	25%	50%	75%	100%		
6															0.88	2/4				0.99	
8															0.90	2/4				1.03	
10															0.90	2/4				1.03	
12															0.90	2/4				1.02	

**Table F-39: Formula/FEM ratios [-] for various weld throats [mm], plastic strains [%] and failure criteria [#] (Reye = 100mm, e = 0mm, t = 40mm, dh = 82mm, dp = 80mm, Rcheek = 80mm, Tcheek = 30mm)**

tcheek	0%							0.5%							1%						
	1	2	3	5	1 cheek	3 cheek	weld	1	2	3	5	1 cheek	3 cheek	weld	1	2	3	5	1 cheek	3 cheek	weld
0	1200		750					2300		1250					2900		1800				
20	2200		2250	3950	2100	1050	4400	3800		3700		3550	1750	5450	5200		4350		4900	2500	5500
25	2450		2550	3750	2300	1000	4100	4200		4250		4000	1700		5350		5100		5300	2450	
30	2700		2950	3550	2500	1000	3900	4600		4650		4450	1700							2400	
40	3250		3800	3350	2900	850	3550	5450		5300		5500	1500	5300						2100	
tcheek	5%							15%							Section yield		F ratio mid plate				
	1	2	3	5	1 cheek	3 cheek	weld	1	2	3	5	1 cheek	3 cheek	weld	Criteria	25%	50%	75%	100%		
0	3050		2500					3300		2900					2850	1	100%	100%	100%	100%	
20			5300												4850	5	59%	59%	61%	62%	
25															4850	5	54%	54%	55%	57%	
30															4900	5	50%	50%	51%	53%	
40															5200	5	43%	43%	43%	44%	

**Table F-40: FEM results [kN for various cheek plate thicknesses [mm], plastic strains [%] and failure criteria [#] (Reye = 100mm, e = 50mm, t = 40mm, dh = 82mm, dp = 80mm, Rcheek = 80mm, weld = 10mm)**

tcheek	0%							0.5%							1%						
	1	2	3	5	1 cheek	3 cheek	weld	1	2	3	5	1 cheek	3 cheek	weld	1	2	3	5	1 cheek	3 cheek	weld
0	1128	3607						2084	3943												
20	1867	5973			2145			3450	6529			3454									
25	1988	6358			2454			3673	6949			3953									
30	2142	6851			2691			3958	7488			4334									
40	2572	8227			3025			4752	8992			4872									
tcheek	5%							15%							Section yield		F ratio mid plate				
	1	2	3	5	1 cheek	3 cheek	weld	1	2	3	5	1 cheek	3 cheek	weld	Criteria	25%	50%	75%	100%		
0			1925							2689					2849	1				100%	
20			3187			4864				4452			6728		4717	1				60%	
25			3393			5567				4739			7700		5021	1				57%	
30			3656			6104				5107			8442		5411	1				53%	
40			4390			6862				6132			9491		6497	1				44%	

**Table F-41: Formula results [kN] for various cheek plate thicknesses [mm], plastic strains [%] and failure criteria [#] (Reye = 100mm, e = 50mm, t = 40mm, dh = 82mm, dp = 80mm, Rcheek = 80mm, weld = 10mm)**

tcheek	0%							0.5%							1%						
	1	2	3	5	1 cheek	3 cheek	weld	1	2	3	5	1 cheek	3 cheek	weld	1	2	3	5	1 cheek	3 cheek	weld
0	0.94							0.91													
20	0.85				1.02			0.91				0.97									
25	0.81				1.07			0.87				0.99									
30	0.79				1.08			0.86				0.97									
40	0.79				1.04			0.87				0.89									
tcheek	5%							15%							Section yield		F ratio mid plate				
	1	2	3	5	1 cheek	3 cheek	weld	1	2	3	5	1 cheek	3 cheek	weld	Criteria	25%	50%	75%	100%		
0			0.77							0.93					1.00	1				1.00	
20			0.60			0.98									0.97	1				0.98	
25															1.04	1				0.99	
30															1.10	1				1.00	
40															1.25	1				1.00	

**Table F-42: Formula/FEM ratios [-] for various cheek plate thicknesses [mm], plastic strains [%] and failure criteria [#] (Reye = 100mm, e = 50mm, t = 40mm, dh = 82mm, dp = 80mm, Rcheek = 80mm, weld = 10mm)**

PINNED CONNECTIONS

e	0%							0.5%							1%						
	1	2	3	5	1 cheek	3 cheek	weld	1	2	3	5	1 cheek	3 cheek	weld	1	2	3	5	1 cheek	3 cheek	weld
0	1900	3100	3000	3000	1750	1250	2950	3300	4400	4400	4700	3100	1950	4450	3950	4750	4950		3900	3450	4800
10	2150	4150	3000	3350	1950	1100	3350	3650	5300	4750	5100	3500	1700	5300	4450		5300		4400	2750	
20	2350	5150	3000	3600	2150	1050	3650	3950		4600	5450	3800	1650		4850				4800	2550	
30	2450		2950	3750	2250	1050	3850	4200		4650		4000	1700		5100				5100	2500	
40	2600		2950	3700	2400	1050	3900	4400		4650		4250	1700		5400				5450	2450	
50	2700		2950	3550	2500	1000	3900	4600		4650		4450	1700							2400	
e	5%							15%							Section yield		F ratio mid plate				
	1	2	3	5	1 cheek	3 cheek	weld	1	2	3	5	1 cheek	3 cheek	weld	Criteria	25%	50%	75%	100%		
0	4950	5150			4850		5150	5150					5150		4300	2/4	48%	48%	48%	51%	
10															4300	2/4	48%	48%	48%	49%	
20															4500	5	48%	48%	49%	50%	
30															4600	5	49%	49%	50%	51%	
40															4750	5	50%	49%	50%	52%	
50															4900	5	50%	50%	51%	53%	

**Table F-43: FEM results [kN for various eccentricities [mm], plastic strains [%] and failure criteria [#] (Reye = 100mm, t = 40mm, dh = 82mm, dp = 80mm, Rcheek = 80mm, Tcheek = 30mm, weld = 10mm)**

e	0%							0.5%							1%						
	1	2	3	5	1 cheek	3 cheek	weld	1	2	3	5	1 cheek	3 cheek	weld	1	2	3	5	1 cheek	3 cheek	weld
0	1651	3224			1825		2950	2888	4054				2950								
10	1776	3879			2054			3063	4672				3430								
20	1885	4616			2250			3276	5369				3767								
30	1981	5376			2418			3503	6089				4012								
40	2066	6127			2564			3733	6801				4194								
50	2142	6851			2691			3958	7488				4334								
e	5%							15%							Section yield		F ratio mid plate				
	1	2	3	5	1 cheek	3 cheek	weld	1	2	3	5	1 cheek	3 cheek	weld	Criteria	25%	50%	75%	100%		
0			3834			6495				5041			8274		3798	2/4				53%	
10			3786			6491				5059			8322		4450	2/4				53%	
20			3745			6365				5074			8361		4968	2/4				53%	
30			3711			6262				5086			8393		5389	2/4				53%	
40			3681			6176				5097			8420		5411	1				53%	
50			3656			6104				5107			8442		5411	1				53%	

**Table F-44: Formula results [kN] for various eccentricities [mm], plastic strains [%] and failure criteria [#] (Reye = 100mm, t = 40mm, dh = 82mm, dp = 80mm, Rcheek = 80mm, Tcheek = 30mm, weld = 10mm)**

e	0%							0.5%							1%						
	1	2	3	5	1 cheek	3 cheek	weld	1	2	3	5	1 cheek	3 cheek	weld	1	2	3	5	1 cheek	3 cheek	weld
0	0.87	1.04			1.04			0.88	0.92			0.95									
10	0.83	0.93			1.05			0.84	0.88			0.98									
20	0.80	0.90			1.05			0.83				0.99									
30	0.81				1.07			0.83				1.00									
40	0.79				1.07			0.85				0.99									
50	0.79				1.08			0.86				0.97									
e	5%							15%							Section yield		F ratio mid plate				
	1	2	3	5	1 cheek	3 cheek	weld	1	2	3	5	1 cheek	3 cheek	weld	Criteria		25%	50%	75%	100%	
0															0.88	2/4				1.04	
10															1.03	2/4				1.07	
20															1.10	2/4				1.05	
30															1.17	2/4				1.03	
40															1.14	1				1.01	
50															1.10	1				1.00	

**Table F-45: Formula/FEM ratios [-] for various eccentricities [mm], plastic strains [%] and failure criteria [#] (Reye = 100mm, t = 40mm, dh = 82mm, dp = 80mm, Rcheek = 80mm, Tcheek = 30mm, weld = 10mm)**

PINNED CONNECTIONS

Rcheek	0%							0.5%						1%							
	1	2	3	5	1 cheek	3 cheek	weld	1	2	3	5	1 cheek	3 cheek	weld	1	2	3	5	1 cheek	3 cheek	weld
60	1650	3550	2200	2650	1500	1800	1650	2950	4100	3200		2800		3400	3850	4250	3750		3500		3950
70	2000	4000	2450	3050	1750	1700	2400	3400	4550	3550		3100		4150	4250	4750	4250		3850		4650
80	2250	4400	2650	3500	1950	1250	3150	3800	5000	4100		3600	2000	4950	4750	5250	4700		4700	3150	5250
90	2450	4750	2800	3800	2150	1100	3600	4200	5450	4400		4050	1750	5600	5400	5700	5000		5500	2700	5800
100	2650	5100	2850	3950	2300	1050	3950	4550	5950	4400	6650	4550	1600	6000	5700	6150	5400		6050	2500	6200
Rcheek	5%							15%						Section yield		F ratio mid plate					
	1	2	3	5	1 cheek	3 cheek	weld	1	2	3	5	1 cheek	3 cheek	weld	Criteria	25%	50%	75%	100%		
60	4300	4500	4350		4250		4400	4450		4500		4450		4532.5	3850	2/4	55%	54%	56%	60%	
70	4900	5100	4950		4800		5050	5100		5150		5050		5167.5	4250	2/4	51%	50%	52%	55%	
80	5400	5600	5500		5300		5600	5600		5650		5600		5760	4700	2/4	50%	49%	49%	52%	
90	5850	6100	5950		5750	5900	6150	6100		6150		6100			5350	2/4	49%	49%	49%	52%	
100	6300	6550	6300		6200	5950	6550	6550		6600		6500	6600		5800	2/4	49%	49%	50%	52%	

**Table F-46: FEM results [kN for various cheek radii [mm], plastic strains [%] and failure criteria [#] (Reye = 120mm, e = 0mm, t = 40mm, dh = 82mm, dp = 80mm, Tcheek = 30mm, weld = 10mm)**

Rcheek	0%							0.5%						1%							
	1	2	3	5	1 cheek	3 cheek	weld	1	2	3	5	1 cheek	3 cheek	weld	1	2	3	5	1 cheek	3 cheek	weld
60																					
70	1991	4347			1357			4507	4792				2323								
80	2057	4491			1869			4657	4951				3022								
90	2098	4581			2319			4750	5050				3861								
100	2126	4643			2719			4814	5118				4755								
Rcheek	5%							15%						Section yield		F ratio mid plate					
	1	2	3	5	1 cheek	3 cheek	weld	1	2	3	5	1 cheek	3 cheek	weld	Criteria	25%	50%	75%	100%		
60																					
70			3526			6921				4835			8724		4583	2/4				56%	
80			3643			6653				4996			8475		4735	2/4				54%	
90			3716			6504				5096			8359		4830	2/4				53%	
100			3766			6313				5164			8299		4895	2/4				52%	

**Table F-47: Formula results [kN] for various cheek plate radii [mm], plastic strains [%] and failure criteria [#] (Reye = 120mm, e = 0mm, t = 40mm, dh = 82mm, dp = 80mm, Tcheek = 30mm, weld = 10mm)**

Rcheek	0%							0.5%						1%							
	1	2	3	5	1 cheek	3 cheek	weld	1	2	3	5	1 cheek	3 cheek	weld	1	2	3	5	1 cheek	3 cheek	weld
60																					
70	1.00	1.09			0.78			1.33	1.05				0.75								
80	0.91	1.02			0.96			1.23	0.99				0.84								
90	0.86	0.96			1.08			1.13	0.93				0.95								
100	0.80	0.91			1.18			1.06	0.86				1.05								
Rcheek	5%							15%						Section yield		F ratio mid plate					
	1	2	3	5	1 cheek	3 cheek	weld	1	2	3	5	1 cheek	3 cheek	weld	Criteria	25%	50%	75%	100%		
60																					
70			0.71							0.94					1.08	2/4				1.01	
80			0.66							0.88					1.01	2/4				1.03	
90			0.62			1.10				0.83					0.90	2/4				1.01	
100			0.60			1.06				0.78			1.26		0.84	2/4				1.00	

**Table F-48: Formula/FEM ratios [-] for various cheek plate radii [mm], plastic strains [%] and failure criteria [#] (Reye = 120mm, e = 0mm, t = 40mm, dh = 82mm, dp = 80mm, Tcheek = 30mm, weld = 10mm)**

Rcheek	0%							0.5%							1%						
	1	2	3	5	1 cheek	3 cheek	weld	1	2	3	5	1 cheek	3 cheek	weld	1	2	3	5	1 cheek	3 cheek	weld
60	1100	1800	1800	1650	1150	1400	1300	2000	3050	3	2750	2050	2400	2450	3300	3	3150	2600	3 cheek	2800	
65	1250	1950	2100	1850	1250	1550	1500	2200	3250		3050	2200	2500	2650	3550		3450	2750		2850	
70	1400	2100	2350	2050	1350	1700	1700	2350	3500		3400	2350	2600	2850	3850		3850	2950		3000	
75	1500	2300	2600	2250	1450	1700	1850	2550	3700		3750	2500	2800	3050	4100		4100	3150		3200	
79	1600	2400	2750	2400	1500	1450	1950	2700	3900		3900	2650	2900	3250	4300		4200	3300		3350	
Rcheek	5%							15%							Section yield		F ratio mid plate				
	1	2	3	5	1 cheek	3 cheek	weld	1	2	3	5	1 cheek	3 cheek	weld	Criteria	25%	50%	75%	100%		
60	3400	3520			3350	3500	3510					3510			2300	2/4	60%	59%	58%	58%	
65	3700	3835			3650	3825	3835					3835			2750	2/4	57%	56%	54%	56%	
70	3950	4145			3900	4050	4135					4125			3250	2/4	55%	54%	53%	55%	
75	4200	4400			4150	4150	4400					4400	4450		3500	2/4	54%	53%	51%	54%	
79	4400	4650		4673	4350	4300	4600					4600	4550		3800	2/4	53%	52%	51%	54%	

**Table F-49: FEM results [kN for various cheek radii [mm], plastic strains [%] and failure criteria [#] (Reye = 90mm, e = 0mm, t = 40mm, dh = 82mm, dp = 80mm, Tcheek = 30mm, weld = 6mm)**

Rcheek	0%							0.5%							1%						
	1	2	3	5	1 cheek	3 cheek	weld	1	2	3	5	1 cheek	3 cheek	weld	1	2	3	5	1 cheek	3 cheek	weld
60																					
65																					
70	1325	2317			1345		2205	3325				2303									
75	1344	2350			1617		2237	3373				2639									
79	1356	2371			1821		2257	3403				2944									
Rcheek	5%							15%							Section yield		F ratio mid plate				
	1	2	3	5	1 cheek	3 cheek	weld	1	2	3	5	1 cheek	3 cheek	weld	Criteria	25%	50%	75%	100%		
60																					
65																					
70			3715			6861				4774			8649		3094	2/4				55%	
75			3768			6744				4843			8548		3139	2/4				54%	
79			3801			6674				4885			8494		3166	2/4				54%	

**Table F-50: Formula results [kN] for various cheek plate radii [mm], plastic strains [%] and failure criteria [#] (Reye = 90mm, e = 0mm, t = 40mm, dh = 82mm, dp = 80mm, Tcheek = 30mm, weld = 6mm)**

Rcheek	0%							0.5%							1%						
	1	2	3	5	1 cheek	3 cheek	weld	1	2	3	5	1 cheek	3 cheek	weld	1	2	3	5	1 cheek	3 cheek	weld
60																					
65																					
70	0.95	1.10			1.00		0.94	0.95				0.98									
75	0.90	1.02			1.12		0.88	0.91				1.06									
79	0.85	0.99			1.21		0.84	0.87				1.11									
Rcheek	5%							15%							Section yield		F ratio mid plate				
	1	2	3	5	1 cheek	3 cheek	weld	1	2	3	5	1 cheek	3 cheek	weld	Criteria	25%	50%	75%	100%		
60																					
65																					
70															0.95	2/4				1.00	
75															0.90	2/4				1.00	
79															0.83	2/4				0.99	

**Table F-51: Formula/FEM ratios [-] for various cheek plate radii [mm], plastic strains [%] and failure criteria [#] (Reye = 90mm, e = 0mm, t = 40mm, dh = 82mm, dp = 80mm, Tcheek = 30mm, weld = 6mm)**

## F.2 Formulas

### Determined formulas

#### Tension in the net section 0%

$$0.000305 \left( -3810. E G^2 + 220. E^2 + 3600. E G + 1310. G^2 - 140. E + 2090. G - 232. \right) t dh \left( 1. - 0.0391 0.221^{G+E} + 0.435 0.221^{G+E} 0.3^{82. clear} \right)$$

#### Tension in the net section 0.5%

$$0.000305 \left( \left\{ \begin{array}{ll} 37600. E^2 G + 37300. E G^2 - 13000. E^2 - 34900. E G + 13700. G^2 + 8820. E - 4000. G + 800. & G < -0.165 E + 0.481 \\ -460. E G + 972. G^2 + 3630. E + 13000. G - 4090. & otherwise \end{array} \right. \right) t dh \min(1.5, 1. - 4.82 e^{-3.81 E - 12.2 G} + 53.5 e^{-3.81 E - 12.2 G} 0.3^{82. clear})$$

#### Fracture beyond the hole 0%

$$0.000305 \left( 3.28 10^5 E G^3 - 4.64 10^5 E G^2 - 58300. G^3 + 7980. E^2 + 2.15 10^5 E G + 79100. G^2 - 29800. E - 25700. G + 2890. \right) t dh \left( 1. - 0.422 \max(0., -2.09 E + 0.598) + \max(0., -2.09 E + 0.598) 0.65^{82. \max(0.005, clear)} \right)$$

#### Fracture beyond the hole 0.5%

$$\max(\text{Fracture beyond the hole } 0\%, 0.000305 \left( 11600. E G^2 + 7620. E^2 - 6610. E G + 4740. G^2 + 3610. E + 3000. G + 49.6 \right) t dh \left( 1. - 0.672 \max(0., -0.828 E + 0.398) + \max(0., -0.828 E + 0.398) 0.82^{82. \max(0.005, clear)} \right))$$

#### Bearing 0%

$$0.000305 \left( 8220. E G^2 - 777. E^2 - 8590. E G - 4050. G^2 + 2210. E + 3470. G + 509. \right) t dh \min(1.6, 0.299 + 2. 0.6^{82. \max(0.005, clear)} - 0.79 \max(0.005, clear))$$

#### Bearing 5%

$$0.000305 \max(1880., \min(2050., 1720. E G - 1000. E - 828. G + 2370.)) t dh \left( 0.482 + 0.9 0.78^{82. clear} - 1.2 clear \right)$$

#### Bearing 15%

$$0.000305 \left( -356. E G + 253. E + 447. G + 2470. \right) t dh \left( 0.663 + 0.47 0.88^{82. clear} - 1.12 clear \right)$$

#### Yielding in the net section

$$0.000305 \left( \left\{ \begin{array}{ll} -13200. + 73800. G - 84600. G^2 + 1.45 10^5 (0.418 - 1. G) E - 1.85 10^5 (0.175 - 1. G^2) E & G < 0.418 \\ 27300. G^2 - 17800. G + 5530. & otherwise \end{array} \right. \right) t dh$$

#### Yielding on top of the hole

$$0.000305 \left( -20700. E G^2 - 1040. E^2 + 26100. E G + 8460. G^2 - 3440. E - 120. G + 569. \right) t dh \left( 1. - 0.689 \max(0., -0.684 E + 0.364) + \max(0., -0.684 E + 0.364) 0.83^{82. \max(0.005, clear)} \right)$$

## Yielding criteria

$$\left\{ \begin{array}{l} \text{Yielding on top of the hole} \\ \min \left( \text{Yielding on top of the hole}, \max \left( \left( \begin{array}{l} \text{Yielding In the net section} \\ 8.33 G^2 - 17800 \cdot G + 5530 \end{array} \right) \begin{array}{l} G < 0.418 \\ \text{otherwise} \end{array} \right) t dh, 0.457 dh t \right) \end{array} \right\} \begin{array}{l} G < \min(0.374, -4.56 E + G + 1.14) \\ \text{otherwise} \end{array}$$

## Load % through midplate

$$\frac{2.9 t}{t + 2 \cdot t_{cheek}} + 78.9 + 5.02 Gg - 39.1 Tt - 13.9 W$$

## Formulas for spreadsheet

In this part of the appendix the formulas are just copied as text, so they are easy to copy in an excel spreadsheet. The variables are:

- G
- E
- clear
- dh
- t
- Gg
- Tt
- W
- tcheek

### Tension in the net section 0%

$$\begin{aligned} &=(1/3280)*(- \\ &(47218621204436583/12408017747200)*E*G^2+(254241904/1153333)*E^2+(22351200644513861/6 \\ &204008873600)*E*G+(14050729539/10758400)*G^2- \\ &(346788977760819/2481603549440)*E+(11227197999/5379200)*G-2500653941/10758400))*t*dh*(1- \\ &0.3914549318e-1*.2213773495^(G+E)+.4349499242*.2213773495^(G+E)*.3^(82*clear)) \end{aligned}$$

### Tension in the net section 0.5%

$$\begin{aligned} &=(1/3280)*\text{if}(G < -(9348/56485)*E+38/79; \\ &(368452563201/9790100)*E^2*G+(16333174643832/437690375)*E*G^2- \\ &(126913615059/9790100)*E^2- \\ &(5737685076041301/164571581000)*E*G+(11500578687/840500)*G^2+(1450942359979167/164571 \\ &581000)*E-(6728304007/1681000)*G+1344372919/1681000; - \\ &(6563833663527/14269169525)*E*G+(454846023899991/468028760420)*G^2+(51806295020613/14 \\ &269169525)*E+(6068642346354669/468028760420)*G- \\ &957552397212531/234014380210))*t*dh*\min(1.5; 1-4.816311860*\exp(-3.810985034*E- \\ &12.22815746*G)+53.51457622*\exp(-3.810985034*E-12.22815746*G)*.3^(82*clear)) \end{aligned}$$

### Fracture beyond the hole 0%

$$\begin{aligned}
 &= (1/3280 * ((6885947853981336459/20996093440000) * E * G^3 - \\
 &(9738769797714188503/20996093440000) * E * G^2 - \\
 &(3601236456194619/61753216000) * G^3 + (127743/16) * E^2 + (13555777226664988051/629882803200 \\
 &00) * E * G + (4882578849673703/61753216000) * G^2 - (15772923425344177/529313280000) * E - \\
 &(1588336603433137/61753216000) * G + 178401596170541/61753216000)) * t * dh * (1 - .4225 * \max(0; - \\
 &2.088000000 * E + .5980000000) + \max(0; -2.088000000 * E + .5980000000) * .65^{(82 * \max(0.5e-2; \text{clear}))})
 \end{aligned}$$

### Fracture beyond the hole 0.5%

$$\begin{aligned}
 &= \max((1/3280 * ((2198225329017222417/188711050304000) * E * G^2 + (3972192514587/521212640) * E^2 - \\
 &(8104484534483278649/1226621826976000) * E * G + (44592974943/9413600) * G^2 + (88553800715457 \\
 &63681/2453243653952000) * E + (14125387273/4706800) * G + 466899603/9413600)) * t * dh * (1 - \\
 &.6724 * \max(0; -.8280000000 * E + .3980000000) + \max(0; - \\
 &.8280000000 * E + .3980000000) * .82^{(82 * \max(0.5e-2; \text{clear}))}); \\
 &(1/3280 * ((6885947853981336459/20996093440000) * E * G^3 - \\
 &(9738769797714188503/20996093440000) * E * G^2 - \\
 &(3601236456194619/61753216000) * G^3 + (127743/16) * E^2 + (13555777226664988051/629882803200 \\
 &00) * E * G + (4882578849673703/61753216000) * G^2 - (15772923425344177/529313280000) * E - \\
 &(1588336603433137/61753216000) * G + 178401596170541/61753216000)) * t * dh * (1 - .4225 * \max(0; - \\
 &2.088000000 * E + .5980000000) + \max(0; -2.088000000 * E + .5980000000) * .65^{(82 * \max(0.5e-2; \text{clear}))})
 \end{aligned}$$

### Bearing 0%

$$\begin{aligned}
 &= (1/3280 * ((1478344132584/179740925) * E * G^2 - (6869505/8836) * E^2 - \\
 &(4645570460651451/540660702400) * E * G - \\
 &(87096492483/21516800) * G^2 + (1197031607633877/540660702400) * E + (37385433797/10758400) * G \\
 &+ 10962246477/21516800)) * t * dh * \min(1.6; .2992682927 + 2 * .6^{(82 * \max(0.5e-2; \text{clear}))} - .79 * \max(0.5e-2; \\
 &\text{clear}))
 \end{aligned}$$

### Bearing 5%

$$\begin{aligned}
 &= (1/3280) * \max(1880; \min(2050; (3527961/2050) * E * G - (2054339/2050) * E - \\
 &(1696653/2050) * G + 4848897/2050)) * t * dh * (.4817082927 + .9 * .78^{(82 * \text{clear})} - 1.2 * \text{clear})
 \end{aligned}$$

### Bearing 15%

$$\begin{aligned}
 &= (1/3280 * (- \\
 &(584307/1640) * E * G + (414813/1640) * E + (91656/205) * G + 505796/205)) * t * dh * (.6633490732 + .47 * .88^{(82 * \\
 &\text{clear})} - 1.12 * \text{clear})
 \end{aligned}$$

### Yielding in the net section

$$\begin{aligned}
 &= (1/3280) * \text{if}(G < 59/141; -13203.63800 + 73770.43920 * G - \\
 &84617.57760 * G^2 + 1.447036504 * 10^5 * (59/141 - G) * E - 1.853051270 * 10^5 * (3481/19881 - G^2) * E; \\
 &27317.05898 * G^2 - 17830.47611 * G + 5526.986436) * t * dh
 \end{aligned}$$

### Yielding on top of the hole

$$\begin{aligned}
 &= (1/3280 * (- (12821047017035169/619414880000) * E * G^2 - \\
 &(80195566/77315) * E^2 + (380417396866113837/14556249680000) * E * G + (1941947997/229600) * G^2 - \\
 &(100167209290287383/29112499360000) * E - (13816493/114800) * G + 130671017/229600)) * t * dh * (1 - \\
 &.6889 * \max(0; -.6840000000 * E + .3640000000) + \max(0; - \\
 &.6840000000 * E + .3640000000) * .83^{(82 * \max(0.5e-2; \text{clear}))})
 \end{aligned}$$

### Yielding criteria

$$\begin{aligned}
 &= \text{if}(G < \min(.374; -4.558823529 * E + G + 1.142441176); (1/3280 * (- \\
 &(12821047017035169/619414880000) * E * G^2 - \\
 &(80195566/77315) * E^2 + (380417396866113837/14556249680000) * E * G + (1941947997/229600) * G^2 - \\
 &(100167209290287383/29112499360000) * E - (13816493/114800) * G + 130671017/229600)) * t * dh * (1 - \\
 &.6889 * \max(0; -.6840000000 * E + .3640000000) + \max(0; - \\
 &.6840000000 * E + .3640000000) * .83^{(82 * \max(0.5e-2; \text{clear}))}); \min((1/3280 * (- \\
 &(12821047017035169/619414880000) * E * G^2 - \\
 &(80195566/77315) * E^2 + (380417396866113837/14556249680000) * E * G + (1941947997/229600) * G^2 - \\
 &(100167209290287383/29112499360000) * E - (13816493/114800) * G + 130671017/229600)) * t * dh * (1 - \\
 &.6889 * \max(0; -.6840000000 * E + .3640000000) + \max(0; - \\
 &.6840000000 * E + .3640000000) * .83^{(82 * \max(0.5e-2; \text{clear}))}); \max((75/164) * dh * t; (1/3280) * \text{if}(G < \\
 &59/141; -13203.63800 + 73770.43920 * G - 84617.57760 * G^2 + 1.447036504 * 10^5 * (59/141 - G) * E - \\
 &1.853051270 * 10^5 * (3481/19881 - G^2) * E; 27317.05898 * G^2 - 17830.47611 * G + 5526.986436) * t * dh))
 \end{aligned}$$

### Load % through midplate

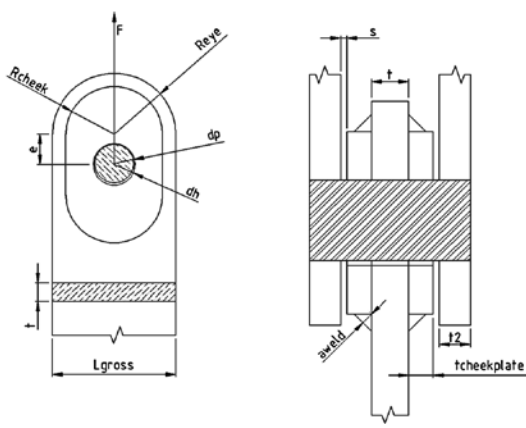
$$= (2.9 * t / (t + 2 * t_{\text{cheek}}) + 78.94 + 5.02 * G_g - 39.09 * T_t - 13.93 * W) * 0.01$$

# G Spreadsheet

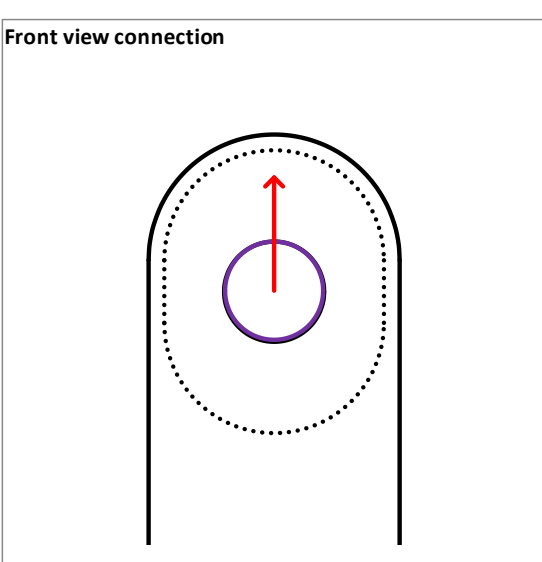
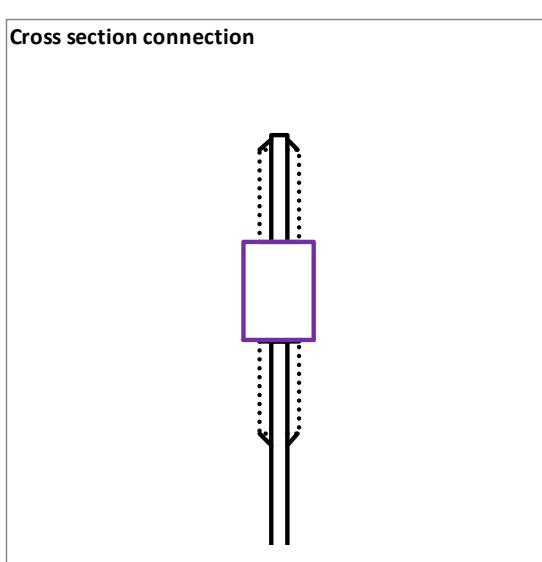
In this appendix an example of a spreadsheet is shown for different input parameters.

## Example with cheek plates

Input			
Cheekplates applied?	<input type="checkbox"/> Yes		
<b>Geometry</b>			
$R_{eye}$	=	<input type="text" value="320"/>	[mm] outer radius eye
$e$	=	<input type="text" value="80"/>	[mm] eccentricity
$d_h$	=	<input type="text" value="255"/>	[mm] diameter hole
$d_p$	=	<input type="text" value="250"/>	[mm] diameter pin
$t$	=	<input type="text" value="40"/>	[mm] thickness eye
$R_{cheek}$	=	<input type="text" value="280"/>	[mm] outer radius cheek plate
$t_{cheek}$	=	<input type="text" value="30"/>	[mm] thickness cheek plate
$a_{weld}$	=	<input type="text" value="20"/>	[mm] weld throat
<b>Material</b>			
$f_y$	=	<input type="text" value="690"/>	[N/mm <sup>2</sup> ] yield stress eye
$f_u$	=	<input type="text" value="770"/>	[N/mm <sup>2</sup> ] ultimate tensile stress eye
$\epsilon_u$	=	<input type="text" value="15%"/>	[-] ultimate tensile strain



Drawing connection	
<p><b>Front view connection</b></p> 	<p><b>Cross section connection</b></p> 

**Calculation parameters and restrictions**

Additional calculation parameters			Restrictions & Formulas		Restrictions/Recommendations
G	=	0.43 [-]	$0.25 \leq G = \frac{R_{eye} - d_h/2}{R_{eye} + d_h/2} \leq 0.6$		
E	=	0.20 [-]	$0 \leq E = \frac{e}{e + R_{eye}} \leq 0.45$		
clear	=	1.96% [-]	$0 \leq clear = \frac{d_h - d_p}{d_h} \leq 0.25$		
Gcheek	=	0.37 [-]	$0.25 \leq G_{cheek} = \frac{R_{cheek} - d_h/2}{R_{cheek} + d_h/2} \leq 0.6$		
Gg	=	1.15 [-]	$G_g = \frac{G}{G_{cheek}}$		
Tt	=	0.75 [-]	$0 \leq T_t = \frac{T_{cheek}}{T} \leq 1$		
W	=	0.67 [-]	$W = \frac{a_{weld}}{T_{cheek}}$		
Echeek	=	0.22 [-]	$0 \leq E_{cheek} = \frac{e}{e + R_{cheek}} \leq 0.45$		

**Output**

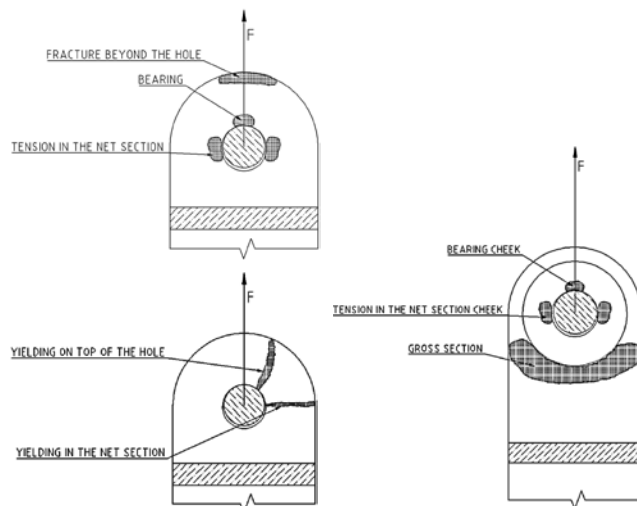
Load % through midplate 47% [-]

**Midplate output**

Tension in the net section 0%	7018	[kN]
Tension in the net section 0.5%	12604	[kN]
Fracture beyond the hole 0%	18303	[kN]
Fracture beyond the hole 0.5%	20751	[kN]
Bearing 5%	13765	[kN]
Bearing 15%	18152	[kN]
Yielding on top of the hole	18875	[kN]
Dishing	60705	[kN]

**Cheek plate output**

Tension in the net section 0%	7971	[kN]
Tension in the net section 0.5%	13513	[kN]
Bearing 5%	12742	[kN]
Bearing 15%	18689	[kN]
Gross section yield	13248	[kN]
Dishing	61069	[kN]
Weld	31416	[kN]



**Example without cheek plates**

**Input**

Cheekplates applied?

**Geometry**

$R_{eye}$	=	<input type="text" value="50"/>	[mm]	outer radius eye
$e$	=	<input type="text" value="0"/>	[mm]	eccentricity
$d_h$	=	<input type="text" value="32"/>	[mm]	diameter hole
$d_p$	=	<input type="text" value="30"/>	[mm]	diameter pin
$t$	=	<input type="text" value="20"/>	[mm]	thickness eye
$R_{cheek}$	=	<input type="text" value="0"/>	[mm]	outer radius cheek plate
$t_{cheek}$	=	<input type="text" value="0"/>	[mm]	thickness cheek plate
$a_{weld}$	=	<input type="text" value="0"/>	[mm]	weld throat

**Material**

$f_y$	=	<input type="text" value="690"/>	[N/mm <sup>2</sup> ]	yield stress eye
$f_u$	=	<input type="text" value="770"/>	[N/mm <sup>2</sup> ]	ultimate tensile stress eye
$\epsilon_u$	=	<input type="text" value="15%"/>	[-]	ultimate tensile strain

---

**Drawing connection**

**Front view connection**

**Cross section connection**

**Calculation parameters and restrictions**

Additional calculation parameters				Restrictions & Formulas		Restrictions/Recommendations
G	=	0.52	[-]	$0.25 \leq G = \frac{R_{eye} - d_h/2}{R_{eye} + d_h/2} \leq 0.6$		
E	=	0.00	[-]	$0 \leq E = \frac{e}{e + R_{eye}} \leq 0.45$		
clear	=	6.25%	[-]	$0 \leq clear = \frac{d_h - d_p}{d_h} \leq 0.25$		
Gcheek	=	-	[-]	$0.25 \leq G_{cheek} = \frac{R_{cheek} - d_h/2}{R_{cheek} + d_h/2} \leq 0.6$		
Gg	=	-	[-]	$G_g = \frac{G}{G_{cheek}}$		
Tt	=	-	[-]	$0 \leq T_t = \frac{T_{cheek}}{T} \leq 1$		
W	=	-	[-]	$W = \frac{a_{weld}}{T_{cheek}}$		
Echeek	=	-	[-]	$0 \leq E_{cheek} = \frac{e}{e + R_{cheek}} \leq 0.45$		

**Output**

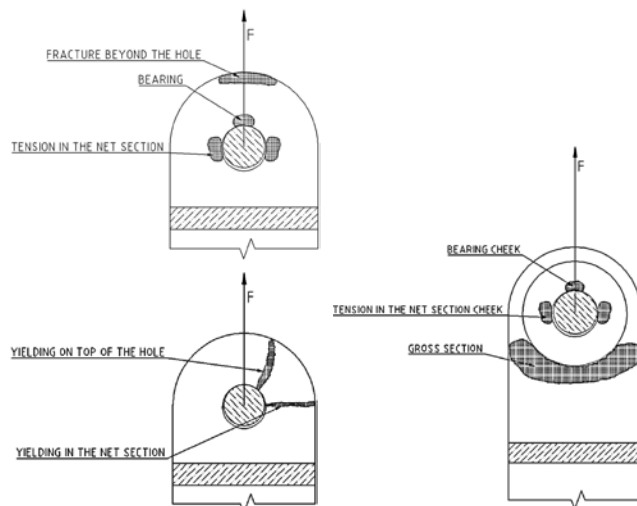
Load % through midplate 100% [-]

**Midplate output**

Tension in the net section 0%	228	[kN]
Tension in the net section 0.5%	558	[kN]
Fracture beyond the hole 0%	420	[kN]
Fracture beyond the hole 0.5%	489	[kN]
Bearing 5%	253	[kN]
Bearing 15%	445	[kN]
Yielding on top of the hole	477	[kN]
Dishing	21016	[kN]

**Cheek plate output**

Tension in the net section 0%	-	[kN]
Tension in the net section 0.5%	-	[kN]
Bearing 5%	-	[kN]
Bearing 15%	-	[kN]
Gross section yield	-	[kN]
Dishing	-	[kN]
Weld	-	[kN]



**Example unfulfilled geometry restrictions**

**Input**

Cheekplates applied? No

**Geometry**

$R_{eye}$	=	100	[mm]	outer radius eye
$e$	=	-10	[mm]	eccentricity
$d_h$	=	125	[mm]	diameter hole
$d_p$	=	80	[mm]	diameter pin
$t$	=	20	[mm]	thickness eye
$R_{cheek}$	=	0	[mm]	outer radius cheek plate
$t_{cheek}$	=	0	[mm]	thickness cheek plate
$a_{weld}$	=	0	[mm]	weld throat

**Material**

$f_y$	=	690	[N/mm <sup>2</sup> ]	yield stress eye
$f_u$	=	770	[N/mm <sup>2</sup> ]	ultimate tensile stress eye
$\epsilon_u$	=	15%	[-]	ultimate tensile strain

---

**Drawing connection**

**Front view connection**

**Cross section connection**

**Calculation parameters and restrictions**

Additional calculation parameters			Restrictions & Formulas	Restrictions/Recommendations
G	=	- [-]	$0.25 \leq G = \frac{R_{eye} - d_h/2}{R_{eye} + d_h/2} \leq 0.6$	$G \geq 0.25$
E	=	- [-]	$0 \leq E = \frac{e}{e + R_{eye}} \leq 0.45$	$E \geq 0$
clear	=	- [-]	$0 \leq clear = \frac{d_h - d_p}{d_h} \leq 0.25$	clear $\leq 0.25$
Gcheek	=	- [-]	$0.25 \leq G_{cheek} = \frac{R_{cheek} - d_h/2}{R_{cheek} + d_h/2} \leq 0.6$	
Gg	=	- [-]	$G_g = \frac{G}{G_{cheek}}$	
Tt	=	- [-]	$0 \leq T_t = \frac{T_{cheek}}{T} \leq 1$	
W	=	- [-]	$W = \frac{a_{weld}}{T_{cheek}}$	
Echeek	=	- [-]	$0 \leq E_{cheek} = \frac{e}{e + R_{cheek}} \leq 0.45$	

**Output**

Load % through midplate - [-]

**Midplate output**

Tension in the net section 0%	<span style="background-color: #90EE90; padding: 2px;">-</span>	[kN]
Tension in the net section 0.5%	<span style="background-color: #90EE90; padding: 2px;">-</span>	[kN]
Fracture beyond the hole 0%	<span style="background-color: #90EE90; padding: 2px;">-</span>	[kN]
Fracture beyond the hole 0.5%	<span style="background-color: #90EE90; padding: 2px;">-</span>	[kN]
Bearing 5%	<span style="background-color: #90EE90; padding: 2px;">-</span>	[kN]
Bearing 15%	<span style="background-color: #90EE90; padding: 2px;">-</span>	[kN]
Yielding on top of the hole	<span style="background-color: #90EE90; padding: 2px;">-</span>	[kN]
Dishing	<span style="background-color: #90EE90; padding: 2px;">-</span>	[kN]

**Cheek plate output**

Tension in the net section 0%	<span style="background-color: #90EE90; padding: 2px;">-</span>	[kN]
Tension in the net section 0.5%	<span style="background-color: #90EE90; padding: 2px;">-</span>	[kN]
Bearing 5%	<span style="background-color: #90EE90; padding: 2px;">-</span>	[kN]
Bearing 15%	<span style="background-color: #90EE90; padding: 2px;">-</span>	[kN]
Gross section yield	<span style="background-color: #90EE90; padding: 2px;">-</span>	[kN]
Dishing	<span style="background-color: #90EE90; padding: 2px;">-</span>	[kN]
Weld	<span style="background-color: #90EE90; padding: 2px;">-</span>	[kN]

